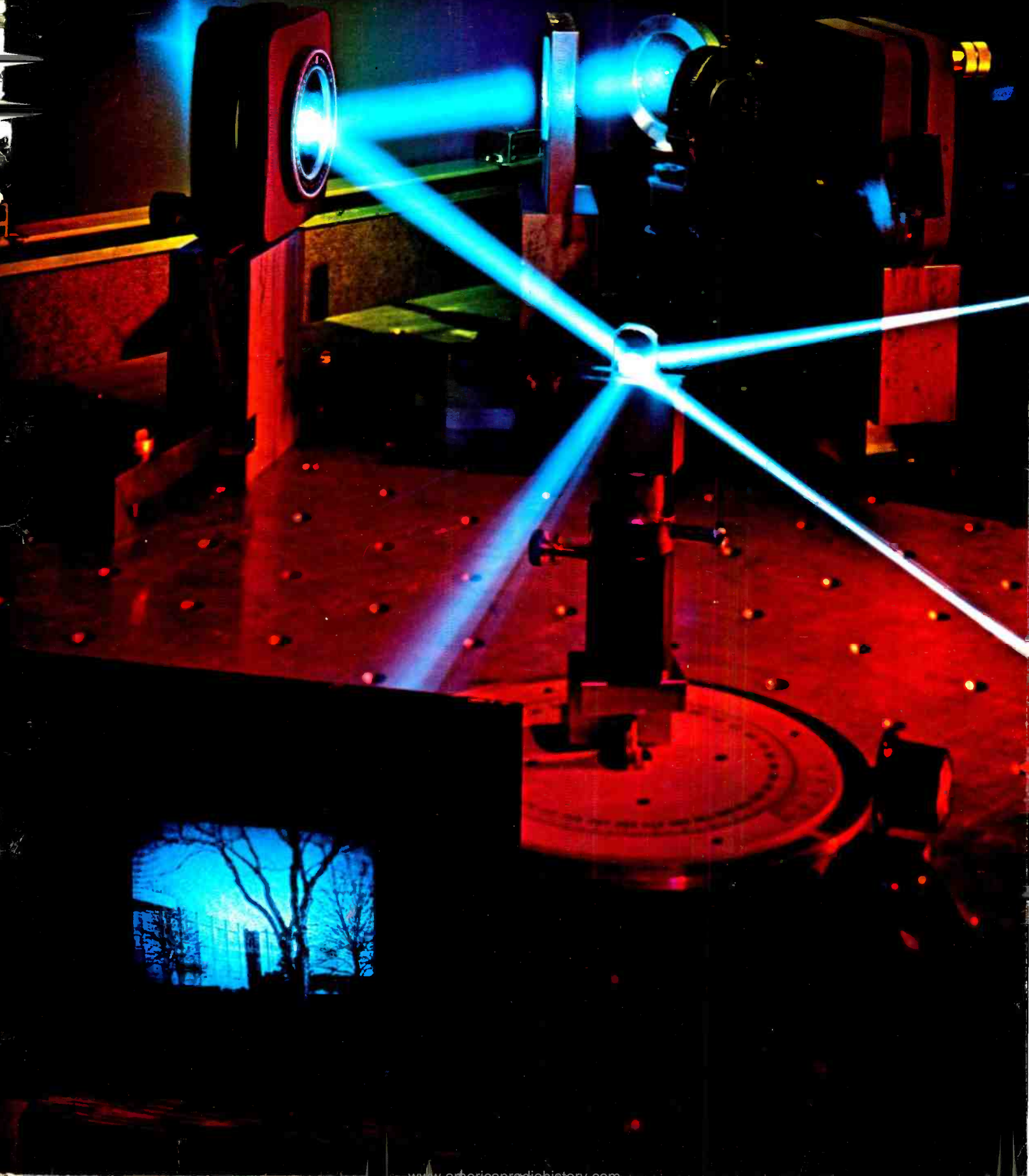


RCA Engineer

Vol 17 No 2
Aug | Sept
1971



Optics

Optics and electronics are inseparable in many systems. As a result, photochromics, cathodochromics, holography, and lasers have become tools of the modern electronics engineer.

To illustrate this relationship, consider the need to store and access the ever-increasing fund of human knowledge. Electro-optical systems of the future can meet this need. For example:

- Such systems are likely to use holographic memories as computer-accessible libraries. These libraries will permit the selection of a page from a book and its retrieval in a fraction of a second.
- "Soft copy" displays will present the page to the viewer for 10 seconds or 2 hours as he desires. New cathodochromic materials will eliminate the need for continuously refreshing "soft copy" displays at television rates.
- Printed or "hard copy" pages will be an alternate output from the library. A new method of printing using a laser beam to transfer ink shows promise.

I am sure this issue will suggest other applications of this exciting new technology to you.



Dr. H. J. Woll
Division Vice President
Government Engineering
Moorestown, N.J.

RCA Engineer Staff

Editor

Associate Editor

Assistant Editor

Editorial Secretary

Design and Layout

Subscriptions

Consulting Editors

Technical Publications Adm.,
Electronic Components

Technical Publications Adm.,
Laboratories

Technical Publications Adm.
Corporate Engineering Services

Editorial Advisory Board

VP, Technical Operations,
Systems Development
Division, Computer Systems

Staff VP, Industrial
Relations—International
and New Business

Mgr., Quality and Reliability
Assurance, Solid State Div.

VP, Engineering, NBC
Television Network

Mgr., Technical Information
Services, RCA Laboratories

Manager, Consumer Products
Adm., RCA Service Co.

Chief Engineer,
Record Division

Chief Technical Advisor,
Consumer Electronics

Div. VP, Technical Planning
Electronic Components

VP, Engineering and
Leased Systems,
Global Communications, Inc.

Director, Corporate
Engineering Services

Manager, Engineering
Professional Development

Division VP,
Government Engineering

Our cover shows the reconstruction of one of several holograms stored and fixed in a gamma-irradiated LiNbO₃ crystal. The converging beam coming in from the left is the reference beam being used for readout. In addition to the reconstructed object beam projecting the image (a view of the Labs in Princeton) the photo shows the transmitted (undiffracted) reference beam and the reflected part of the reference beam. **Photo credit:** Tom Cook, RCA Laboratories, Princeton.

P. R. C. America

OCT 1 1971

RCA Engineer

Vol 17 | No. 2
Aug | Sept
1971

A technical journal published bi-monthly by
RCA Corporate Engineering Services 2-8,
Camden, N.J.

RCA Engineer articles are indexed
annually in the April-May Issue and
in the "Index to RCA Technical Papers."

• To disseminate to RCA engineers technical information of professional value • To publish in an appropriate manner important technical developments at RCA, and the role of the engineer • To serve as a medium of interchange of technical information between various groups at RCA • To create a community of engineering interest within the company by stressing the interrelated nature of all technical contributions • To help publicize engineering achieve-

ments in a manner that will promote the interests and reputation of RCA in the engineering field • To provide a convenient means by which the RCA engineer may review his professional work before associates and engineering management • To announce outstanding and unusual achievements of RCA engineers in a manner most likely to enhance their prestige and professional status.

Contents

Editorial	Reactions to reader survey 4	2
Engineer & the Corporation	Solid state: where it's been and where it's headed	W. C. Hittinger 3
Optics research	Optics and electron optics as competitive and complementary technologies	Dr. E. G. Ramberg 8
	Cathodochromic image display applications	Dr. I. Gorog 12
	Holographic recording in crystals	Dr. J. J. Amodei Dr. W. Phillips Dr. D. L. Staebler 16
	Inorganic photochromic and cathodochromic recording materials	R. C. Duncan, Jr. Dr. B. W. Faughnan Dr. W. Phillips 23
Optical systems & techniques	Low-light-level color photography	E. Hutto, Jr. 28
	The ideographic composing machine	W. F. Heagerty 31
	Color decoding projector for low-light-level color photography	Dr. L. J. Nicastro E. Hutto, Jr. 34
	Measuring optical properties of water <i>in situ</i>	Dr. L. E. Mertens W. H. Manning, Jr. 38
	Material transfer recording	M. L. Levene Dr. R. D. Scott B. W. Siryj 43
Special reports	RCA & Apollo 15	48
	Fourth RCA Engineer readership survey	P. C. Farbro 50
Optical systems & techniques	Laser Beam Image Reproducer (LBIR)	S. M. Ravner 53
	Videovoice	S. N. Friedman 58
	High-power GaAs close-confinement laser diodes	T. Gonda R. B. Gill 62
Division profile	Laboratories RCA Ltd—a profile	R. F. Holtz 66
Of general interest	Piezoceramic device applications	P. Nelson 76
	Speech bandwidth compression by analytic rooting	E. J. Sass G. E. Mackiw 82
Notes	Phase-change heat-transfer techniques	B. Shelpuk 88
	Chip collection	M. Novick 89
Departments	Pen & Podium	90
	Patents	93
	News & Highlights	94

Copyright 1971 RCA Corporation
All Rights Reserved

Application to mail at second-class postage rates
is pending at U.S. Post Office, Camden, N.J.

editorial input

reactions to reader survey 4

If editors were seers endowed with supreme insight, reader surveys would not be necessary. Sweating out this issue on optics and optical systems didn't perceptibly improve our clairvoyance. So, we turned to the best method we know—and pored over 1500 questionnaires from reader survey 4 to see if present courses of action and future editorial plans match reader interests.

Reflecting on our request to complete survey 4, you readers could reasonably ask the editors . . .

Q—Why are the editors so eager to get our guidance?

A—If the journal is to remain "by and for the RCA engineer," its editors must remain always in close touch with readers, as well as editorial representatives and advisory board members.

Q—Don't the editors have good "directivity" from previous surveys?

A—Through the constant help of editorial representatives in every area, the editors manage to stay "on course" reasonably well. But, your reactions constitute the perfect barometer to measure the present publication and steer its future course.

Q—Don't the editors know desired themes and the best mix of articles?

A—Over a short period of time this is true. But the journal must follow carefully the rapid technological changes within RCA so that the *RCA Engineer* can truly represent the technical character and makeup of RCA.

With the need for the new survey completely justified, at least in our own minds, what then did we learn from you?

You generally supported our editorial convictions: you expressed pride in the journal's professional approach and its personalized characteristics; and you expressed appreciation of being kept informed—both technically and managerially. This all provides us a new strength of purpose to move forward.

However, in several areas, we have already (based on your suggestions) established new objectives. For example,

we plan to step up the tempo of publishing certain types of articles, especially in management planning areas. We know there is an increased need for close contact between the editorial representatives and the readers. Specifically, you told us again that we must remain broad in purpose and continue to serve all the technical areas, large and small, embracing electrical, mechanical, chemical, physical, management, computer programming, and even technical processing and manufacturing skills.

As might be expected a minority of readers in advanced development and research areas preferred a modest increase in theoretical approaches, but other engineering areas committed to the challenges of mechanical engineering and manufacturing engineering disagreed with this idea. So, the challenge of maintaining an intelligent and *diversified balance* remains, as always, a primary editorial goal. You have suggested that the *RCA Engineer* continue a modified thematic approach that includes a prescribed number of good survey papers, occasional tutorial papers, and (in the majority of cases) articles that both inform and teach. Emphasis will be given to new sciences and fields of engineering, new developments, new techniques, and advanced development and research.

A substantial reader response indicates desire for more articles on company plans, objectives and policy. This editorial approach, already begun, will be stepped up through more "division profiles", more "Engineer-and-the Corporation" papers, and by increased use of interview type or question-and-answer articles. Our recent quest for papers dealing with engineering and its relationship to ecology seems justified by your response and will be continued. Another area you voted for emphatically is the increased use of engineering-and-

research notes. These ideas constitute some of the important areas of feedback resulting from survey 4.

Finally, in satisfying your recommendations . . . and pursuing the major goal—to produce a journal by and for the engineer—we welcome your day-to-day ideas and suggestions—and your professional papers to share with the technical community.

References:

1. P. C. Farbro, "Results of Readership Survey #1," *RCA Engineer*, Vol. 2, No. 3 (Oct/Nov, 1956).
2. P. C. Farbro and J. M. Cook, "Second RCA Engineer, Readership Survey," *RCA Engineer*, Vol. 5, No. 4 (Dec 1959/Jan 1960).
3. P. C. Farbro, "Third RCA Engineer Readership Survey," *RCA Engineer*, Vol. 14, No. 1, (June/July 1968).
4. "Editorial input: Reactions to reader survey 3," *RCA Engineer*, Vol. 14, No. 2 (Aug/Sept 1968).
5. P. C. Farbro, "Fourth RCA Engineer Readership Survey," this issue.

Future issues

The next issue of the *RCA Engineer* discusses integrated circuits and solid-state technology. Some of the topics to be covered are:

Design automation and test technology

Semiconductor IC technology

COS/MOS memory array design

Materials and processes

Hybrid and packaging technology

Power technology and reliability

IC fabrication and applications

Discussions of the following themes are planned for future issues:

Additional developments in solid-state technology

Computer peripherals

Displays

Advanced Technology Laboratories

Systems programming

Semiconductor memories and COS/MOS circuits

Solid state: where it's been and where it's headed

W. C. Hittinger

RCA's role in the solid state market is becoming one of increased selectivity—relying on leadership in distinct areas, such as power transistors and COS/MOS devices, or in areas that offer significant potential return on investments, such as linear IC's and semiconductor memories. In this paper, Mr. Hittinger examines the business and marketing considerations, the design and applications, and the new materials and processes that should maintain RCA's position as a major supplier of solid state products for the home, industry, and government.

SOLID STATE RESEARCH was begun by RCA Laboratories in 1938, but it wasn't until 1948—the year Bell Labs announced the invention of the transistor—that the operating division at Harrison became actively involved in solid state work. By the end of 1948, six RCA engineers and technicians were working in the Harrison plant on development projects for point-contact transistors.

Out of these beginnings grew the Solid State Division, now comprising 6,000 employees and five major plants in Somerville, N. J. (opened in 1956), Findlay, O. (1959), Mountaintop, Pa. (1960), Taoyuan, Taiwan (1967) and Liege, Belgium (1970). Our Division is a world-wide leader in a number of solid-state areas, including power transistors, linear IC's for home entertainment equipment, and COS/MOS (complementary symmetry metal-oxide-semiconductor) IC's.

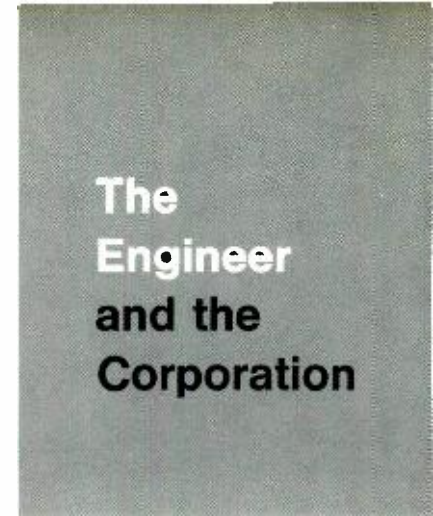
For many years, the Division had been a major supplier of small signal transistors, having delivered more than 500 million since 1957. But the popularity of the small signal transistor is waning; its functions are being assumed by segments of IC's which are performing larger, more complex, integrated functions. In a sense, by our very development of linear IC's, we have helped eliminate a major, profitable product line.

The signal transistor story is illustrative of one of the most challenging and rewarding, yet frustrating, aspects of the solid state business. It is evo-

lutionary at a startling rate, with changes induced by repeated improvements in materials, processes and design concepts.

We have been recognized for our technical leadership in several areas, with our image much stronger in power semiconductors than in IC's, simply because we did not enter the IC market until 1965.

In power devices, for example, we have sold more RF transistors and triacs than any other manufacturer. We marketed the first practical commercial silicon power transistor in 1962



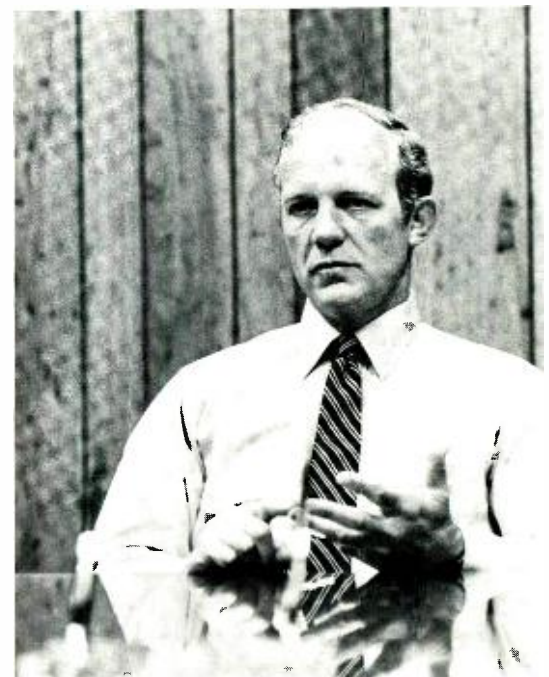
The
Engineer
and the
Corporation

and, that same year, were the first company to detail second breakdown ratings. In the latter area, only a few months ago we were the first semiconductor organization to disclose a practical rating system for evaluating thermal fatigue.

We invented the overlay transistor and the all-diffused SCR. And we have achieved several firsts for consumer electronic products. Two examples are transistors for the first commercial U.S. auto radios produced in volume, and transistors for power stages in the first volume-produced solid state phonographs. From the earliest days of

William C. Hittinger
Vice President and General Manager
Solid State Division
Somerville, New Jersey

graduated from Lehigh University in 1944 with the BS in Metallurgical Engineering. Mr. Hittinger was appointed Vice President and General Manager of the Solid State Division in April 1970. In this newly-created post, he has responsibility for all solid-state technology throughout the company. A veteran of almost 25 years in electronics, Mr. Hittinger had been President of General Instrument Corporation since March, 1968. Prior to that, he held a number of top executive positions with affiliated companies of the Bell Telephone System. Following service with the U.S. Army in World War II, Mr. Hittinger joined Western Electric Company in 1946 as a Materials Engineer. After two years with the National Union Radio Corporation, Hatboro, Pa., where he served as Production Manager of its Semiconductor Division, he joined the Bell Telephone Laboratories as a member of its technical staff. In 1957, he was named Director of its Semiconductor Device Laboratory and in 1962 became Executive Director of its Semiconductor Device and Electron Tube Division. In 1966, he was elected President of Bell-Comm, Inc., a company jointly owned by American Telephone & Telegraph Company and Western Electric Company which engaged in systems engineering for NASA's manned spaceflight program.



Reprint RE-17-2-23
Final manuscript received August 16, 1971.

solid state radios, record players, and TV's, we have been a dominant supplier.

We are strengthening our position now through our recent line of linear IC's, including op amps, that combine related functions of discrete parts into a single chip.

My greatest enthusiasm is for cos/mos which is beginning to challenge saturated logic in performance and in cost-effectiveness. Its low voltage and low power levels, its high noise immunity, and its interface compatibility with saturated logic should chase saturated logic right out of the ball park in many areas.

Clearly, RCA has been the chief mover of cos/mos technology since the David Sarnoff Research Laboratories announced the scientific breakthrough in 1963. We have strung together an impressive list of cos/mos firsts since then: *first* to introduce developmental types (1967), *first* to announce circuits capable of operating in the 6-to-15 volt range (1968), *first* to make available plastic packages (1970) and, last March, *first* to offer circuits operating in the 3-to-15 volt range. The reaction has been tremendous; we are being designed into many systems, and by last July we had already overbooked the number of custom circuits we had projected in our 1971 business plan. The cos/mos success still lies ahead, but we cannot help but react positively to the many indicators.

Our look at the future, I think, can be divided into three separate, but closely related and probably inseparable, areas: business and marketing considerations, circuit design, and material and process changes and refinements.

The changing marketplace

Our future has been fashioned to some extent by the past and the present, where the combination of semiconductor production overcapacity and a general depression in the entire economy created a severe roadblock for continued growth in the solid state industry. The birth and growth of solid state technology have become classics and, in some cases, legends, attesting to the success of free enterprise. Yet, the very factor that was so

essential to success in the industry's dynamic growth atmosphere—namely, overcapacity—severely hampered continued success when the economy turned down in 1970.

Despite current market conditions, the future is bright. U.S. plus export sales volume last year exceeded \$2 billion, with Latin America, the Far East, and Europe still offering great opportunities for market expansion.

Latin America

Latin America offers great challenge because its potential is virtually untapped. Market development will be slow, however, because the industrialization process lags behind other parts of the world. Full realization of the area's potential may not be achievable until the 1980's.

The Far East

In the Orient, Japan is an excellent market, despite the formidable competition of native suppliers and restrictive laws that hamper foreign competition. But the Far Eastern markets extend well beyond Japan, encompassing Australia, Taiwan, Singapore, Hong Kong, and the Philippines. Our production plant on Taiwan, where we assemble and test IC's, gives us a natural base from which we are and will continue to expand our international marketing activities.

Europe

Europe offers the greatest opportunities for overseas market development at this time. That is why we began production of semiconductor power devices in our new plant near Liege, Belgium, late last fall. That is why we have greatly expanded our basic applications and final testing operation at Sunbury-on-Thames, England. And that is why we have established a separate Solid State-Europe organization under Dr. D. J. Donahue to relate marketing, application engineering, production, and customer services in Europe. We recognize that we cannot compete against European semiconductor houses and overseas American operations unless we are on the scene, conversant with local needs and problems, and able to respond on that scene to those needs and problems.

Market selectivity

Despite all of the foregoing, we cannot be successful either domestically or internationally unless we adhere to a single criterion: selectivity. We must concentrate on areas of distinct leadership or uniqueness, such as power transistors, thyristors, and cos/mos. Or we must carefully enter market segments that offer significant returns on well-calculated investments such as linear IC's and semiconductor memories.

Power transistors

Our activity in power transistors is a case in point. Our amplifiers and high-current switches are acknowledged industry leaders. Yet we have looked to the future with our developmental types of hybrid power arrays that combine several functions. We now offer customers a much lower cost per function, or cost per watt, whichever may be his yardstick, by combining a number of power functions in a single package.

Linear integrated circuits

Linear IC's certainly represent another significant market segment. We have established ourselves as a major supplier to radio and TV manufacturers, and we are moving ahead in many industrial, commercial and consumer markets with the product line. The market was in the neighborhood of \$70 million in 1970 and, contrary to most of the market, was up from 1969. We expect the market to continue to expand, and we expect to grow with it, particularly in light of our op amp work.

Memory devices

Finally, we are busy developing solid state memory devices, which have a broad range of applicability. Mainframe use represents only one segment of the computer market, albeit a major one. But we do not intend to disregard other memory uses, such as industrial process and machine control units, small business computers, etc.

Design: how critical is it?

Cost per function has become so critical that we have entered a new era where custom design is becoming critical. By custom design, I mean using the basic elements of gain, logic, and

memory in unique ways. Conventional partitioning in computers offers an excellent example.

Computer design

Historically, a large mass storage and large logic often have had to communicate over long paths, thereby increasing complexity and costs. It is now very inexpensive to combine logic and memory in esoteric and innovative ways. Thus, we can get away from the concept of reducing cost per bit by increasing core memory size. Instead, we will restructure the computer to take advantage of our abilities to combine logic and memory, either at the chip or subsystem level.

Very clearly, IC's have pushed the interface between device and system to a higher level in the system hierarchy. Thus, instead of pushing systems designers into the background, as some people have implied, semiconductor technology is demanding a higher level of sophisticated interaction between device and systems designers.

Clearly, the device designer does not understand all of the problems. Let's look at memories and computer design as an example. The device designer does not know enough about partitioning of memory systems and subsystems, power distribution, or coding/decoding on a chip vs. on a subsystem level to solve the problems without a close, active interchange with the computer designer.

Automotive electronics

We also have many new markets opening to us. Perhaps the most immediate is automotive electronics, where safety, pollution, and even government pressures are causing drastic changes in the automobile. Yet, in the process we have been forced into a massive education program with the car builders because of their basically mechanical, rather than electrical, background. Not unnaturally, some automotive people have been puzzled how we can derive a reliable device when a manufacturing yield from a silicon wafer to final product can be 10 to 20%. They have always thought in terms of electro-mechanical components where scrap rates are kept very low by reworking defective units.

Cost is of paramount importance. Get-



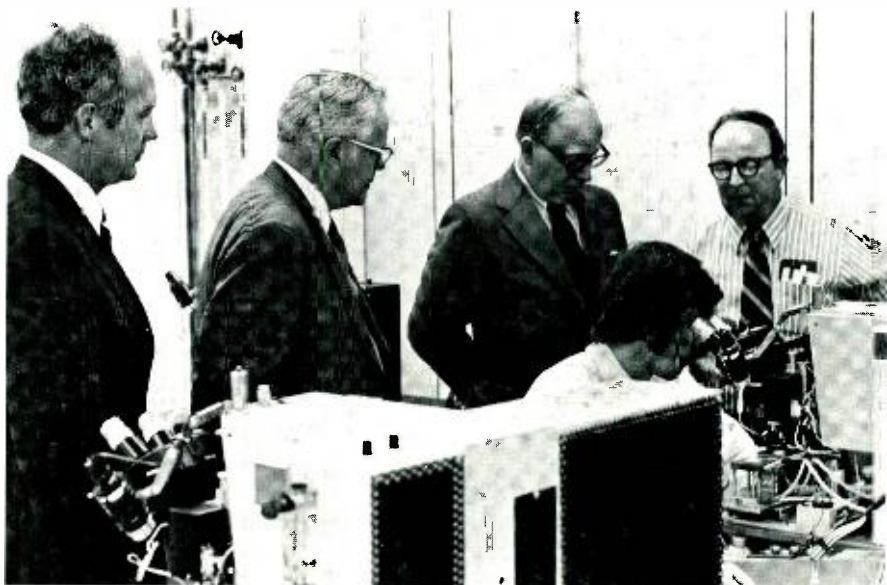
Ultrasonic bonding area for integrated circuit production at Solid State Division plant in Findlay, Ohio.



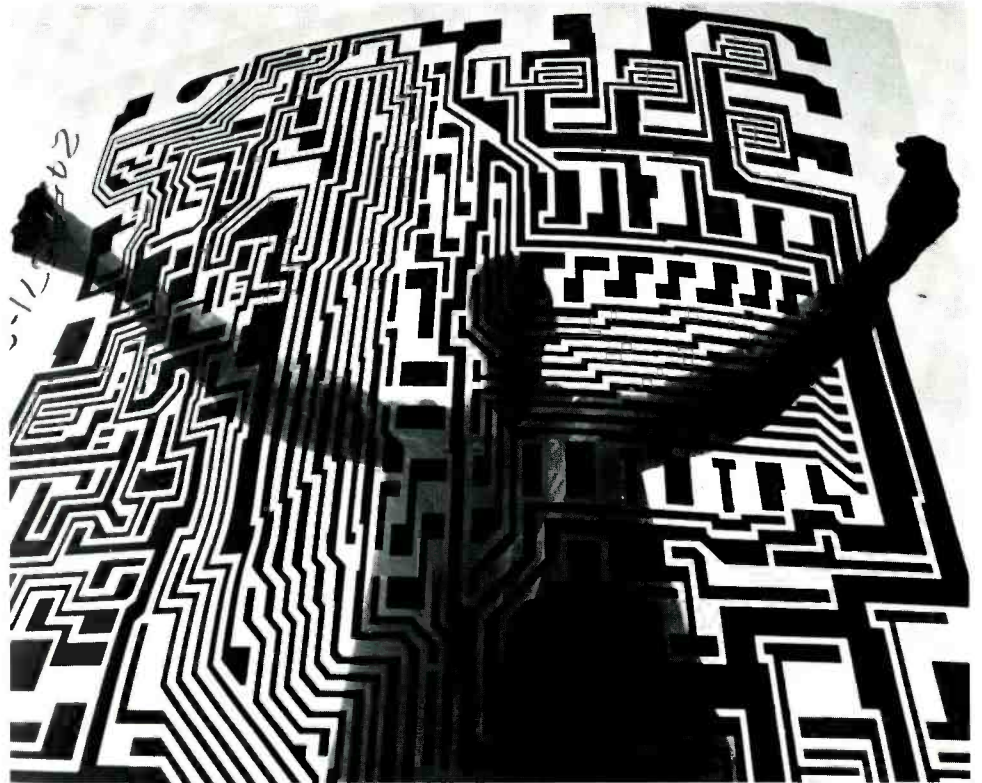
Production equipment sometimes combines functions. In this case one machine tests and sorts silicon rectifiers.



This computer controlled IC tester has 25 probes for specific tests and a 26th station to ink pellets which fail one of the tests.



Anthony L. Conrad, President of RCA, watches a beam lead bonding operation with William C. Hittinger, Vice President and general manager, Solid State Division; Dr. James Hillier, Executive Vice President, Research and Engineering; and William Grieg, Engineering Leader, Thin Film Technology.



This photomask will be reduced 500× prior to being reproduced by pattern generators.

ting better performance for slightly higher cost has been difficult to justify. In the same vein, redundancy has been totally alien; the benefits could not be rationalized against the competitive cost factor.

The combined impact of all the foregoing considerations has been hard. But we seem to have arrived. Automotive engineers have recently turned to solid state for solutions to electronic ignition (and therefore reduced exhaust pollution), fuel injection, anti-skid braking, obstacle detectors, passive restraint sensors, variable speed windshield wipers, drunk-driver detectors, antispin systems, automatic vehicle speed control, and the more prosaic applications of voltage regulators, alternators, radios and tape players. And this list of automotive applications is far from complete. We can now realistically see at least 100 solid state devices on every car by the end of this decade.

More applications

We see that same proliferation in other areas. The home, for example, is already being overwhelmed with solid state devices. Televisions, radios, and stereo players are being joined by electric coffee pots, ranges, washers

and dryers, blenders, mixers, dishwashers, toasters, heating and air conditioning units, burglar and fire alarms, light controls, and automatic door openers. We're doing it all with digital and linear ic's and with power transistors and thyristors.

Evolution of materials and processes materials

Packaging

Obviously, we simply must learn more about assembling and packaging to reduce the cost per function. That is why we have been striving so mightily with beam leads, sealed junctions, and film substrates. It is very clear, for example, that we simply cannot develop solid state memories by using existing techniques in bonding the literally tens of thousands of wires that would be required to build a 128-kilobyte computer memory. Nor can we afford the hermetic packages of these beastly 12-, 16-, 24- and yes, even 72-lead packages, which can cost anywhere from one to four dollars in extreme cases.

Materials

Semiconductor material, understanding and control has been a major factor in solid state progress. Germanium was the most widely used since its properties were well understood. To-

ward the end of the decade silicon began to emerge as a preferred material of the '50s.

It was more troublesome to work with than germanium because of its cantankerous nature. It was refractive, reacted at high temperatures with everything we tried to grow it from, and surface properties were very unpredictable. But we learned much about diffusion, oxide masking, and planar technology, which led to transistors with lower cost and higher performance than germanium devices, and then to integrated circuits in the 1960's.

The quest for new materials has continued. We are finding many that intrigue us with their potential. Yet, we are amazed by silicon's lattice as such an effective carrier for so much that we want to do. We understand the material, we now know how to produce it repeatedly and reliably, and we know how to modify its properties by the addition of elements in a variety of ways.

In the '70s, then, we must learn how we can better use silicon. In the past our interests have been primarily in silicon in bulk form. We start with large crystals and shape them to thinner and thinner substrates, discarding damaged material in the process.

We now know a great deal about depositing silicon directly in film form without going through the shaping steps. RCA's pioneer work in silicon on sapphire at the Laboratories has shown how to eliminate the unwanted parasitic losses in unessential bulk materials by using the silicon lattice only where we want it. We should refine ion implantation techniques—a somewhat controversial subject today. Ion implantation should become an important fabrication tool. The ability to deposit impurity elements where you want them, very closely controlled, and in distributions that might differ from the classic distributions inherent in diffusion, will be most important. Perhaps not as important as diffusion itself, but not far behind.

New materials

In terms of new devices, the basic silicon/insulator/metal structure, so important to MOS devices, will lead to new device structures. For example, N-MOS looks both attractive and interesting as a simple memory device.

However, it stresses the state of the art in that it requires very thin insulator layers with known, controlled properties. We can almost say that we must quickly learn a great deal about atom layers—the layers are almost that thin.

The question of other materials is most intriguing. Quite clearly, there is room for new materials. Gallium arsenide and its subsets, for example, should become increasingly important. How large their volume usage will become is problematic. These materials are now appearing primarily in special optical and microwave products. Beyond that we can only conjecture.

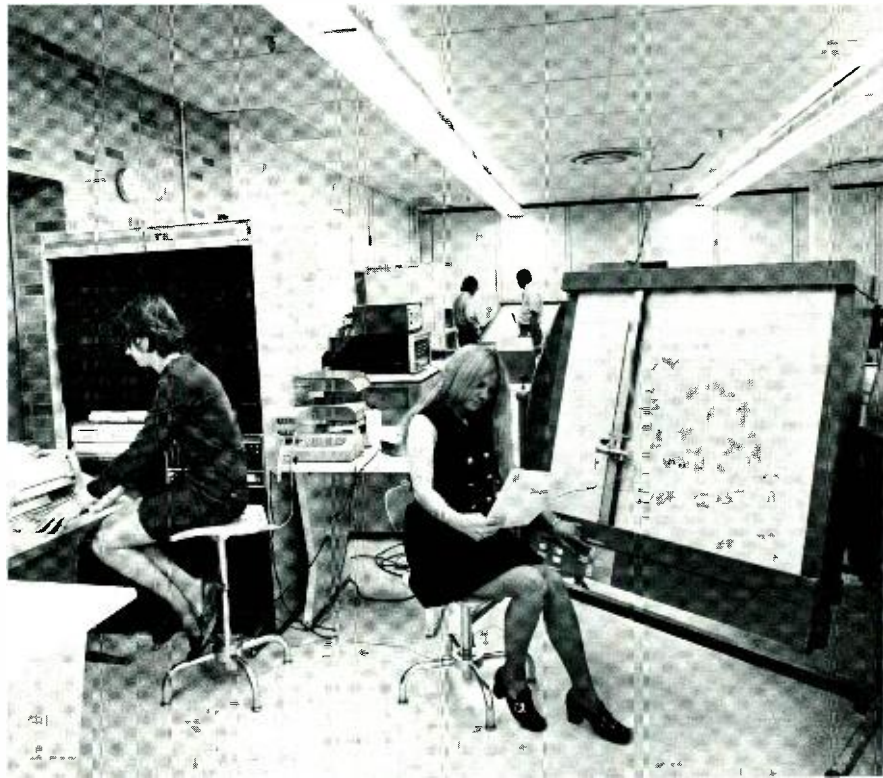
Liquid crystals are fascinating almost everyone, with their intriguing applications in displays, digital readouts, and timing devices. But liquid crystals and gallium arsenide complement, rather than replace, silicon. We therefore are expanding our store of useful materials rather than developing replacements.

We could continue with other materials that show promise—orthoferites, for example, with their property of "magnetic bubble" formation which

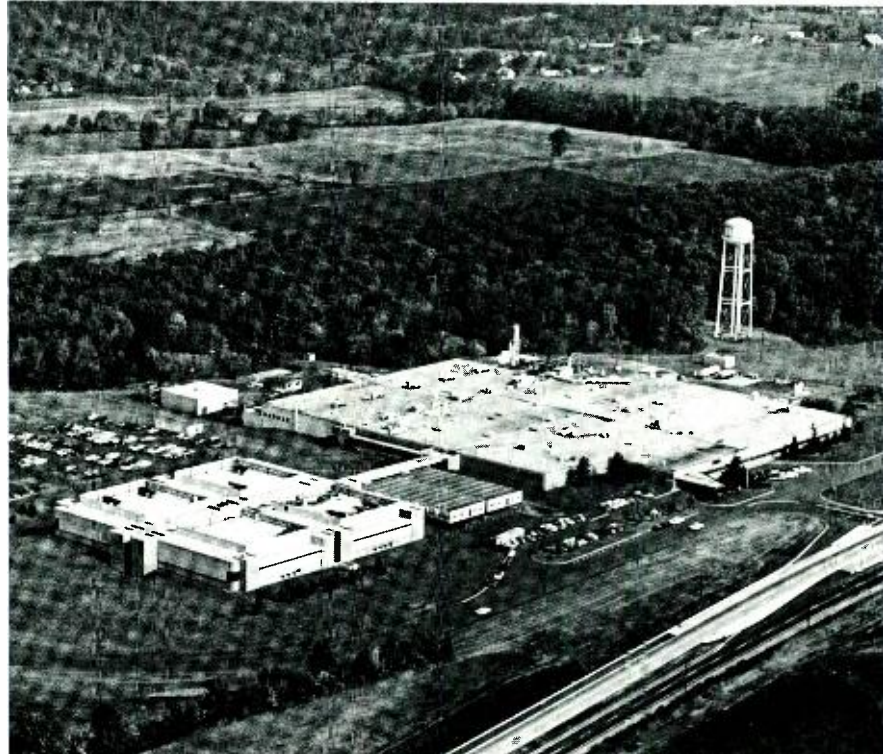
can be used to represent digital information. But such materials are too far down the road to see clearly where their true possibilities lie.

At this point in time, therefore, we

will continue to stress a combination of design, material, and process developments with perhaps our greatest concentration—and our greatest prospects for success—on silicon materials and processes during the 1970's.



Automated design facility uses digitizers and teletypes to feed photomask pattern data to computer in Princeton.

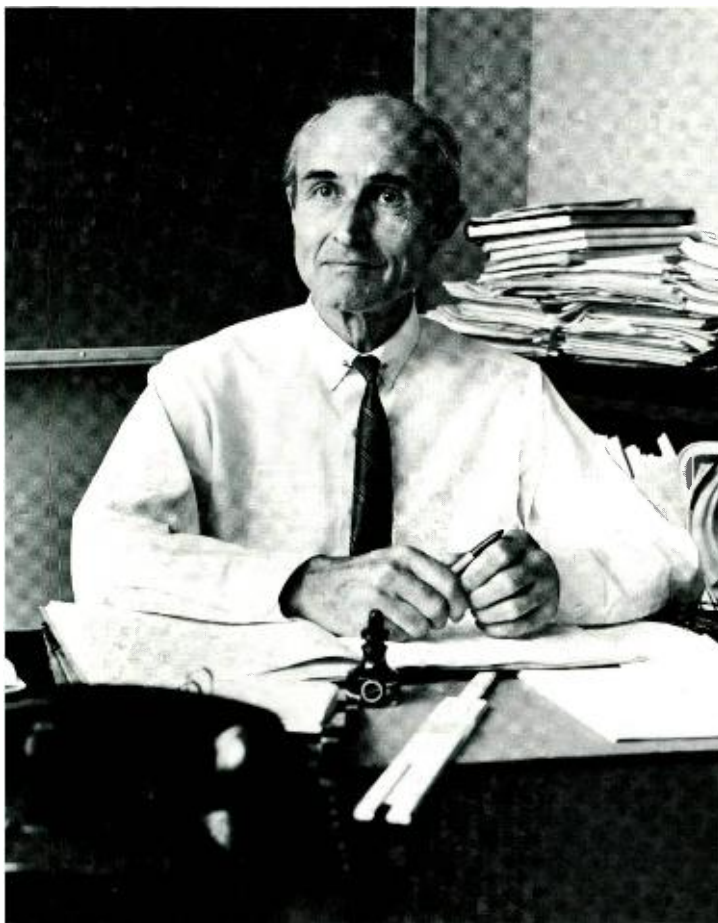


Solid State Division headquarters in Somerville, New Jersey.

Optics and electron optics as competitive and complementary technologies

Dr. E. G. Ramberg

Television became a practical reality when the electron beam became a replacement for the light beam. With the advent of laser technology, however, light optics has become competitive in areas which, for a while, appeared reserved to purely electronic devices. Computer memories and micro-machining and welding are better examples of this than are television displays. Electron optics has an unchallenged monopoly only in the recording of patterns with least resolvable elements that are small compared to the wavelength of light. The competition of optics and electron optics is, however, more than outbalanced by their complementary roles. This may be illustrated from all phases of television practice and is accentuated in some of the more recent developments.



Dr. Edward G. Ramberg, Materials and Device Research, RCA Laboratories, Princeton, New Jersey, received the AB from Cornell University in 1928 and the PhD in theoretical physics from the University of Munich in 1932. After working on the theory of x-ray spectra as research assistant at Cornell, he joined the Electronic Research Laboratory of RCA in Camden in 1935. He has been associated with the RCA Laboratories in Princeton since their establishment in 1942. He has worked primarily on electron optics as applied to electron microscopy and television, various phases of physical electronics, thermoelectricity, and optics. In 1949, he was visiting professor in physics at the University of Munich and, in 1960 and 1961, Fulbright Lecturer at the Technische Hochschule, Darmstadt. Dr. Ramberg is a Fellow of the IEEE and the APS and a member of Sigma Xi and the Electron Microscope Society of America.

THE SUBSTITUTION of the electron pencil for the light beam made possible the transmission of two-dimensional scenes in real time, with definition limited only by the normal visual limitations of the viewer. In brief, it brought television as we know it today. The design of the electronic apparatus for attaining this goal was facilitated by the recognition, expressed by William Rowan Hamilton over one hundred years ago, that the paths of material particles, subject to external force fields, obeyed the same mathematical laws as light rays in media of varying refractive index. Much later, Hans Busch¹ showed that free electrons in a vacuum, moving under the influence of axially symmetric electric and magnetic fields, were indeed converged by these fields in the same manner as light rays are converged by lenses. The analogy between the geometrical optics of electrons and light is best expressed by writing down the refractive index, n , of an electric and magnetic field for electrons. Its most general form is

$$n = \frac{mv}{m_0c} - \frac{eA}{m_0c} \cos \chi \quad (1)$$

$$= 1.978 \times 10^{-3} (V + 0.978 \times 10^{-6} V^2)^{1/2} - 587 A \cos \chi \quad (2)$$

Here m is the mass of the electron, m_0 its rest mass, v its velocity, c the velocity of light in vacuum, e the electron charge, A the magnetic vector potential

Reprint RE-17-2-13

Final manuscript received June 26, 1970.

of the field, χ the angle between the direction of the electron path and the magnetic vector potential, and V the electrostatic potential of the field (set equal to zero where the kinetic energy of the electron vanishes). The numerical coefficients are consistent with V measured in volts and A in webers/meter. Thus, knowing the electric and magnetic fields in which the electrons move, we can infer the effective refractive index of the medium, and Fermat's law

$$\int_A^B n ds = 0 \quad (3)$$

can be used to determine the path of an electron from an initial point A to a final point B in the same manner that the course of a light ray through a medium of varying refractive index might be determined.

We are not concerned, at this point, with the actual determination of the electron paths from known fields. Nor are we concerned with the prior problem of determining the electric fields from the potentials of electrodes, the magnetic fields from magnetic field measurements, or in the (unusual) absence of ferromagnetics, the magnetic fields from solenoidal current distributions. These constitute the art of the electron optician. We are, however, concerned with the differences between light and electrons, which have made the exploration of electron optics worthwhile.

Differences between light and electron optics

These are two. One of them is the ease of modulating electron-optical elements, by the simple modulation of electrode potentials or of magnetic-field generating currents. The effect of optical elements—mirrors, prisms, lenses—on a light beam can, on the other hand, only be altered by mechanical displacement or rotation. The difference can readily be illustrated quantitatively. Let an electron beam of cross section area A and accelerating voltage V be deflected through an angle α by an electrostatic field of length l . The energy required to establish the deflecting field is readily shown to be

$$E_d = 2 \alpha^2 V^2 \epsilon_0 A / l = 1.77 \times 10^{-11} V^2 \alpha^2 A / l \quad (\text{in MKS units}) \quad (4)$$

For a magnetic deflecting field we find instead:

$$E_m = (mV / \mu_0 e) (\alpha^2 A / l) = 4.5 \times 10^{-8} V \alpha^2 A / l \quad (5)$$

If a light beam of the same (square) cross section area A is to be deflected by a mirror within a deflection period t , the mirror (of mass M) must be given an angular velocity $\omega = \alpha / 2t$, so that the energy required for the deflection becomes

$$E_{m\text{ech}} = I \omega^2 / 2 = MA \alpha^2 / 96 t^2 \quad (6)$$

Compare the results for

$V = 20,000$ volts, $A = 10^{-4}$ m² (1 cm²), $\alpha = 0.5$ ($\approx 30^\circ$), $l = 0.05$ m (5 cm), $M = 10^{-4}$ kg (0.1 gram), $t = 6 \times 10^{-5}$ sec (period of horizontal television deflection)

We then find $E_{e1} = 3.5 \times 10^{-6}$ joule, $E_{mag} = 4.5 \times 10^{-5}$ joule, and $E_{m\text{ech}} = 0.29$ joule.

These numbers illustrate the tremendous advantage of electric or magnetic electron-beam deflection over mechanical light-beam deflection at high-frequency aperiodic deflection rates. In the television application, light-beam deflection could be made more suitable by using multifaceted mirrors of much greater moment of inertia (and hence stored kinetic energy) and by conserving kinetic energy from cycle to cycle. Even so, the great simplification resulting from electron-beam deflection in the cathode-ray tube was the first step toward practical home television reception.

The other important property of electrons compared with light is the possibility of increasing their energy by acceleration and, correspondingly, increasing the refractive index by a very large factor. For both light and electrons, the flux density j_1 in a spot formed by a source of flux density j_0 is limited by the Helmholtz-Lagrange relation,

$$\frac{j_1}{j_0} \leq \frac{n_1^2 \sin^2 \alpha_1}{n_0^2 \sin^2 \alpha_0} \quad (7)$$

Here n_1 and n_0 are the refractive indices at spot and source, respectively, and α_1 and α_0 are the beam divergence angles at these two points. For light, n_1 and n_0 are either equal or differ by a factor of the order of unity.

The electrons emitted by a hot cathode of absolute temperature T have a mean kinetic energy

$$2kT = T / 5800 \text{ electron volts} \quad (8)$$

As Langmuir² has shown, summing over the velocity distribution of the electrons, with a maximum emission angle $\alpha_0 = \pi/2$, translates Eq. 7 into the form

$$j_1 \leq j_0 (1 + eV/kT) \sin^2 \alpha_1 \quad (9)$$

Since, at the same time, the kinetic energy of the electron is increased, on the average, from $2kT$ to $2kT + eV$, the power density of the electron beam increases from P_0 to P_1 , with

$$P_1 \leq P_0 (1 + eV/2kT) (1 + eV/kT) \sin^2 \alpha_1 \approx j_0 V (eV/kT) \sin^2 \alpha_1 \quad (10)$$

By comparison, for a Lambertian light source and image spot in air or vacuum ($n_1 = n_0$; $\alpha_0 = \pi/2$) we find

$$j_1 \leq j_0 \sin^2 \alpha_1 = j_0 / (2F)^2 \quad (11)$$

where $F = 1 / (2 \sin \alpha_1)$ is the effective f-number of the lens forming the spot. Furthermore, since the power density is simply proportional to the photon flux density

$$P_1 \leq P_0 / (2F)^2 \quad (12)$$

Thus with light, the power density at the spot can never be larger than that at the source. For electrons, on the other hand, Eq. 10 prescribes an upper limit for the power density ratio P_1/P_0 which exceeds 10^6 , for $kT/e = 0.1$ volt (oxide cathode), $V = 25,000$ volt, and $\alpha = 10^{-2}$ radian (i.e., small enough that the aberrations of the electron-optical system need not be a severe limiting factor).

Let us consider this case more closely, applying it to the formation of an image on the screen of a cathode-ray tube, and compare the highlight brightness which we might achieve in this manner with that which we might realize by scanning a screen of the same size with a light beam derived from a high-intensity conventional light source.

Let the screen size be 30×40 cm (50 cm in diameter) at a distance of 25 cm from the deflection plane, at which point we assume the beam diameter to be 0.5 cm. To achieve the resolution required for a television display, the spot diameter must be $2r_s = 0.05$ cm. Eq. 9 can now be used to compute the spot current $i_s = \pi r_s^2 j_1$ for $j_0 = 1$ amp/cm², $V = 25,000$ volt, $kT/e = 0.1$ volt, and $\alpha = 10^{-2}$ radian and find

$$i_s \leq 50 \times 10^{-3} \text{ amp} \quad (13)$$

This is much larger than the spot currents realized in actual kinescopes, which are at best a few milliamperes. The spot enlargement due to space-charge repulsion within the beam in the drift space between the electron gun and the screen has not been included. As Schwartz³ has shown, the upper limit to the current in the spot prescribed by space charge can be written

$$i_{sp} = \alpha_1^2 V^{3/2} f(r_s/r_d) \quad (14)$$

Here α_1 is the convergence angle in the absence of space-charge repulsion (i.e. 10^{-2} , as before) and f is a universal function of the ratio of the spot radius to the radius of an effective beam-defining aperture at the gun, which we shall set equal to the beam radius in the deflection plane, making $r_s/r_d = 0.1$. Since $f(0.1) = 5 \times 10^{-3}$ amp^{1/2}/volt^{3/2} (as given by Schwartz's curve),

$$i_{sp} = 10 \times 10^{-3} \text{ amp} \quad (15)$$

Actual spot currents are somewhat smaller. This is due, in part, to the circumstance that an emission current density of 1 amp/cm² is not maintained over the entire emitting area of the cathode and, in part, to the fact that with the practical restriction imposed on gun dimensions, the adverse effect of electron-optical aberrations on beam concentration may be significant.

To remain conservatively within the realm of spot currents realized in practice, assume the high-light beam current to be 10^{-3} amp. The power dissipated in the screen then becomes 25 watts. For an aluminized white phosphor screen with a (practically realized) conversion efficiency of 15 candles/watt, a high-light brightness

$$B_s = 375\pi / (40) (30) (1.2) = 0.82 \text{ lambert} \quad (16)$$

can be obtained, without filterglass! The factor 1.2 in the denominator accounts for the blanking time.

Next we compute the high-light brightness which might be realized for the same dimensions of the screen, the spot, the beam diameter, and the distance between the deflection plane and the screen for an H-6 water- or air-cooled high-pressure mercury arc lamp as light source, with a maximum surface brightness of 30,000 candles/cm². If the (transmission) screen is perfectly diffusing and loss-free, its high-light brightness will be given by

$$B_s = \frac{1}{2} \frac{(30,000 \times 10^{-4}) (\pi 6.25 \times 10^{-4}) \pi}{(40) (30) (1.2)} = 0.64 \times 10^{-3} \text{ lamberts} \quad (17)$$

The factor 1/2 results from the fact that light is scattered backward as well as forward. The brightness could be increased in two ways: 1) by increasing the beam diameter in the deflection plane (at the cost of increasing the difficulty of maintaining the required spot size over the entire screen area and increasing the inertia of the scanning system) and 2) by using a directional screen, concentrating the light emission in the preferred viewing directions. However, these measures could not begin to overcome the indicated superiority factor of 10^5 of the electron-optical system.

Significance of laser technology

For high resolution displays

The preceding analysis would suggest that, in applications which demand high energy concentrations in small elements of area as well as rapid access to any element, light beams could not hope to compete with electron beams. This was, in fact, the situation before the advent of the laser and various technological developments which have accompanied its introduction. The laser beam can, in effect, be expanded or compressed by a telescopic lens sequence to the diameter desired in the scanning system and will then yield a focused spot with a diameter given, in rough measure, by

$$2r_s \cong \lambda / \sin \alpha_1 \quad (18)$$

For a single-mode argon laser with $\lambda = 515$ nm (2×10^{-5} in.) and $\alpha_1 = 10^{-2}$ radian we find, for our example, $2r_s \cong 0.005$ cm, which is much less than required. Thus the entire energy of the laser beam can be utilized for recording the picture. The high-light brightness achieved with the laser is thus given by

$$B_s = \frac{1}{2} \frac{P_L C \pi}{(40) (30) (1.2)} \quad (19)$$

where P_L is the laser power and C is the luminous efficiency of the laser light. As before, we assume a perfectly diffusing, loss-free screen. For $\lambda = 515$ nm we have

$$C = (0.6) (621) / \pi = 118 \text{ candles/watt} \quad (20)$$

We thus find from Eq. 16 that, to

match the high-light brightness of the electron-excited phosphor screen (0.82 lambert), the laser power must be 6.4 watts.

This would suggest that, for television displays, the laser represents a feasible light source, but that laser displays are scarcely competitive with cathode-ray tube displays. This certainly appears valid in the entertainment field. However, for special high-resolution displays, the great resolution reserve of the laser display can give it an advantage over the cathode-ray tube display.

For machining and welding

On the other hand, the laser is becoming increasingly competitive with the electron beam in another area, namely beam-machining and welding. The features most desirable for beam-machining—a very high concentration of energy on a small area in a very short span of time—may be achieved with electronically pulsed electron beams and with pulsed lasers. The upper limit to the peak power density achieved with either has been estimated at 10^9 watts/cm².⁴ The short time span reduces the total energy required to achieve a prescribed localized temperature rise and, hence, the extent of thermally induced structural changes in the surrounding material. The loss mechanisms for electrons and light differ greatly; they arise primarily from nuclear electron scattering in one instance and reflection and transmission in the other; hence the relative efficiencies of the two techniques also vary greatly from material to material. However, the basic mechanism for the removal of material is similar since it depends primarily on the thermal properties of the work piece.

The choice between the electron beam and the laser in machining and welding applications is thus commonly one of convenience. The simplicity of the laser equipment and the possibility of operating in any kind of atmosphere may often be the deciding factor. The avoidance of charging difficulties with dielectric materials and, in problems involving the machining of thin films (e.g., in microelectronics applications), the very small penetration of the laser beam into metallic materials can be additional advantages of the laser. Thus lasers currently find application in drilling diamond dies for wire

drawing,⁵ trimming resistors, balancing gyroscope rotors, and fabricating microelectronic devices.⁶

The electron beam, on the other hand, has the advantage that magnetic deflection permits precise programming and, hence, the cutting of precisely defined, complex patterns of arbitrary shape. It is also uniquely adapted for drilling with very high depth-to-diameter ratios, as exemplified by 0.013 cm holes in 1.3-cm-thick stainless steel plate, and for deep vacuum welds, as applied to airframe structures and nuclear fuel elements.⁷

Electron beams can, furthermore, be counted on to retain a monopoly in the recording of patterns with least resolvable separations small compared to the wavelength of light. For example, in the microrecorder, the controlled magnetic deflection of an electron beam has been used to record gratings of 23 lines/micron and printed matter with word lengths of the order of a half micron on thin films of collodion, carbon, beryllium, and photoresist.^{8,9} A special application of such a device is the preparation of zone plates for x-ray imaging.¹⁰ However, it has been shown that zone plates for soft x-rays can also be prepared by laser beam interference, provided that the resolution to be achieved does not exceed that attainable with the light microscope.¹¹

Rapid-access computer memories represent an interesting example of the transition from an electron-optical to an optical approach. The earliest such memories, exemplified by the Selectron,¹² the Williams tube,¹³ and the MIT Storage Tube,¹⁴ employed electron beams for element selection. These were presently replaced by magnetic core memories and other matrix memories in which electric pulses are used directly to store and read information, without the mediation of electron or light beams. For a discussion of more recent work on holographic memories, employing an optical approach to the problem, we refer to the paper of J. A. Rajchman which appeared in a previous issue.¹⁵

Optics and electron optics as complementary technologies

We have, so far, discussed optics and electron optics as competitors, with the

laser beam taking over, at various points, the functions of the electron beam. The more typical situation is that the two techniques complement each other, a familiarity with both being required for the most satisfactory solution of a given problem.

Many examples of this may be cited from the field of television. Here the basic signal-generating and display devices, namely, the camera tube and the kinescope, are both founded on electron optics. While there are alternatives which do not rely on electron optics, it is unlikely that they will challenge the dominance of the electron-optical devices for years to come. At the same time, the zoom lenses¹⁶ which form so prominent a part of most television cameras are obvious outward manifestations of the dependence of electronic television on optics; so are the modified Schmidt mirror systems¹⁷ of theater television projectors employing conventional kinescopes and the Schlieren projection optics¹⁸ of the light-valve television projectors. The optics of scattering media play a role in determining the grain size and thickness of phosphor screens.¹⁹

In present-day shadow-mask color kinescopes, the control of the deposition of the phosphor dots on the screen is an optical process which utilizes the optical simulation²⁰ of the electron paths in the finished tube to assure registration of the electron spots projected by the scanning beams with the appropriate phosphor dots deposited on the screen. In conventional color television cameras dichroic prisms, incorporating wavelength-selective interference filters,²¹ serve to separate the incident light into different chromatic components and to direct them to the appropriate camera tubes. Finally, in single-tube color cameras,²² interference filter gratings effect a separation of the color components in the output signal on a frequency basis—the quality of the color reproduction relying both on the precision of the optical filter gratings and the electron-optical sharpness of the scanning beam. These are only a few examples of the role of optics in current television practice.

An excellent example of the interplay of optical and electron-optical techniques is provided by the method of hologram motion picture recording

and play-back described by Hannan in an earlier paper.²³ Such complementary employment of electron-optical and optical methods, using each where it is most advantageous, can be expected to become increasingly general as their inherent advantages and limitations are more fully recognized.

References

1. Busch, H., "On the Operation of the Concentrating Coil in the Braun Tube", *Arch. Electrotechn.* Vol. 18 (1927) pp. 583-594.
2. Langmuir, D. B., "Limitations of Cathode-Ray Tubes", *Proc. IRE* Vol. 25 (1937) pp. 977-991.
3. Schwartz, J. W., "Space Charge Limitation on the Focus of Electron Beams", *RCA Review* (Vol. 18 (1957) pp. 1-11.
4. Anderson, J. F. and Jackson, J. E., "An Evaluation of Pulsed Laser Welding", *6th Electron Beam Symposium* (1964); Nuclide Corp., Medford, Mass.) p. 1.
5. Epperson, J. P. and Dyer, R. W., "The Laser Now a Production Tool", *8th Annual Electron and Laser Beam Symposium* (1966); U. of Mich., Ann Arbor, Mich.) pp. 187-204.
6. Smith, J. F., "Drilling, Trimming, Welding", *Laser Focus* (March 1969) pp. 32-37.
7. Nyenhuis, H. N., "Practical Application of Electron Beam Welding and Milling", *6th Electron Beam Symposium* (1964); Nuclide Corp., Medford, Mass) pp. 124-143.
8. Schief, R., "Television-Controlled Electron Micro-Recording", *Optik* Vol. 29 (1969) pp. 416-436.
9. Holl, P., "An Electronic Micro-Recorder of High Stability and Its Application", *Optik* Vol. 30 (1970) pp. 116-137.
10. Grote, K. V., Möllenstedt, G., Jönson, C., "X-Ray Optics and X-Ray Microanalysis," (Academic Press; New York; 1963).
11. Schmal, G. and Rudolph, D., "Efficient Zone Plates as Imaging Elements for Soft X-Rays", *Optik* Vol. 29 (1969) pp. 577-585.
12. Rajchman, J. A., "Selectron", *Mathematics Tables and Other Aids to Computation* Vol. 2 (1947) pp. 359-361; *RCA Review* Vol. 12 (1951) pp 53-97.
13. Williams, F. C. and Kilburn, T., "A Storage System for Use with Binary-Digital Computing Machines", *Proc IEE (London)* Vol. 96, pt. II (1949) pp. 183-202; Vol. 100, pt. II (1953) pp. 523-539.
14. Dodd, S. H., Klemperer, H., and Youtz, P., "Electrostatic Storage Tube", *Electrical Engineering* Vol. 69 (1950) pp. 990-995.
15. Rajchman, J. A., "Research in optical memories," RCA reprint PE-516, *RCA Engineer*, Vol. 16, No. 6 (Apr-May 1971).
16. Cook, G. H., "Television Zoom Lenses", *J. Soc. Motion Pict. Telev. Eng.* Vol. 68 (1959) pp. 25-28.
17. Bendell, S. L. and Neely, W. J., "Medium Screen Color Television Projection", *J. Soc. Motion Pict. Telev. Eng.* Vol. 67 (1958) pp. 166-168.
18. Baumann, E., "The Fischer Large-Screen Projection System", *J. Brit. IRE*, Vol. 12 (1952) pp. 69-78.
19. Nicoll, F. H., "Some Observations on Light Absorption of Powdered Luminescent Materials", *Preparation and Characteristics of Solid Luminescent Materials*, G. R. Ronda and F. Seitz, Eds. (Wiley; New York; 1948) p. 418.
20. Epstein, D. W., Kaus, Pa., and Van Ormer, D. D., "Improvements in Color Kinescopes Through Optical Analogy", *RCA Review* Vol. 16 (1955) pp. 491-497.
21. Widdop, M. E., "Review of Work on Dichroic Mirrors and Their Light-Dividing Characteristics", *J. Soc. Motion Pict. Telev. Eng.* Vol. 60 (1953) pp. 357-366.
22. Briel, L., "A Single-Vidicon Television Camera System", *J. Soc. Motion Pict. Telev. Eng.* Vol. 79 (1970) pp. 326-330.
23. Hannan, W. J., "Holographic movies for TV viewing," RCA reprint PE-478, *RCA Engineer*, Vol. 16, No. 1 (June-July, 1970).

Cathodochromic image display applications

Dr. I. Gorog

Cathodochromic materials have been used in image display and storage devices since the early 1940's. Recent efforts at the RCA Laboratories have led to new materials and devices which have improved both the display and the storage capabilities of these devices. Several of these improvements are described in this paper, and a two-way communication system that utilizes both the cathodochromic and the photochromic properties of certain materials is described.

Dr. Istvan Gorog, Head
Optical Electronics Research
Solid-State Research Laboratories
RCA Laboratories
Princeton, New Jersey

attended the University of California at Berkeley, where he received the BSc (1961), MSc (1962) and PhD (1964) in Electrical Engineering. In September 1964, Dr. Gorog joined the RCA Laboratories where his main areas of concern have been quantum electronics and electro-optical systems. His activities included gas laser research, holography, investigation of "pre-recorded video" recording and playback techniques, laser deflection, photochromic and cathodochromic devices and systems. Currently he is head of the Optical Electronics Research Group in the Solid-State Research Laboratory. During 1968, he was on leave of absence from RCA as a National Science Foundation Post-Doctoral Fellow in Frascati, Italy where he worked on laser related problems in plasma research. Dr. Gorog is a member of the American Physical Society and of Eta Kappa Nu.

IN A MANNER ANALOGOUS to photochromism, coloration can be induced in certain materials by electron-beam bombardment. To emphasize this analogy, the term *cathodochromism* is used in this paper to describe the latter phenomenon. Earlier literature employed various terminology, including calling the phenomenon of either electron-beam or x-ray induced absorption *tenebsesence* and the materials exhibiting it *scofophors*.¹ Cathode-ray tubes employing such materials have been called *skiatrons*,² *dark trace tubes*, or *color-center tubes*.³ Here we shall

Reprint RE-17-2-15
Final manuscript received April 27, 1970.



use *cathodochromism*, *cathodochromic materials* and *cathodochromic tubes*. Cathodochromism was first observed in alkali-halides at the end of the last century.¹ The first suggestion for a cathodochromic CRT was made by Rosenthal.² He proposed to use a thin layer of single-crystal alkali-halide as the screen material in a cathode-ray tube equipped with an off-axis electron gun and windows suitable for projecting light through the CRT screen. In the original proposal, this CRT was to be incorporated into a slide-projector optical system, thereby producing a high-brightness large-viewing-screen television display. It has been found, however, that the contrast achievable with single crystal alkali-halides is too small to be practical. During the Second World War, a systematic examination of various alkali halides revealed that, in terms of its absorption properties and sensitivity, polycrystalline potassium chloride was the most suitable CRT screen material for long-persistence-display applications.³ King and Gittins⁴ and Nottingham³ described operational radar display tubes employing polycrystalline *KCl*. In the system of King and Gittins, the tube was illuminated from the front and the reflective image projected onto the rear of a viewing screen. The image persistence was a function of the illumination level, temperature, exposure (charge incident per unit area), and rate of exposure of the CRT screen. Low contrast and brightness of the viewing screen were the chief limitations of this system.

In addition to the alkali-halides, a number of other crystals—e.g. *ZrSiO₄*, *CaF₂*, *BaTiO₃*—have been known for some time to be cathodochromic.⁶ The suitability of sodalite as a cathodochromic screen material was suggested by Ivey,⁷ and direct-view storage display tubes employing sodalite have been constructed.^{8,9}

Even though displays remain the most important practical application of cathodochromic tubes, a number of other interesting possible applications exist. For example, Fyler¹⁰ suggested the use of cathodochromic tubes for digital data storage. In Fyler's tube, the screen has a sandwich structure that consists of successive layers of phosphor, cathodochromic material, and a transparent resistive heater for

thermal erasure. Digital information stored in the cathodochromic layer is retrieved by detecting the intensity of the light emitted by the phosphor and passed through the cathodochromic layer.

At RCA Laboratories, cathodochromism has been the subject of extensive investigation during the past few years. The aims have been to improve material properties in terms of their cathodochromic sensitivity, erasability, and contrast and to study appropriate device applications. Important advances made by materials research include

- 1) The synthesis of *sodalite:Br* and *sodalite:I*, in addition to the well known *sodalite:Cl*;¹¹
- 2) The development of new methods of sodalite preparation that resulted in materials with very high contrast ratios;¹² and
- 3) The discovery of cathodochromism in double-doped *CaTiO₃*.¹³

In the device area, we have demonstrated

- 1) Improved projection¹¹ and direct view display-tubes;
- 2) Memory-and-display cathodochromic-phosphor combination tubes with grey scale capability;¹⁴ and
- 3) Two-way video systems (suitable for slow-scan transmission) employing a single cathodochromic tube for pick-up, storage, and display.

Mechanism of cathodochromic color switching

The mechanism of cathodochromic coloration can be understood in terms of a model, similar to the one employed for the explanation of photochromism, involving charge transfer between two centers. The only difference is in the details of the charge-transfer process. In photochromic switching, a free electron is created by the absorption of a quantum by one of the centers; the free electron is then captured by the other center. In cathodochromic switching, it is more plausible to assume that an incident high-energy electron creates a number of electron-hole pairs; the holes are captured by one of the centers and the electrons by the other. For both, switching involves the increase of the valence of one of the centers and the decrease of the valence of the other. The characteristic induced absorption band is primarily due to the center whose valence has been decreased.

According to Medved,¹⁵ the induced coloration in sodalite is due to an *F* center created by the capture of an electron at a halogen vacancy. The nature of the other center is unclear.¹¹ In *CaTiO₃*, the two centers are introduced by appropriate doping. For example, in *CaTiO₃:Fe,Mo* in the thermally stable state, iron is trivalent and molybdenum is hexavalent. Cathodochromic switching then involves the trapping of a hole by the trivalent iron, creating *Fe³⁺*, and the trapping of an electron by the hexavalent molybdenum, creating *Mo⁵⁺*. The induced absorption band is due to *Mo⁵⁺*.¹³ The bleaching process involves the removal of an electron from a *Mo⁵⁺* to the conduction band. The free electron thus created can be re-captured by either a *Mo⁶⁺* or by an *Fe³⁺*. The efficiency of the bleaching process is strongly dependent on the relative capture probabilities. As a general rule, high cathodochromic switching sensitivity for a given material implies low bleaching sensitivity and vice versa.

Applications of cathodochromic tubes

The oldest application of cathodochromic tubes is in displays. A direct-view cathodochromic storage display device has the following desirable features: contrast independent of light level, high resolution (resolution limited primarily by the electron-beam spot size), grey scale capability, and an inherent device simplicity that results in low cost. Cathodochromic projection displays have been also constructed.^{11,16} In a typical projection display, the cathodochromic CRT is placed into a Schmidt optical system of the type used for television projection. The tube face is illuminated by a bright light source located on axis, and the reflected light is collected by the optical system and projected onto the viewing screen.

A number of interesting applications exist for CRT's utilizing the phosphor-cathodochromic sandwich-screen structure described above. One of these is the electronic storage tube mode of operation mentioned earlier.^{10,11,17} Another is the possibility of displaying simultaneously rapidly varying "real time" information and slowly varying stored "background" information. Independent excitation of the phosphor and of

the cathodochromic layers can be accomplished by using different ultor voltages for the addressing of the two layers. The real time information can be displayed on the phosphor; "the background" information to be stored is written as a dark trace into the cathodochromic layer, with an ultor voltage high enough to penetrate through the phosphor into the cathodochromic. If the cathodochromic material used in this type of tube is also optically sensitive, then the stored information can also be entered into the cathodochromic by optically projecting it from an external source. A communication system utilizing the dual photo- and cathodochromic properties of some materials is described in greater detail in the following section.

Cathodochromic two-way video system

A two-way video system that employs a single cathodochromic CRT for the pick-up, storage, and display of pictorial information has been constructed. The tubes used for this application are built with phosphor-cathodochromic sandwich-screen structures. Video information is entered by first coloring the cathodochromic material uniformly by a constant-beam-current raster and then using a slide projector to project the pictorial infor-

mation on the screen. The information is bleached into the precolored screen and stored there. Transmission is accomplished by scanning a uniform raster on the phosphor with low beam current and low ultor voltage and using a photomultiplier to detect the phosphor light modulated by the absorption in the cathodochromic layer. When information is received, the cathodochromic tube functions in the ordinary reflective storage-display mode.

A block diagram of the system is shown in Fig. 1. (The system constructed accepts standard 30-frame/sec 15-kHz-line-rate tv signals. The potential for arbitrary scan rates, however, is obvious.) System operation is programmed by the *set-up, transmit, receive* switch. Set-up corresponds to the uniform coloring of the cathodochromic prior to optically entering information from the projector. The T/R relay switches either the input or the output end of the system to the main video cable (*composite video in/out*). *Video processor #1* and γ -corrector #1 together accomplish the correction for tube non-linearity and optional video polarity inversion on the input signal. (Note that a dark trace display device produces polarity inversion if driven by standard tv-type signal.) *Video processor #2* and γ -corrector #2 operate on the output signal. Era-

sure of the information stored on the tube face is accomplished by a bright light source not shown on the diagram. The cathodochromic tube is operated at 30 kV in the set-up and receive modes and at 20 kV in the transmit mode.

Cathodochromic tube

Four types of tubes have been studied in detail in conjunction with the system shown in Fig. 1. They are the three known cathodochromic sodalites: iodine, bromine and chlorine, and $CaTiO_3$ double doped with Fe and Mo . A detailed description of these materials can be found elsewhere.¹⁸ Because of its good relative cathodochromic sensitivity and high contrast ratio, combined with complete optical erasability, sodalite:iodine was found to be the best cathodochromic material for this application.

Standard 5-in. kinescope bottles were used. The screens consisted of 4 mg/cm², 10 to 20 μ particle size, sodalite:iodine deposited onto the inside of the faceplate using standard phosphor settling techniques. On top of the cathodochromic 1.4 mg/cm² sub 5 μ particle size $YAG:Ce$ phosphor was deposited. The screens were then aluminized (~1000 Å thick). The aluminum serves the dual purpose of ultor plate and optical reflector. The phosphor used has a fast flying spot type of decay characteristic and an emission spectrum that matches well the induced absorption spectrum of the sodalite.

In Fig. 2 the lower curve, SY-4, shows the cathodochromic sensitometric data for the tube used in the two-way system. The upper curve, SI-A, corresponds to a sodalite:iodine tube without phosphor. (Here *contrast ratio* is defined as the ratio of the light reflected from the uncolored screen to that reflected by the colored screen. All contrast measurements were made in white light illumination using a spot brightness meter with a spectral response corresponding to that of the average human eye.)

The high contrast achieved with the tube SY-4 is somewhat surprising. The penetration of electron beams into solids is governed by the Thomson-Whiddington law¹⁹

$$dV_x/dx = -b/2V_x \quad (1)$$

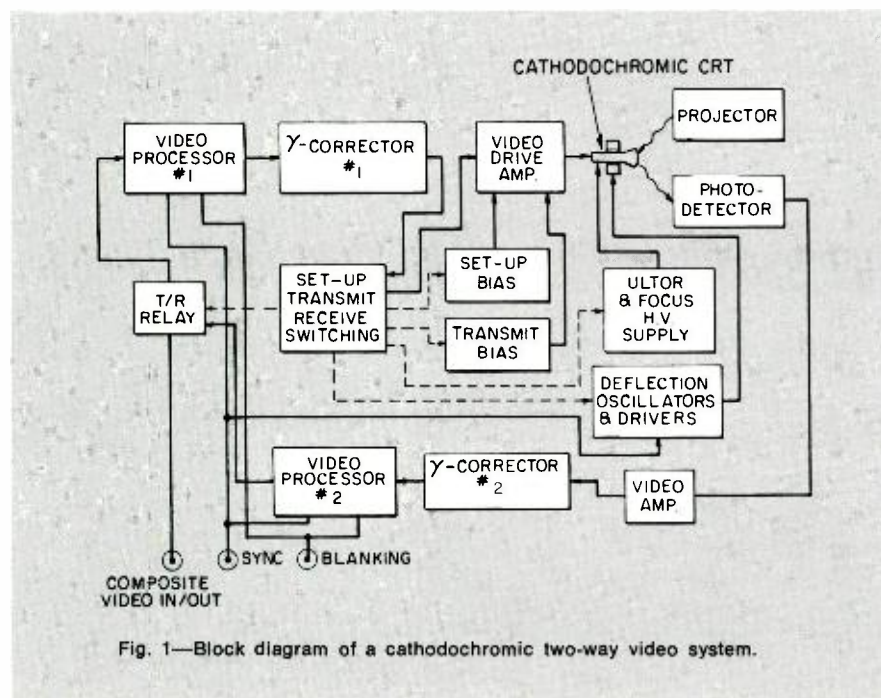


Fig. 1—Block diagram of a cathodochromic two-way video system.

where V_x is the beam energy, x is the thickness penetrated, and b is a constant proportional to the density of the solid penetrated. If x is written in units of mass thickness (mg/cm^2) and V in kilovolts, the value of b is $2.3 \times 10^{-3,20}$. According to Eq. 1 then, approximately 25 kV energy loss occurs in the 1.4 mg/cm^2 phosphor layer. Fig. 3 shows the exposure requirement for 2:1 contrast ratio on the tube SI-A having no phosphor layer. According to Fig. 3, approximately 20 kV of beam energy is required at the phosphor-cathodochromic interface to produce the coloration indicated by Fig. 1. The apparent anomaly may be explained in part by assuming a microscopically non-uniform distribution of the phosphor.

The persistence of the stored image depends on the ambient illumination and temperature. In a typical 10 foot-lambert room environment during the time interval 5 seconds to 100 seconds after exposure, the contrast decay can be approximated by an empirical relation of the form

$$CR = \alpha - \beta \log_{10} t \quad (2)$$

where CR is the contrast ratio, α and β constants, and t the time lapse since exposure. For example, in a given set of measurements, tube SY-4 yielded the following results: at $t=5$ sec, $CR=1.95$; at $t=10$ sec, $CR=1.75$; and at $t=100$ sec, $CR=1.43$. During the first few seconds, the decay rate is faster than Eq. 2 predicts; after approximately one hundred seconds, it is slower.

The tube resolution in the display mode is primarily limited by the electron beam spot size. If, however, the cathodochromic material is driven strongly into the contrast saturation region (see Fig. 2), the wings of the current distribution in the spot cause significant coloration, and the result is a loss in resolution. The resolution in the transmit mode of operation is determined by beam spot size, the screen thickness and uniformity, and the phosphor decay time. The limit on pick-up resolution is currently set by the high frequency noise caused by microscopic non-uniformities in the screen structure, primarily in the phosphor layer. In the display mode of operation, the image displayed on the cathodochromic screen is subjectively noise free.

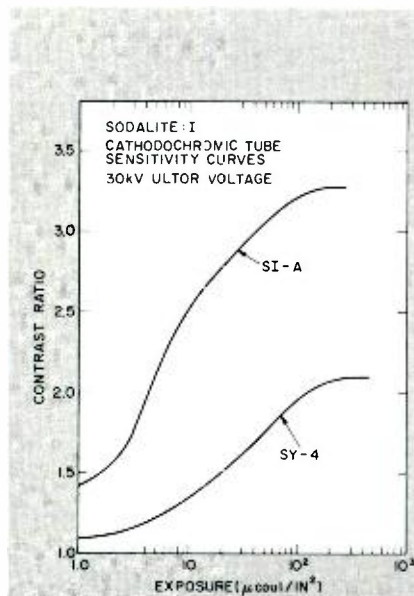


Fig. 2—Cathodochromic sensitometric curves for sodalite iodine tubes at 30-kV ultor voltage. Tube S-4 has a phosphor-cathodochromic-sandwich screen structure; tube SI-A has no phosphor in it.

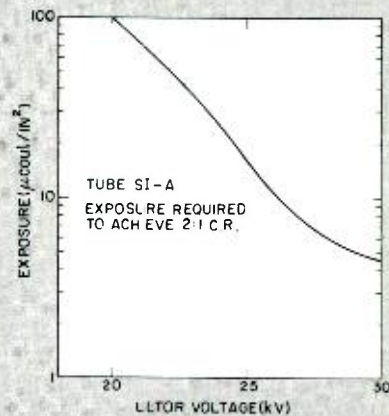


Fig. 3—Exposure required to achieve 2:1 contrast ratio in tube SI-A as a function of ultor voltage.

Conclusion

Cathodochromic tubes under current development are expected to find extensive applications in the area of data transmission, display, and processing. Utilizing the dual cathodochromic and photochromic properties of certain materials, information to be stored on the tube faceplate can be entered either electronically by writing with the electron beam or optically from an external scanned light source or projector. The stored information can be either viewed directly as a reflective display or extracted electronically by the flying spot scanning method. Long persistence cathodochromic tubes are excellent display devices for narrow bandwidth transmission channels. Cathodochromic page composers to couple electronic transmission links directly to holographic storage banks are within reality.

References

- Leverenz, H. W., *An Introduction to Luminescence of Solids* (John Wiley and Sons, Inc.: New York; 1950) p. 146.
- Rosenthal, A. M., "A System of Large Screen Television Reception Based on Certain Electron Phenomenon in Crystal," *Proc. IRE* Vol. 28 (1940) pp. 203-212.
- Nottingham, W. B., "Screens for Cathode Ray Tubes," *Cathode Ray Tube Displays*, MIT Radiation Laboratory Series, Vol. 22 (McGraw-Hill Book Co., Inc.: 1948) pp. 664-705.
- Early references are quoted in ref. 3 above.
- King, P. G. R. and Gittius, J. F., "The Skia-

- tron or Dark-Trace Tube," *J. of IEE* (London) Vol. 93, IIIA (1946) pp. 822-831.
- Leverenz, *op. cit.*, p. 312.
- Ivey, H. F., "Screen Material," U.S. Patent No. 2,752,521 (June 26, 1956).
- Phillips, W. and Kiss, Z. J., "Photo Erasable Dark Trace Cathode-Ray Storage Tube," *Proc. IEEE*, Vol. 56 (1968) pp. 2072-2073.
- Forrester, P. A., Marshall, D. J., McLaughlan, S. D. and Taylor, M. J., "Colour Centers in Sodalites for Storage Displays," North Atlantic Treaty Organization, *AGARD Conference Proc. No. 50* (1970) pp. 14-1-14-9.
- Fyler, N. F., "Cathode Ray Storage Tube Using a Dark Trace Layer and a Phosphor Layer," U.S. Patent No. 3,148,281 (September 8, 1964).
- Phillips, W., *Cathodochromic Projection CRT*, Final Report, Contract No. N00024-68-C-1173, U.S. Navy Ship Systems Command, Dept. of the Navy, Washington, D.C. (August 1969).
- Yocom, P. N. and Shidlovsky, I., *Private communication*.
- Kiss, Z. J. and Phillips, W., "Cathodochromism in Photochromic Materials," *Phys. Rev.*, Vol. 180 (April 15, 1969) pp. 924-925.
- Bosomworth, D. R. and Moles, W. H., *Cathodochromic Storage Device*, Final Report, Contract No. NAS 5-10636, Goddard Space Flight Center, Greenbelt, Maryland (April 1969).
- Medved, D. B., "The Optical Properties of Natural and Synthetic Backmanite," *J. Chem. Physics*, Vol. 21 (1953) pp. 1309-1310.
- Soller, T., Dressel, R. W. and Sherwin, C. W., "Mechanical and Optical Devices," *Cathode Ray Tube Displays*, MIT Radiation Laboratory Series, Vol. 22 (McGraw-Hill Book Co., Inc.: 1948) pp. 578-584.
- Kazan, B. and Kuoll, M., *Electronic Image Storage* (Academic Press; New York; 1968) pp. 182-185.
- Duncan, R. C., Faughnan, B. W. and Phillips, W., "Inorganic Photochromic and Cathodochromic Recording Materials," *this issue*. See also, Faughnan, B. W., Staebler, D. L. and Kiss, Z. J., "Inorganic Photochromic Materials," *Applied Solid State Science*, Vol. 11, Academic Press, New York (1971) pp. 107-172.
- Leverenz, *op. cit.*, p. 158.
- Pritchard, D. H., "Penetration Color Screen, Color Tube, and Color Television Receiver," U.S. Patent No. 3,204,143 (August 31, 1965).

Holographic recording in crystals

Dr. J. J. Amodei | Dr. W. Phillips | Dr. D. L. Staebler

This paper describes some of the latest advances in materials and techniques for storage of high efficiency phase holograms. The process relies on the electro-optic properties of crystals, such as lithium niobate or barium sodium niobate, and on the optical absorption and electron trapping characteristics of impurities and defects in the lattice. The latest materials combine good sensitivity with diffraction efficiencies that reach well over 50% for sample thickness of a few millimeters. The fixing techniques described in the paper offer the additional choice of non-destructive readout for images or other information stored in the material.

Dr. Juan J. Amodei, Solid State Research Laboratory, RCA Laboratories, Princeton, New Jersey, received the BSEE from Case Institute of Technology in 1956, the MSEE from the University of Pennsylvania in 1961, and the PhD from the University of Pennsylvania in 1968. Dr. Amodei began his career in 1956 with the Philco Corporation, where he worked on transistor radio developments. In 1957, he joined the Advanced Development Department of RCA's Industrial Electronic Products Division in Camden, N. J., where he developed a high-accuracy analog-to-digital converter, a novel pressure telemetering system for medical applications, and a high resolution sampling oscilloscope system that later became a product. He transferred to RCA Laboratories in 1959, working on the development of high-speed computer circuits and subsystems. He later became engaged in research and development of integrated circuits. Since 1966, he has been working in the investigation and development of materials and devices for optical information storage. The work included research on the optical storage properties of doped and pure $SrTiO_3$ crystals, and the study of magneto-optic and metallic thin films for holographic storage. In 1967, he developed an analytical model for electron migration effects in photochromic materials that led to the proposal of an electro-optic holographic storage device. He presently has responsibility for a program aimed at developing better materials and techniques for high-sensitivity, erasure-resistant electro-optic storage systems. Since 1962, Dr. Amodei has been a lecturer at LaSalle College in Philadelphia, where he has been Chairman of the Electronic Physics Department of the Evening Division since 1967. He has authored or co-authored 30 technical papers and has more than 20 U.S. patents issued or pending. Dr. Amodei is a member of the American Physical Society, the IEEE, and Eta Kappa Nu.



Left to right, authors Amodei, Phillips, and Staebler.

Dr. William Phillips
Solid State Research Laboratory
RCA Laboratories
Princeton, New Jersey

received the AB in Physics from Columbia University in 1958. He did graduate work at the Carnegie Institute of Technology, receiving the MS in Physics in 1961 and the PhD in Electrical Engineering in 1964. He joined the technical staff of RCA Laboratories in 1964, and from 1964 to 1967 was engaged in research on the synthesis and properties of crystalline materials for laser applications. In 1967 he became involved in work on the synthesis and evaluation of photochromic, and later cathodochromic, materials. He received RCA Laboratories Achievement Awards for this work in 1968 and 1970, and shared in an IR-100 Award for development of the cathodochromic CRT in 1969. Dr. Phillips is currently engaged in research on improved materials for volume holographic storage. He has authored or co-authored nine technical articles and has two patents pending. Dr. Phillips is a member of the American Physical Society, the IEEE, the American Ceramic Society and Sigma Xi.

Dr. David L. Staebler
Solid State Research Laboratory
RCA Laboratories
Princeton, New Jersey

received the BSEE with Distinction and the MSEE from the Pennsylvania State University in 1962 and 1963 respectively. He then joined RCA Laboratories and worked with narrow band phosphors, laminated ferrite memories, and injection diode lasers. In 1964, he began studies on oxidation-reduction processes in gamma-irradiated rare earth doped fluorites. This work led to his subsequent investigation of photochromic behavior in CaF_2 . In 1966, he entered Princeton University, receiving a PhD in Electrical Engineering in 1970. His doctoral research involved optical studies of photochromic CaF_2 and resulted in the identification of a general class of rare earth associated color centers in CaF_2 . Upon returning to RCA Laboratories, he has worked on electric field coloration of transition element doped titanites, and is now involved in the study of electro-optic materials for holographic storage. Dr. Staebler is co-author of a number of technical papers including a chapter on photochromics in a forthcoming issue of *Applied Solid State Science*. He is a member of Eta Kappa Nu, Sigma Tau, Tau Beta Pi, and the IEEE.

THE POTENTIALLY HIGH INFORMATION STORAGE DENSITY of optical techniques has received so much publicity in the past few years that it scarcely requires further review. The great promise of this technology is that the information packing density is theoretically limited only by the wavelength of light, and figures of 10^{22} bits/cm³ are often loosely quoted by workers in the field. These astronomical storage densities are obviously far from practical for the present or near future, but nevertheless offer the incentive to improve the areas of technology that could make these techniques useful. One of the most important areas in need of further development is that of storage media suitable for holographic recording, and one approach to this problem is the subject of this paper.

The storage of information in a medium that operates on the phase rather than the amplitude of the light traversing it has long been recognized as the more efficient process. Phase modulation of the wavefront permits reconstruction efficiencies of nearly 100%, as opposed to about 6% for amplitude type of holograms where the light is modulated through absorption. Many different types of phase holographic storage media have been investigated in the past, ranging from dichromated gelatin that gives up to 90% efficiencies when properly developed, to reversible *MnBi* films² whose efficiencies are below 0.1% but offer the important feature of reversibility.

An additional advantage of thick phase-holographic storage media is that their high angular selectivity permits random access of holograms within a given volume by simply changing the angle of the readout beam. That is, changing the angle of incidence by a few tenths of a milliradian is sufficient to permit a switch from one hologram to the other. There is no need for separating spatially the two beam positions, such as is the case when reading thin holograms, because the holograms that were recorded at different angles do not meet the Bragg condition for reconstruction and thus do not interfere.

Reprint RE-17-2-8

Final manuscript received May 21, 1971.

The work described in this paper was supported in part by the Naval Air Development Center, Department of the Navy.

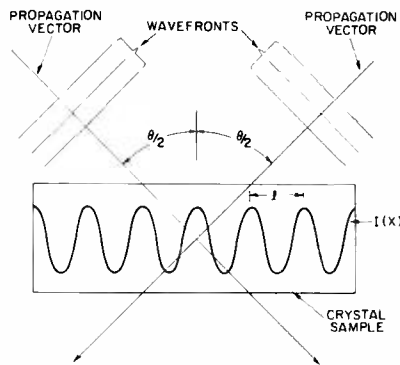


Fig. 1—Schematic description of a plane-wave interfering pattern.

This paper describes the mode of operation and the latest advances in the new field of electro-optic holographic storage—an approach that was demonstrated only a few years ago and which shows promise of becoming a most serious contender for many storage applications. This approach represents the only type of holographic storage that combines very high efficiency with reversibility. In addition, newly developed materials have reached very useful levels of sensitivity, and techniques have been worked out that make possible the fixing of holograms for non-destructive readout.

Principles of Operation

Pattern storage

High efficiency holographic storage in electro-optic crystals of lithium niobate and lithium tantalate was first reported by Chen, LaMacchia and Frazer in 1968.¹ The phenomenon relies on the migration and subsequent retrapping of electrons that have been excited from localized centers by the light.

To clarify the details of the process, it is best to use the example of the simplest form of holographic pattern—the sinusoidal grating. This type of grating is formed when a linear medium is exposed to the interference pattern created by the superposition of two coherent plane waves intersecting within its volume. Since through Fourier decomposition any arbitrary pattern can be thought of as the superposition of sinusoidal patterns, the results obtained by using this simplified picture are quite general. The intensity pattern created by the intersection of two coplanar coherent plane waves of light within the crystal is sinusoidal and is

ELECTRO-OPTIC MEDIUM

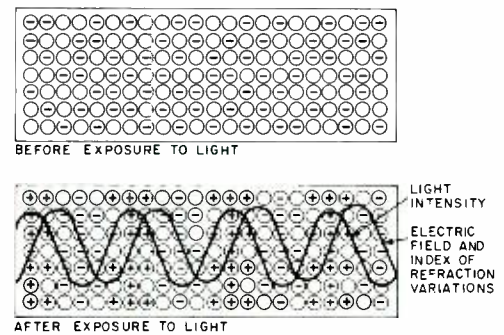


Fig. 2—Pictorial representation of hologram storage by diffusion of photogenerated free electrons.

shown in Fig. 1. If both beams make an angle $\theta/2$ with the normal to the surface, the intensity-interference pattern, which varies only along one direction, x , can be written as:

$$I(x) = I_0 (1 + m \cos Kx) \quad (1)$$

where I_0 is the average level of intensity; m is the modulation ratio ≤ 1 ; $K = 2\pi/l$; $l = \lambda/2 \sin(\theta/2)$; and λ is the wavelength of the light.

The essential features of the storage process are shown in Fig. 2. A pictorial representation of the crystal containing localized traps (e.g., impurity centers, vacancies, or other defects) is shown at the top of Fig. 2. Some of the localized states are assumed to contain optically excitable electrons, the remaining ones should be empty so that they may act as traps to allow for redistribution of the charge. All the traps are assumed to be thermally stable and charge neutrality exists throughout the volume before it is exposed to light. When the light-interference pattern is applied as shown in Fig. 2b, its effect is to generate a free electron concentration of the same shape in the conduction band. In the absence of an electric field, these electrons will diffuse from the regions of high intensity of the light-interference pattern and into the regions of low intensity. This net migration and subsequent retrapping gives rise to a space charge and accompanying electric field. The polarity of the charge and the resulting field are illustrated in Fig. 2b. The space charge build-up continues until the field completely cancels the effect of diffusion and makes the current zero throughout. At this point, the equilibrium space-charge field produced by a

sinusoidal light-intensity pattern can be shown to be:²

$$E(x) = (kT/q) mK [\sin Kx / (1 + m \cos Kx)] \quad (2)$$

where k is the Boltzman constant; T is the temperature; and q is the electronic charge.

A similar effect can take place when there is a strong DC electric field, that is either applied externally or generated internally in ferro-electric crystals.^{3,4} If this field is very large compared to the fields that can be generated through thermal diffusion, the space-charge field that builds up through drift remains sinusoidal as long as its magnitude is considerably smaller than the applied field and is given by:⁵

$$E(x) \approx -E_0 \cos Kx \quad (3)$$

where E_0 depends on the exposure time and material parameters.

If the material has a high linear electro-optic coefficient, its index of refraction would be modulated in accordance with the electric field. It follows, therefore, that exposure to a light interference pattern would result in variations in the index of refraction that would approximate the shape of the light intensity pattern, and the changes would persist as long as the space charge remains in its place.

Record and readout processes

The processes of recording and reading out a hologram of a given image in a crystal medium are illustrated in Fig. 3. Recording is achieved by exposing the crystal to the interference pattern of a reference beam and a beam that has either been reflected from an object or has traversed a transparency of the object. Readout is accomplished by exposing the crystal to the reference beam only, which in turn gets diffracted by the pattern stored in the crystal, and reconstructs the object beam with the image pattern that it contained.

For the case where there is no absorption and the beams are arranged as described above, the holographic efficiency of a sinusoidal grating is:⁶

$$\eta = \sin^2 (\pi n_1 d / \lambda \cos \theta / 2) \quad (4)$$

where n_1 is the peak value of the assumed sinusoidal variation in index of refraction, and d is the thickness of the medium.

For grating thickness of 1 cm, the above formula shows that a diffraction

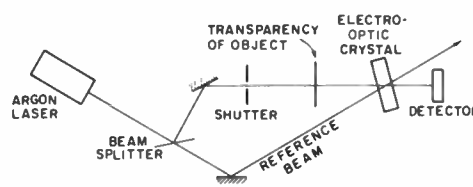


Fig. 3—Experimental setup for recording and reading out holograms in thick single crystals of electro-optic materials.

efficiency of 100% can be obtained with values of n_1 in the range of 10^{-5} , which requires fields of a few thousand volts per centimeter in materials such as lithium niobate or barium sodium niobate.

The actual modulation of the light by the stored pattern is due to the electro-optic effect of the intrinsic crystal, but the formation of the field and all the other performance characteristics depend on the properties and concentration of the localized centers. The impurity or defect concentration that is needed to support a given field intensity can be calculated easily for a sinusoidal field distribution and is given by:⁵

$$N = 2\pi \epsilon E_0 / gl \quad (5)$$

where ϵ is the static dielectric constant of the material.

For a peak field of 10^4 V/cm, a fringe spacing $l = 10^{-4}$ cm, and a relative dielectric constant of 30, the minimum trap concentration would be:

$$N \approx 10^{16} \text{ cm}^{-3} \quad (6)$$

Unless the trap density is considerably larger than the minimum required to sustain the desired field as given by Eq. 5, the resolution of the material will be trap-limited. That is, the minimum fringe spacing, l , at which a given diffraction efficiency can be maintained will be restricted by the inability to develop sufficient space charge to support the field.

In addition, the sensitivity (i.e. the incident light energy needed to reach a certain diffraction efficiency) is determined by the concentration and absorption cross section of the electrons in the impurity centers and by the quantum efficiency of the process. The quantum efficiency is a function of the average number of times that an electron must be re-excited before it migrates the required distance. If one assumes unity quantum efficiency, a theoretical maximum can be calculated for the light energy required to reach

100% diffraction in a given material. The minimum amount of light energy that needs to be absorbed works out typically to be around 0.1 to 1 mJ/cm². The best measured value so far has been 1 J/cm² of incident light energy, to achieve 40% diffraction efficiency in iron-doped lithium niobate. Crystals of lithium niobate, as grown, exhibit storage effects but with very low sensitivity, of the order of 500 J/cm². This is due to the low concentration and optical absorption of the intrinsic defects or residual impurities that are responsible for the effect. Other materials, such as barium sodium niobate, exhibit negligible storage effect when grown undoped.

Since the concentration and type of impurities play such a crucial role in the performance of the crystal, our materials development program put major emphasis on experimenting with different types and concentrations of impurity ions and induced defects. The methods used included irradiation with X-rays and gamma-rays, and doping during growth with a variety of impurities. Most of the work was carried out with lithium niobate and barium sodium niobate.

Effect of radiation on storage

Exposure of most materials to high energy electromagnetic radiation, such as X-rays or gamma-rays, is known to produce defects in the lattice. This occurs when intrinsic ions in their normal lattice sites are dislodged into interstitial positions. The resulting vacancy and the interstitial atom are both sources of localized states that can harbor or trap electrons. If their energy depth is sufficient so as to be thermally stable, and if the electrons trapped in such states can be excited into the conduction band by light of a convenient wavelength, these defects can improve the optical storage properties of the material.

Samples of lithium niobate were irradiated with 40-kV X-rays and with 1.2 MeV gamma-rays with qualitatively similar results. The latter is preferred because of its longer penetration depth. The fact that gamma-irradiation generates localized centers which have absorption in the visible is illustrated by the two curves of Fig. 4. They show the optical density of a 0.3-cm sample a) before and b) after irradiation. The dosage was about 10^6

rads of 1.2 MeV gamma-rays from a cobalt source.

The large improvement in sensitivity and diffraction efficiency achieved through the gamma-irradiation is illustrated in Fig. 5. The curves show a comparison between the recording rates of grating holograms in the sample, before and after gamma-irradiation. The test used an Argon laser operating at 4880 Å with a power density of 0.6 W/cm²; the grating spacing was 10⁻⁴ cm. The sample was aligned with its *c*-axis horizontal and perpendicular to the bisector of the two beams; the polarization of the beams was horizontal also. The improvement in sensitivity is seen to be about 20/1 and the diffraction efficiency after 10 minutes of recording is about 10 times higher in the sample after irradiation.

Radiation treatment of barium sodium niobate did not result in significantly improved storage performance. It appears that the traps induced by irradiation in this material are too shallow in energy to give useful storage times.

Improvements through impurity doping

While the radiation treatment was

shown highly effective in improving the performance of the materials, it is largely limited to a single type of center. Impurity doping during growth of the crystal, on the other hand, gives a much wider range of centers from which to choose. A variety of dopants were tried in lithium niobate and barium sodium niobate, many with good and some with remarkable improvements of the storage properties of the crystals.

Iron was found to be the most effective of the dopants tried in both materials, with improvements in sensitivity of lithium niobate of more than two orders of magnitude. With iron doped lithium niobate diffraction efficiencies of 60% in a 0.25 cm thick sample were achieved, and the exposure required to reach 40% diffraction efficiency was only 1 J/cm².

Barium sodium niobate, which shows little or no storage effect in its nominally pure form or even after irradiation, also becomes an excellent storage material when doped with iron or iron and molybdenum. The curve in Fig. 6 shows the performance of a 0.3-cm sample of barium sodium niobate doped with iron and molybdenum,

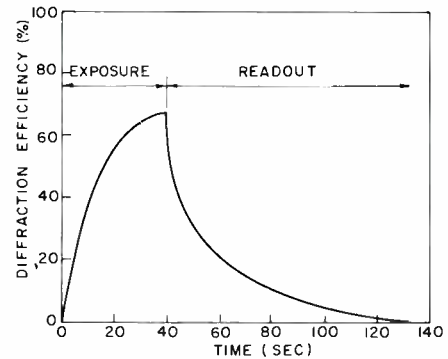


Fig. 6—Diffraction efficiency vs. time during recording and readout in a 0.3 cm Ba₂NaNb₅O₁₅ sample doped with 0.036 w/o Fe and 0.002 w/o Mo.

which was grown by Dr. A.W. Stephens and A. Cafiero. Based on the above results, it appears that these dopants provide the right type of centers for enhancing this phenomenon in a wide variety of host lattices, and other electro-optic crystals are now being tried.

Fixing techniques

To take full advantage of the features of volume recording, it is often necessary or at least highly desirable to have nondestructive readout capabilities. The electro-optic storage process described above produces a hologram that erases optically unless longer wavelength light is utilized during readout. Unfortunately, because of the nature of thick holograms, readout at a different wavelength is difficult to implement without introducing distortion. In an effort to find a solution to this problem, we investigated techniques of "fixing" the holographic pattern in the electro-optic material. The basic idea behind the various schemes that were tried consists of using the optically generated field to produce a more stable pattern through drift or reorientation of ions, vacancies, or impurity complexes that had been made temporarily mobile. Some of the possible mechanisms for achieving this effect are the following: recording during or immediately after high-energy irradiation, exposure to high-energy irradiation after recording, and heating above the threshold temperature for ionic or vacancy migration during or after recording.

The high energy radiation techniques have so far been successful only when recording immediately after gamma-

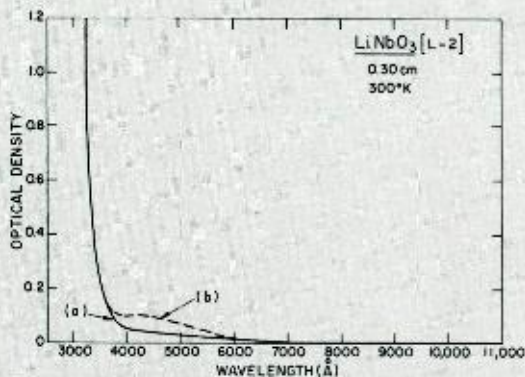


Fig. 4—Absorption spectrum of a LiNbO₃ sample (a) untreated and (b) after γ -ray irradiation.

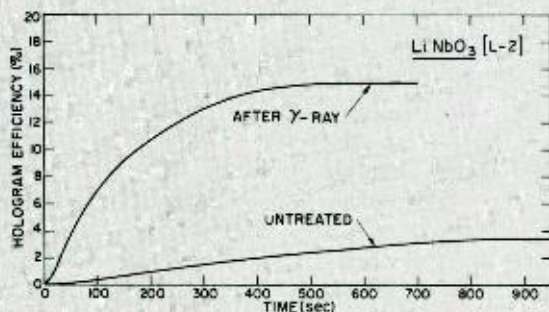


Fig. 5—The effect of the γ -irradiation on the hologram storage in the same sample. This shows the diffraction efficiency during exposure to both beams.

irradiation. Here, presumably, the "fixing" is due to short lived ionic defects that are mobile enough to rearrange themselves under the influence of the holographic field. Irradiation with gamma-rays after recording, on the other hand, caused the holographic pattern to disappear and no fixing was observed. This was probably due to fast erasure of the electric field by the large number of electrons freed by the irradiation. Recording while the sample is being irradiated has not been tried yet because of the experimental complexity involved.

Thermal fixing techniques⁷ have been the most successful and consist simply of heating the crystal for 20 to 30 minutes to 100°C during or after recording. Because the activation energy for ionic or vacancy motion appears to be lower than that for exciting the trapped electrons, it is possible to allow ionic migration without erasing the electronic pattern constituting the hologram. The sequence for the formation of a fixed hologram starts with the creation of a space-charge pattern due to the optically excited electrons. Subsequent heating increases ionic mobility allowing the ions to drift and neutralize the "electronic" space charge. At this point the hologram is nearly erased but it is quickly brought back by exposure to readout light, that has the effect of redistributing the electrons evenly over the volume. This leaves the ionic space charge unneutralized, and since the ions are not excited by the light, the new pattern is resistant to optical erasure. The curves in Fig. 7 show the decay during readout of a normal hologram in lithium niobate (curve A) and the build-up of diffraction efficiency of a hologram



Fig. 8—Photograph showing actual reconstruction of a fixed hologram in $LiNbO_3$.

fixed by heating in the same crystal (curve B). The higher diffraction efficiency of the fixed pattern is due to a self enhancement effect where the fixed hologram creates an additional electronic pattern that increases the field. This effect is described in more detail in a previous publication.⁷ The photograph in Fig. 8 shows the reconstruction of one of several holograms stored and fixed in a gamma-irradiated $LiNbO_3$ crystal. The converging beam coming in from the left is the reference beam being used for readout. Besides the reconstructed object beam projecting the image, the photo shows the transmitted (undiffracted) reference beam and the reflected part of the reference beam.

Similar fixing results were obtained with doped barium sodium niobate crystals, indicating that the technique is likely to be widely applicable to a variety of materials. The process is

made even more attractive by the fact that it is reversible. A thermally fixed hologram can be erased by either heating the crystal to 300°C, or by heating to 100°C while exposing it to uniform light of the proper wavelength to excite the trapped electrons, and the storage process can then be repeated.

Conclusions

The electro-optic storage phenomenon has always appeared to be a potentially attractive approach for holographic storage. Improvements in material performance over the last year have changed considerably the practical outlook and competitiveness of these media. For any given level of diffraction efficiency, the sensitivity of the materials described above is considerably better than that of most photochromics and their storage time is much longer. At the present state of development, therefore, these improved electro-optic crystals should be regarded as serious contenders for dynamic storage and read-write memory applications, where their usage was precluded in the past by their low sensitivity.

The successful implementation of fixing techniques have also opened new application areas for these materials, such as read-only memories, storage for display devices, and holographic optical components.

It is expected that these developments will greatly spur the work towards further material improvements and towards the implementation of practical systems utilizing these media.

Acknowledgements

It is a pleasure to acknowledge the skillful assistance of Messrs. G. Latham, L. Levin and R. Wer in the experimental work that was carried out.

References

1. Chen, F. S., LaMacchia, J. T., and Fraser, D. B., "Holographic Storage in Lithium Niobate," *Appl. Phys. Letters*, Vol. 13 (Oct 1968) pp. 223-225.
2. Amodei, J. J., "Electron Diffusion Effects During Hologram Recording in Crystals," *Appl. Phys. Letters*, Vol. 18 (Jan 1971) pp. 22-24.
3. Chen, F. S., "Optically Induced Change of Refractive Indices in $LiNbO_3$ and $LiTaO_3$," *J. Appl. Phys.*, Vol. 40 (July 1969) pp. 3389-3396.
4. Johnston, Jr., W. D., "Optical Index Damage in $LiNbO_3$ and Other Pyroelectric Insulators," *J. Appl. Phys.*, Vol. 41 (July 1970) pp. 3279-3284.
5. Amodei, J., *J. Appl. Phys.*, to be published.
6. Kogelnik, H., "Coupled Wave Theory for Thick Hologram Gratings," *Bell System Tech. J.*, Vol. 47 (Nov 1969) pp. 2909-2947.
7. Amodei, J. J., and Staebler, D. L., *Appl. Phys. Letters*, to be published.

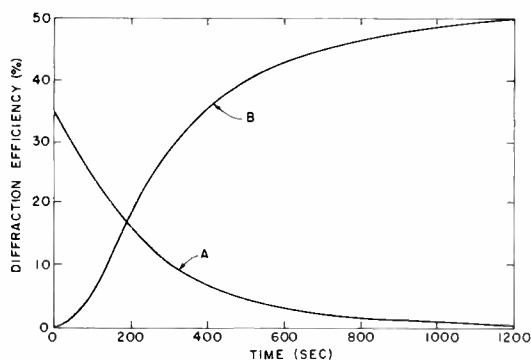


Fig. 7—Readout of (a) normal (optically erasable) hologram in a 0.3 cm sample of $LiNbO_3$ and (b) a hologram fixed by heating the crystal after recording a normal hologram.

Inorganic photochromic and cathodochromic recording materials

R. C. Duncan, Jr. | Dr. B. W. Faughnan | Dr. W. Phillips

Photochromic materials have the property of changing color under light illumination. Inorganic photochromic materials are frequently cathodochromic as well, that is, they can be colored by electron-beam irradiation. This paper describes recent studies at RCA Laboratories of three classes of inorganic photochromic materials: 1) rare-earth-doped CaF_2 ; 2) transition-metal-doped SrTiO_3 and CaTiO_3 ; and 3) iron- or sulfur-doped sodalite. Photochromic properties of these materials in both single crystal and powder form, and cathodochromic properties of powders, are discussed.

PHOTOCHROMIC MATERIALS change color reversibly when illuminated by light. Typically, they are transparent or lightly colored in the normal or thermally stable state, and become more darkly colored after irradiation with ultraviolet or blue light. The induced photochromic optical absorption decays thermally at room temperature in times ranging from seconds to days depending on the material. The materials can also be returned to their original state by irradiation with visible light. Many applications of photochromic materials are possible. For example, single crystals may be used for information storage and optical processing; powders may be used for cathodochromic storage tubes and hard copy applications.

Organic photochromic materials have been studied for many years, and several review articles have been written about them.^{1,2} Reviews of inorganic photochromic materials are also available.^{3,4} However, only relatively few inorganic materials have been studied in any detail. The earliest examples are alkali halides containing F -centers.³ For the past several years, a group at RCA Laboratories has been studying the photochromic properties of calcium fluoride doped with rare earths

($\text{CaF}_2:\text{RE}$), strontium and calcium titanate doped with transition metals ($\text{SrTiO}_3:\text{TM}$ and $\text{CaTiO}_3:\text{TM}$), and sodalite doped with iron or sulfur.

In this paper we are concerned with the properties of these three materials. In the first part we deal with single crystals. This is followed by a discussion of photochromic powders. Finally, the cathodochromic properties of these powders, i.e., their behavior under electronbeam excitation, are considered.

Single crystals of CaF_2 used in this study were grown at RCA Laboratories. Crystals of SrTiO_3 and CaTiO_3 were obtained from National Lead Company, and CaTiO_3 was synthesized in powder form at RCA. Crystalline sodalite was supplied by Airtron, a division of Litton Industries.

Photochromic single crystals

Photochromic mechanism and spectra

The photochromic process in inorganic crystals can be understood in terms of the photo-induced charge transfer of an electron from one localized impurity or defect state in the crystal to another via the conduction band. This process is illustrated schematically in Fig. 1; A and B represent two different defect centers in their thermally stable states. Centers A and B may or may not have optical absorption bands in the visible; if not, then the crystal will be colorless in its normal state. In the photochromic process, an ultraviolet photon removes an electron from A. This electron is

free to move in the conduction band until it is trapped by B (if not retrapped by A), thereby producing two new centers A^+ and B^- . Either or both of these centers must now have absorption in the visible for the material to be photochromic. If the incident photon has an energy greater than the band gap, then an electron-hole pair will be created. If the hole is trapped by A and the electron by B, the final result will be the same as for direct excitation of the A center. However, if the photon energy is greater than band-gap, the light will be absorbed close to the surface of the crystal because of the high optical edge absorption.

The photochromic optical absorption bands observed in $\text{CaF}_2:\text{RE}$, $\text{CaTiO}_3:\text{TM}$, and sodalite are shown in Fig. 2. In Fig. 2a, the unswitched or thermally stable absorption arises from the $\text{La}^{2+}:\text{F}$ -center complex which is created when $\text{CaF}_2:\text{La}$ is additively colored.^{3,5} The switched curve results after an electron is removed from this center by ultraviolet irradiation and is subsequently trapped by a La^{3+} ion in a cubic site. The optical absorption arises from both the ionized $\text{La}^{2+}:\text{F}$ -center complex and the newly created cubic

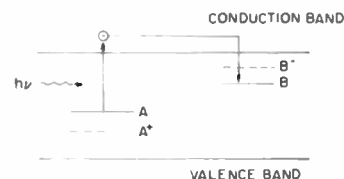


Fig. 1—Photo-excitation and transfer of an electron from one localized impurity center, A, to another center, B.

Reprint RE-17-2-9

Final manuscript received April 30, 1970.

Portions of the work described in this paper were supported by the Defense Atomic Support Agency under Contract No. DASA-01-68-C-0064, the National Aeronautics and Space Administration under Contract No. NAS 5-10335, and the U.S. Navy Ship Systems Command under Contract No. N00024-68-C-1173

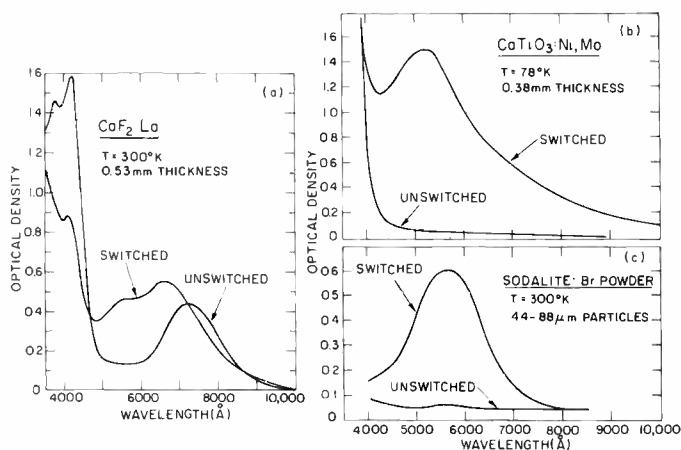


Fig. 2—(a) Optical absorption spectra of a $\text{CaF}_2:\text{La}$ crystal wafer before and after photochromic switching with ultraviolet light. (b) Optical absorption spectra of a $\text{CaTiO}_3:\text{Ni,Mo}$ crystal wafer before and after photochromic switching with ultraviolet light. (c) Diffuse reflectance spectra of Fe-doped sodalite before and after photochromic switching with ultraviolet light.

La^{2+} center. Gd -, Tb -, and Ce -doped CaF_2 also show similar effects.

Fig. 2b shows the photochromic absorption in CaTiO_3 doped with Ni and Mo .^{3,4,7} In the transparent state the impurity ion valences are Ni^{2+} and Mo^{6+} . The effect of ultraviolet light near the band edge is to remove an electron from the Ni^{2+} ion. The electron is then trapped by the Mo^{6+} . The net result is the creation of Ni^{3+} and Mo^{5+} , both of which have absorption bands in the visible. The Ni^{3+} absorption band peaks at 5000 Å, while the Mo^{5+} absorption band peaks at 6500 Å.

Chloride sodalite has the chemical

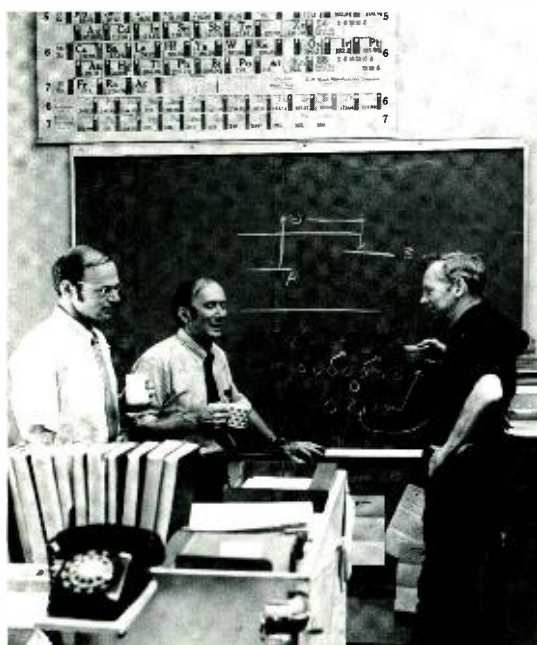
formula $\text{Na}_8\text{Al}_6\text{Si}_6\text{O}_{24}\text{Cl}_2$. In place of the chlorine in the more common chloride sodalite, bromine or iodine can also be fully incorporated into the lattice. The structure consists of an aluminosilicate cage with the halogen ion at its center tetrahedrally coordinated with Na ions.⁸ The color center in sodalite has been identified as an F -center at a halogen site.^{9,10} The photochromic absorption band arising in bromide sodalite is shown in Fig. 2c. The donor supplying the electron for the F -center is a chemical impurity such as sulfur or iron. The data shown in Fig. 2c were taken on a sodalite powder, rather than a single crystal.

Optical density vs concentration

The maximum optical density ($OD = \log [I_0/I]$) that can be obtained in a photochromic crystal of given thickness is a most important quantity for applications. A high optical absorption coefficient allows the use of a thin crystal wafer to obtain a desired optical density change. This coefficient is directly proportional to the number of switching centers/cm³, which, in turn, is dependent on the dopant concentration. All three materials have been studied in detail to optimize the number of switching centers. Some results of this study for typical samples of SrTiO_3 and sodalite are shown in Fig. 3.

The peak absorption coefficient is plotted, in each case, against the weight percent of transition element. (The sodalite data were taken on powder samples, and the raw diffuse reflectance data converted to absorption coefficients using the theory discussed below.) The maximum number of centers that switch has been estimated from electron spin resonance measurements to be about $10^{18}/\text{cm}^3$ for both CaTiO_3 and sodalite. The peak absorption in Fig. 3 occurs for a dopant concentration an order of magnitude or more greater than this.

The situation for $\text{CaF}_2:\text{RE}$ is more complicated since the crystal must be additively colored before it becomes photochromic, and this process itself depends on the rare earth concentra-



Authors (left to right), Phillips, Faughnan, and Duncan.

Dr. William Phillips

Solid State Research Laboratory
RCA Laboratories
Princeton, New Jersey

received the AB in Physics from Columbia University in 1958. He did his graduate work at the Carnegie Institute of Technology, receiving the MS in Physics in 1961 and the PhD in Electrical Engineering in 1964. He joined the technical staff of RCA Laboratories in 1964, and from 1964 to 1967 was engaged in research on the synthesis and properties of crystalline materials for laser applications. In 1967 he became involved in work on the synthesis and evaluation of photochromic, and later cathodochromic, materials. He received RCA Laboratories Achievement Awards for this work in 1968 and 1970, and shared in an IR-100 Award for development of the cathodochromic CRT in 1969. Dr. Phillips is currently engaged in research on improved materials for volume holographic storage. He has authored or co-authored nine technical articles and has two patents pending. Dr. Phillips is a member of the American Physical Society, the IEEE, the American Ceramic Society and Sigma Xi.

Dr. Brian W. Faughnan

Solid State Research Laboratory
RCA Laboratories
Princeton, New Jersey

graduated from McGill University in 1955 with a B.Eng. in Engineering Physics. He was awarded the MSEE in 1957 from the Massachusetts Institute of Technology. In February 1957 he entered the Physics Department of M.I.T. and was awarded the PhD in 1959. In 1959, he joined RCA Laboratories and has carried out research in a variety of topics in solid state physics. These include: the study of negative mass cyclotron resonance effects in germanium, radiation damage to solar cells, the study of radiation damage centers in silicon by electron spin resonance techniques. From August 1963 to June 1964 he was at the RCA Tokyo Laboratories studying the propagation of Alfvén waves in the semimetal bismuth. Since his return to Princeton, he continued work on semimetals including device applications. From 1966 to 1969 he has engaged in fundamental studies of various photochromic single crystals, especially SrTiO_3 , using combined electron spin resonance and optical techniques. For the past 2 years he has been studying the electron beam coloration of materials especially sodalite with the goal of understanding the physical mechanism and optimizing materials for device applications. He is a member of Sigma Xi and the American Physical Society.

tion. If this concentration is made too high, undesirable coloration side effects are produced during the additive coloration step. However, the same general conclusion applies: in the best material the rare earth concentration is roughly ten times higher than the actual number of switching centers.

Thermal decay rate

The thermal decay rate is an exponential function of temperature. The thermal decay time depends principally on the thermal depth of the relevant electron trap. In general, if the bandgap is large, the trap depth will also be large. In CaF_2 , which has a bandgap of 10.2 eV, the decay times in the dark are several days to a week. Sodalite, with a bandgap of 5.2 eV, has thermal decay times of hours to

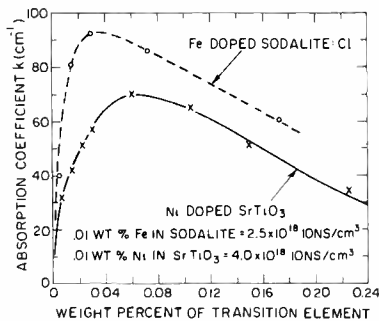


Fig. 3—Photochromic optical absorption change as a function of transition metal dopant concentration for a $SrTiO_3:Ni$ single crystal and an Fe -doped sodalite powder.

Robert C. Duncan, Jr.
Solid State Research Laboratory
RCA Laboratories
Princeton, New Jersey

holds BS (1951) and MS (1958) degrees in physics from Union College and Cornell University, respectively. For the MS he carried out thesis research using the total reflection of x-rays to study the structure of evaporated metallic films. Mr. Duncan joined the research staff of the RCA Laboratories in 1957, and from 1957 to 1962 did both experimental and theoretical work on the electronic and microwave properties of semiconductors. This work included studies of space charge regions in semiconductor surfaces and cyclotron resonance of negative effective mass charge carriers in germanium. Since 1962, Mr. Duncan has carried out both fundamental and applied research on the optical properties of insulating crystals, particularly rare-earth-doped calcium fluoride. This work has included development of several new optically-pumped laser materials, demonstration of the first band-pumped and laser-pumped infrared quantum counters, and contributions to the understanding, development and evaluation of inorganic photochromic crystals and powders. Mr. Duncan has authored or co-authored over a dozen technical papers, and was awarded an RCA Laboratories Achievement Award in 1963. He is a member of the American Physical Society and Sigma Xi.

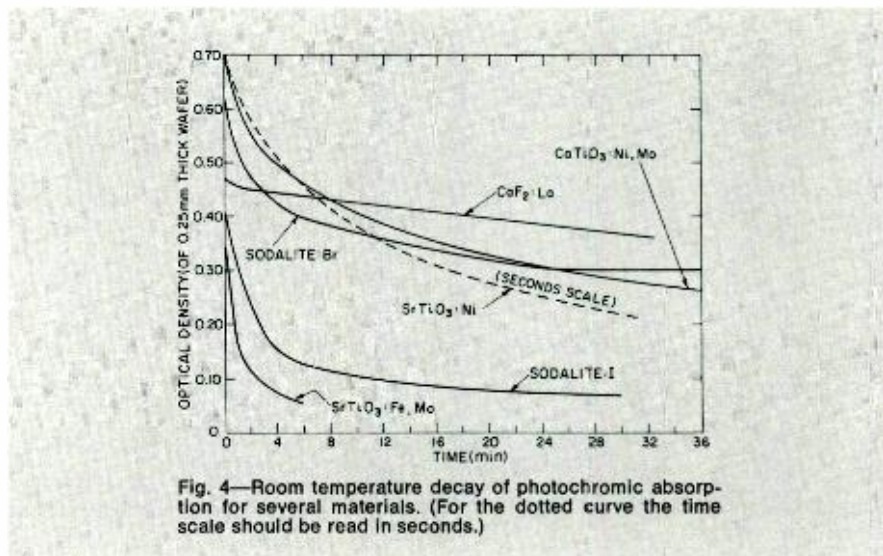


Fig. 4—Room temperature decay of photochromic absorption for several materials. (For the dotted curve the time scale should be read in seconds.)

days. In $SrTiO_3$, with the much smaller bandgap of 3.2 eV, the decay times vary from seconds to minutes. The Mo^{5+} trap depth in $SrTiO_3$ has been measured to be 0.7 eV below the conduction band.¹¹

Even in the same material and with the same electron trap, as for example with Fe, Mo - and Ni, Mo -doped $SrTiO_3$, the thermal decay times will differ because the electron capture cross sections of the different ions differ. If the charge states of the ions are different, e.g., Fe^{2+} and Ni^{2+} , the differences in thermal decay times can be as large as a factor of 10. Decays for the three materials are shown in Fig. 4. Note that for the dotted curve the time scale should read in seconds.

Coloring and bleaching efficiency

The photochromic process, unlike the photographic one, has no built-in gain mechanism. The unavailability of high power light sources in the ultraviolet region of the spectrum frequently places limitations on the switching speeds of photochromic crystals. The growing number of laser sources in this frequency range is helping to alleviate this problem.

A lower limit on the energy required to switch a photochromic can be estimated from Smakula's equation for color centers.¹² This can be written,

$$Nf = 0.87 \times 10^{17} [n / (n^2 + 2)^2] k_{max} W_{1/2}$$

where N is the number of absorbing centers/cm²; f is the oscillator strength

of the transition; n is the index of refraction of the material; k_{max} is the absorption coefficient, in cm⁻¹, at the peak of the absorption band; and $W_{1/2}$ is the full width, in eV, of the absorption band at half intensity.

For a typical F -center-like transition, $f \sim 0.5$ and $W_{1/2} \sim 0.4$ eV. To produce an optical density change of 0.3 (a 2:1 contrast ratio) in a crystal thickness t , it is necessary that $Nt = 4 \times 10^{15}$ centers/cm² switch. If we further assume that every ultraviolet photon incident on the crystal is absorbed and excites one color center (unity quantum efficiency), the energy required is approximately 2.5 millijoules/cm².

This is an optimistic estimate. For the materials under study here, a quantum efficiency of approximately 10-15% is usually found. This means that for sodalite and CaF_2 approximately 25 mJ/cm² of energy is required to produce an optical density change of 0.3. In $SrTiO_3$, the oscillator strength is somewhat smaller and the absorption bandwidths are about twice as great, so that approximately 40 mJ/cm² of energy is required. The quantum efficiency can be reduced by so-called "dead bands" which absorb energy but do not lead to photochromic switching.

Photochromic bleaching is accomplished by irradiation with visible light. In general, bleaching efficiencies are usually at least ten times lower than coloring efficiencies. Typically they are a few percent.

Photochromic powders

Why powders?

For many applications, photochromic materials are more useful in powder form than as single crystals. Several mechanical, optical and photochromic properties of these powders are responsible. First, in powder form, these materials lend themselves particularly well to large-area displays. Such displays are not possible with single crystals except in the form of carefully polished and fitted mosaics. Second, the diffuse reflectance of a powder surface is ideally suited to reflective readout in ambient light. Third, because of their large surface-to-volume ratio, the small powder particles achieve a more complete and uniform bulk coloration under greater than bandgap ultraviolet or electron-beam switching than do even the thinnest single crystal wafers. And fourth, the readout contrast of a recorded image is enhanced by multiple internal reflection of readout light trapped within the powder particles.

These properties suggest the use of photochromic powders on flexible large-area substrates, such as sheets or moving belts for semi-hard copy, reflective display, and buffer memory applications. Perhaps the most important use to date of these powders is in dark-trace cathode-ray tubes. The cathodochromic properties of these powders pertinent to that application will be specifically discussed later in this paper.

Photochromic $SrTiO_3$, $CaTiO_3$, and sodalite have all been studied in powder form. Samples were prepared by direct powder synthesis or by crushing crystalline or sintered material. The powders were sized, by mechanical sieving, into several particle-size ranges between 20 and 88 μm . Powder of a single particle size range was used in the preparation of thick (usually many particle diameters) loose-powder samples for study.

Diffuse reflectance of absorbing powders

A detailed theory for the diffuse reflectance of absorbing powders has been developed by Melamed.¹³ This theory relates the diffuse reflectance of a powder to the particle size, its bulk absorption coefficient, and its refractive index. Its basic assumptions—

- 1) A Lambertian (perfectly diffuse) re-

flecting powder surface;

- 2) A total reflectance given by the Fresnel relations for each angle of incidence;

- 3) An infinitely thick powder; and

- 4) Spherical powder particles of uniform size

—are generally consistent with properties of photochromic powder samples studied. The very nearly Lambertian nature of their surface reflectance was experimentally verified; their thickness was essentially infinite; particle sizes were approximately uniform ($\pm 30\%$ or better); and we have assumed, with Melamed, that the spherical particle assumption is a good approximation to a real powder of randomly oriented and randomly shaped particles. The second assumption above has not been explicitly verified.

For all of the powders studied, the bulk absorption coefficient (for both the switched and unswitched states), k , and the powder particle diameter, d , lie in the regions $0 < k < 150\text{cm}^{-1}$ and $0.0020 < d < 0.0088\text{ cm}$ respectively. Thus the kd product lies in the range $0 < kd < 1.4$. The index of refraction, n , is about 2.4 for the titanates and about 1.5 for sodalite.

It is useful to summarize some of the predictions of the Melamed theory which are applicable to these powders:

- 1) For a given value of $k > 0$, the diffuse reflectance R should decrease monotonically with increasing d .
- 2) Within the limited range $kd < 1.4$, a

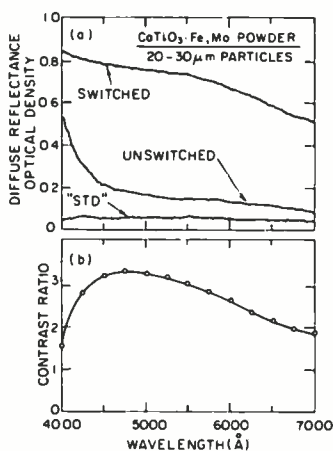


Fig. 5—(a) Optical diffuse reflectance spectra of a $CaTiO_3:Fe,Mo$ powder before and after photochromic switching with ultraviolet light. (b) Spectral dependence of the corresponding photochromic diffuse reflectance contrast ratio.

given photochromically induced change Δk should produce a diffuse reflectance contrast ratio, $C \equiv R_{unswitched}/R_{switched}$, which increases with increasing d .

- 3) For very large Δk , or Δkd , the value of C should approach a maximum which is independent of d but which decreases with increasing n . This C_{max} should be about 8:1 for the titanates and about 20:1 for sodalite.

Diffuse reflectance spectra

The photochromic behavior of a powder sample of $CaTiO_3:Fe,Mo$ is illustrated in Fig. 5. The data in Fig. 5a were obtained using a modified integrating sphere accessory for the Cary 14 Spectrophotometer. Measured diffuse reflectance optical densities ($\equiv \log [R_{reference}/R]$) are shown for a $MgCO_3$ block "standard" ($R_{standard} = 0.97$), the $CaTiO_3$ powder in its unswitched state, and the same powder in its saturated switched state. With small instrumental and "standard" corrections applied, these optical densities can be converted directly to absolute reflectances. The ratio of these reflectances then gives the saturated diffuse reflectance contrast ratios plotted in Fig. 5b. The broad wavelength region of high contrast ratio is well suited for nearly black-on-white visual readout in ambient light. Sodalite powders, on the other hand, have considerably narrower visible absorption bands (See Fig. 2c) and produce a colored image.

The wavelength dependence of the photochromically induced change Δk in the bulk absorption coefficient can be obtained from data such as that of Fig. 5a by using the Melamed theory. Induced absorption spectra obtained in this way have been compared with those of single crystal samples of the same material. The close similarity in the shapes of these spectra tends to confirm both the applicability of the theory to these photochromic powders and the similarity of the photochromic processes in the crystal and powder forms of the materials. Generally, however, the powder data yield larger values of Δk . This discrepancy will be discussed later.

Saturated photochromic contrast ratio

The saturated photochromic contrast ratio is the ratio of the diffuse reflectances of a powder in its normal or unswitched state and its saturated switched state, $C \equiv R_u/R_s$. The value of C , depends on the wavelength at

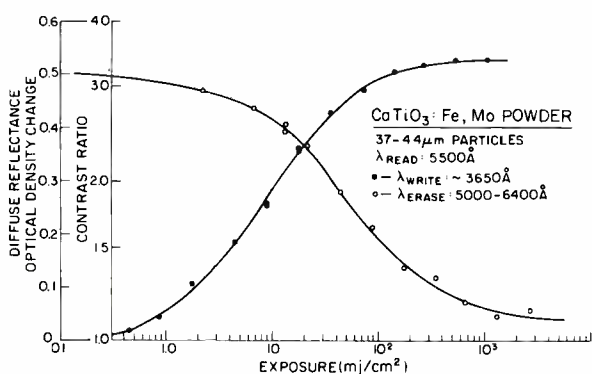


Fig. 6—Photochromic sensitometric characteristic for CaTiO_3 : Fe, Mo powder for ultraviolet write radiation and visible erase radiation (see legend).

which the appropriate diffuse reflectances are determined; the spectral dependence of C , for a CaTiO_3 : Fe, Mo powder sample was shown in Fig. 5b. Saturated contrast ratios at 5500 Å for CaTiO_3 : Fe, Mo powder samples of several different particle-size ranges are given in Table I. These values are among the highest observed to date for SrTiO_3 or CaTiO_3 powders. Values of C , between 2:1 and 3:1 are exhibited by typical sodalite powders of 20-40 μm particles.

The values of C , given in Table I exhibit a progressive increase with increasing particle size. This again is consistent with the predictions of the Melamed theory, and illustrates the contrast enhancement that can be achieved in display applications where large powder particle sizes do not conflict with resolution requirements.

The diffuse reflectances used in determining the values for C , in Table I can also be used, in conjunction with the Melamed theory, to compute the change Δk in the bulk absorption coefficient for each powder sample. The results, shown in the last column of Table I, are essentially independent of particle size. This observation lends still further support to the applicability of this theory to these photochromic powders and, at the same time, tends to confirm that the Δk so determined is indeed a bulk property of the material.

Table I—Saturated diffuse reflectance contrast/ratios for powder samples of CaTiO_3 : Fe, Mo . (Readout $\lambda \cong 5500 \text{ \AA}$)

Particle Diameter d (μm)	Saturated contrast ratio (C_s)	Bulk absorption coefficient Δk_{max} (cm^{-1})
20-30	3.1 ± 0.1	140 ± 15
30-37	3.4 ± 0.1	125 ± 15
33-44	3.6 ± 0.1	135 ± 15

It is interesting, therefore, to compare this deduced value, $\Delta k_{max} \cong 135 \pm 15 \text{ cm}^{-1}$, with bulk values determined by direct transmission measurements on single crystal samples of CaTiO_3 : Fe, Mo . The largest values so determined are $\Delta k_{max} \cong 90 \text{ cm}^{-1}$, and are only observed for very thin crystalline samples in which the greater-than-bandgap switching radiation reaches a larger fraction of the sample volume. The greater Δk_{max} observed for powder material may, then, represent a still more efficient penetration of this switching radiation into the small particles.

Photochromic switching sensitivity

The photochromic switching sensitivity of good quality CaTiO_3 : Fe, Mo powder sample is illustrated in Fig. 6. About 8 mW/cm^2 of switching radiation near 3650 Å was used. The initial rate of diffuse reflectance optical density change with exposure is about 0.08 OD/mJ/cm^2 . The optical-density-versus-log-exposure format of Fig. 6 places major emphasis on the middle exposure range in which the greatest optical density changes occur and corresponds to the standard display format used for sensitometric data for photographic film.

The effective threshold for significant photochromic coloration is about 1 mJ/cm^2 . Saturation becomes important at exposures of somewhat less than 100 mJ/cm^2 . The approximately 10 mJ/cm^2 exposure necessary to achieve a contrast ratio of 2:1 is less than the 40 mJ/cm^2 required to produce the same contrast in transmission in a single crystal, and considerably closer to the 2.5 mJ/cm^2 estimated for an ideal crystal (see the discussion of *Photo-*

chromic Single Crystals above; SrTiO_3 and CaTiO_3 have similar oscillator strengths). This is consistent with the previously noted higher efficiency with which switching radiation is absorbed in powder samples and increased uniformity and completeness of coloration of such samples.

The effective slope or γ of the nearly linear portion of the switching curve of Fig. 6 is $\gamma = 0.3$.

Photochromic erase sensitivity

The photochromic erase sensitivity of the same material is also shown in Fig. 6. Here the powder was switched to near saturation with 3650 Å radiation and subsequently erased in about 20 mW/cm^2 of 5000 Å to 6400 Å light. The data has been corrected for the thermal decay in coloration which is assumed to proceed independently during optical erasure and which is easily measured (see below).

The exposures corresponding to the effective threshold and effective completion are each nearly a factor of ten greater for erasure than for switching. This is consistent with the behavior of single crystal photochromics and is common (qualitatively) to all inorganic photochromics we have studied. The effective γ of the erase mode is approximately $\gamma = -0.3$.

Switched-state lifetimes

The lifetimes of the switched states of photochromic powders vary, as do those of their single crystal counterparts, for different host crystals and different dopants. The decay rates of bulk absorption coefficients appear to be identical for the two forms of the material (see Fig. 4). The resulting decay of the diffuse reflectance contrast ratios for powder samples of three materials are shown in Fig. 7.

Cathodochromic excitation of powders

Cathodochromic mechanism

When powdered photochromic materials are bombarded by an electron beam, they undergo a color change that closely resembles the photochromic color change induced by ultraviolet irradiation, and in fact differs from the latter only in the way in which electrons are transferred from the A-centers to the B-centers (see Fig. 1). In the cathodochromic process the electron beam creates electron-hole pairs in the

material.¹⁴ Electrons are trapped at B-centers and holes at A-centers, exactly as in the case of greater-than-bandgap ultraviolet irradiation (refer to the discussion of *Photochromic Single Crystals*), producing the colored state of the material. Thermal decay of optically induced bleaching of the cathodochromic coloration proceeds in the same manner as for photochromic coloration.

Interest in the cathodochromic mode of excitation stems from the fact that it provides a relatively simple solution to the problem of addressing photochromic materials. One can, for example, construct cathode-ray tubes having cathodochromic screens instead of phosphor screens.¹⁵ These tubes constitute inexpensive display-storage devices having a number of unique attributes.

Fabrication and properties of screens

Cathodochromic screens are made by settling powdered material from aqueous suspension onto glass substrates, using well-known phosphor settling techniques. The screens are then aluminized to eliminate light transmission and increase reflectivity. Most of the data presented here were obtained using 5-cm square glass slides in a demountable electron-beam apparatus.

The powder particle size used is determined by a compromise. Larger particles are capable of greater contrast ratios for a given Δk (refer to the discussion of *Photochromic Powders*), while smaller particles can be more fully and more uniformly colored by an electron beam of given energy. The empirically determined optimum size

is several times larger than the estimated electron-beam penetration depth.¹⁶ For sodalite screens excited by 28-kV electrons, this optimum is approximately 25 microns.

The screen weight (mass of material/cm² of screen surface) used also represents a compromise. As much material as possible should interact with the readout light, yet the electron beam should completely penetrate the screen to color the particles in direct view of the observer. Optimum screen weights have been found by D. R. Bosomworth to be equivalent to between one and two monolayers of particles.

Although the parameters of particle size and screen weight are usually optimized to produce the maximum contrast capability, they also influence the sensitivity (defined below) of the screens. There are applications in which sensitivity considerations take precedence over contrast capability.

Performance of screens

Measurements are made by exciting screens with known electron beam exposures and observing the changes in diffuse reflectance with a spot brightness meter. The results are conveniently represented as curves, such as those in Figs. 8 and 9, showing the contrast ratio achieved for a given electron beam exposure. From such curves one determines both the sensitivity and the maximum contrast capability of the screen. In the present discussion, the term *sensitivity* is used in a relative sense to refer to the amount of coloration achieved for a given electron beam exposure. A useful practical measure of sensitivity is

the exposure (in units of microcoulombs/cm²) required to reach a contrast ratio of 2:1. Lower required exposures, of course, imply higher sensitivities.

The cathodochromic materials that have been studied in the greatest detail are the sodalites and calcium titanate. These are the materials with the greatest cathodochromic as well as photochromic absorption coefficients. The behavior of $CaTiO_3$ and sodalite screens differs in a number of important respects, one of which is sensitivity. Fig. 8 shows electron beam exposure curves for representative sodalite (in this case, iodide sodalite) and $CaTiO_3$ screens. Sodalite screens usually require between one and two microcoulombs/cm² to reach a 2:1 contrast ratio. Calcium titanate screens are less sensitive, typically requiring 8 microcoulombs/cm² to reach 2:1.

The most significant practical difference between sodalite and $CaTiO_3$ screens is the way in which they approach their maximum reversible contrast. The contrast that can be achieved by a $CaTiO_3$ screen is limited by the onset of saturation (see Fig. 8). When the maximum coloration at a given electron-beam voltage has been reached, additional exposure at that voltage will not increase the contrast. When the excitation is removed, thermal decay commences in the normal manner. In practical screens optimized for voltages of 30 kV, saturation occurs at contrasts of somewhat greater than 2.5:1.

On the other hand, sodalite, particularly chloride and bromide sodalites, usually show an increase in contrast with increasing electron-beam exposure until considerably higher contrast ratios are achieved. Once the material is colored beyond a certain point, however, the image can no longer be completely erased with light. The situation for chloride sodalite is illustrated in Fig. 9. The upper curve indicates the total contrast, while the two lower curves show the portions of this total which are and are not erasable with light. At higher contrast levels, the total coloration curve and the optically irreversible curve tend to converge.

The advantages of sodalite are that both its ultimate contrast capability at any given accelerating voltage and its

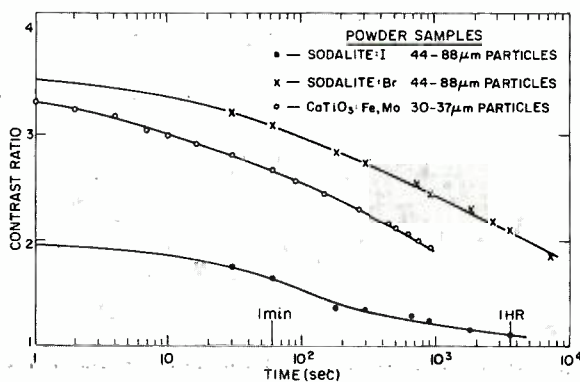


Fig. 7—Room temperature thermal decay of the photochromic diffuse reflectance contrast ratio for sodalite:I, sodalite:Br, and $CaTiO_3:Fe,Mo$.

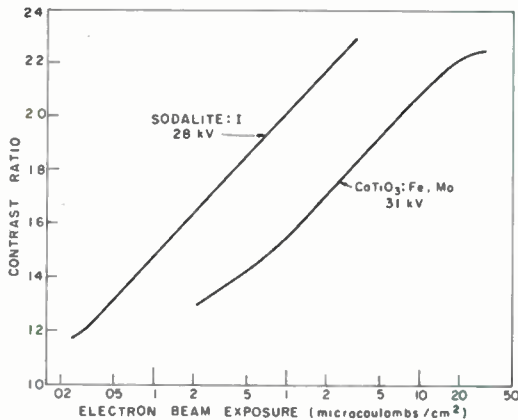


Fig. 8—Diffuse reflectance contrast ratio as a function of electron beam exposure for an iodide sodalite and a $\text{CaTiO}_3:\text{Fe,Mo}$ screen.

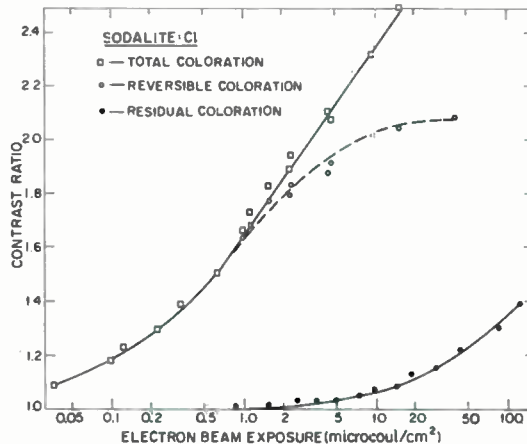


Fig. 9—Diffuse reflectance contrast ratios corresponding to the total coloration, reversible coloration, and irreversible coloration of a chloride sodalite test screen, as functions of the electron beam exposure.

sensitivity are higher than those of CaTiO_3 . CaTiO_3 screens, on the other hand, are virtually immune to optically irreversible coloration effects produced by excessive electron beam exposures. The appearance of irreversible coloration represents a potentially serious weakness of sodalite screens, since it is difficult to operate them without sometimes exceeding the threshold for permanent coloration. This problem has been pursued on two fronts. On one hand, efforts have been made to produce materials with reduced permanent coloration sensitivity. We have developed iodide sodalite materials with contrast capabilities exceeding 3:1 in which the irreversible coloration sensitivity has been reduced to nearly negligible values. When these materials undergo continuous electron beam exposure, they gradually develop a small amount of residual coloration. This can be removed, however, by exposure to erase illumination for a period of one half hour.

Another approach to the problem is to make use of the fact that the optically irreversible coloration bleaches thermally when the screens are heated to about 200°C. The thermal erase technique can, in fact, be applied to optically reversible materials as well.

Applications of cathodochromic materials

As mentioned previously, cathodochromic CRT's have a number of valuable attributes which are not found, or are achieved with difficulty, in other

display-storage systems. They can be made in almost any size. Because no separate storage structure is involved, the resolution is limited by the electron beam optics or the powder particle size. In direct view display tubes, the electron-beam spot size typically exceeds 50 to 75 microns diameter and defines the minimum resolution element.

The most striking attribute of these tubes is that the contrast of the display is independent of ambient illumination. Phosphor CRT displays tend to be completely washed out in direct sunlight, for example, whereas cathodochromic screens exhibit essentially the same contrast in direct sunlight and at low light levels. A more detailed discussion of cathodochromic CRT applications appears elsewhere in this issue.¹¹

Acknowledgments

We would like to acknowledge the assistance of R. Infanti, R. E. Nielsen, and R. L. Quinn who prepared most of the samples and slides and took much of the data. We wish to express our thanks to D. R. Bosomworth for permission to use his unpublished CaTiO_3 data in Fig. 9 (and elsewhere at noted), and to Peter Norris for the use of his sodalite data in Fig. 2c and for making other measurements on sodalite. CaTiO_3 was prepared in powder form by P. N. Yocom, and CaF_2 crystals were grown by H. Temple, both of RCA Laboratories.

References

1. Exelby, R., and Grinter, R., "Phototropism (or photochromism)," *Chem. Rev.* Vol. 65 (1965) p. 247.
2. Brown, C. H., and Shaw, W. G., "Phototropism," *Rev. Pure Appl. Chem.*, Vol. 11 (1961) pp. 2-32.
3. Faughnan, B. W., Staebler, D. L., and Kiss, Z. J., in *Applied Solid State Science*, Wolfe, R., Ed. (Academic Press, Inc.; New York; Vol. 2) to be published.
4. Kiss, Z. J., "Photochromics," *Physics Today*, Vol. 23 (1970) p. 42.
5. Staebler, D. L., and Kiss, Z. J., "Photo Reversible Charge Transfer in Rare-Earth-Doped- CaS_2 ," *Appl. Phys. Letters* Vol. 14 (1969) p. 93.
6. Faughnan, B. W., and Kiss, Z. J., "Photo-induced Reversible Charge-Transfer Processes in Traditional Metal-Doped Single-Crystal SrTiO_3 and TiO_2 ," *Phys. Rev. Letters* Vol. 21 (Oct 1968) pp. 1331-1334.
7. Faughnan, B. W., and Kiss, Z. J., "Optical and EPR Studies of Photochromic SrTiO_3 Doped with Fe/Mo and Ni/Mo ," *IEEE J. Quantum Electron.* QE-5 (Jan 1969) pp. 7-21.
8. Wells, A. F., *Structural Inorganic Chemistry* (Oxford University Press, London, 1950) 2nd ed., pp. 590-591.
9. Medved, D. B., "Hackmanite and its tenebrescent properties," *Am. Mineralogist* Vol. 39 (1954) p. 615.
10. Hodgson, W. G., Brinen, J. S., and Williams, E. F., "Electron Spin Resonance Investigation of Photochromic Sodalites," *J. Chem. Phys.* Vol. 47 (1967) p. 3719.
11. Amodci, I. J., "A Study of Dynamics of Photochromic Switching in Strontium Titanate Materials," PhD Thesis, U. of Pa. (1968).
12. Dexter, D. L., in *Solid State Physics*, Seitz, F., and Turnbull, D., Eds. (Academic Press, Inc., New York, 1958) Vol. 6 p. 370.
13. Melamed, N. T., "Optical Properties of Powders. Part I—Optical Absorption Coefficients and the Absolute Value of the Diffuse Reflectance; Part II—Properties of Luminescent Powders," *Appl. Phys.* Vol. 34 (March 1963) pp. 560-570.
14. Kiss, Z. J., and Phillips, W., "Cathodochromism in Photochromic Materials," *Phys. Rev.* Vol. 180 (1969) p. 924.
15. Phillips, W., and Kiss, Z. J., "Photo Erasable Dark Trace Cathode-Ray Storage Tube," *Proc. IEEE*, Vol. 56 (Nov 1968) pp. 2072-2073.
16. Leverenz, H. W., *An Introduction to the Luminescence of Solids* (John Wiley & Sons, Inc.; New York; 1950) pp. 156-159.
17. Gorog, I., "Cathodochromic image display applications," *this issue*.

Low-light-level color photography

E. Hutto, Jr.

Multistage image intensifier tubes have extended the ability of monochrome photography to be effective at starlight illumination levels. Consideration has been given to color photography at moonlight conditions but most methods become too complex to be practical. The use of three intensifier tubes can be ruled out because of severe registration problems. Single-tube cameras using rotating color filter discs are unattractive because of mechanical components and the necessity to relay the output image to the film. This paper describes an experimental low-light-level camera using a color encoding technique.

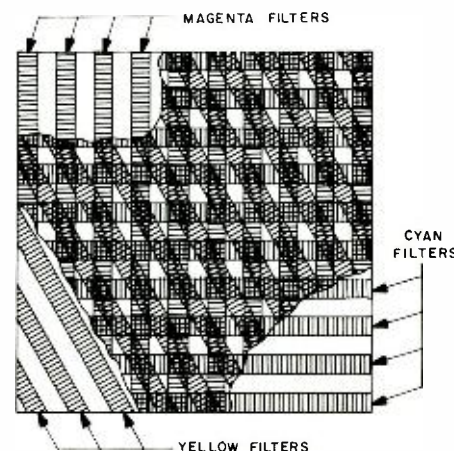


Fig. 1—Encoding filters.



E. Hutto, Jr.
Electro-Optics Laboratory
Advanced Technology Laboratories
Camden, New Jersey

received the BSEE from Clemson College in 1947 and joined RCA as a member of the engineer training program. From 1948 to 1953, he was with the Home Instrument Optical Group working on optical components for Schmidt projection television systems and in colorimetry for home color TV receivers. In 1953, he joined the Optics, Sound, and Special Engineering Section, responsible for an electronic lens bench for the evaluation of television and photographic lenses. His work has also included optical systems for color television cameras and projectors. Mr. Hutto has participated in studies involving aerial reconnaissance by television and photographic techniques. He was project engineer on two programs utilizing image tubes in photographic cameras and a study program investigating techniques for low-light-level color photography. He is currently engaged in the development of a camera in which color information is encoded on black-and-white film. Mr. Hutto has been actively concerned with optical systems for use with injection and gas lasers in illuminator and scanning devices.

THE COLOR ENCODING TECHNIQUE using multicolored gratings has been investigated by several RCA groups concerned with single-tube color television cameras and at Stanford Research Institute under RCA sponsorship. Its application to color encoding on black-and-white film has been described by Mueller.¹ The encoding filter is placed in contact with the input fiber optics faceplate of the image tube; otherwise, there is no modification of the monochrome camera.

The encoding filter

The encoding filter shown in Fig. 1 was prepared on Eastman color print film. It consists of a cyan grating at 0°, a magenta grating at 90°, and a yellow grating at 120°. When black-and-white film is exposed at the output faceplate by contact printing, the grating structure is superimposed upon the image of the scene photographed. The

presence or absence of the particular grating structure is dependent upon the color of the object photographed. A positive transparency is produced from the negative and color information is restored using a color retrieval projector such as shown in Fig. 2. In the retrieval projector, a decoding filter is placed in the Fourier plane where the diffracted orders appear. Apertures in the decoding filter permit the passage of the diffracted orders but the central zero order common to the three color information channels is either completely blocked or a small fraction is transmitted. Red, blue, and green filter segments are placed over the appropriate apertures to impart color to the three information channels. This results in a reconstructed color image at the viewing screen.

Camera description

The details of the low-light-level color camera utilizing the encoding technique are shown in Fig. 3, and the camera itself is shown in Fig. 4. The camera consists of:

Reprint RE-17-2-1
Final manuscript received August 14, 1970.

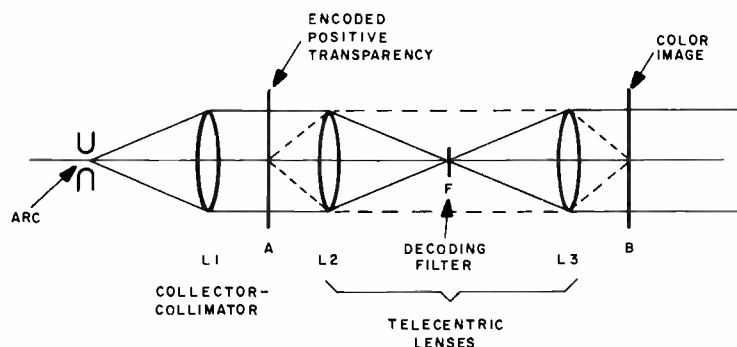


Fig. 2—Color retrieval projector.

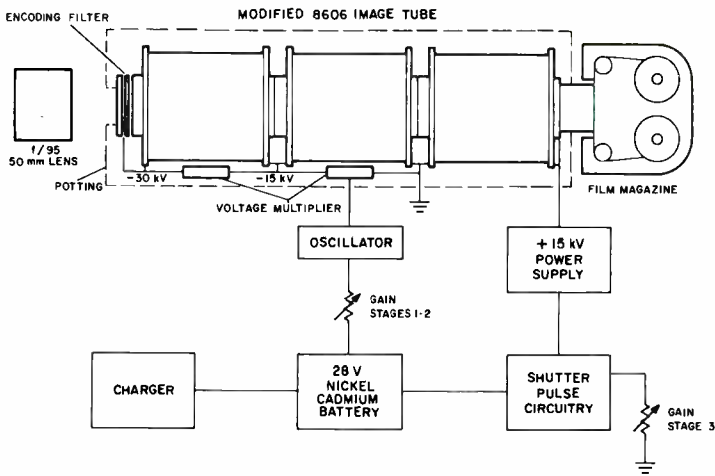


Fig. 3—Block diagram of camera.



Fig. 4—Camera.

- 1) A modified RCA 8606 three-stage (or RCA 8605 single-stage) electrostatic image tube with a 12-line/mm encoding filter,
- 2) A 50-mm f0.95 Canon lens,
- 3) A battery-operated power supply, and
- 4) 70-mm, roll and sheet film Hasselblad magazines.

The encoding filter is held in contact with the fiber optics input faceplate by a glass plate and plastic fixture. Silicone oil is used at the film glass interfaces to prevent Newton's rings. A conductive coating on the inner surface of the glass plate is connected to the photocathode flange to protect the fiber optics faceplate from electrical breakdown. For the three-stage tube, the potting extends over the glass plate and the encoding filter cannot be changed without repotting. For the single-stage tube, the photocathode is at ground potential and there is no conductive coating and no potting.

The three-stage tube is operated with the interface between the second and third stages at ground. The third stage is operated as a shutter and is turned on by a positive pulse applied to the output phosphor screen electrode. Stages one and two operate continuously at -30 kV and -15 kV from the multiplier units potted in the tube housing. A 1500-Hz, 2800-volt oscillator located in the power supply drives the voltage multipliers.

A 0.5-inch-long fiber optics plug in contact with the output faceplate of the image tube transfers the image to the film magazine. It also provides electrical isolation. A conductive coat-

ing on the inner face of the plug is connected to the output flange of the image tube in order to protect the faceplate. When the single-stage tube is used, it is operated as a shutter in the same manner as the last stage of the three-stage tube.

The film magazines are attached to the camera by catches and light seals which are identical to those of the Hasselblad camera. The mounting surface is moved relative to the tube by a knurled ring. In this manner, the film is brought into contact with the fiber optics plug for exposure and is withdrawn for film advance or insertion of the dark slide.

The power supply unit contains these major components:

- 1) An operating panel with controls for turning on and varying the gain of stages one and two or stage three, and setting exposure time at intervals of 0.04, 0.02, 0.01, 0.004, 0.002, 0.001 second or continuously on,
- 2) A 28-volt nickel-cadmium battery and a charging circuit,
- 3) An oscillator for driving the voltage multipliers, and
- 4) A shutter pulse circuit which drives a fast rise time high-voltage supply.

The luminance gain of the 8606 image tube was 120,000 prior to the installation of the fiber optics plug at its output faceplate. With a transmittance of 0.3 for the encoding filter and 0.5 for the fiber optics plug and transparent coatings required for faceplate protection, the effective luminance gain of the three-stage tube is estimated to be 18,000. Other test data on the 8606 before mounting the fiber optics plug were:

Center resolution 36 line pair/mm;
Resolution at 11 mm from center 30 line pair/mm;
Contrast transfer function at center 48% at 12 line/mm;
Magnification at center 0.845;
Magnification 16 mm from center 1.004 (which gives 18.8% distortion at 16 mm).

The 8605 single-stage tube had a luminance gain of 90 prior to installation of the fiber optics plug. The estimated gain in the camera is 17. Its center resolution of 80 line pair/mm was reduced to 56 with the attachment of the fiber optics plug. The center magnification is 0.946, the edge magnification is 1.001 which gives a distortion of 5.81%.

Performance tests

Camera performance tests were made with Panatomic-X film rated at ASA 100 when developed in Acufine. With the single-stage tube, an illumination level of 50 footcandles, a lens aperture of f8 and exposure times from 0.02 to 0.004 second were used. For the three-stage tube, exposures were made at 0.01 footcandles illumination. This simulated full moon light was obtained by attenuating a daylight fluorescent lamp. Lens apertures of f2 to f4 were used with 0.02 to 0.004 second exposure times.

The color performance of the camera is dependent upon the fidelity of the reproduction of the grating at the positive transparency that is placed in the color retrieval projector. The three-stage tube contrast transfer function is 48% at the grating frequency. The

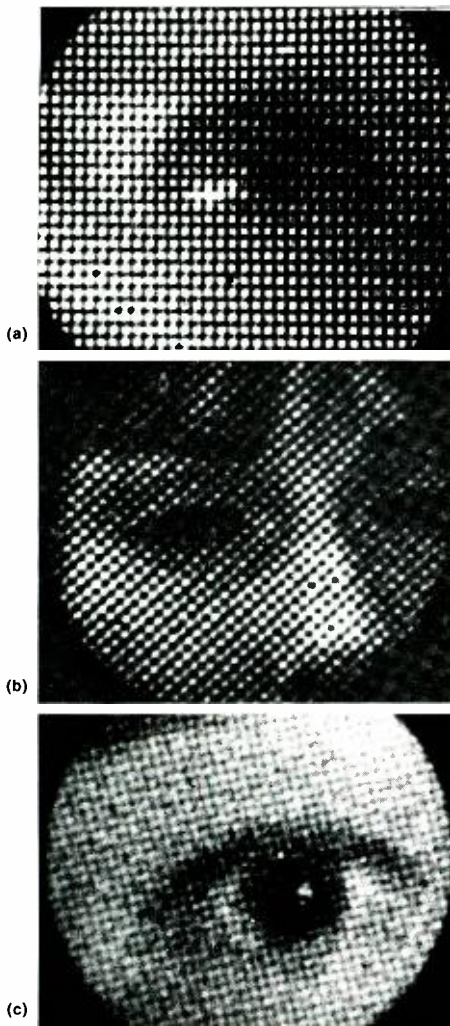


Fig. 5—Microphotographs of grating structure images: (a) encoding filter in direct contact with film, (b) imagery through single-stage tube, and (c) imagery through three-stage tube.

fiber optics plug and contact losses at the encoding filter input faceplate and film output faceplate further degrade imagery. This is illustrated in Fig. 5. A microphotograph of an encoded positive is shown in Fig. 5a when the encoding filter was in direct contact with film in a press camera. In Fig. 5b is shown the imagery through the single-stage tube; and Fig. 5c shows the imagery through the three-stage tube.

Fig. 6 is a print made from the encoded negatives exposed with the single-stage tube at the 50-footcandle illumination condition. The retrieved color image of the cat in Fig. 6 gave reasonably faithful color reproduction over about two-thirds of the area of the tube. The area within the picture frame contains good color reproduction. The cat's tan and white fur as well as green eyes are

well reproduced. In the outer positions of the tube, large red and green areas occur. This color shift is due in part to off-axis aberrations in the image tube which tend to favor certain orientations of the grating lines. In general the reproductions are blue deficient. This can be attributed to imperfections in the yellow grating in the encoding filter and to the low luminosity of the blue decoding filter in the retrieval projector.

The reproduction in Fig. 7 was made from the encoded negatives made at the 0.01 foot candle illumination condition with the three-stage tube and shows the lower resolution and increased distortion given by this tube; also, the effects of noise are apparent at the low illumination level. The colors are correct but subdued. In field tests with the camera, photographs were made with the multistage tube three nights prior to full moon. Retrieved color imaging was obtained from exposures made at 0.01 second and f4.

Conclusions

Tests made with the camera have shown that encoding with multispectral gratings can provide color photography at low light levels with image tubes. Improvements must be made in the imagery of the grating structure at the film in order to enhance performance with multistage tubes. Areas of possible improvement include: use of an interference type encoding filter to



Fig. 6—Retrieved display, single stage camera.

replace the absorption filter (this will have a better defined grating structure and higher light transmission); eliminating the fiber optics plug and conductive coating at the output and replacing with a thick fiber optics faceplate. Magnetic image tubes which have high resolution over a greater area, more gain, and less distortion than electrostatic tubes should be considered if magnet weight and the more stringent power supply performance requirement can be tolerated. Second generation tubes employing micro-channel multipliers should be considered for the color camera when their performance exceeds that of the three-stage electrostatic tubes.

Acknowledgements

Acknowledgment is given to F. E. Shashoua and to K. C. Hudson for the original concept for the low-light-level camera, to R. E. Herr for the mechanical design, to J. F. Schanne for the electrical design. J. C. Moor, W. K. Peifer, and R. G. Stoudenheimer of Electronic Components provided helpful suggestions and assistance in the procurement of the modified image tubes. The camera was constructed for the United States Army Electronics Command under contract DAAB07-69-C-A-109.

Reference

1. Mueller, P. F., "Color Image Retrieval from Monochrome Transparencies," *Applied Optics* (1969) Vol. 8, p. 2051.

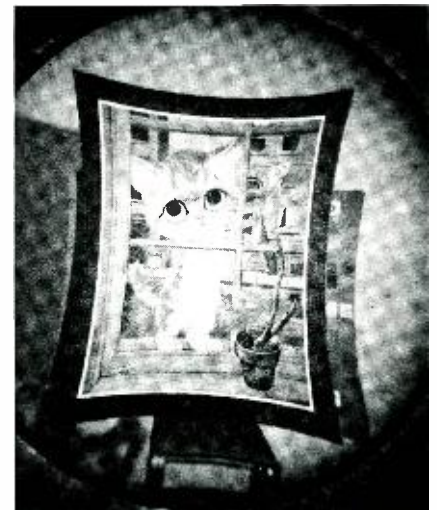


Fig. 7—Retrieved display, three stage camera.

The ideographic composing machine

W. F. Heagerty

This article reports the work being done at Advanced Technology Laboratories on the Ideographic Photocomposing Machine.¹ This effort, which started with Dr. S. H. Caldwell's design of the Sinotype,² has expanded on two fronts. First, the language studies have resulted in a machine vocabulary of over 10,000 characters, including Chinese, Japanese, and Korean. Second, the use of a holographic memory system has resulted in a machine capable of rapid access to the characters while maintaining reasonable machine size and reliability.

William F. Heagerty

Electro-Optics Laboratory
Advanced Technology Laboratories
Camden, New Jersey

received the BEE from Syracuse University in June, 1960 and the MSEE from the University of Pennsylvania in August, 1967. Upon completion of the RCA Design and Development training program, in November 1960, he joined the Applied Research Reading Machine Development Group. In June 1963, he became a member of the design group responsible for the development of a prototype Ideographic Photocomposing Machine. In 1965, Mr. Heagerty was made project engineer, partially responsible for the construction of two engineering models of the photocomposing machine. Since completion of this assignment he has been involved with classified programs. Mr. Heagerty is a member of Tau Beta Pi, Eta Kappa Nu, Pi Mu Epsilon, and IEEE.



A MAJORITY of the people in the world communicate in writing by the use of ideographs. The most common ideographic language is Chinese; however, Japanese and Korean also make use of this form of writing. When considering the intricacy of the ideographs shown in Fig. 1 and the fact that the current Chinese-Japanese Dictionary³ contains 48,902 unique characters (and these are not all in use). The immensity of the communication problem becomes more apparent.

Language studies

The complex structure of the characters (ideographs), plus the highly developed sense of taste for good calligraphy among the readers, necessitates that the characters be stored in machine memory in total rather than in the subcharacters. As the number of stored characters increases to provide composition flexibility, the problem of addressing the memory becomes more formidable. This had been the stumbling block in the development of an ideographic printing machine.

Traditionally the characters have been ordered in a number of ways,⁴ all with difficulties:

- 1) Telegraphic code number—In this system a character is assigned an arbitrary number. The coders who use this method can remember about 2500 code groups. This level of performance is achieved after a long training period.
- 2) Alphabetical order by Romanization of pronunciation—Within this listing there is no direct relationship between character form and pronunciation. Also, a single pronunciation may contain a long list of characters.

Reprint RE-17-2-3
Final manuscript received April 30, 1970



Fig. 1—Typical ideographs.

3) Radical index—This index orders the characters under 214 radicals. The character radical may be difficult to locate and sometimes does not exist in the structure of the character. Further subdivision by residual stroke count is helpful, but the residual stroke count may be difficult to determine.

4) Total number of strokes—Since a character may contain more than 36 strokes, determining the count is difficult. Then, long lists of characters appear under various counts.

5) The four corner system—This system is based on the form of the corners of the character. Here many forms are ambiguous.

The efforts of Dr. Caldwell resulted in another cataloging system. Twenty-one basic strokes that are used to handwrite the characters were determined. Characters were then cataloged by the stroke sequence used in handwriting. Fig. 2 illustrates the stroke sequence concept with Romanization of strokes.

This cataloging method has the distinct advantage of being easily learnable. Chinese students are taught the stroking sequence in a fairly rigid manner in school. Hence, the composing machine operator need not learn a new indexing method. The uniqueness of the stroking sequence as a cataloging method has been ascertained as a result of the language studies. Within the 10,000 characters there are 271 pairs, 15 triads, and a single quad of "ambiguous" characters. The ideographic composing machine (ICM) is designed to handle these cases.

One form of Korean writing uses ideographs. The Korean ideographs

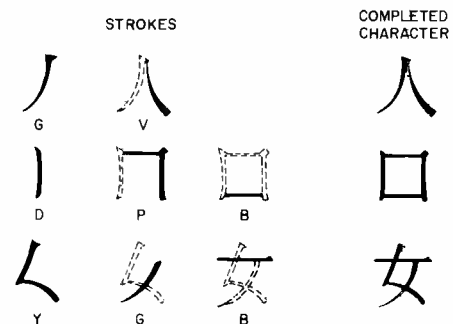


Fig. 2—Stroke sequences.

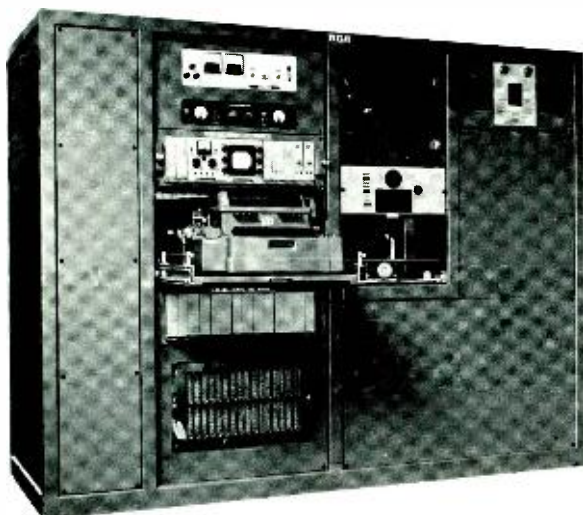


Fig. 3—Ideographic composing machine.

are interchangeable with the Chinese except the meanings change. Since some current Korean characters are not current on the Chinese list, a portion of the machine memory is allotted to these characters. The remainder of the memory is reserved for Japanese.

Japanese uses ideographs as the Korean language does. That is, the ideographs are written as the Chinese except meanings change. Some ideographs in current usage in Japanese are not current in either Chinese or Korean. The Japanese Kana forms are also included in the machine vocabulary.

The results of the language studies are

that 3865 characters are common to all languages. The total ICM character count for the various languages are as follows:

Language	Total characters
Chinese	9958
Japanese	5394
Korean	4834

System description

To use the ICM (see Fig. 3) an operator familiar with the language to be composed enters the proper stroke sequence at the keyboard. Along with the 21 basic strokes, the keyboard has punctuation, ambiguous character selection, operational, and entity keys. The entities are stroke sequences or

“phases” frequently used in the construction of ideographs.

All outputs from the keyboard enter the gating logic shown in the system block diagram of Fig. 4. The code groups entering the gating logic are sorted into four categories. Operational codes such as “photograph” are gated to perform their function. Punctuation and strokes enter the shift register as 5-bit codes. Entities are converted to their equivalent stroke sequence and are gated into the shift register.

The shift register stores the 5-bit stroke codes as they are entered from the keyboard. A maximum of twenty strokes are stored and sent to the coincidence detector. The coincidence detector also receives all legitimate stroke combinations from a magnetic drum. When coincidence is detected, the contents of a drum counter are gated to the storage register; the entered stroke sequence has been identified as a legitimate character. This sequence has been assigned a number which identifies its position in the optical memory. The optical memory is read out and displayed on a kinescope for operator verification. When verified, the character is recorded on film by operation of the keyboard photograph bar. The operational keys (photograph, line shift, space shift) can cause the film camera to perform in a manner analogous to a typewriter. The erase key allows correction of erroneous stroke sequences. The characters are recorded on 5-inch film in any of four font sizes. An engraved plate is made from the film for the final step of printing.

Optical memory

The ideographs used in the photo-composing machine are stored in the optical memory as holograms. The storage medium is a Kodak 649 silver halide emulsion on a glass disc as illustrated in Fig. 5.

The hologram is addressed as shown in the optical memory block diagram of Fig. 6. The digital address store contains 14 bits to select one of 10,000 characters. This word is broken into three parts consisting of 3 bits, 7 bits, and 4 bits. The first 3 bits are used to address the galvanometer driver and cause selection of one of five disc

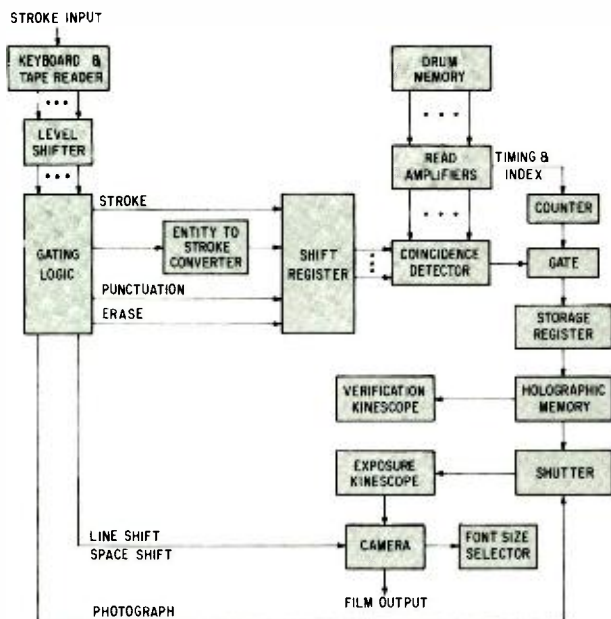


Fig. 4—System block diagram.

Color decoding projector for low-light-level color photography

Dr. L. J. Nicastro | E. Hutto, Jr.

A color decoding projector has been designed to retrieve color images from encoded monochrome transparencies obtained with the low-light-level camera described in this issue.¹ The method of color encoding monochrome transparencies uses the Fourier transform property of lens systems in the decoding process. Thus, in the encoding-decoding system described, storage of the encoded image on the transparency provides the transition mechanism between an incoherent optical recorder (a camera used with ordinary illumination) and a coherent retrieval device (the color decoding projector which utilizes a spatial filtering system).



Dr. L. J. Nicastro

Electro-Optics Laboratory
Advanced Technology Laboratories
Camden, New Jersey

received the BA in Physics from La Salle College in 1953, the MS in Radiation Biology from the University of Rochester in 1956, and the PhD in Physics from Temple University in January, 1970. Dr. Nicastro was an instructor in Chemistry and Physics at La Salle College, 1953-1954; a Physicist in Ballistics at the Frankford Arsenal, 1954-1955; and a Health Physicist at the Brookhaven National Laboratories during the summer of 1956. From 1956 to 1959, he worked in the Neutron Physics Section of the National Bureau of Standards on neutron spectrometry, measurements of neutron age and neutron cross-sections, neutron detection methods, and the response of various scintillators to alpha particles. Since coming to RCA early in 1959, Dr. Nicastro has done experimental work in the areas of gaseous molecular frequency standards, laser radar, measurement of fluorescent time constants of laser materials, and measurement of plasma properties using lasers. Dr. Nicastro has been involved in experimental and analytical studies in the general area of display techniques, including modulation of light by means of magneto-optic rotators and electro-optic crystals, laser displays, and measurements of the negative resistance effect in cadmium selenide powders. Recently, Dr. Nicastro has been engaged in work on the development of liquid crystal displays.

E. Hutto, Jr.

Electro-Optics Laboratory
Advanced Technology Laboratories
Camden, New Jersey

received the BSEE from Clemson College in 1947 and joined RCA as a member of the engineer training program. From 1948 to 1953, he was with the Home Instrument Optical Group working on optical components for Schmidt projection television systems and in colorimetry for home color TV receivers. In 1953, he joined the Optics, Sound, and Special Engineering Section, responsible for an electronic lens bench for the evaluation of television and photographic lenses. His work has also included optical systems for color television cameras and projectors. Mr. Hutto, has participated in studies involving aerial reconnaissance by television and photographic techniques. He was project engineer on two programs utilizing image tubes in photographic cameras and a study program investigating techniques for low-light-level color photography. He is currently engaged in the development of a camera in which color information is encoded on black-and-white film. Mr. Hutto has been actively concerned with optical systems for use with injection and gas lasers in illuminator and scanning devices.

Reprint RE-17-2-2

Final manuscript received March 9, 1971.

IN RECENT YEARS, stimulated by the discovery of the laser, studies in coherent light techniques have uncovered or rekindled interest in several optical phenomena. One of these is the Fourier transformable property of lens systems.² That is, just as one-dimensional electrical signals can be looked upon as having an integrally related time domain and frequency domain, two-dimensional optical images can have two-dimensional spatial frequencies which have similar integral relationships. The front and back focal planes of lenses possess the desired Fourier transform relationship.

In electrical communication systems, frequency multiplexing allows many information signals to exist on a single link by having each signal modulate a different carrier frequency. When this same powerful technique is applied to optical images, it offers the potential for storing many images on a single two-dimensional surface. For example, one image can be stored on a transparency by exposing the film through a vertical diffraction grating held in contact with the film, while another image can be superimposed through a horizontal diffraction grating. From a spatial frequency viewpoint, each image contains only DC and relatively low spatial frequencies. Each image also amplitude-modulates the relatively high spatial frequency due to the grating, so that the resultant spectrum contains the original low-frequency signal plus a modulated high-frequency signal.

If collimated light is passed through the transparency and focused by a lens, the Fourier transform of the

transparency's spatial frequency spectrum is obtained at the focal plane of the lens; in terms of diffraction grating theory, the Fraunhofer diffraction pattern of the transparency is displayed at the focal plane. The most significant feature of the Fourier transform plane is that the two superimposed images are spatially separated, and can be reimaged to recreate each image separately. Using this technique, Mueller^{3,4} has devised a method of recording and retrieving full color images with panchromatic black-and-white film. Hutto⁵ also has used the technique in developing a camera for low-light-level color photography. In fact, the color decoding projector described below was designed to retrieve color images from encoded monochrome transparencies obtained with Hutto's low-light-level color camera.

Color encoding and decoding

Color encoding of black-and-white film is carried out by placing a specific set of gratings in contact with the film to be exposed. The gratings that are used are similar to Ronchi rulings, which are made up of alternate clear and opaque bars of equal and constant width. When an exposure is made through a Ronchi ruling held in contact with the recording film, the image obtained contains alternating bars of low and high density. If collimated light is passed through either the original Ronchi ruling, or one of the gratings produced on film, some fraction of the transmitted light is diffracted. When the diffraction pattern is observed at the transform plane, it appears as a linear array of spots oriented perpendicular to the direction of the grating bars (see Fig. 1). The bright central spot of the array, which represents the light that is not dif-

fracted by the grating, is referred to as the DC or zero order. The spots symmetrically distributed on either side of the central maximum are the first, second, third, etc. orders. For Ronchi rulings, all the even orders (2, 4, 6, etc.) are missing. This comes about because the distance between clear bars is twice the width of a clear bar, and this is just the condition for having all even orders missing.⁶

When the grating is rotated, the orders of the diffraction pattern are angularly displaced from their original positions in the transform plane. Thus it can be seen that if Ronchi rulings of different angular orientation are overlapped, the various sets of orders will be spatially separated in the transform plane. To achieve a color system, three gratings must be constructed such that each has the capability of modulating a single primary color. The required gratings have clear bars alternating with bars of a subtractive color: cyan to modulate red, magenta to modulate green, and yellow to modulate blue.

The encoding filter used in the low-light-level color camera was fabricated by superimposing three gratings at different angles on a single substrate of Eastman color print film. This filter, depicted in Fig. 2, consists of a cyan grating oriented at 0°, a magenta grating oriented at 90°, and a yellow grating at 120°; each grating has 12 line pairs per millimeter. When black-and-white film is exposed, the encoding filter is held in contact with it, so that the grating structure is superimposed upon the image of the photographed scene. The presence or absence of a particular grating structure in the exposed film is determined by the color of the object photographed: the cyan grating produces alternate light and dark bands at 0° if the object is red; the magenta grating produces alternate light and dark bands at 90° if the object is green; and the yellow grating produces alternate light and dark bands at 120° if the object is blue. Other colors produce structures corresponding to a combination of the gratings. Thus the color of the photographed scene is stored on the exposed black-and-white film by the superimposed structure of the gratings. For retrieving the color, a positive transparency must be ob-

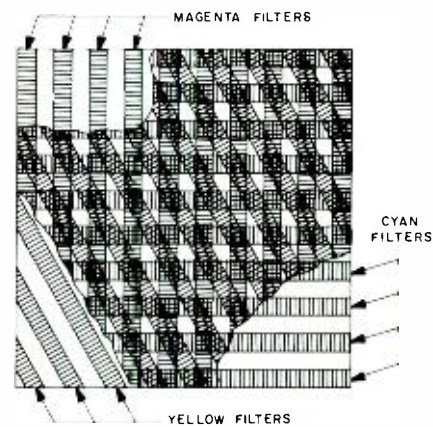


Fig. 2—Encoding filter.

tained from the negative of the photographed scene, and this in turn is used in the color decoding projector.

To reconstruct the original color scene, an intense collimated beam of white light is passed through the encoded film transparency. The beam is diffracted and a spatial separation of the diffraction patterns due to the three gratings superimposed on the transparency is obtained at the transform plane. An example of the diffraction pattern obtained from an encoded transparency is shown in Fig. 3. In the figure, the central DC order is surrounded by several diffraction orders for each of the three gratings; the even orders of the diffraction patterns are missing, just as is required for Ronchi rulings.

In encoding the transparency, the cyan grating was oriented at 0°. Therefore, from Fig. 1, the diffraction pattern at the transform plane due to the red information is oriented at 90°. Simi-

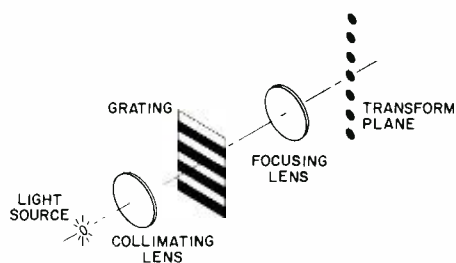


Fig. 1—Illustration of diffraction by a grating.

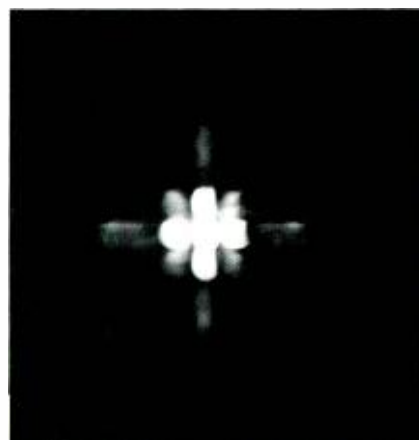


Fig. 3—Fourier transform (Fraunhofer diffraction pattern) of a color encoded transparency.



Fig. 4—Decoding filter.

larly, because of the orientations of the magenta and yellow gratings in the encoding process, the diffraction pattern at the transform plane due to the green information is oriented at 0°, and that due to the blue information is oriented at 30°. Since all three gratings superimposed on the transparency diffract all the colors of the collimated white light source, the primary color information at 0° (green), 30° (blue), and 90° (red) must be extracted by means of filters. This is accomplished by placing at the transform plane a specially designed mask with apertures oriented at 0°, 30°, and 90°. When the apertures at the appropriate angles are fitted with green, blue, and red filters, the mask is called the decoding filter. One of the decoding filters used in the projector is shown in Fig. 4. This figure shows that the central DC order is prohibited from passing through the filter. When all of the DC order is allowed to pass,

a black-and-white projection of the transparency is obtained because the weaker color information is completely desaturated. When the DC order is not allowed to pass, a color image of the original scene is projected onto the screen.

Detailed description

The essential components of the spatial filtering system of the color decoding projector are illustrated in Fig. 5. In the projector, a plane wave illuminates the color encoded positive transparency, and the Fourier transform of the transparency is produced at the back focal plane of the focusing lens. The images encoded on the transparency are spatially filtered at the transform plane, then projected onto the screen. The mirrors in the system are used for folding the optical path, so that the length of the projector does not become cumbersome.

The projector was designed for use with transparencies obtained with the low-light-level color camera. These transparencies have a diameter of 1.65 inches and are encoded at a grating frequency of 12 line pairs per millimeter. Provisions have also been made for accommodating transparencies encoded with higher grating frequencies.

Referring to Fig. 5, two 100-mm focal length lenses image the 450-watt xenon arc lamp at unity magnification on a pinhole aperture. A 0.05-inch diameter pinhole is used for the transparencies encoded at 12 line pairs per millimeter; larger pinholes are also available for transparencies encoded at higher frequencies. Identical 191-

mm focal length doublet lenses are used for the collimating and focusing lenses. Thus an image of the pinhole with unit magnification is formed at the decoding filter-transform plane.

The decoding filter has green, blue, and red absorption filters covering 1/32- by 1/4-inch slotted apertures oriented at 0°, 30°, and 90°. The slots, which allow the diffracted orders to pass through, extend radially from the center of the decoding filter beginning at a radius of 0.033 inch. If the slots were brought any closer to the center, then some of the light from the zero order might pass through them.

The positions of the diffracted orders at the transform plane can be determined from the grating equation:

$$m\lambda = d \sin \theta = (1/F) \sin \theta, \quad (1)$$

and the equation that determines the lateral displacement of the diffracted order at the focal plane:

$$s = f \tan \theta. \quad (2)$$

In these equations, m is the order of diffraction, λ is the wavelength, d is the grating spacing, F is the grating frequency, θ is the angle of diffraction, f is the focal length of the focusing lens, and s is the lateral displacement of the diffracted order. Since the diffraction angle is small,

$$\sin \theta \approx \tan \theta \approx \theta.$$

Therefore, Eq. 1 and 2 may be combined to give

$$s = mfF\lambda. \quad (3)$$

With $m = 1$, $f = 191$ -mm, $F = 12$ line pairs per mm, and $\lambda = 5000 \text{ \AA}$, the maximum of the first diffraction order will fall at a distance of 0.045 inch from the center of the decoding filter when it is properly positioned at the transform plane. Since the slotted apertures of the decoding filter begin at a radius of 0.033 inch, the maxima of the first diffraction orders fall at a position only 0.012 inch inside the edges of the decoding filter slots. These considerations dictated the design of the decoding filter. The diffracted orders could have been made to fall further out from the center by selecting longer focal length collimating and focusing lenses, but then the light collection efficiency of the system would have been lower.

The decoding filter is provided with rotational, horizontal, vertical, and longitudinal motions so that alignment with the diffraction image may

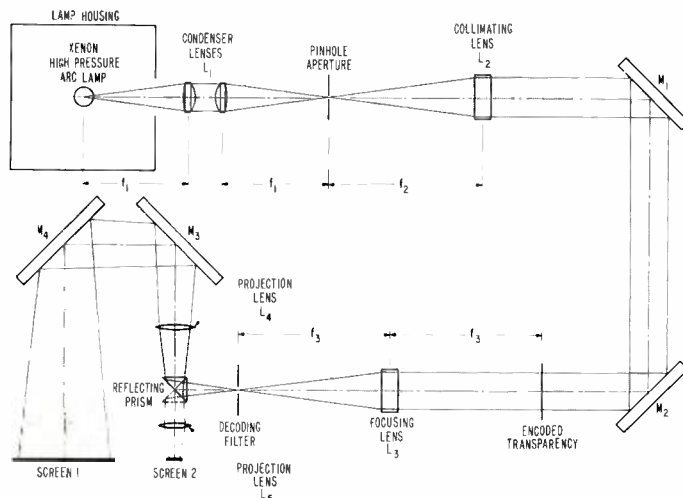


Fig. 5—Schematic diagram of color decoding projector.

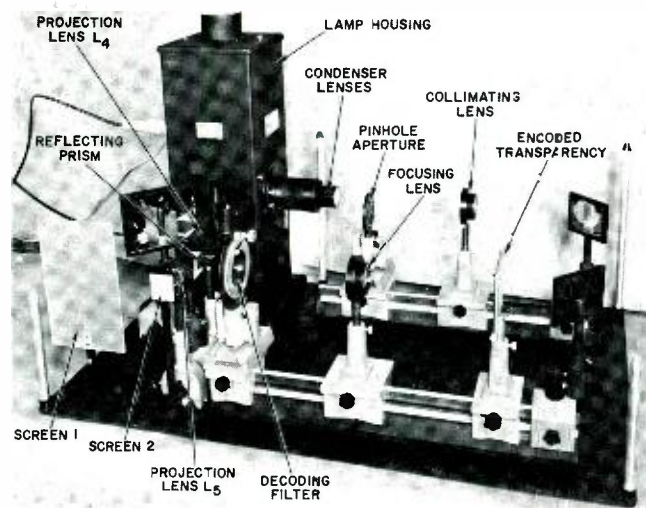


Fig. 6—Color decoding projector.

be easily optimized for maximum light transmission. A plug at the center of the filter normally prevents the undiffracted zero order from being transmitted. However, a small fraction of the zero order may be passed to desaturate the projected display. This is done by removing the plug and covering the hole with a neutral density filter that passes 1 or 2% of the zero order. The decoding filter that has been described can be used for transparencies encoded with grating frequencies up to about 60 line pairs per millimeter. For use with encoded transparencies having even higher grating frequencies, decoding filters with larger apertures can also be accommodated in the filter mount.

A prism located in the optical path beyond the decoding filter can be rotated to direct the light through either of two projection lenses. When directed to the 500-mm focal length lens (L_4 of Fig. 5), the color decoded image of the transparency is projected onto a rear projection screen and enlarged 2.6 times to a diameter of 4.35 inches. In the other position, the prism directs the light to a 55-mm focal length lens (L_5) which projects a 0.48-inch diameter image at 0.29 times magnification onto a small high-resolution screen. At this screen the small image may be photographed with color film or viewed with a microscope.

Results and conclusions

The color decoding projector is shown in Fig. 6, where the components are

labeled the same as in Fig. 5. A closeup view of a projected color image obtained from an encoded transparency is shown in Fig. 7. The principal difficulty with this projection system, low light efficiency, is clearly illustrated in this last figure, where it may be noticed that the brightness of the projected image is low compared to the brightness at the encoded transparency. Using a high-gain screen, the highest brightness obtained with a projected color image is about 10 footlamberts. This low brightness is due to the small pinhole aperture and the long focal length collimating and focusing lenses, both of which are required because of the 12 line pairs per millimeter grating frequencies. Since it is estimated that

only about 10% of the lamp light is collected, significant improvement in brightness could be obtained by encoding the transparencies with higher grating frequencies. This would allow the use of a larger pinhole aperture and shorter focal length collimating and focusing lenses, thus increasing the amount of collected light. Another large loss in light is due to the fact that four mirrors and a reflecting prism are used for folding the optical path to keep the size of the projector within reasonable limits. This loss could be reduced by using antireflection coated prisms in place of the metallic mirrors. When these improvements are made, the brightness of projected images should increase by as much as 10 times.

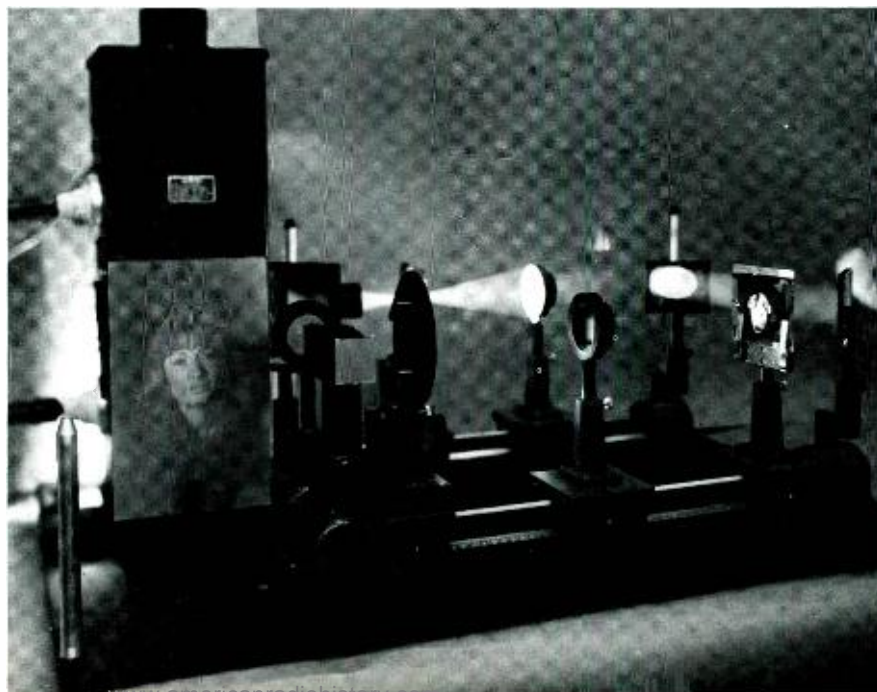
Acknowledgements

The authors thank J. J. Rudnick for many helpful suggestions concerning the overall design of the color decoding projector, and B. W. Siryj, J. Bonacquisti and J. Cies for assistance in the mechanical design. The projector was constructed for the United States Army Electronics Command under Contract No. DAAB07-70-C-A144.

References

1. Hutto, Jr., E., "Low-Light-Level Color Photography," *this issue*, RCA Reprint RE-17-2-1.
2. Goodman, I. W., *Introduction to Fourier Optics*, McGraw-Hill (New York) 1968.
3. Mueller, P. F., "Linear Multiple-Image Storage," *Applied Optics* (1969) Vol. 8, p. 267.
4. Mueller, P. F., "Color Image Retrieval from Monochrome Transparencies," *Applied Optics* (1969) Vol. 8, p. 2051.
5. *Op. Cit.*, Hutto, Jr., E.
6. Jenkins, F. A. and White, H. E., *Fundamentals of Optics*, 2nd Edition, McGraw-Hill, New York (1950) p. 324.

Fig. 7—Projected color image and an encoded transparency.



Measuring optical properties of water *in situ*

Dr. L. E. Mertens | W. H. Manning, Jr.

An underwater instrumentation system has been developed to permit virtually simultaneous *in situ* measurement of those optical parameters useful in predicting performance of long-range underwater imaging and communications systems. This paper describes the basic design and performance of this instrumentation system.



Walter H. Manning

Dr. L. E. Mertens, Chief Scientist
Missile Test Project
Eastern Test Range
Patrick AFB, Florida

has staff responsibility for RCA scientific and technical work on the Eastern Test Range. He is a technical consultant on the ARPA Advanced Sensors Programs and on range calibration for the AUTEK range. Prior to his present assignment, he held a variety of positions with RCA Government and Commercial Systems including Manager, Systems Engineering, Manager, Digital Communications Equipment Engineering, and on the technical staff of the Chief Defense Engineer.

Walter H. Manning, Jr., Director
Range Measurements Laboratory
Advanced Research Projects Agency
Office of the Secretary of Defense

holds the BS and MS in Physics. Mr. Manning is Director of the Range Measurements Laboratory (RML), which is responsible for investigations and analyses of the effects of various physical phenomena on instrumentation associated with the development of spacecraft and missiles. The RML has developed many advanced techniques in tracking, electro-optical, and underwater systems in connection with projects carried out for the Advanced Research Projects Agency of the Office of the Secretary of Defense.

TRANSMISSION of optical images in water is controlled by a large number of parameters which determine the photon level, contrast, and resolution of the image. The basic parameters describing the optical properties of water are well known and include the volume attenuation, scattering, and absorption coefficients as well as the volume scattering function which describes the angular distribution of the scattered light.

Conventional instrumentation for measuring these parameters is not entirely adequate for studying image transmission and communications over long water paths. The principal difficulty is associated with the very strong narrow-angle scattering of light produced by water. Scattering at angles as small as a hundredth of a degree or less can be important for image propagation, and conventional instrumentation does not respond appropriately in this narrow-

angle region. In addition, measurement accuracy must be exceptionally high. This is particularly true for propagation over long paths since many of the relations describing light transmission in water are exponential in nature. Small errors in the propagation constants become very significant when operation is attempted over many attenuation lengths. For example, a 0.01m^{-1} measurement error in the volume attenuation coefficient leads to an error of a factor of nearly 3 in transmission loss over a 100 meter path.

In principle, appropriate measurements of the above basic quantities are sufficient for analysis and prediction of image transmission in water. In practice, however, it is desirable to also have additional measurements of a) thermal and salinity microstructure and b) the water path transmission for certain conceptually simple signals such as a point sources, collimated beams, and spatial squarewave or sine-

Reprint RE-17-2-71

Final manuscript received May 11, 1971.



Dr. Larry Mertens

wave patterns. It is well known that small thermal and salinity fluctuations (inhomogeneities) produce gradients in the refractive index of the medium and are thus responsible for a significant portion of the scattering in the narrow-angle region. Microstructure measurements can be used to supplement conventional volume scattering measurements for predicting image resolution.

The complex multiple scattering of light which occurs in water is very difficult to describe accurately in terms of the basic absorption and scattering parameters. As a result, it is desirable to perform a number of measurements over relatively long paths. These measurements can be used to confirm the various transmission models and are also more easily and accurately extended to the actual imaging system geometry.

It would be most convenient if suitable optical measurements could be made on water samples in either shipboard or shore-based labs. Unfortunately, such measurements are subject to many sources of error due to contamination in sampling and handling and changes in particle concentration. Bio-

logical particles are known to be responsible for a significant portion of the optical scattering and absorption in seawater. The relative concentration of the various biological particles is subject to large change in periods of only a few hours. Even with special storage and handling procedures, the accuracy of data from water samples is subject to question. Furthermore, the very narrow-angle scattering properties of water are largely due to the thermal and salinity microstructure, which we have no practical way to preserve in the sampling procedure. Consequently it is essential to measure the important optical parameters *in situ*.

Furthermore since the water properties are subject to change with time and location it is desirable to make the necessary measurements as near simultaneously as possible.

The original goal was to develop a single cluster of instruments for measuring the above quantities to depths of approximately 300 meters. Practical problems associated with the size of the instruments, the number of measurements, and deployment at sea made it desirable to divide the instrumenta-

tion into two separate systems. One of these instrumentation systems, called the *cluster*, measures the more or less conventional optical and oceanic parameters; it is relatively small and readily deployed. The second instrumentation system, called the *long optical bench*, is used for measurements requiring longer optical paths. The long bench requires a larger ship such as the Deep Look support vessel for deployment.

Cluster

The cluster (Fig. 1) is basically a combination of conventional optical and oceanic instrumentation. It weighs approximately 125 pounds in air and is normally adjusted for slightly negative buoyancy in water. A mechanical damper is used in conjunction with the cluster to decouple it from wave action on the support vessel.

The cluster measures volume attenuation coefficient, α ; volume absorption coefficient, a ; diffuse attenuation coefficient, k ; salinity; temperature; current direction; current speed; and depth. Resolution of the salinity and temperature measurements is sufficient for measuring the microstructure fluctuation.

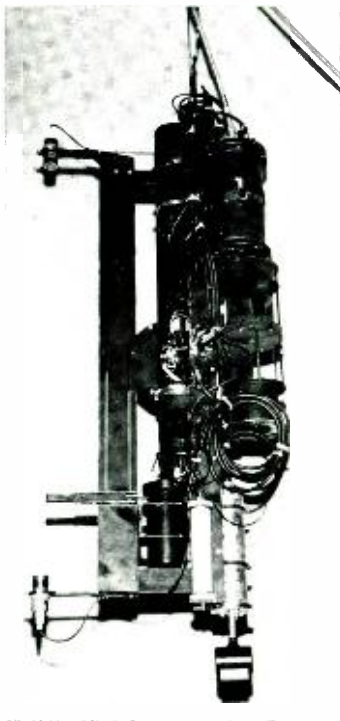


Fig. 1—Instrumentation cluster.

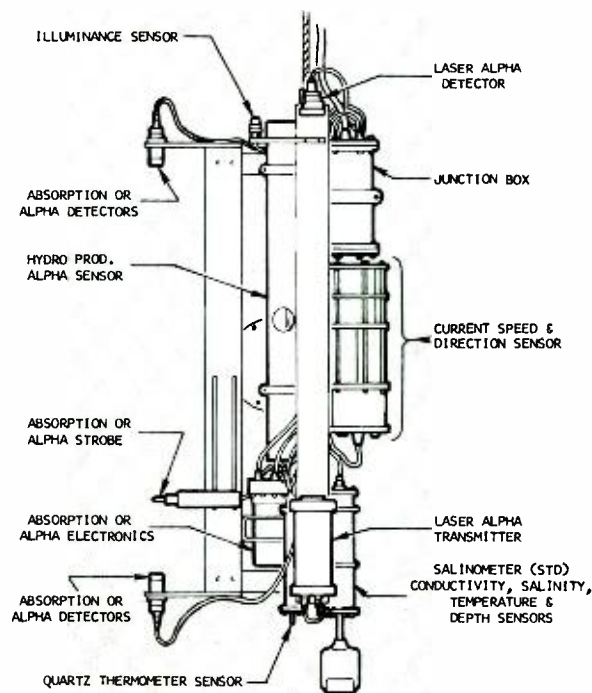


Fig. 2—Schematic drawing of the instrumentation cluster showing location of the various sensors.

RT TIME	TEMP	COND	TIMS	SRMS	ALP	ABS	SCAT	SPD	DIR	DP
13:46:19	22.845	00.046	7777	0054	.046	.001	.851	2.00	0004	0001
13:47:19	22.418	00.046	3225	0078	.030	.002	.032	2.00	0079	0001
13:48:19	27.863	00.046	0552	0078	.030	.001	.022	2.00	0080	0001
13:49:19	27.794	00.047	0054	0078	.028	.001	.027	2.00	0078	0001
13:50:19	27.543	01.757	3443	7777	.062	.007	.024	2.55	0109	0004
13:51:19	26.338	56.247	0191	0197	.111	.046	.064	0.32	0111	0004
13:52:19	26.323	56.234	0163	0182	.115	.043	.071	0.70	0150	0004
13:53:19	26.326	56.230	0144	0113	.105	.048	.056	0.75	0150	0004
13:54:19	26.330	56.225	0156	0156	.105	.043	.062	0.10	0157	0005
13:55:19	26.321	56.215	0156	0054	.106	.047	.058	0.67	0142	0005
13:56:19	26.307	56.196	0163	0095	.100	.047	.058	0.67	0144	0006
13:57:19	26.077	56.168	0156	0134	.125	.053	.052	0.63	0146	0009
13:58:19	26.268	56.148	0078	0197	.106	.054	.051	2.55	0151	0017
13:59:19	26.247	56.125	0099	0173	.106	.066	.039	2.62	0141	0019
14:00:19	26.242	56.118	0156	0054	.106	.063	.042	2.57	0149	0026
14:01:19	26.222	56.099	0156	0095	.106	.062	.043	2.63	0142	0031
14:02:19	26.217	56.096	0144	0095	.107	.066	.041	2.62	0153	0031
14:03:19	26.218	56.096	0078	0095	.106	.064	.042	2.63	0148	0031
14:04:19	26.219	56.097	0078	0078	.106	.069	.037	2.57	0148	0031
14:05:19	26.221	56.098	0163	0163	.106	.065	.042	0.39	0150	0031
14:06:19	26.221	02.105	0173	7777	.105	.067	.038	0.59	0149	0031
14:07:19	26.219	56.094	0054	0095	.106	.067	.039	0.56	0151	0033
14:08:19	26.185	56.088	0325	0003	.106	.068	.037	0.54	0146	0039
14:09:19	26.109	56.081	0163	0122	.105	.067	.038	0.53	0153	0043
14:10:19	26.261	55.907	0588	0552	.125	.065	.040	2.48	0159	0052
14:11:19	25.942	55.863	0054	0163	.107	.068	.038	2.56	0144	0051
14:12:19	25.924	55.839	0034	0290	.108	.070	.038	2.54	0146	0056
14:13:19	25.882	55.786	0163	0027	.103	.070	.038	2.55	0145	0062

Fig. 3— Typical data printouts.

tuations as well as gross profiles. A multiconductor video cable is used to transmit data from the sensors to the instrumentation processing units on deck. A low-noise multiconductor slip ring is employed so that data can be recorded while the cluster is being raised and lowered.

Data recording

Data is recorded in real time on an 8-channel analog recorder. Certain of the quantities such as temperature, salinity, and depth can be recorded with expanded resolution and automatic scaling. The expanded resolution permits display of 0.01°C full scale, and the automatic recycling feature keeps the pen recorder from exceeding full scale by changing the zero reference in known steps. The resulting recordings are, of course, ambiguous to within integral multiples of the full cycle value, but absolute measurements can be reconstructed by tracing the record from a known absolute value or by referencing the time point to digital records which are also made.

All of the instrumentation data is digitized for input to a XDS-CF16 mini-computer. The computer records data points on a magnetic tape at a nominal 1 per second rate but has the capability of recording certain quantities such as the microstructure fluctuations at rates up to 10 per second. The computer can print out in near real time any desired combination of the optical or oceanic parameters. The print outs are nor-

mally made in either a *time* or *depth* mode. The time mode prints out the selected parameters at equal time intervals—normally 10, 20, 30, 40, 50 or 60 seconds. In the depth mode, a print-out is made for equal increments in depth—normally 5, 10, 15, 20, 25 or 30 meters. Certain simply derived functions of the parameters such as the scattering coefficient and RMS fluctuations of the parameters can also be printed out.

An analog magnetic recorder is also available as a backup to the digital data recorder. Either of these recorders can be played back through the shipboard computer to check system performance or for quick look data analysis. The digital magnetic recording is used for post-tests reduction on a XDS Sigma-7 computer.

Volume attenuation coefficient

Two types of instrumentation are available on the cluster for measuring α , the volume attenuation coefficient. One instrument employs a pulsed Xenon flash tube with reference and data paths of 0.25 and 1.25 meters respectively. The light beam is shaped by a series of apertures and is on the order of 1/2 inch. Wratten filters are used in the detectors to obtain a peak response in either the 480 or 530-nm spectral ranges. Infrared filters are employed to block any red or infrared light passed by the Wratten filters. The electronics associated with the α -meter computes the α and displays the result

on direct digital read outs, as well as supplying electrical signals to the analog and digital recorders. Considerable effort has been employed to make the electronics drift free, insensitive to background ambient light, and independent of source intensity. The α -meter can be simply calibrated on deck using an air path for reference. Calibrated neutral density filters are available to confirm system accuracy and linearity.

The second α measurement is made with a small pulsed Argon laser. The laser output is collimated with a simple optical system and projected over a 1.5 meter path. Longer paths are not normally employed in view of the desire to keep the system small and easily deployed. Individual spectral lines of the Argon laser can be selected by means of interference filters. The laser α -meter is normally calibrated in air. However, calibration in water by moving the detector position is occasionally performed to verify the in-air calibration. The major calibration factor is due to a change in reflection from the optical windows when the device is immersed in water. A beam splitter and reference cell are employed to compensate for any drift in the laser power output.

Volume absorption coefficient

The volume absorption coefficient is measured with a pulsed Xenon system based on a design of Gilbert and Honey of SRI. The absorption instrumentation is actually the same physical system as used for the pulsed Xenon α -meter. The only difference is that the beam-forming baffles are removed and the system then responds to light scattered from the nearly omni-directional source. The principal difficulties encountered with the absorption measurement involve reflections from nearby instrumentation. Reflections can be calibrated out by measurements made on deck before or after testing. The accuracy of the absorption measurements is also degraded in shallow water where surface or bottom reflections cause additional light input to the photo cells. The accuracy goals for the α and a measurements of the cluster are $\pm .01m^{-1}$. Extensive testing indicates that the instrumentation can achieve this accuracy with the exception of absorption in shallow water.

Diffuse attenuation coefficient

The cluster also contains upward- and downward-looking irradiance detectors which are used to determine the diffuse attenuation coefficient of ambient light. A reference cell on deck is employed to correct for the changes in ambient light. The digital computer system can fit and smooth the observed irradiance data to determine its slope and thus the diffuse attenuation coefficient. The diffuse attenuation coefficient is compared with the absorption meter readings for possible calibration errors.

Temperature

Temperature is measured by Hewlett-Packard 2801A Quartz thermometer. This thermometer has excellent accuracy and great flexibility for microstructure measurements. Pushbutton controls permit selection of 0.01, 0.001, and 0.0001° Celsius resolution. The sampling times associated with these resolutions are 0.1, 1, and 10 seconds respectively. The thermometer has two probes and the temperature indicated by either probe or the temperature difference between the probes can be selected for display and recording. The probes have a thermal time constant on the order of 1 to 2 seconds and thus limit the frequency response on the lower resolution scales. The sampling rate, however, is the basic frequency response limitation for the high resolution scale.

Salinity and depth

Salinity and depth are measured by a CM² Model 513 instrument. With slight modification, resolutions of a few parts per million in salinity have been obtained. The salinometer computes the salinity from conductivity, temperature, and pressure measurements. The temperature probe used in the salinometer has a relatively long time constant, and it is preferable to compute salinity in the digital computer from conductivity and depth measurements of the salinometer and temperature measurements from the Quartz thermometer described above.

Depth is measured with the pressure transducer in the CM² salinometer. Resolution of the depth channel can be increased as desired so that fluctuations less than one foot can be monitored to determine decoupling from wave action.

Current speed and direction

Current speed and direction are measured with a Hydro Products Model 460/465A current meter. This data is useful in analyzing the microstructure and in directing the support vessel.

Long optical bench

The long optical bench has been configured around a high-power cw Argon laser. The ionized Argon laser can be operated at a number of discrete wavelengths in the blue-green transmission window of oceanic water. Long mea-

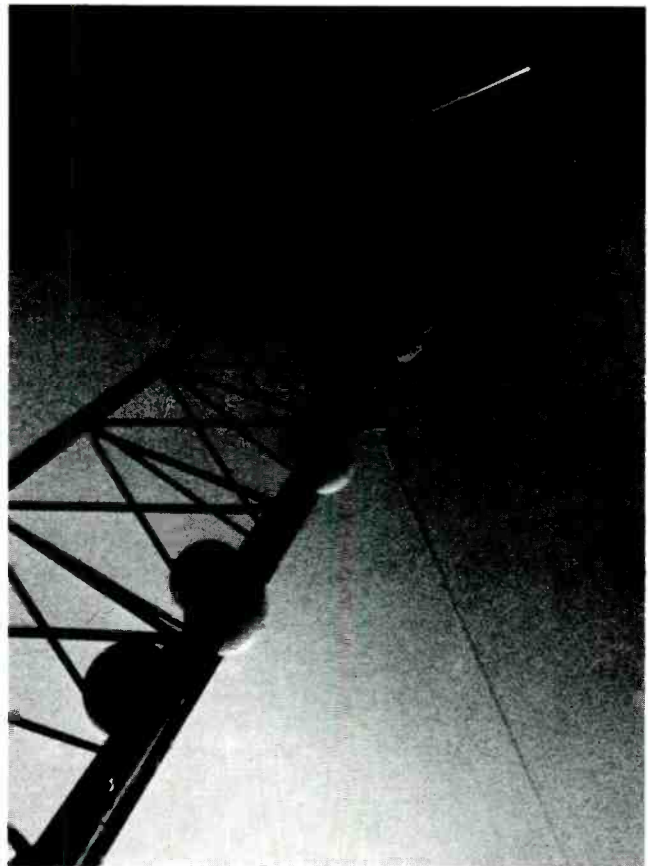


Fig. 4—Photograph of the long optical bench used for a measurement. Spherical balls attached to tower are used to adjust buoyancy.

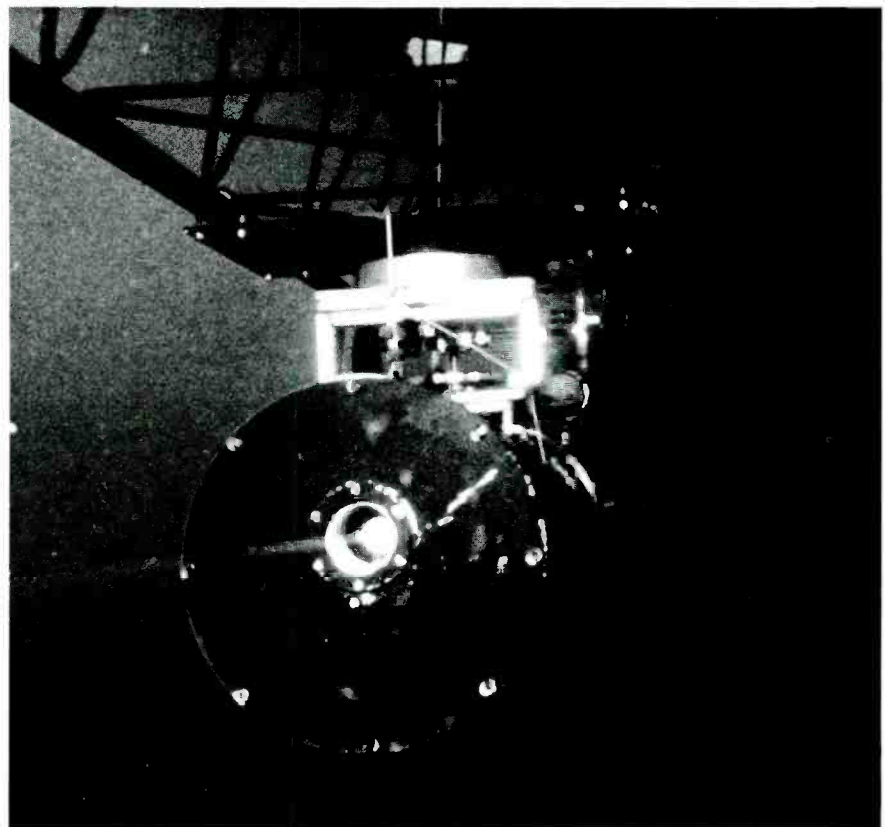


Fig. 5—Close-up of the underwater laser and mount on the long optical bench.

surement path lengths are desired for this instrument so that high accuracy measurements can be performed with instruments having only modest accuracy. Fig. 4 is a photograph of the long optical bench being used to measure α . The bench is constructed of triangular aluminum tower sections approximately two feet on a side and 20 feet long. As normally used, the bench provides an optical path length of approximately 20 meters. Additional sections, however, can be readily added so that the optical path length can be extended as desired to approximately 100 meters. Flexure of the bench provides a practical limit for path length for certain of the experiments. The 20-meter path has less than 1-cm laser-beam deflection when operating in three-foot seas with no special attention to decoupling from wave motion.

The basic performance objective for the long optical bench was to obtain the spectral transmission characteristics of water to an order of magnitude better accuracy than achieved by the cluster. The 20-meter configuration is adequate for this objective. The high accuracy measurements of the long bench measurements can be used to check the performance and calibrate the instrumentation on the cluster. The Argon laser provides a convenient method of generating collimated and monochromatic beams of light. The Argon laser is capable of emitting a number of discrete wavelengths in the blue-green band of water. Normally, we use the 4579, 4727, 4880, 5017, 5145Å lines which are very nearly equally spaced in wavelength across the band. For some purposes, additional lines at longer wavelengths would be desirable but unfortunately are not obtainable with an Argon laser. The 2-watt RCA LD2101 laser has been used for most of the long baseline measurements for the past year. A higher power laser with special anodic bore is planned for future measurements since it is easier to package for deep oceanic operation and can be operated in a vertical orientation. High power output of the laser is not essential for the α measurements even for the 20-meter path. The high power becomes desirable when measuring off-axis irradiance.

A number of sensors can be used in conjunction with the laser. The Cintra Model 101 radiometer has proven both

convenient and accurate. This instrument can measure power levels down to 10^{-8} watts and its output is digital and the automatic ranging feature simplifies operation over the very wide power ranges encountered. As normally configured, the optical bench uses sensors close to the laser window and at 10 and 20 meter ranges along the tower. The laser is collimated for the wavelength employed and is aimed to irradiate each of the detectors in turn. The detector area is sufficiently large to collect the entire direct beam of the laser. Some care must be exercised since the present detectors have relatively wide field of view. Ambient light level is monitored and corrected as necessary in shallow water daylight conditions. In addition, a series of manually inserted apertures and blocks along the beam are available to insure that appreciable scattered light is not collected. Early versions of the long bench required manual (diver) operation of the wavelength and collimating controls. Planned modifications will permit remote control from the support vessel. By rotating the laser assembly, it is possible to measure the off-axis beam irradiance as a function of both angle and wavelength. Appropriate volume integration of this data can be used to determine the absorption coefficient.

Volume scattering function

By employing an additional detector with suitable optics to produce a narrow field of view, it is also possible to measure the volume scattering function (VSF). The VSF sensor is presently mounted on a 1-meter rotatable arm so that the beam can be viewed from forward direction to within approximately 10° of the back direction. The Cintra radiometer is used for the VSF as well as the other measurements. The laser output is linearly polarized and is normally polarized perpendicular to the observation plane of the VSF instrument. When desired, the laser polarization can be rotated 45° and 90° and linear polarizing filters and quarter-wave plates can be used in conjunction with the VSF detector to investigate the effect of polarization on scattering.

Image transmission

As previously indicated, other optical measurements are frequently used in the prediction of image transmission. Most common of these measurements are the images produced by an impulse

or point source and the images produced by bar or sinewave spatial patterns. Cameras mounted on the long bench make it possible to record images from point and resolution chart sources. A Mercury Arc "point" source and a strobe back-illuminated USAF resolution chart are employed for these measurements. By combining the VSF, impulse response, and resolution chart response data, the modulation transfer function of the water path over a very wide range of spatial frequencies can be determined.

Temperature and particle sampling

The long optical bench is being modified to contain a series of Quartz temperature transducers similar to those used for the cluster. The greater separation possible with the long bench makes it possible to measure the structure function of the turbulences over a greater range of separation.

Water-sample bottles will also be included on the bench to provide samples for particle analysis using a Coulter counter and/or phase contrast microscope.

Summary and Conclusions

The cluster permits convenient measurement of profiles of conventional optic and oceanic parameters with depth. Conventional accuracies are obtained for most of the measurements, but extremely high resolution is provided for the microstructure measurements. The long optical bench features high accuracy and spectral resolution due to its long path length and collimated monochromatic laser source. The instruments can be operated simultaneously or independently. Long bench measurements have been valuable in calibrating and assessing the accuracy of the cluster instrumentation. Operation of both instrumentation systems permits near simultaneous *in situ* measurements of the important optical parameters useful in predicting performance of long range imaging systems and communications systems.

Acknowledgment

The equipment described in this paper has been developed as part of the Advanced Research Projects Agency/Advanced Sensor project Deep Look. The advanced planning and many of the system concepts were contributed by Mr. R. S. Cesaro, Director and Mr. A. M. Rubenstein, Deputy Director ARPA/Advanced Sensors.

B. W. Siryj

Engineering
Advanced Technology Laboratories
Government and Commercial Systems
Camden, New Jersey

received the BSME in 1959 and the MSME in 1966 from Drexel Institute of Technology. He has had professional experience at Navigation Computer Corporation (NAVCOR), Philco (computers), and RCA. His overall experience includes laser film transport and scanner design, helical and digital magnetic tape transport design, pneumatic design, precise dynamic mechanism design, and material transfer investigations. Mr. Siryj is a registered professional engineer in Pennsylvania. He has a patent for a conception of an electro-mechanical automatic programmer and a disclosure for an adjustable tape guide roller.

M. L. Levene, Leader

Advanced Mechanics Group
Advanced Technology Laboratories
Government and Commercial Systems
Camden, New Jersey

received the BSME and MSME from the University of Pennsylvania in 1954 and 1958, respectively. In 1963, he returned to U. of Pa. as a David Sarnoff Fellow and completed course work for the doctorate in Mechanical Engineering. Mr. Levene joined RCA in 1954. His major work has included mechanical memory devices for computers, color kinescope film recording, quadruplex tape recording, continuous burning carbon-arc mechanisms for simulation of solar radiation, and Electrofax printing devices and high-speed Electrofax character and document printers. In 1960, Mr. Levene was appointed Leader, Mechanical Data Processing, in the Electro-Mechanics Group. In 1966, on his return from academic leave, Mr. Levene was appointed to his present position. He has been granted nine U.S. Patents and has authored or co-authored several technical papers. He is a registered Professional Engineer in Pa. He is a member of the ASME, the IEEE, the National Society of Professional Engineers, and the Society of the Sigma Xi.

Material transfer recording

M. L. Levene | Dr. R. D. Scott | B. W. Siryj

The advent of the laser has been closely followed by its applications in film recording,¹ in micro-machining,² and in "non-photographic" data systems.^{3,4,5,6} Material removal as described in Refs. 2, 3, 4, is an occurrence common to many of these processes. Advanced Technology Laboratories is developing a technique in which a focused laser beam is used not only to remove material from a substrate but also to transfer it to a recording medium. No other processing is required; the recording is fully formed merely by material transfer and is instantly available for readout. Transfer can be accomplished using a variety of ink- or dye-bearing substrates and almost any recording medium (paper, metal, mylar). Transfer of material has been made across gaps of several mils without evidence of line spread. Transfer has also been made in the reverse direction.

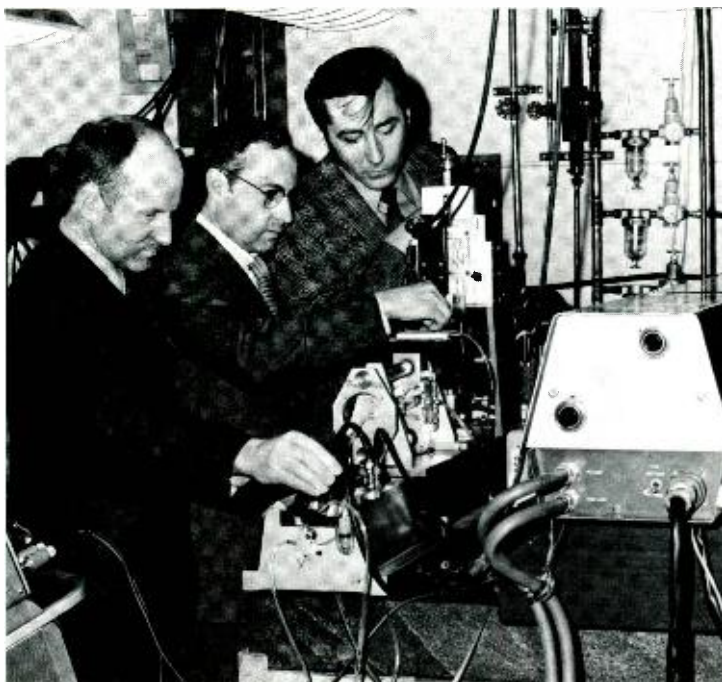
Dr. R. D. Scott

Design and Development
Advanced Technology Laboratories
Government and Commercial Systems
Camden, New Jersey

received the BSME from MIT in 1953. He received the MSME in 1959 and PhD in 1965 from the U. of Pa. After completing active duty with U.S. Army Ordnance, he joined RCA as a mechanical engineer in Advanced Technology Laboratories. He worked on refinement of audio recording heads with respect to miniaturization and improvement of assembly techniques, and was also responsible for the design and construction of various tape handling machines. He worked on the packaging of magnetic recording heads for digital computers, and reduced the size of the existing heads 60% over those previously used. Dr. Scott has been closely involved with fluid mechanics. He has also participated in several energy conversion projects. Dr. Scott has been an instructor and lecturer at the Summer institute for computer mathematics at U. of Pa. and is responsible for the creation and instruction of an after-hours course in numerical programming techniques at RCA.

THE DISCOVERY of the material transfer technique of laser writing is a classic example of serendipity. Experiments were being conducted on the removal of material from a dye-coated mylar strip. The coated mylar was wrapped around a solid aluminum shaft. Lines of removed material were created by rotating the shaft relative to a stationary laser beam, focused at the mylar surface. Preparing the sample for one test sequence, the experimenter happened to inadvertently place the dye-coated surface facing the shaft surface rather than facing the laser source. On completing the test, the experimenter noticed a line formed on the metal surface of the shaft corresponding perfectly with the clear line created on the dye-coated mylar. Intentional repetition of this assembly "mistake" produced consistent transfers of material.

Although in its relative infancy as a recording process, the foremost applications for the new technique include the recording of line scanned imagery, the printing of letters and numbers in communications systems and in computer peripheral equipment, the optical recording of data, and the selective marking of process materials. Featuring instant viewability, near-real-time high-resolution "moving-window" display systems become feasible with material transfer recording. Requiring no process chemicals, the material transfer method may be used in operating environments in which sloshing of fluids and replenishment of chemicals would be unacceptable. Not being light sensitive in the usual sense, ma-



Authors (left to right), Scott, Levene, and Siryj.

Reprint RE-17-2-4

Final manuscript received July 27, 1971

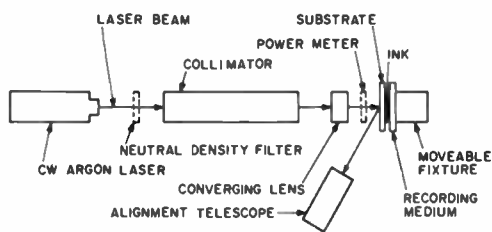


Fig. 1—Early experimental setup.

terial transfer images may be created in open, well-illuminated areas. Being inherently a non-contact, non-impact printing system, material transfer printers can be built featuring acoustically quiet operation.

These applications and features will become practical realities as further research and development establishes gray-scale capability and decreases laser power requirements while maintaining the achieved high writing rate. This article relates some of the observed phenomena associated with transfer recording, presents representative test data, and offers suggested physical models to explain the observed transfer action.

Experimental test setup

A cylindrical mandrel was used to support the recording media in the early experiments. A polyethylene-backed typewriter ribbon was the most regularly used ink source material, and a number of colored dyes applied to a mylar base were also successfully transferred. The basic arrangement for material transfer recording is shown in

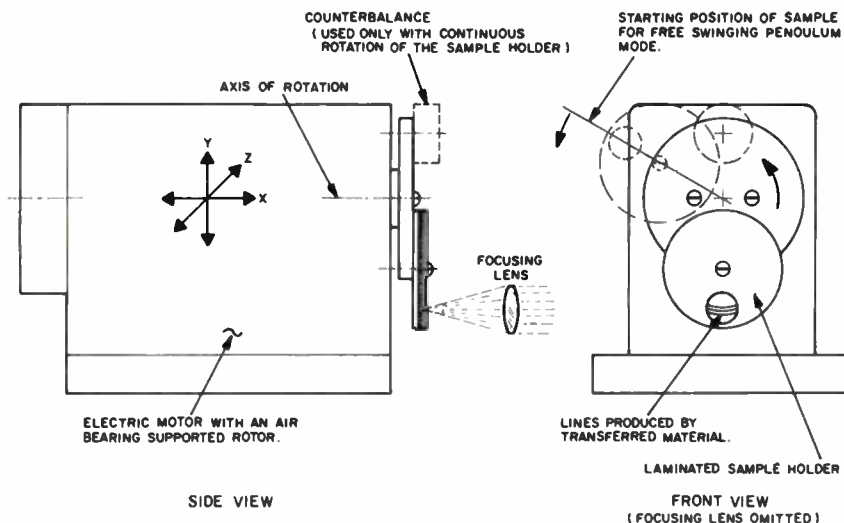


Fig. 2—Principal experimental setup.

Fig. 1. The first experiment used small argon lasers,⁷ but as higher power was desired to permit faster writing speed, the laser source was changed to Nd^{3+} :YAG. The substitution of laser sources and improvement in test setup increased the writing rate from several centimeters per second to over 3500 cm/s; subsequent refinements and improved laser-material combinations increased the writing rate to 15,000 cm/s.

Later experiments used a 1.06- μm Nd^{3+} :YAG laser with a maximum output power of 22 joules/s (22W) as the energy source. Because of losses through the optical system, the highest power available at the recording spot was 11 joules/s (11 W).

The latest experimental test setup developed (see Fig. 2), employs a 5-watt argon laser as the power source. High-reflectivity dielectric mirrors are used wherever possible to maintain overall laser power efficiency at 48%. A "flying spot" scan has been accomplished by directing the focused cone of light coaxially into a single-faced rotating mirror. The transfer material was developed at RCA Laboratories and is designated *EBER*.

Experiments were performed by transferring material either in the forward or reverse directions as shown in Figs. 3 and 4.

Summary of the observed phenomena

In order to transfer material either in the forward or reverse directions, in

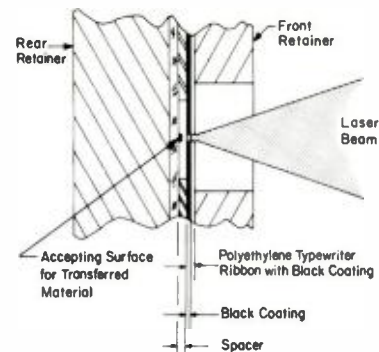


Fig. 3—Forward transfer through a gap.

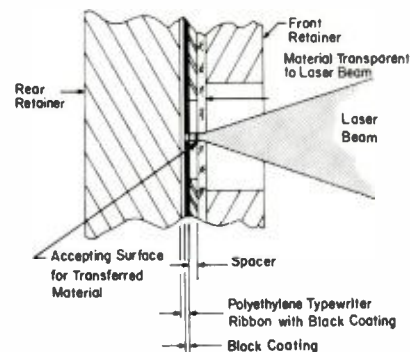


Fig. 4—Reverse transfer through a gap.

contact or out of contact, an energy density level ranging from 1 to 3 joules/cm² was required, for the Nd^{3+} :YAG-carbon ribbon combination, while only 0.1 joule/cm² was needed for the more effective *Argon-EBER* combination. ("In contact" refers to the transferrable material being in contact with the accepting medium at the time of laser beam impact.) In the earlier systems, the focused spot diameter was calculated to be 80 μm and a depth of focus of 200 μm was predicted. The spot diameter was experimentally confirmed by the width of the recorded line. The depth of focus, a distance over which the recorded line width remained approximately constant, was measured to be about 300 μm . In the latest system (Fig. 2), the calculated diffraction-limited spot diameter is 10 μm , while the depth of focus is 64 μm .

Forward transfer

The test setup for forward transfer is shown in Fig. 3. Magnified recorded lines made both in and out of contact are shown in Fig. 5a and 5b. The out of contact recording was made with a 100- μm gap. Interestingly, the line produced by the forward transferred material from the carbon ribbon consisted of fine granules, similar to exposed and developed film, as well as

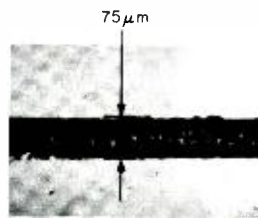
“chunks of melt” randomly distributed. The observed “chunks of melt” appeared as particles substantially larger than the previously described granules. It is postulated that the “melt chunks” consist of incompletely vaporized carbon material transferred along with the other vaporized particles.

Reverse transfer

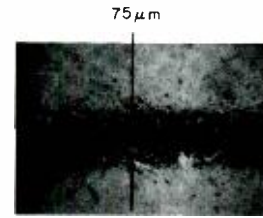
The test setup for reverse transfer is shown in Fig. 4. Magnified recorded lines made both in and out of contact are shown in Fig. 5c and 5d. The reverse-transfer recorded line has a fine granular structure without evidence of “melt chunks” as shown in Fig. 5b and 5c. The line starts to lose definition and spreads when the transfer gap exceeds 130 μm . At a gap of 300 μm the definition of the line is almost completely lost. Fig. 5e shows the latest results using the 5-watt argon laser and EBER recording materials. The words MATERIAL TRANSFER were written through an opaque mask stencil.

Discussion of experimental results

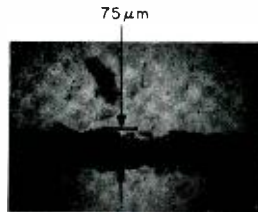
The absence of the “melt chunks” when transferring material in the reverse direction may be explained as follows. In the forward direction, the transferrable material to be heated first is located at the common boundary with the ribbon. This implies that the material closest to the transferrable surface will be vaporized last. The locally heated region would resemble a pressurized bubble with a hard shell. Once the shell fractures, before it has an opportunity to vaporize, solid particles will be set in motion. This condition, however, does not exist in the reverse direction. Here the transferrable material is struck by the laser beam directly and removed gradually until all has been removed clear through to the ribbon. The amount of material removed can be controlled by controlling the energy density supplied to the area of interest. As would be expected, when transferring material in the forward direction, the area on the ribbon where the material was removed usually appears clean (all material removed). However, when transferring material in the reverse direction, only an excess amount of power would result in removal of all of the material. In the forward direction, the



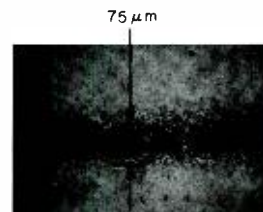
(a) Forward transfer, in contact.



(b) Forward transfer, across 100- μm gap.



(c) Reverse transfer, in contact.



(d) Reverse transfer, across 100- μm gap.

transferrable material was either completely removed or not removed at all, but in the reverse direction small amounts of material could be removed gradually. When all of the material was not removed, a groove in the transferrable material could be observed.

If an excessive amount of power was supplied to the ribbon when transferring material either in the forward or reverse directions, the center of the transferred line was usually partially or completely “blown out” with the edge material remaining.

In order to determine whether a recorded line could be erased, some material was transferred onto a glass slide. Next, the transferred lines on the glass slide were scanned with a focused laser beam of the same intensity as was utilized for the original transfer. The end results were etched lines in glass with no apparent trace of the transferred material. Subsequent tests indicated that etching did not occur in the glass when the original transfer was made. However, further experiments have shown that whenever mylar is used as the medium upon which the transferred material is deposited, line etching can be made to occur during the original recording. Throughout all of the tests conducted, it was obvious that the energy density needed to transfer material is highly dependent upon the light energy absorption capability of the transferrable material.

	1000 in/s	3000 in/s	6000 in/s
SPEED —			
POWER AT RECORDING SPOT —	1.9 W	1.9 W	2.3 W
LINE WIDTH —	1.5 mils	.9 mils	1 mil

MATERIAL TRANSFER

MATERIAL TRANSFER*

*ENLARGED 3:1 TO SHOW LINE STRUCTURE

(e) Latest results.

Fig. 5—Photomicrographs of lines formed by transferred material.

Physical models

A proposed model must account for the results observed for cases of high- and low-energy absorption, and also for effects of contact and separation. The conditions, which represent limits on the range of possible interactions, are steady-state with low energy density with the surfaces in contact, and higher energy density with the surfaces separated.

Low energy input

Assume the existence of a transparent substrate, which forms an infinite plane boundary in space (see Fig. 6). Assume the entire boundary to be coated with a thin opaque substance with uniform properties throughout and with constant thickness normal to the interface. At time t_0 , the coating is illuminated from within the substrate

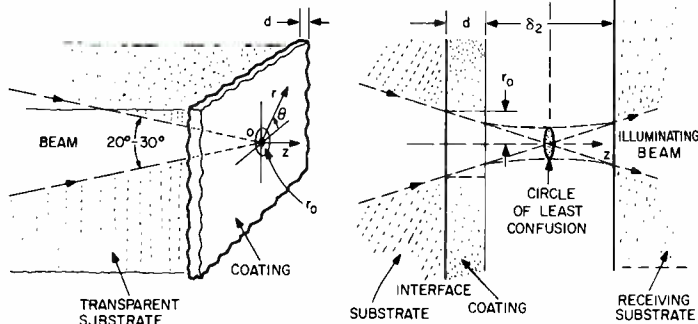


Fig. 6—Substrate with coating.

by a beam with energy density E at the interface and with a pulse width τ . If the incident energy is completely absorbed without reflections, the following series of events occur: At time $t=t_0$, the temperature of the opaque material within the beam at the interface begins to rise as a linear function of time. (This assumes that the coating is insulated from the substrate and is thin in relation to the spot size.) The dividing line between the “thin” and “thick” coating designations is the penetration depth, which defines the region within which the energy is assumed to be uniformly physically absorbed. For metals, this is roughly 10^{-6} to 10^{-5} cm or 1 to $10 \mu\text{m}$.⁸ For dispersed dyes, using translucent binders, the penetration depth is probably larger than this value. The temperature will rise until either the beam is turned off or a change of state of the material is observed. For extremely high energy levels, a change of state can easily occur within an area of the order of that defined by the diameter of the beam; for very low levels, a steady-state temperature can be obtained with a continuous beam, without state change.

If no change of state occurs, classical thermoelastoplastic relations can be applied. In general, the area surrounding the beam expands with a positive surface curvature.

If the energy and temperature are raised until melting begins, it may be possible to capture a pool of molten material situated roughly within the beam. The shape of the pool meniscus depends in part on whether or not the molten material wets the substrate. Under these conditions, it would be possible to generate a drop of fluid

with a radius several times the thickness of the original coating if the substrate is non-wettable. Transfer can then be made if the receiving substrate is in contact with the fluid drop; or nearly so if the fluid is in a turbulent state. It is worth pointing out that elastic deformation of the interface can shift the relative location of the focus of the optical system, and cause an increase or decrease of incident energy density.

Consider next a substantial rise in energy flux, which causes boiling and/or vaporization of the molten surface. If the change in state of the surface material involves chemical reactions, the mechanism is complicated in detail, but qualitatively, vapor will be emitted with an attendant buildup in pressure. If the emission is sufficiently violent, fluid will be ejected along with the vapor. If the surface fractures due to thermal strains, solid particles may also be included in the emission. The existence of the latter (liquid and solid particles) is contingent upon a “sufficiently” thick coating, which allows the formation of these products before complete vaporization occurs.

If the incident energy is retained long enough, the opaque material and its residues will be removed, and the temperature of the substrate will return (relatively slowly) to that value which it would attain alone. At this point, a hole in the opaque coating has been formed. The amount of thermal penetration into the substrate depends on the time of exposure and energy level of the beam. The opaque coating acts as the heat source on the boundary of the interface; the temperature is assumed low enough that the thermal energy is transferred primarily by conduction.

High energy input

Although the literature shows experimental evidence that strong acoustic shock waves can be produced by thermal shock,^{9,10,11} it seems likely that the vaporization of the material with consequent high local pressures is the principal contributor to the development of the momentum of the mass that is transferred. Surface pressures of the order of 10^3 atmospheres have been measured, with plasma velocities in the supersonic range.¹² In fact, once gross material particles have been separated from the present surface, they remain in the path of the beam for an appreciable time, and are further acted upon.¹²

For high energy rates, most of the heat absorbed resides in the molten and gaseous material, ejected outwards by the vaporization of the surface. The vapor forms at the interface. If the opaque coating has a thickness of the order of the penetration depth, vaporization will occur virtually instantaneously at the surface. If the coating is sufficiently thick, the vapor will literally blast a hole in the opaque material before the surface has time to vaporize completely. The ejected particles will assume trajectories which depend on the pressure gradient and momentum of the expanding gas. Pressures of the order of 10^3 atmospheres can be obtained at the surface. As the ejected mass moves outward, the portion that remains within the energy beam continues to be heated. A reaction force can perhaps be generated which will propel the particles away from the beam.¹²

A physical model based on shock wave propagation was initially proposed by Braudy.⁷ The existence of a shock wave generated by the intense, nearly instantaneous thermal expansion of a point area at the surface of the illuminated material was theoretically investigated by Ready, et al.⁸ Typical laser pulse widths of 30 ns were assumed, and high peak stresses of the order of 700 kg/cm^2 were shown to result for an input of roughly 1.2 joules/cm^2 . In fact, stress amplitudes approaching the material yield stress are possible. Wave shapes are more or less material independent. The stress wave is reflected at the interfaces and may produce a standing wave of short duration. The

time of transit of the wave depends on the material properties and thickness, but is typically less than the duration of the pulse if the specimen is very thin. The suggestion was made, therefore, that the acoustical shock wave thus generated would provide the required bursting of the surface and initial momentum of the dye particles.

Effect of receptor surface

If an opposing surface is placed near the opaque surface, the quality of the transfer is affected by the intensity and duration of the beam. For slow heating, it is possible for a liquid drop to contact the opposing surface and be deposited as previously noted. As the drop contacts the receiving surface the latter is heated by conduction, and thermal fixing can be accomplished.

For rapid heating, the ejected material is driven towards the receptor surface, and whether or not the portion of the mass which is not vaporized will tend to adhere to the opposing surface depends on the character of the receptor surface. Fixing may be aided by the transmitted beam. If the beam illuminates the transferred material for an additional time, the vaporization process may continue with further removal of material and burning of the opposing surface. The presence of vapor near the receiving surface will cause transfer by condensation, again depending on the condition of the surface.

The fixing of the material which remains in the beam will yield an apparent focusing of the ejected material. Although natural focusing arises from a notch or crater, it is unlikely that ejected material from a thin coating will tend to focus unaided.

Two other accompanying forces may contribute to focusing: pressure gradient and vortex action. The pressure gradient will cause accelerations of the gas-fluid mixture which are proportional to the gradient, and in the same direction. The pressure field associated with an exploding surface of the type contemplated is difficult to define analytically due to the absence of suitable known boundary conditions. Similarly, vortex action, which may provide stabilization of the particle jet (e.g., smoke rings) is also difficult to account for

analytically. It might be noted in passing that an excellent example of a fluid jet originating in a liquid bath is given by the thermal mud pots of Yellowstone Park. The jets are initiated by steam percolation through the viscous bath, and the jet so resulting is extremely well collimated. Whether these mechanisms are applicable to the case in point is pure speculation at this level of investigation, however.

Summary of model

Contact—Low-level heating causes a droplet of molten or softened material to form, and contact is made with the transfer surface, aided by thermal distortion of the substrate. Fixing is enhanced by further heating by the beam, and the properties of the transfer surface. This is the most probable explanation of the observed results at the present state of knowledge.

Out of contact—High-level heating causes fracture of the surface by shock wave and gas formation. Solid and liquid particles mixed with vapor are ejected in a dispersion pattern characteristic of an explosion. Those particles encountering the transfer surface within the beam are heat-fixed. Those particles outside of the beam migrate away as condensed dust. Some particles in the transition region may adhere weakly to the transfer surface, but will be extremely vulnerable to erasure by mechanical wiping of the surface. Vaporized material near the transfer surface will tend to condense on the surface, in a manner dependent on the conditions of the surface.

Out of contact (beam reversed)—If the receiving substrate is transparent, it is possible to illuminate the opaque coating, shown in Fig. 6, by a beam which first penetrates the receiving surface. In this mode, the opposite side of the coating is heated, with consequent vaporization of the surface without buildup of pressure between the coating and its carrier.

The action is primarily sublimation and condensation on the receiving surface. It is also possible that violent surface boiling may cause sputtering of the receptor as well.

Conclusions

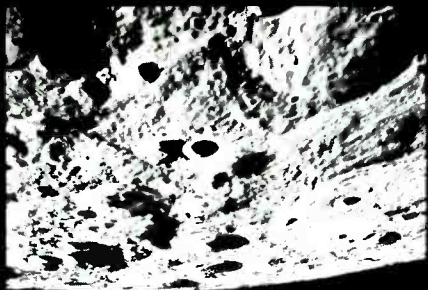
Three basic transfer modes have been examined: 1) transfer with supply and

recording surfaces in contact; 2) forward transfer across an air gap; and 3) transfer across a gap in the reverse direction. Each of these three modes of transfer has practical applications, and each has somewhat unique transfer characteristics.

As evidence of the potential practicality of material transfer recording, recording was accomplished with a variety of dyes and "ink" materials over a range of speeds from zero to 15,000 cm/s. Line widths from less than 30 μm to more than 130 μm have been recorded. Energy density requirements have been in the range of 0.1 joule/cm² for most effective combinations of laser and recording material.

References

1. Woywood, D. J., "Laser Recording: Key to High-Resolution Image/Signal Reproduction," *Laser Focus* (Feb. 1968) p. 28.
2. Lavoie, F. J., "The Blue-Collar Laser," *Machine Design* (Feb. 19, 1970) pp. 140-146.
3. Schawlow, A. L., "An Example of Laser Erasing," *Laser Focus* (Sept. 1967) p. 9.
4. Becker, C. H., "UNICON Computer Mass Memory System," Proceedings of AFIPS Joint Computer Conference, Vol. 29 (Fall 1966) pp. 711-716.
5. Rostron, Jr., D. D., and Young, T., "Printing by Means of a Laser Beam," IBM Technical Disclosure Bulletin, Vol. 7, No. 3 (Aug. 1964) p. 224.
6. Woodward, D. H., "Distillation Printing," IBM Technical Disclosure Bulletin, Vol. 9, No. 11 (April 1967) p. 1592.
7. Braudy, R. S., "Laser Writing," Proceedings of the IEEE, Vol. 57, No. 10 (Oct. 1969) p. 1771.
8. Anisimov, S. I., Bonch-Bruевич, A. M., Elyushevich, M. A., Imas, Ya. A., Pavlenko, N. A., and Romanov, G. S., "Effect of Powerful Light Fluxes on Metals," *Zh. Tekhn. Fiz.* Vol. 36 (1966) p. 1273. English translation: *Soviet Physics—Tech. Phys.* Vol. 11 (1967) p. 945.
9. DeMaria, A. I., "Optically-Induced Ultrasonic Waves in Transparent Dielectrics," Proceedings of the IEEE, Vol. 52, No. 1 (1964).
10. Chiao, R. Y., Townes, C. H., and Stoicheff, B. P., "Stimulated Brillouin Scattering and Coherent Generation of Intense Hypersonic Waves," *Physics Review Letters*, Vol. 12 (1964) p. 592.
11. White, R. M., "Elastic Wave Generation by Electron Bombardment or Electromagnetic Wave Absorption," *Journal of Applied Physics*, Vol. 34, No. 7 (1963) p. 2123.
12. Askar'yan, G. A., and Moroz, E. M., "Pressure on Evaporation of Matter in a Radiation Beam," *Zh. E. T. F.*, Vol. 43 (1962) p. 2319. English translation: *Soviet Physics—JETP*, Vol. 16, p. 1638.
13. Ready, J. F., Bernai, G. E., and Shepherd, L. T., "Mechanisms of Laser-Surface Interactions," Honeywell, Inc. Research Center. AD 666-245 (1967).



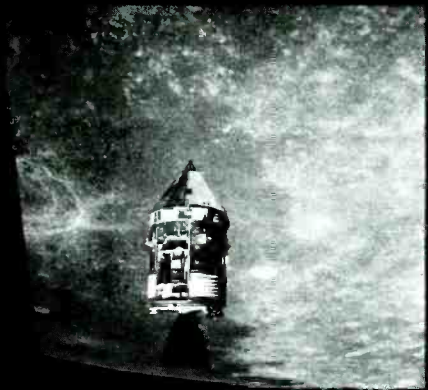
View of lunar farside as photographed from CM in lunar orbit.



Apollo Lunar Surface Experiments Package (ALSEP) deployment site.



LM, Irwin at Fover, Hadley Delta in background.



Command and Service Modules, with open SIM bay revealed. Sea of Fertility below.



Close-up view Rover track, bootprints and hole in lunar soil.



Suprathermal Ion Detector Experiment (SIDE) and the Cold Cathode Ion Gauge (CCIG) of ALSEP.



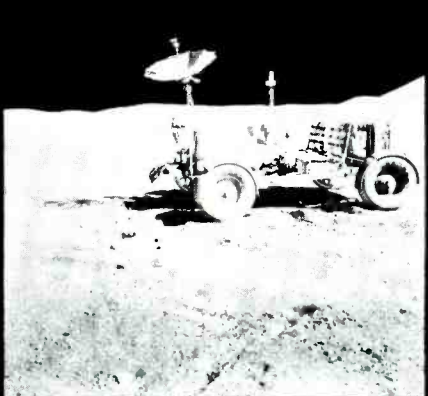
Command and Service Modules above lunar horizon, photographed from LM.



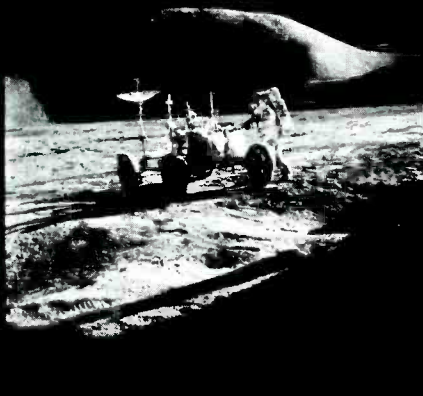
Irwin saluting, flag, LM, Rover, Hadley Delta. RCA built equipment visible on the Lunar Rover.



Close-up of gnomon, color chart bootprints, lunar soil.



Rover in foreground Mount Hadley in right background.



Irwin at Rover, Mount Hadley in background.



Scott working with lunar drill. Solar Wind Experiment in foreground.

RCA & Apollo 15

THE PHOTOGRAPHS on these pages document the most ambitious and successful space venture in the history of man. RCA played a major role in this success. Our contributions were:

The Ground Commanded Color Television Assembly provided color TV coverage of the Astronauts at work. The Assembly, consisting of a camera and control unit, was built by the Astro-Electronics Division. It contains a revolutionary Silicon Intensifier Target tube developed by the RCA Laboratories.

The Lunar Communications Relay Unit transmitted voice, telemetry and color television directly from the moon, and received transmissions directly from earth. It consists of a pressurized housing containing the S-band and VHF-band systems. The LCRU was built by the Communications Systems Division. The S-band antenna that allowed the astronauts to operate independently from the Lunar Module was designed by the Missile and Surface Radar Division.

The VHF System linked the Lunar Module and Command when the two spaceships were separated in space, handling voice and astronaut biomedical data. In addition, the sets provided the CM pilot with the range between the two spacecraft.

The Extra Vehicular Communications Systems provided communication for the astronauts exploring the Moon. It linked the Astronauts with one another, with the LM and (via LM) with mission controllers on earth. In addition, the system transmitted biomedical data and telemetry information on the condition of the spacesuit systems. The VHF and EVCS systems were built by the Communications Systems Division.

The Laser Altimeter provided precise determination of the Moon's topography, measuring the altitude above the Moon's surface to within one meter. The Laser Altimeter was built by the Aerospace Systems Division.

The Rendezvous Radar/Transponder System was a critical source of data for the rendezvous of the Lunar Module and the Command/Service Module. The X-band radar, mounted on LM determined range, direction and velocity of the LM relative to the CSM. The rendezvous radar is the first gimbaling radar ever flown in space. These units were built by the Aerospace Systems Division, and the Missile and Surface Radar Division.

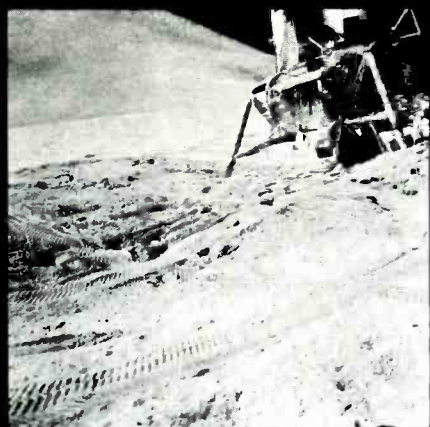
The Lunar Module Landing Radar provided continuous measurements of the LM altitude and velocity relative to the lunar surface during the final phases of the descent and landing. It used a three-beam doppler velocity sensor and a single beam altimeter. The radar information was integrated with other LM sensors, computers and control systems to aid the astronauts in making a gentle touchdown on the Moon. The landing radar is the responsibility of the Aerospace Systems Division. Electronic Components built the solid-state transmitter for the landing as well as a similar solid-state transmitter for the rendezvous radar.

The Descent Engine Control Assembly provided on and off and throttling signals to the Lunar Module descent engine, which can operate from 10% thrust to full capability. (This is the first throttlable rocket engine ever flown.) The DECA was built by Aerospace Systems Division.

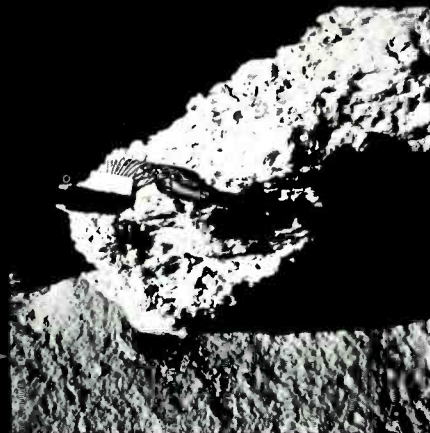
The Attitude Translation and Control Assembly sent control signs to the LM's 16 reaction-control jets. When the automatic systems or astronauts dictated an attitude or translation change, ATCA selected the proper jets to fire. Since a host of combinations were possible among the 16 jets, ATCA had extensive logic circuits. The ATCA was built by the Aerospace Systems Division.

The Two Saturn Countdown Computers checked out the Saturn launch vehicles during the countdown leading to lift off. The mobile launcher computer checked out the rocket by commanding it to exercise valves, engines, relays, etc., and measuring the resultant performance. It monitored more than 3,000 parameters in this way. The LCC computer controlled the sequence of checkout and launch countdown programs performed by the mobile launch computer. The Saturn countdown computers are built by the Electromagnetic and Aviation Systems Division.

Tracking Radar Support of Apollo was provided at NASA and DoD land stations and aboard ships around the globe to track Apollo/Saturn during powered flight and earth orbit. The radars are the AN/FPS-16, including a special shipboard version; the AN/FPS-6 and the CAPRI (Compact All-Purpose Range Instrument). The Missile and Surface Radar Division built the radars.



Portion of LM. Rover tracks Hadley Delta in background.



Close-up of lunar rocks lunar rake.



VHF antenna on right, docking antenna on left, St. George Crater in center background during SEVA.



Apollo 15 Hadley-Apennine landing area from CM.

Photo credits: Scott and Irwin, NASA.

Fourth *RCA Engineer* readership survey

P. C. Farbro

Readership surveys were conducted in 1956 (the second year of publication), in 1959, and in 1968. Now, in the sixteenth year of publication, it was felt advisable to assess again the acceptance and value of the journal among the readership to further guide editorial decisions.

PAST READERSHIP SURVEYS have furnished the Editors and the Editorial Board with information for their planning in achieving the aim of the publication—a journal “by and for the RCA engineer.” The Editors suggested that the readers of the publication may be interested in a summary of the results of the recent survey and asked that this article be prepared to feedback the findings.

A questionnaire was developed by the RCA Staff Personnel Research function and was distributed with the February-March and April-May, 1971 issues of the *RCA Engineer*. Instructions accompanying the questionnaire asked that it be answered and then returned anonymously to the Editor. Close to 1500 questionnaires (approximately 20% of the distribution) were returned voluntarily which is considered a very good reply for mailed surveys.

Reprint RE-17-2-17
Final manuscript received July 30, 1971



Several findings from the survey indicated that the *RCA Engineer* is well accepted by the engineering population as follows:

In answer to the question, “How would you rate the *RCA Engineer*?”, 82% rated the publication “excellent” or “good”. Fig. 1 shows the response to this question.

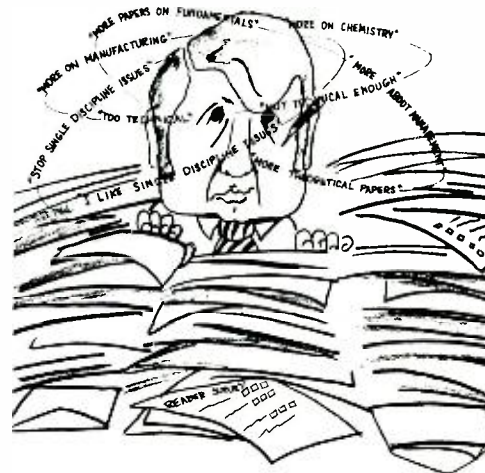
In answer to the question, “From which of these sources (11 sources were listed) do you get the major amount of your technical information about RCA?”, 65% indicated the *RCA Engineer*—showing the publication as the primary source. Fig. 2 shows the response to this question.

Image of the *RCA Engineer*

Several statements describing the journal were developed in an attempt to establish an “image” of the *RCA Engineer* as held by the engineer readership. For each of these statements, the questionnaire asked the respondent to indicate whether or not he *strongly agreed*, *agreed*, was *neutral*, *disagreed*, or *strongly disagreed* with it. From

Patrick C. Farbro, Director
Personnel Policy and Research
RCA Staff
Camden, New Jersey

received the AB and MS in psychology from the University of Tulsa (1947) and Purdue University (1948) respectively. His occupational experience includes work as a graduate teaching assistant in psychology at Purdue University, 1947-1948; Personnel Research Analyst, RCA Victor General Office, 1948-1949; Employment Supervisor, Lancaster Plant, 1949-1951; Manager, Personnel Research, RCA Staff, 1951; Manager, Training and Personnel Research, 1957; Manager, Professional Personnel Programs, 1959; and Director, Professional Personnel Programs 1965. Mr. Farbro was appointed to his present position this year. He is a member of the American Psychological Association, the N.J. Psychological Association, the N.Y. Academy of Science, the American Assoc. for the Advancement of Science, the American Personnel and Guidance Assoc., the Industrial Relations Research Assoc., the American Society of Training and Development (1967 National President), the International Assoc. of Applied Psychology, Psi Chi (honorary in Psychology), and Sigma Xi. Mr. Farbro is also listed in *American Men of Science* and *Who's Who in the East*.



these responses a “composite image” of the magazine as viewed by its readers was developed.

These “image” statements were scored by giving a weight of +2 or -2 if the reader checked *strongly agree* or *strongly disagree*, respectively, in responding to the statement; +1 or -1 if he checked *agree* or *disagree*, respectively, to the statement. A weight of zero was given to the neutral responses.

Table I is made up of those image statements which reflect the opinion of more than one-half of the respondents. The statements are listed in order of the strength of the engineers' feelings based on the scores for each statement described above.

Diverse interests of readers

The population for which the *RCA Engineer* is written is one of widely varying interests. Even though the readers are engineers, the businesses of RCA to which they apply their engineering disciplines are diverse—space programs, home entertainment products, defense and commercial systems, information processing, etc. Of natural concern to the Editors and the Editorial Board is the development of a journal that can serve this broad interest.

It appears that the publication is serving well this diversity of interests. Table II shows that in each of the major operating units of the Company shown, over three-quarters of the engineers rated the *RCA Engineer* as “excellent” or “good.”

Table I—Readers' "image" of the *RCA Engineer*.

- Distributing the *RCA Engineer* outside the company would enhance the technical image of RCA.
- The journal has a professional character.
- The publication helps the company's engineers to be better informed.
- The *RCA Engineer* is valuable to younger engineers.
- The *RCA Engineer* is valuable to the experienced engineer.
- The *RCA Engineer* encourages "professionalism".
- The reputation of RCA and its engineers is increased by the journal.
- As a source of information, the *RCA Engineer* compares favorably with external nonspecialized journals (e.g., *Spectrum*, *Electronic Design*, *Electronics*).
- The *RCA Engineer* provides an open communication channel for the entire technical staff.
- The publication encourages engineers to write.
- Papers published in the *RCA Engineer* would be of interest to scientists and engineers outside of RCA.
- The *RCA Engineer* is helpful in furthering my insight into RCA as a corporation.

Statements presented in order of strength of response; statements shown reflect the opinion of more than one-half of the respondents.

Future articles

Two items in the questionnaire attempted to assess among the readers ideas and subjects that the Editors and Editorial Board might use in planning future issues.

The questionnaire asked the respondents to suggest articles which would be of interest to them and to suggest possible authors for these articles. A large proportion of the respondents suggested ideas for articles and authors. These are on file in the Editorial office and will be used by the Editors and the Editorial Board in conceiving future issues.

In addition, the following shows the per cent of readers who responded to the item, "The *RCA Engineer* should have more about:

Company plans and objectives	62%
Company policy	44%
Research activities	28%
Product Engineering	24%
The balance is about right	23%
Social implications of engineering	22%
Well known RCA "personalities"	13%

It appears that the substantial response concerning company plans, objectives and policy indicates a desire for more management-oriented articles. Expansion of the "Engineer and the Corporation" articles which have appeared in the publication may be a way to accomplish this.

Engineers' comments

Two "open-ended" items were included in the questionnaire:

"I like the *RCA Engineer* because . . ."
 "I would like to see the following changes made to the *RCA Engineer*:"

Table II—Per cent who rate the *RCA Engineer* excellent or good.

Major Operating Unit*	%
RCA Service Company	87
Aerospace Systems	86
Missile & Surface Radar	86
Globcom	86
RCA Limited	86
Communications Systems	84
Astro-Electronics	83
TV Picture Tube	83
Solid State	82
Government Engineering	81
Electromagnetic & Aviation Systems	79
Computer Systems	79
Consumer Electronics	79
Industrial Tube	78
Receiving Tube	77
Laboratories	76

*Only Major Operating Units with twenty or more questionnaire returns are listed.

Following is a sample of the comments given. They are reported here verbatim and are typical:

Like "RCA Engineer" because . . .

- "It is well written.
- It informs me about developments outside my specialty.
- It has professional character.
- It is a high quality technical magazine.
- It is informative from a research viewpoint and provides some insight into future business endeavors.
- Different format than usual journals—gives better 'feel' for RCA Corporation. Extremely well-edited and shows real quality in layout and assembly.
- It keeps me in touch with progress throughout the Corporation.
- It gives me contacts with people in RCA that are doing similar work as myself. Keeps me informed on other design work performed within RCA.

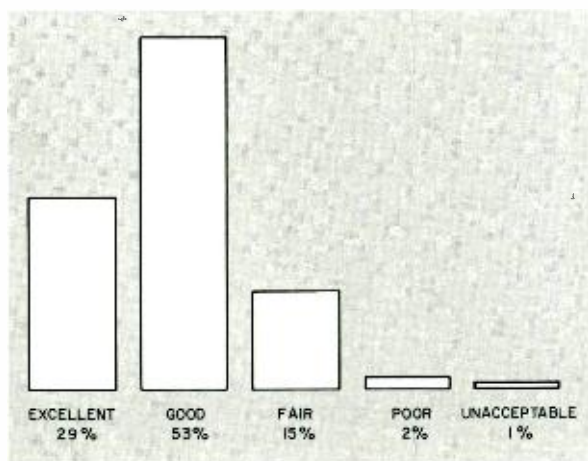


Fig. 1—Rating of the *RCA Engineer* by the Readership.

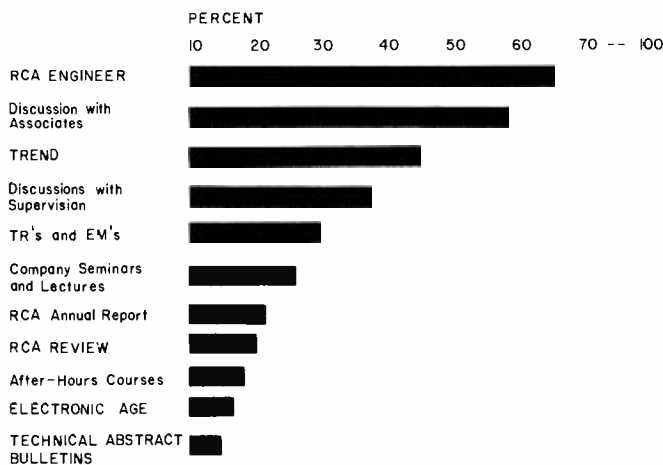


Fig. 2—Choice of eleven sources of technical information from which the readers receive the major amount of technical information about RCA.

It is done in a very professional manner, the technical level is just right, and the variety of subjects.

It shows where the research and the highly specialized engineering is aiming—the end result they are reaching for/or new business areas to be developed.

It's informative, reasonably well-balanced and a credit to RCA.

There is more emphasis on the technological breakthroughs that are expected to have the greatest impact on the Company's objectives and goals.

It is thoroughly professional in nature and most importantly it provides the only real source of corporate technology available to me.

I enjoy reading it.

It keeps me up with what's going on elsewhere in RCA, and gives me an occasional look at the work of people I know or have known.

It helps me to be part of RCA.

Since I work overseas, it is my main source of information about the overall technical and engineering progress.

It is informative, current and broad based in its reporting of engineering articles.

Information is presented in a 'highly readable' manner—if a highly mathematical treatment is desired, the IEEE can provide.

It covers a wide variety of technical areas in electronics and physics.

It's an easy reading, yet informative publication. It's a good way to keep up with the broad front of RCA's engineering activities.

It provides good interchange of ideas for engineers.

It groups a related segment of the industry into the articles of each issue. The presentations are clear and well edited. Important technical papers are presented.

It is one of the channels reminding the engineer that RCA is still a technically oriented company in spite of its recent emphasis on a purely business image.

It presents state of the art applications of electronic engineering and important current major projects.

Fairly large range of subject material. Obviously presents a 'quality' appearance. The sincerity of the staff in helping authors. The editorials.

The educational value of the technical articles.

It also allows me to keep up to date re: promotions and changes in activities of my old friends.

I like issues dedicated to particular subjects or disciplines.

It gives me a company-wide picture of the types of activities going on at RCA and a chance to see how *real world* problems are solved by our engineers.

Induces ideas for design and instills a

friendly competitive feeling to accomplish.

I like information on papers, patents, etc. by RCA engineers. I like articles on new RCA developments; e.g., laser recording, Apollo Mission, etc.

It informs me of the RCA 'Big Picture'. I recently came from DuPont and they have nothing that approaches the *RCA Engineer*.

I save the back issues and read some papers several years later.

It is a research and theoretical type.

It is a quality publication presented on a professional level.

I like the idea of using one issue to cover one subject thoroughly rather than having articles on many subjects in the same issue.

Excellent format—easy reading—right mix of articles and general interest items.

It is highly informative in detail, innovation, presentation, and insight not found in other sources."

Would like to see the following changes . . .

"Have tutorial papers, *less* highly specific technical papers."

How about management and relation to economics.

Review articles dealing with major areas of interest to RCA but including the business as well as technical aspects; e.g., competition, volume, rank in the industry.

More articles by top management outlining the future direction of RCA in the electronics industry."

None that I can think of. I like it very much just the way it is.

Publish only review articles on a variety of subjects. Most articles are too specific and directed toward a rather small audience of specialists.

More non-technical articles dealing with RCA projects and plans.

More emphasis on communications and more interest in technical relations between science and ecology and relevant social implications.

As an ME, I find relatively little of technical interest. Most EE articles are too advanced for me.

More details on Company objectives and achievements.

Articles tend to be too technically oriented.

My opinion is that the magazine should reflect the times of RCA and its relation to the socio-economic climate nationally and internationally. What is RCA doing for mankind? How can it do more? What can the RCA engineer do in his community, etc."

A much greater emphasis on manufacturing. This would be especially significant since manufacturing is more common to all RCA Divisions than any other engineering activity.

More articles on RCA Systems.

Expand 'Engineering and Research Notes' feature.

Change to a monthly publication.

A general discussion of RCA's role in different technical fields such as space, communications, TV, radio, Consumer Products.

Additional articles on Management, Management Philosophy, and the Proper Interaction between Management and Engineers throughout the Corporation. (Planning, Control, etc. to get the job done.)

Since every piece of electronics or theory has mechanical aspects and/or problems, therefore I feel it would be beneficial to include more articles involving mechanical engineering.

Editorials on new developments in the field of electronics.

Stop single-discipline issues or single-division issues.

More articles that have state of art techniques instead of articles which have little or no *new* developments.

Additional chemistry-oriented articles.

One tutorial paper per issue, for product line engineer's need.

More communication from management to the engineers.

Would like to see more emphasis on the theoretical or mathematical applications to the solution of engineering problems.

There is a strong need for marketing information at the engineers level. Could this gap be filled through this medium?

More articles on engineering management. Research projects from Princeton.

More papers on fundamentals.

More articles dealing with semiconductor technology.

Cover software design—operating systems, communication systems, graphic systems.

More articles concerning manufacturing areas; e.g., value analysis, quality control, manufacturing assembly techniques, industrial engineering.

To present more articles (scientific and popular) on RCA computer products.

Fewer 'pure research' reports and more 'practical engineering' reports—research is fine, but products sold to customers pay the bills.

I am a systems programmer; I would like to see software-related articles.

I would like to see more articles on computer hardware, logic design and software (operating systems, communications, real time).

More theoretical articles having practical potential.

Less concentration on highly theoretical subjects and more about RCA as an organization.

More theoretical papers.

Additional space should be given to changes in corporate organizational structure in terms of the goals involved.

Regular feature on social implications of engineering."

Laser Beam Image Reproducer (LBIR)

S. M. Ravner

The Laser Beam Image Reproducer has evolved into an extremely high-performance reproduction device. The present design can generate hard-copy image reproductions from high-resolution video signals with excellent fidelity. The high degree of stability and repeatability, as well as the simplified operating requirements, make the LBIR well suited for field operational applications.

Editors' Note: This paper was originally presented by Mr. S. Ravner at the SPSE Symposium on Electronic Imaging Systems in April 1970. Since that time the continuing LBIR developmental effort at AED has led to a third generation LBIR which faithfully reproduces imagery with a resolution of 20,000 picture elements per scan at a scan rate of a thousand lines per second and with a video bandwidth of 10 MHz. The basic design and the major portion of the actual LBIR are the same as the one described in this paper.

Continuing efforts in LBIR design will be described by Mr. Ravner in another article in a forthcoming issue of the *RCA Engineer*.

THE LASER BEAM IMAGE REPRODUCER (LBIR) was developed at RCA in 1967 to produce faithful, large format (9"×9"), hard copy reproductions of high-resolution (6000 TV lines), single-frame television images generated by the RCA 2-Inch Return-Beam Vidicon (RBV) camera. The prototype LBIR demonstrated the high-quality capabilities of laser image recording, and was used extensively for laboratory testing and field demonstrations.

A design effort was started in late 1968 to build a second generation LBIR that would be suitable for use as opera-

Reprint RE-17-2-16
Final manuscript received April 17, 1970.

Stephen M. Ravner, Mgr., High Resolution Displays, Astro-Electronic Division, Princeton, New Jersey received the BSEE and the MSEE from the Polytechnic Institute of Brooklyn in 1959 and 1963, respectively. He has been active in the design and development of advanced television and display devices at RCA during the past nine years and was responsible for the development, at AED, of a high resolution Laser Beam Image Reproducer (LBIR). Previously, he was associated with ITT Federal Laboratories, where he was concerned with design and development of training simulators and display devices utilizing television techniques. Mr. Ravner joined AED in 1961 and shortly became a lead engineer for the electrical-system design, integration, and testing of the Nimbus Ground Stations; he was also responsible for the study and design of a high-resolution line-scan kinescope display for a dielectric-tape camera system. After his promotion to Leader, Engineering in 1965, Mr. Ravner was responsible for the design and development of all AGE for a classified program as well as early design phases of the improved Apollo Television Scan Converters for NASA. In 1968, he was promoted to Manager of High Resolution Displays and has devoted the major portion of his efforts toward directing the LBIR advanced development program at AED. Mr. Ravner is a member of the IEEE.



Fig. 1—Prototype Laser Beam Image Reproducer.

tional ground equipment. This effort produced the LBIR currently in use at RCA.

Background—the prototype LBIR

The prototype LBIR has been described in several published papers.^{1,2} However, a brief description is given here to provide a basis for comparison in the following discussion of the second-generation LBIR.

Description

Fig. 1 shows the prototype LBIR. The upper portion (under the black, light-tight shroud) consists of the laser, optics, scanner, and film transport while the lower portion houses the electronics, control panel, power supplies, and the air pressure and vacuum systems for the scanner and film platen.

The basic components of the prototype LBIR are shown in Fig. 2. The laser, a 15-mW, continuous-wave, helium-neon unit, provides a constant intensity collimated beam of light (about 1 mm in diameter) to the light modulator. The light modulator is an electro-optic device which, when driven by the processed video signals, modulates the intensity of the incoming laser beam. The intensity-modulated beam then passes through beam-enlarging optics in order to fill the 50-mm aperture of the imaging lens. The scanning mirror intercepts the focused beam and deflects a portion of the beam perpendicularly to the film on the film transport. The imaging spot thus formed at the film is diffraction-limited to about 20 micrometers.

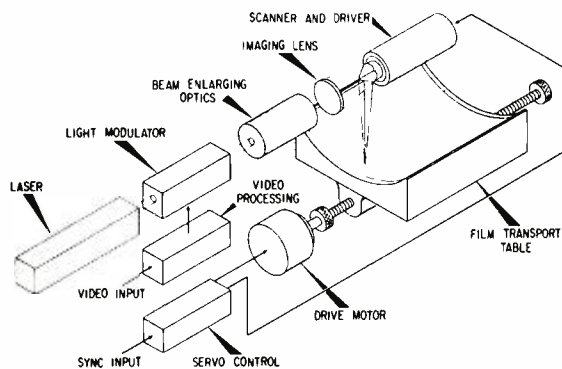


Fig. 2—Prototype LBIR, functional block diagram.

The scanner consists of a precision, four-sided, pyramidal beryllium mirror, an air-bearing motor, and the associated servo electronics. The scanner rotates at 18,000 rpm, synchronous with the incoming video line rate. A focused spot traverses the film, producing 1,200 lines-per-second deflection. The film transport, which provides the vertical deflection, holds the film curved to a precise radius concentric with the scanner and optical axis. Thus, the beam is focused uniformly across the full scan line, and a constant scanner rotational speed yields a linear scan.

Before each exposure the film transport is manually loaded. It has a vacuum film-hold-down system, and is driven at a constant speed, under servo control, parallel to the optical axis during an exposure cycle.

The video electronics provide DC restoration, gain control, gamma correction, and polarity reversal for positive or negative hard-copy output. An elec-

tronic test pattern generator is included for self-test purposes.

Performance

The prototype LBIR performed as shown in Table I. It was designed to appear as a "transparent" element in the total video chain from input scene to hard copy output: it was to faithfully reproduce the images as they were generated by the 2-inch RBV camera, without introducing any additional distortion. For example, while the original RBV camera had limiting resolution of about 4500 elements per scan, the LBIR response was better than 90% at that resolution, and was still 75 percent at 6000 elements per scan. The limiting resolution (limited by the optics) was measured in excess of 25,000 elements per scan.

The prototype LBIR reproduced images which were generated by the RBV camera from live scenes as well as from rear-illuminated, high-resolution glass plate and film transparencies. Exam-

Table I—Prototype LBIR performance.

Parameter	Value
Image format	single frame, 9×9 in. image
Image quality	
Resolution	75% response at 6000 elements per scan
Tone reproduction	13 $\sqrt{2}$ gray steps
Density uniformity	2 %
Linearity	0.5 %
Recording rate	
Scanning	1200 lines/second
Frequency response	5 MHz within ± 1.0 dB

ples of these are shown in Figs. 3 and 4.

In addition to the conventional imagery shown in Figs. 3 and 4, color separation experiments were done for the U.S. Department of the Interior. A set of different black and white negatives (LBIR output) for various spectral regions of a full color scene were made by successively exposing the RBV camera to a color transparency through different spectral filters, and generating the corresponding LBIR output for each exposure. The LBIR negatives were then recombined in a photographic darkroom by a dye-transfer color printing process to reconstruct the original color scene. Different color combinations were used with these negatives to construct a set of various false color pictures. Fig. 5 shows a typical color separation negative set. Since color cannot be reproduced in this printing, the color separation prints are shown instead.

Areas for improvement

Although the prototype LBIR produced relatively good imagery, it lacked many of the essential functions and

Fig. 3—View of Salton Sea reproduced by RBV/LBIR from Gemini V transparency.



Fig. 4—View of Dayton, Ohio from 15th floor of hotel. Reproduced by RBV/LBIR.



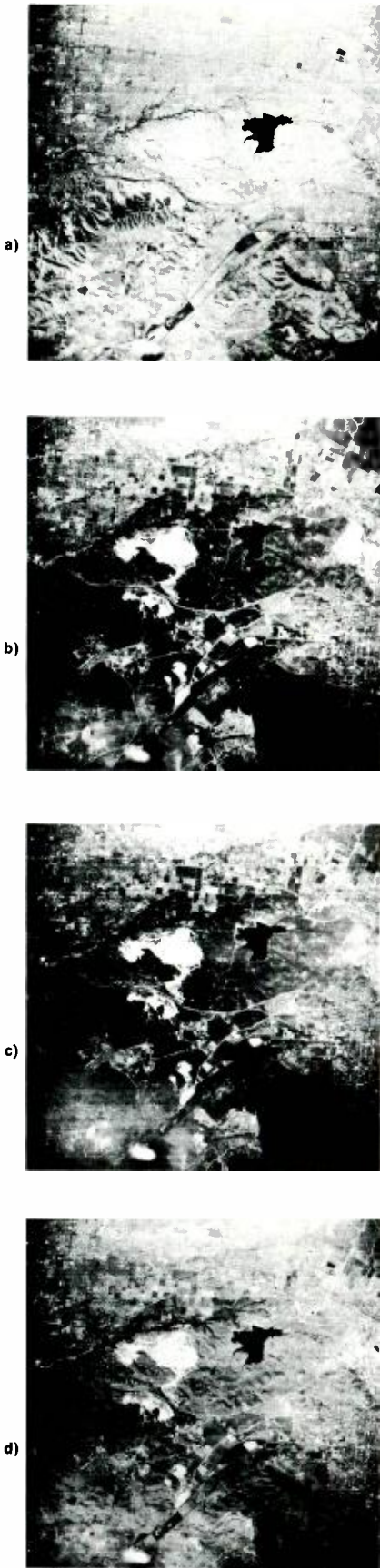


Fig. 5—Color separations and composite images produced by RBV/LBIR from color transparency: a) red, b) blue, c) green, d) composite.

capabilities required for operational use. Some of these were:

- Automatic film handling and rapid sequencing of frames,
- Automatic calibration and exposure control,
- High stability for repeatable drift-free operation,
- Manufacturable and adaptable design,
- Spot shaping for raster line merging, and
- Simple operation, alignment, and maintenance.

In addition, there were a few objectionable patterns which appeared in the images: film-transport-induced “banding”, scanner-servo drift, and scanner-induced “four-line banding.”

Transport banding was visible to the naked eye as faint horizontal streaks running across the full width of the image. These streaks were caused by slight errors in the film transport motion, which in turn caused slight errors in the spacing of scan lines in groups of 10 to 50 scan lines. Although the errors never exceeded ± 30 percent of the 38-micrometer line-to-line spacing (the lines were not displaced enough to touch each other), the effect was quite obvious.

Scanner servo drift caused a low-frequency shift (over a few hundred scan lines) of the scanner phasing relative to the incoming video synchronization pulse train. This caused a waviness to appear in vertical straight lines. Peak-to-peak drift was on the order of one picture element ($1/6000$ of the picture width), yet it was obvious to the naked eye.

The scanner four-line banding pattern



Fig. 6—Laser Beam Image Reproducer.

was caused by excessive tolerance errors in the scanner mirror face-to-axis angles and depth of cut. This effect was only noticeable under magnification.

Second generation LBIR

Based on the experience gained from system tests with the prototype LBIR, and the operational requirements summarized above, new performance and operational concepts were established for the second generation LBIR. This led to design and fabrication phases which resulted in the present LBIR configuration shown in Fig. 6. A few of the improvements and modifications are worth noting:

- Adjustable imaging spot size and shape, for optimum raster merging and resolution;
- Greatly improved geometric fidelity;
- New film transport configuration, capable of single or multiple frame exposure, or continuous strip recording;
- Transport banding reduced to an undetectable level; and

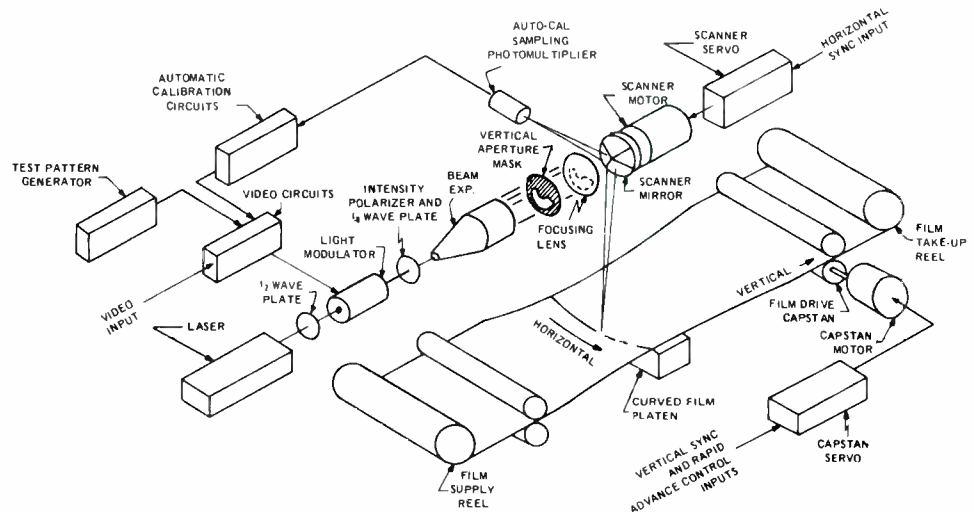


Fig. 7—LBIR, functional block diagram.

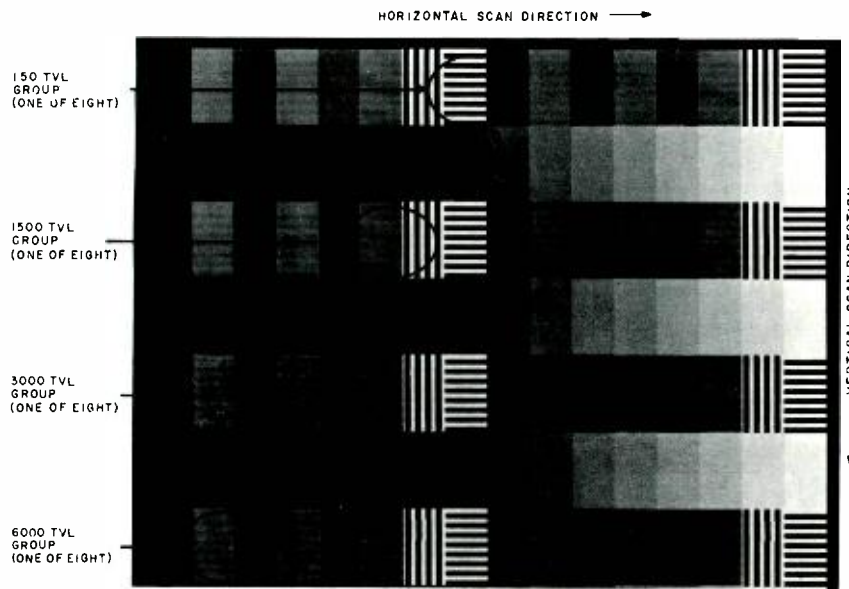


Fig. 8—LBIR composite test pattern.

Automatic exposure calibration for predictable, repeatable output quality. A pictorial diagram of the LBIR is shown in Fig. 7. The new components shown are the test pattern generator, the automatic calibration circuits and photomultiplier, the vertical aperture mask, and the continuous film transport.

Test pattern generator

The test pattern generator provides a variety of highly stable, electronically generated gray scale, resolution, and geometric test-pattern video signals to the video input. These test signals are useful in evaluating LBIR performance during routine calibration checks, and for trouble-shooting. The test-pattern generator also generates various synchronizing signals, including simulated frame cycle modes.

An example of an LBIR test pattern output is shown in Fig. 8. (Note: Moiré patterns may appear in the resolution areas of the image as printed in this publication due to the interaction of the fine bar pattern with the screen used in the half-tone printing process.)

Automatic calibration system

The LBIR exposure level is self-calibrated by an automatic, closed-loop system. This system generates test signals which are fed to the input of the video circuits and samples the resultant modulated light reflected from the scanner; it compares the two, and generates the control signals necessary

to maintain proper exposure parameters (contrast and intensity levels).

The auto-cal system is active whenever the LBIR is "on", but it is automatically switched "off" during an incoming video frame. The auto-cal control levels which were present just prior to an input frame are maintained during the frame exposure cycle and the relative maximum and minimum exposure levels for which the LBIR is calibrated are indicated on front panel meters.

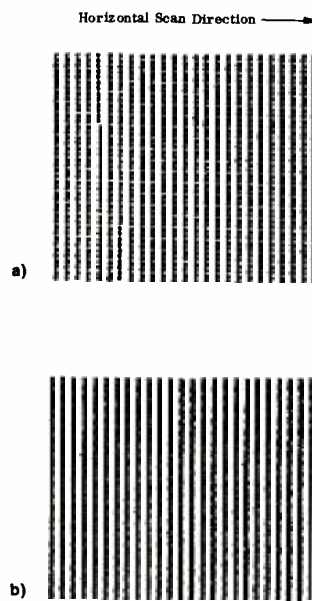


Fig. 9—Vertical expansion of LBIR spot in 6000 TVL bar pattern: a) un-merged raster; b) merged raster.

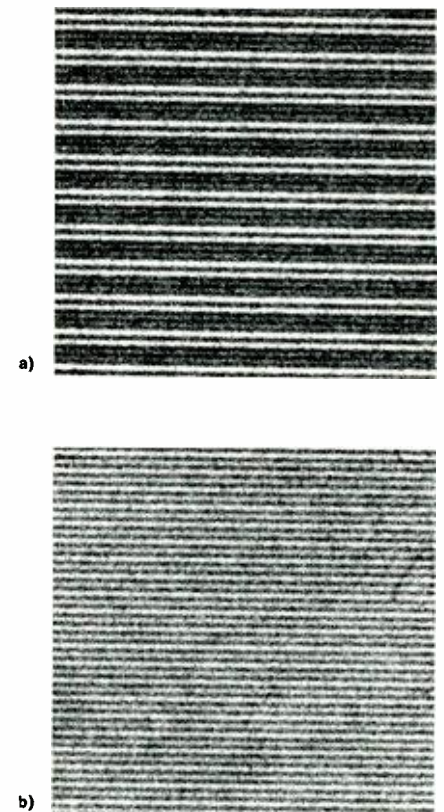


Fig. 10—LBIR scanner banding: a) Prototype scanner with 3-and-1 banding; b) desired scanner performance.

These levels are initially adjusted manually, and may be changed for different photometric characteristics.

Raster line merging

The vertical aperture mask allows adjustment of the vertical dimension of the imaging spot independent of the horizontal dimension. This permits the vertical spot dimension to be expanded for optimum raster line merging without degrading horizontal resolution. Without the vertical aperture mask, the limiting aperture in the diffraction-limited focusing system is the scanner face. The adjustment is continuous, so that raster merging and vertical resolution may be optimized.

The effect of the vertical aperture mask is demonstrated in Fig. 9. The images shown are magnifications of actual LBIR high-resolution test pattern outputs. The black dots in Fig. 9a are the areas of film exposed in a 6000 tv line, horizontal resolution bar pattern. The spaces between adjacent scan lines can be clearly seen. Fig. 9b shows the same pattern, but with the vertical aperture readjusted for a merged

Table II—Current LBIR performance.

Parameter	Value
Resolution (MTF)	6000 TV lines at 80% for 9-inch image.
Imaging spot	Nominally 20 μm horizontal by 38 μm vertical, independently adjustable in both dimensions.
Gray scale	Greater than 100:1 dynamic range.
Video bandwidth	DC to 5 MHz, ± 1 dB.
Film type	Kodak RAR 2496 or equivalent.
Geometric fidelity:	
Linearity	0.01% of raster width, maximum.
Geometric Distortion	0.05% of raster width, maximum.
Repeatability	0.02% of raster width, maximum.
Signal-to-noise ratio (electronics)	50 dB, minimum.
Image format	9-inches wide on 9½-inch-wide film, up to 125 feet long.
Horizontal deflection	
Rates	Continuously selectable between 1000 to 1500 lines per second.
Jitter	0.01% of raster width, maximum.
Vertical deflection (film motion)	
Rates	Continuously selectable up to 4 inches per second.
Length	Intermittent (frame) or continuous up to 125 feet.
Line spacing (banding)	Within 5% of nominal line-to-line dimension.

raster. The horizontal resolution is not affected by the defocusing of the imaging spot in the vertical dimension. In normal operation, the degree of raster merging is optimized for maximum vertical resolution.

Scanner

The minor angular errors present in the prototype scanner mirror caused objectionable banding (as shown in Fig. 10a) because one of the four faces was slightly undercut, and another face had an excessive face-to-axis angular error.

An optimum raster, free of all banding is shown in Fig. 10b. The line-to-line dimension, shown greatly magnified in these pictures, is 38 micrometers.

The current LBIR scanner specification calls for face-to-axis angular accuracies on the order of 5 seconds of arc, and depth of cut accuracies on the order of ± 1.3 micrometers.

The scanner servo was redesigned to a three-loop system. The new scanner servo is capable of rapid synchronization and maintains long-term phase accuracies on the order of $\pm 1/4$ element (better than one part in 10,000), eliminating the problem of waviness in the vertical direction of an image.

Fig. 11—Aerial scene (I) reproduced by RBV/LBIR from high-resolution transparency.



The line-to-line phase stability is too good to be measured.

The high servo accuracy is related to the narrow bandwidth (high inertia) of the scanner servo system. A future addition to the LBIR will be an electronically variable delay line (EVDL) to maintain high performance with an input having poor line rate stability (e.g., a tape-recorded video signal input).

The EVDL can advance or retard the incoming video signal with respect to a fixed delay. The scanner is synchronized to the average line rate of the incoming signal, while the precise phase is achieved by instantaneously shifting the video phase line by line, to coincide with the scanner phasing. This technique is commonly used in transverse-scan video tape recorders.

Continuous film transport

The continuous film transport can record individual images, a rapid sequence of images, or a continuous strip image. In the current LBIR design, the film transport operation is completely automated. A supply roll of 125 feet of film (or 250 feet of special thin-base film) is manually loaded, and the transport automatically cycles for each frame; the exposed images are stored

Fig. 12—Aerial scene (II) reproduced by RBV/LBIR from high-resolution transparency.



in a take-up cassette, and may be removed at any time (in ambient room light) for processing. The transport is currently designed to run at speeds between 0.9 and 4 ips, with the nominal speed of 1.8 ips for the 2-inch RBV camera rates.

The transport performance is well within specifications, which call for film positional accuracies on the order of ± 1 micrometer. This tolerance allows less than ± 3 percent positional displacement of the scan lines, nominally spaced 38 micrometers, and produces images that are virtually free of banding.

Performance

The overall appearance, accuracy, and repeatability of the LBIR output imagery has greatly improved over that of the prototype. In addition, operational features such as alignment, calibration and general operating procedures have been greatly simplified. The LBIR has operated in a virtually hands-off mode for days at a time, and with only minor adjustment over a period of weeks. Current LBIR performance is given in Table II.

Recently, the NASA feasibility model 2-inch RBV camera was interfaced with the LBIR, and several images were reproduced through the system. Some of them are shown in Figs. 11, 12, and 13.

Conclusion

The techniques developed for the LBIR are directly applicable to higher-performance systems. As imaging sensors provide higher resolution, wider dynamic range, and better geometric fidelity, the LBIR technology will be extended to provide maximum utilization of these systems.

References

1. Woywood, D., "Laser Recording: Key to High Resolution Image/Signal Reproduction," *Laser Focus* (Feb. 1968).
2. Thompson, B., "Laser Beam Printing and Recording," *Applications of Lasers to Photography and Information Handling*, SPSE (April 1968).

Fig. 13—Ground scene reproduced by RBV/LBIR from high resolution transparency.



Videovoice

S. N. Friedman

Two-way television communication devices similar to telephones have long held the imagination of the public. The Videovoice system is the only currently available system which can be used in conjunction with existent telephone lines and switching equipment. Because it uses a slow-scan transmission system, the Videovoice system can deliver a single picture in 30 seconds using no more than the 3-kHz audio bandwidth for telephone lines. Where the subject is live, a frame-freeze unit stops all motion; a silicon-target storage tube then allows the receiver to retain single frames for fifteen minutes or more. Potential applications of the Videovoice system include transmission of faces, objects, and scenes; documents; or graphic data for business or medical use; identification and verification of signatures; and transmission of educational materials for a lecture-by-wire.

CONVENTIONAL TELEVISION has been accepted as a "one-way" communication system, where individuals have their own receivers but transmission is restricted to major broadcasting facilities. The absence of a "two-way" capability restricts the individual to the role of viewer and precludes the exchange of information which is vital to total communication.

Samuel N. Friedman, Mgr

Advanced Development & Design Engineering
RCA Global Communications, Inc.
New York, N.Y.

received the BSEE from Polytechnic Institute of Brooklyn in 1956 and has done graduate work at New York University. He joined Radiomarine Corporation of America in 1951 as a design engineer. In 1956 he transferred to RCA's newly formed Advanced Communications Laboratory in New York, where he became Engineering Leader in 1959. Here he gained extensive experience in military and commercial equipment development, both analog and digital, and in advanced military systems for electronic countermeasures and intelligence. Mr. Friedman joined RCA Global Communications in 1968 as Manager, Equipment Design, and in 1970 was made Manager, Advanced Development and Design. He has been very closely associated with the development of new equipments and services such as Simultaneous Voice Record (SVR), Interpolated Voice Data (IVD), Advanced Facsimile, and the present Videovoice. He is a Senior Member of the IEEE, and a Member of the Audio Engineering Society and of the AFCEA.



Although a picture is recognized to be "worth a thousand words," up to now we have not used our television know-how and facilities to the full advantage of the communicator.

What it is

A brief comparison of Videovoice and conventional TV highlights some of the performance characteristics of the slow-scan version. In standard TV, 30 full pictures, or frames, are transmitted every second; that is, a full picture is displayed on the screen and then erased, and the next picture is displayed in its place. This sequential display of full frames at 30 frames per second produces the illusion of motion in the picture. The price we pay for this illusion of motion is the amount of spectrum space required for transmission. Video signals typically fill a bandwidth of 4 MHz, more than 1000 times the bandwidth of a voice circuit and, in addition, pose problems of transmission and recording.

The visual telephone system presently under development by the telephone company appears to be a video system utilizing standard telephone lines. Actually it has a signal bandwidth of 1 MHz: more than 300 times the capacity of the telephone line. This means that new cables and switching systems will be required domestically, and that international use of these systems may be prohibitive.

On the other hand, Videovoice is completely compatible with standard voice-grade circuits and, in addition, allows the user to hold a single desired frame of video; in regular TV, a moving sequence would pass on and be

lost. It is this one-frame-at-a-time transmission capability that allows us to achieve video transmission by telephone line. We can, at the same time, realize additional benefits from the conversion of video to the audio range: video information can be stored on standard audio tape; voice and video can be recorded on stereo tape; and video can be transmitted over standard voice-grade leased circuit facilities alternating with voice, data and teletype.

What it does

Videovoice can transmit standard television video signals over a voice-bandwidth network or over a C2-conditioned (FCC "C2" specifications for tariffed voice-grade telephone lines) voice-grade circuit. The system can be used to photograph a subject with a television camera operating at the standard TV scanning rate, convert to a much lower rate for transmission over voice-bandwidth circuits, store the received picture at the slow rate, and then present it for display on a standard TV screen. Videovoice signals are also compatible with closed-circuit TV and can, therefore be retransmitted at the "receive" terminal over a local closed-circuit TV system.

Videovoice, unlike broadcast TV, does not present motion in the display. Many video requirements, however, can be met without the need for instantaneous transmission, and many users do not require motion in the display received.

The Videovoice transmission process takes between thirty seconds and one minute for each frame of video, depending on the amount of detail desired. Still subjects can be transmitted with a live TV camera. Subjects in motion must have the motion stopped for the duration of the transmission period. To accomplish this, a "frame-freeze" unit has been developed to stop the action in a single frame period and hold that frame for transmission. This frame-freeze capability is made possible by the novel silicon target storage tube designed and developed by Consumer Information Systems Research, RCA Laboratories, Princeton.

Reprint RE-17-2-15
Final manuscript received April 30, 1971.

System description

The basic Videovoice system is shown in Fig. 1. The TV camera and monitor (Fig. 2) are mounted in a custom-designed desk-top unit which allows full rotation of the camera so the "executive" operator can select subjects in the surrounding area. A special 90° reflecting device (not shown) is incorporated in the camera assembly to allow focusing on documents and small objects placed on top of the desk, without tilting the camera. Only familiar TV controls are required.

The same monitor is switched to display the received picture in a bidirectional half-duplex system. In a simplex system, the monitor is available as a separate unit, without camera, for receive only. Also available is an RCA 18 inch TV set, which can be switched to regular VHF-UHF reception when not in use for Videovoice. The large screen may be popular since it allows convenient viewing by a number of people; other sizes or types of monitors can be used to suit individual requirements.

Each desk-top assembly contains a speaker (within the monitor) and a microphone providing hands-free operation of the Videovoice system and independent use of the telephone handset. The balance of the electronic equipment is furnished in an enclosure which can be remotely located.

Duplex system implementation (transmission from either terminal), requires only the complete desk set (camera and monitor) at both terminals. All other pieces of equipment can be used

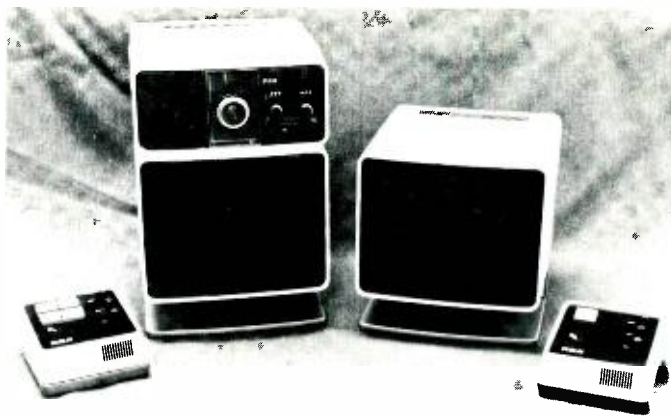


Fig. 2—Videovoice desk-top units.

in either the "transmit" or "receive" modes by actuating a switch. Optional devices include the following:

- 1) A hard-copy printer, which provides a picture of the video in 10 seconds;
- 2) A stereo tape recorder (reel, cartridge, or cassette) which can be used
 - a) For unattended operation at the receive end. Many frames of video can be stored with associated audio and viewed at convenient times. Cost per frame is negligible.
 - b) To store video at the transmit end for later transmission or for record purposes.
 - c) To audit pre-taped recordings with video, which can be viewed as well as heard. This system shows excellent possibilities for educational tapes, training aids, etc. The Videovoice equipment allows both recording and playing back.

System operation

An example illustrates how the system operates. A subscriber at a domestic terminal who wants to send video to his foreign office picks up his telephone and places a voice call in the usual manner (using hot-line, switchboard, or leased channel).

He then rotates his camera to the subject material, and views it on his

monitor. The camera is essentially prefocused, so only minimal adjustment of the focus control is required in most cases. If the subject material is a document or other motionless object, the subscriber presses his TRANSMIT button and the video is sent out over the line. If the subject might move after the camera is set, the subscriber presses his FRAME FREEZE button and views the stopped-action frame which appears on his monitor. He then presses TRANSMIT and the picture is sent out.

At the receive end, the operator switches to Videovoice mode and receives the picture. He can adjust his monitor for contrast and brightness as he would his home tv.

Voice communication is not possible while the video material is being transmitted, but after the full picture has been received, the system automatically switches back to "voice" mode. The video remains on display as long as required (ten to fifteen minutes maximum), and is erased only for presentation of the succeeding frame. Full voice conversation can continue during the no-video-transmission period even though video still being viewed.

Technical considerations

Frame storage

Several approaches have been publicized for this type of slow scan tv frame storage and display (see Fig. 3):

- 1) *High persistence display tube.* A very low resolution picture is transmitted in about eight seconds per frame. The transmission is continuous, and the persistence of the tube creates a still-image effect.
- 2) *Memory tube.* A storage-type cathode-ray tube records the video at the transmission speed but stores it for display over extended periods without requiring continuous transmission.
- 3) *Magnetic disc storage.* A magnetic

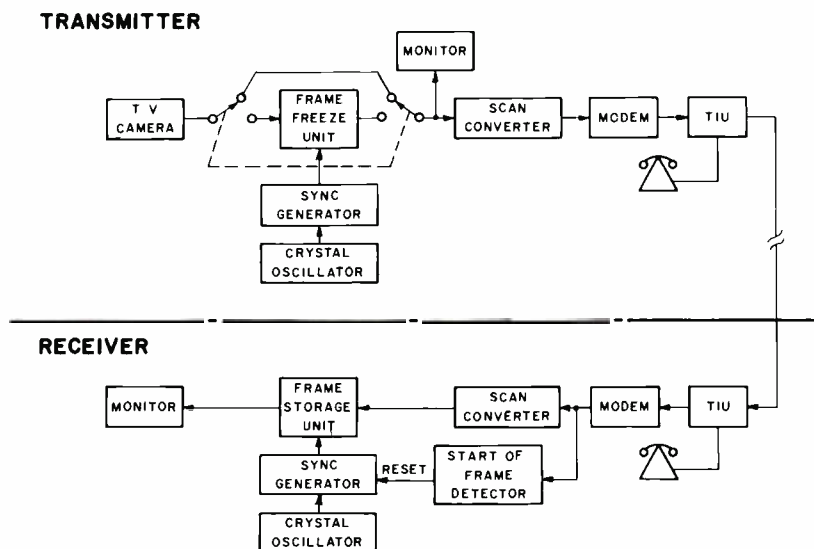


Fig. 1—Videovoice 3-kHz basic (Simplex) system.

disc memory device uses a small disc driven at speeds on the order of 1800 rpm. The video information is laid down on the rotating disc in a prescribed pattern and an associated TV synchronizing signal is recorded directly on the disc itself. The signal can be played back and displayed continuously at standard TV rates.

4) *Silicon target storage tube.* The silicon storage tube is a small, low cost, single-ended, non-destructive read-out storage device. It is particularly useful where video information is to be displayed on conventional TV monitors, or "written" on a target from conventional TV cameras. The video can be recorded at TV speeds and read off at slower rates or, conversely, written at slow speeds and read off to a TV monitor. A video frame can be written onto the target in 1/30 of a second (one TV frame); it can then be continuously read out for display for periods of five minutes or more. At the end of this time, the stored message can be erased in a fraction of a second. A limiting resolution capability of 800 TV lines is typical on present one-inch diameter storage tubes.

The most desirable system lies between the disc approach and the use of a silicon-storage device. The high persistence display tube and the memory tube suffer from serious disadvantages: unacceptably low resolution, limited gray scale capability, requirement for motionless objects, and incompatibility with standard TV components. Neither offers any real advantages to compensate for these shortcomings.

The disc, on the other hand, has many advantages and does present many attractive features such as, a) almost unlimited picture viewing duration, b) very large frame storage capacity (as many as 60 frames) at practically no added cost or increased size, and c) simultaneous read and write capability. However, it has major disadvantages due to the mechanical aspects of the device: high maintenance cost, low reliability, need for synchronization of power sources at the terminals, and other associated problems. For RCA Global Communications applications, where field maintenance is an overriding consideration, these shortcomings ruled out this approach.

The case for the silicon-target storage tube is conclusive. Although it has relatively limited picture duration and restricted storage capacity at present, compromise solutions yield acceptable performance characteristics. The prob-

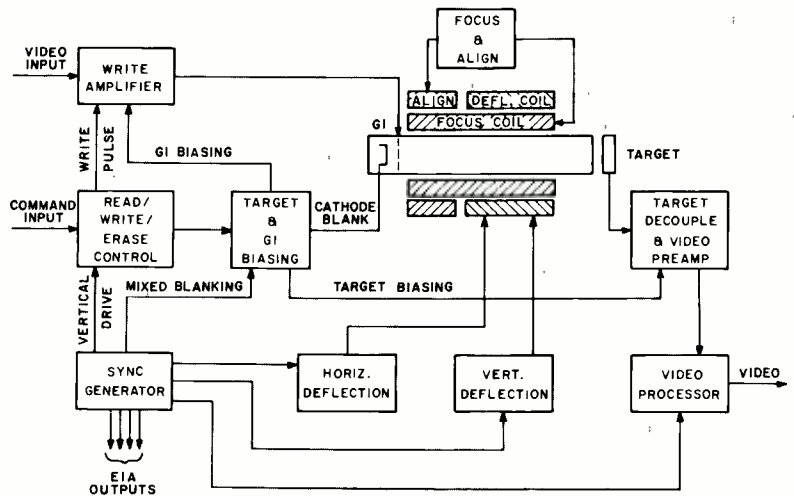


Fig. 3—Frame freeze unit.

ability of improved characteristics in the near-term future is very high. Moreover, the list of advantages for this approach is quite impressive: all electronic, high resolution, high reliability, full compatibility, stop-action capability and versatility.

Scan conversion

The scan converter (Fig. 4) provides for scanning the stored image in the standard video raster format (15,750 lines/second, 60 fields, 30 frames, 2:1 interlace) or in a similar format modified to simplify synchronization. The input to the scan converter is, thus, either a composite video signal from the TV camera or a repetitive version of the stored single frame scan outputted from the frame freeze (storage) unit.

The video scan converter transmitter samples the repetitive single video frame to produce a pulse amplitude modulated (PAM) signal suitable for transmission by standard facsimile-type modem techniques over voice-bandwidth facilities. In essence, the scan converter reduces the single TV frame to approximately 132,000 amplitude modulated sample-pulses; the amplitude of each pulse is proportional to the luminance of the corresponding point in the TV frame.

The present procedure is to sample vertically, taking corresponding points on each of the 525 lines in a specified sequence and proceeding across the target horizontally. The received picture builds up from left to right. With a storage device that has simultaneous read-write capability, the gradually developing picture can be viewed; however, with the present storage tube, the receive display is totally

blanked during transmission, except for a thin vertical line cursor which moves horizontally, indicating the instantaneous position of the scanner.

Synchronization and transmission

Synchronization is more complicated in the slow scan method than in standard TV because the sampling signal is pulsed rather than video; and the sampling period is of very short duration, on the order of 250 nanoseconds per sample. Available circuit bandwidth limitations preclude the transmission of synchronizing signals other than long duration codes such as start of frame. Synchronization is maintained, therefore, by independent, highly-stable crystal oscillators at each terminal. At the receive terminal, the incoming PAM signal is sampled in the same interleaved manner as at the transmitter. Synchronizing signals are provided by the local crystal oscillator system.

The transmission time for a full video frame is a function of the type of modem used. The only commercially available modem is the WE602 Series, which allows for a sampling rate of approximately 1000 samples per second, or a 2-minute-per-frame transmission time. Since our marketing inputs indicate the preference for a 30-second picture with no more than a one-minute picture being acceptable, RCA initiated special in-house developments. This effort first produced a modem design with satisfactory performance at 2000 samples/sec: a one minute picture. Further development aimed at 4000 samples/sec., for the desired 30-second transmission period per frame, was then completed at RCA Globcom.

Control and operation

Because the Videovoice system is intended for "executive" operation, design philosophy calls for minimum manual control and maximum automation consistent with cost effectiveness. In the camera, for example, only two controls are accessible for adjustment: a FOCUS control with three basic settings—normal, distance, and documents—and a lens tilt control. For the monitor, only CONTRAST, BRIGHTNESS, and VOLUME are brought out on the control unit. A MIC switch is also available, to disable the microphone.

The hook switch on the telephone set remains the basic control for activating the overall circuit. The switches on the control unit are of the push-button type and are designated VIDEOVOICE, LIVE CAMERA, FRAME FREEZE, and TRANSMIT. The switches are momentary and are illuminated when energized. They are not interlocked, so that several may be illuminated at the same time; for example, the TRANSMIT button will light when video transmission is in progress, as will the VIDEOVOICE, and either the LIVE CAMERA or FRAME FREEZE, depending on the type of picture being transmitted.

Some functions are automatically switched, including switching from voice to video at start of video transmission and back to voice at the end of the frame; switching the monitor between the camera and the frame freeze unit; switching between the telephone handset and the loudspeaker system; and switching from standby

power on the video equipment to full power when Videovoice is actuated. At the receive end, only the VIDEOVOICE switch is required. All other functions are automatic. Table I summarizes the technical details.

Commercial possibilities

Videovoice is a particularly significant development for RCA Global Communications. It opens the way for visual communications internationally, a capability which was heretofore precluded by both technology and economics. The long-range applications are almost unlimited. For the near term, we can mention the following:

- 1) Videovoice can supplement the capability presently provided to our voice record leased channel subscribers. The Videovoice feature could be offered at only a relatively small additional cost for equipment lease, with no change in circuit requirements or service costs.
- 2) Videovoice can supplement our executive "Hot Line" offering.
- 3) A Videovoice circuit could be leased specifically for the transmission of a wide range of audio and visual material.
 - a) Pictures of parts and assemblies for manufacturing purposes, maintenance and repair instruction, and spare parts catalogs.
 - b) Advertising and sales promotion.
 - c) Materials for the identification of people; signatures.
 - d) Drawings, documents, maps, and schematics for conferences and discussions.
 - e) Educational and training material to support an illustrated lecture, a blackboard-by-wire demonstration, or a textbook-on-audio tape.
 - f) Purchasing and inventory control documents and supporting photographs.
 - g) International live-feed of Closed-

circuit TV material.

h) Cardiograms and other medical graphic data.

i) Airlines arrival departure information.

j) Brokerage display boards.

k) Banking, administration, and account material.

4) Videovoice could be used to input video data into a computer for data processing, and to graphically display computer outputs.

In most situations where communications are required, the use of Videovoice can enhance the efficiency and intelligibility of the system, and at the same time, contribute significantly to circuit utilization.

Table I—Technical details.

System	Description
Format	Standard TV
Vertical lines/frame	525
Fields	60, 2:1 interlaced
Frames/sec	30
Sync, interfaces and levels	Standard EIA
Gray scale	6 or 7 shades
Transmission time	30 sec/frame
Desk set camera	
Reproduction	Monochrome
Horiz. resolution	600 TV lines center, 450 lines corner
S/N ratio	35 dB
Total raster distortion	2.0% max.
Auto. light compensation	2000:1 range with no more than 6 dB change in video output level
Single front and panel control for focus controls range and aperture automatically	
Frame-freeze unit—silicon storage tube	
Resolution	800 TV lines
Retention time	10 min. (approx.)
Frame write time	1/30 sec.
Frame erase time	1/3 second
Deflection, focus, alignment	magnetic
Scan converter operating modes	
Manual	Single frame
Automatic	Continuous sequential frames, automatic start-of-frame triggered by transmitted code
Transmit terminal	
Input	Composite video with EIA sync, 1 V p-p, 75 ohms
Output	Slow-scan video, 0-7 V, 600 ohms
Receive terminal	
Input terminal	Slow-scan video, 0-7 V, 600 ohms
Output	Composite video with EIA sync, 1 V p-p, 75 ohms
Modem	
Baseband	Slow-scan video, 0-7 V, 600 ohms
Line Signal	FM carrier, 0 dBm, 600 ohms
Trunk interface unit (TIU)	
Line signal level adjust	Automatic
Signaling	2600 Hz
Transmission capability	Full duplex
Interface	EIA/CCITT Standard

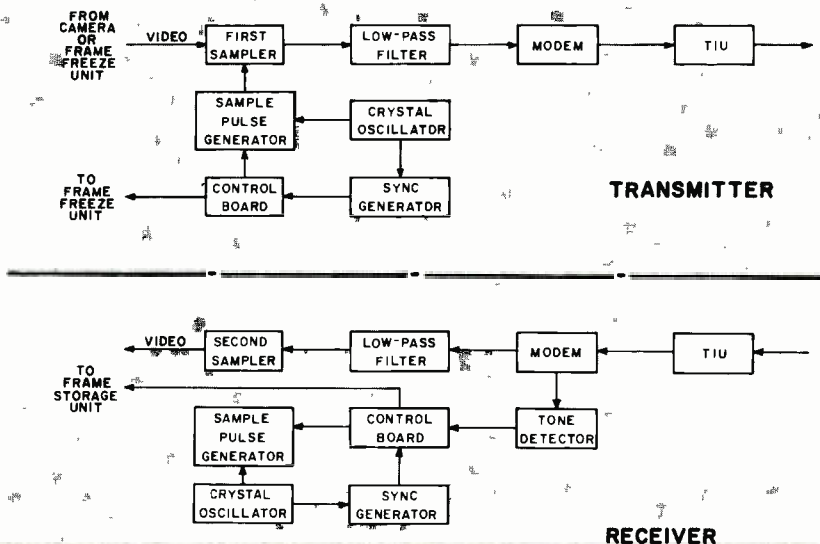


Fig. 4—Scan converter.

High-power GaAs close-confinement laser diodes

T. Gonda | R. B. Gill

The fabrication and characteristics of high-power close-confinement GaAs laser diodes are described. Single pellet devices emitting up to 100-W peak power at 300°K are detailed. These diodes have one GaAlAs-GaAs heterojunction prepared by liquid-phase epitaxy. The parameters considered in the design of these devices are discussed, and the test equipment and measurement techniques used in their characterization are outlined. Test results showing lasing threshold current density, peak optical output power, conversion efficiency, and emitted beam patterns for these devices are presented. Reliability data relating to long-term operational life and mechanical and environmental testing are also presented. A comparison is made of the gradual degradation of units operated at a current density of 50,000 amperes/cm² with units operated at reduced (30,000 amperes/cm²) drive currents.

THE RECENT DEVELOPMENTS in high-peak-power GaAs laser diodes, operating in the pulsed mode at room temperature, have been made possible by two advances in GaAs materials and device technology: the development of the single heterojunction close-confinement GaAs injection laser by Kressel and Nelson¹, and Panish and Hayashi, et al^{2,3}; and the improved quality of the GaAs epitaxial substrate which contains the active laser region. As a result, processes have been developed which yield lasers characterized by

- 1) Room-temperature threshold currents between 7,500 and 20,000 A/cm²;
- 2) External differential quantum efficiencies for single-ended lasers in the range of 30 to 50%; and
- 3) Excellent device uniformity within a wafer and good wafer-to-wafer reproducibility.

In this paper, the performance of devices with emitting facets up to 60 mils in length is discussed; some of the substrate and epitaxial parameters which affect the performance of these devices are described; and the results obtained during a small production program of fifty 60-W diodes are presented. In addition, life test results are presented for the high-power diodes, which indicate that long-term pulse operation is possible in these devices without serious degradation in performance.

Reprint RE-17-2-5 (ST-4656)

Final manuscript received May 13, 1971.

The work reported in this paper was sponsored in part by the U.S. Army Electronics Command, Philadelphia, Pa., under Contract DAABO5-67-C-2709 with technical guidance from U.S. Army Electronics Command, Fort Monmouth, N.J.



Authors, Tibor Gonda (left) and Robert Gill.

Tibor Gonda

Special Products Engineering
Solid State Division
Somerville, New Jersey

received the MSEE from Technical University Graz of Austria in 1957. He also did graduate work in Electrophysics at Polytechnic Institute of Brooklyn. Mr. Gonda joined RCA Electronic Components, Somerville, N.J. in 1962, where he was assigned to the Gallium Arsenide Special Products group. In this capacity, he engaged in applications engineering and circuit development work on solid-state power sources at microwave frequencies. He currently is assigned to the Optical Devices and Tunnel Diode Engineering group of Special Products Engineering, where he is conducting studies of device properties and radiation characteristics of optical diodes and injection lasers. One of his most recent responsibilities was the design, development, and pilot-line fabrication of a 60-W, single-pellet, injection-laser diode.

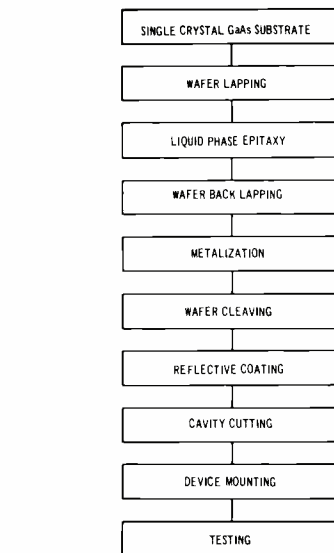


Fig. 1—Material processing sequence for fabrication of high-power laser diodes.

Processing of laser diodes

The processing sequence for fabrication of the high-power diodes is shown in Fig. 1. The GaAs single crystals which were wafered to form the epitaxial substrate were all n-type, Si doped, and grown at RCA by the Horizontal Bridgeman method. The net donor concentrations varied from 2.5×10^{18} to $3.8 \times 10^{18} \text{cm}^{-3}$. The lower number represents the minimum concentration that yielded lasers having (at 300°K) low lasing-threshold currents and high differential quantum efficiencies; the larger number approaches the highest concentration that can be readily attained and still provide a high degree of assurance that the crystal is free of precipitates that degrade laser performance and reliability.

Robert B. Gill

Optoelectronic Products Department
Solid State Division
Somerville, New Jersey

received the BS in physics from Fairleigh Dickinson University in 1963 and the MS in physics from Stevens Institute of Technology in 1967. Mr. Gill was employed at RCA Laboratories in 1963 where he was primarily engaged in the development of semiconductor devices. His responsibilities included the preparation and characterization of materials, device design and evaluation, and process development. In 1968, Mr. Gill transferred to the Optoelectronic Products Departments of the Solid State Division where he was assigned to Semiconductor Engineering. His primary responsibilities have been in the solution of problems associated with GaAs, (GaAl)As and GaP single and multiple epitaxy and the design of electroluminescent devices including injection lasers and visible and infrared emitters utilizing these materials. His work in these areas contributed to the design and development of the first commercial GaAs and (GaAl)As single heterojunction-injection lasers and laser arrays. Mr. Gill is author or co-author of nine technical papers.

All crystals used in this work contained average dislocation densities less than 1000 pits/cm² as determined by etch-pit counts made on [111] wafers taken from the extremities of the useful portion of the ingots. Crystals which contained either dislocation clusters or linge were not used. The crystals were also characterized by photoluminescence in the manner described by Kressel⁴ and were rejected if $\alpha/\beta > 2$, where α is the emission-band peak characteristic of recombination of electrons (with either free holes or holes trapped to shallow Si acceptors) and β is the long-wave-length band peak which is apparently associated with an unknown deep center.

After slicing, lapping, and etching the substrate wafer to remove work damage, a GaAlAs layer was grown on it by liquid-phase epitaxy from a ZnAl-doped Ga melt nearly saturated with GaAs. The melt was brought into contact with the substrate near 980°C and cooled at 5 to 30°C/minute to 600°C, at which point the furnace was freely cooled to room temperature. Because the growth solution was initially unsaturated near 980°C, melt-back of 1 to 2 mils of the substrate surface generally occurred when the melt was brought into contact with it. As the furnace cooling progressed, the melt became supersaturated, and the GaAlAs layer deposited on the wafer surface. The initial melt-back assured the generation of a uniform planar heterojunction interface, which is crucial to the ultimate quality of the devices. The total thickness of the GaAlAs layers obtained is generally 3 mils.



Fig. 2—Cross-section of GaAs single heterojunction laser structure.

Fig. 2 shows a cross-section of a typical epitaxial wafer. The heterojunction interface has been delineated by etching with a solution of 160 mg of AgNO₃, 20 g of CrO₃, 20 cm³ of HF, and 40 cm³ of H₂O, for about 6 seconds. The GaAs p-n junction, which lies about 2 μm below the heterojunction interface, results from the diffusion of Zn from the epitaxial layer into the substrate during the growth cycle. The actual depth, which falls between 2 and 3 μm for optimum device performance at room temperature, can be controlled by an after-growth diffusion. Both the uniformity and planarity of the epitaxial and diffusion front interfaces are characteristic of solution-grown layers on high-quality, low-dislocation, precipitate-free substrate. After growth, the wafers are lapped parallel to the (100)-plane to a total thickness of between 2 and 3 mils.

After ohmic contacts had been applied, the wafers were cleaved into strips, 12 to 18 mils wide, and a reflecting optical coating was applied to one of the cleaved sides. The Fabry-Perot laser cavity was completed by wire-sawing the strips into pellets of

the desired length. The pellets were then soldered to an OP-12 coaxial package shown in Fig. 3, which was hermetically sealed with a cap containing a transparent glass window.

Test facilities

To characterize and evaluate the high-power injection lasers, a pulse power supply with a 300-ampere drive capability was designed and constructed. The pulser output consists of six identical parallel scr pulse circuits, each supplying a peak output current of approximately 50 amperes. The open pulser chassis is shown in Fig. 4; Fig. 5 shows the pulser with a laser diode mounted on a heat sink at the center of the pulser chassis. At room temperature, the pulser is capable of a peak pulse-output current of at least 300 A, with a 100-ns pulse width, and a repetition rate of 100 Hz. The laser output power measurements were made with ITT F-4000 phototubes using calibrations supplied by the manufacturer.

Device performance

During the course of this work, laser diodes having cavity lengths ranging from 9 to 60 mils have been charac-

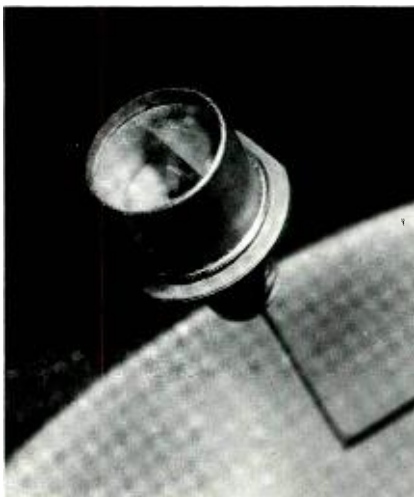


Fig. 3—An OP-12 coaxial package used for diode mounting.

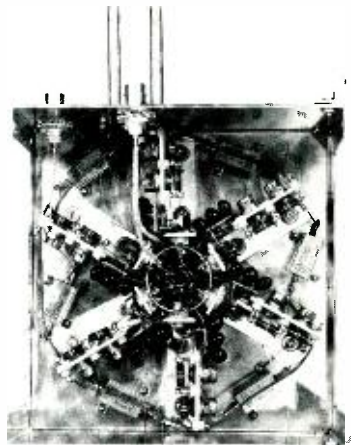


Fig. 4—High current pulser—chassis open.

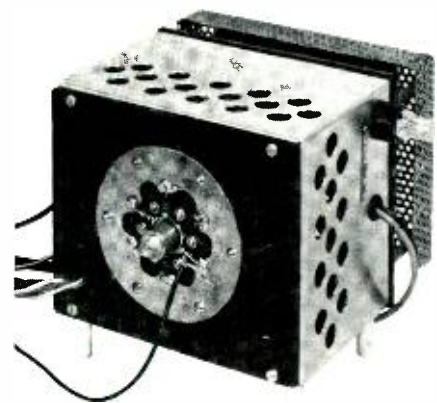


Fig. 5—High current pulser with laser diode mounted at the center.

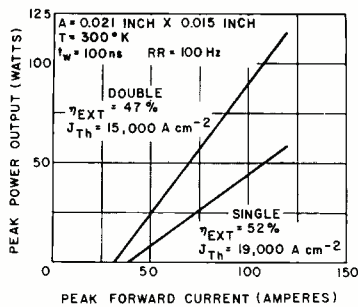


Fig. 6—Moderate-power laser performance.

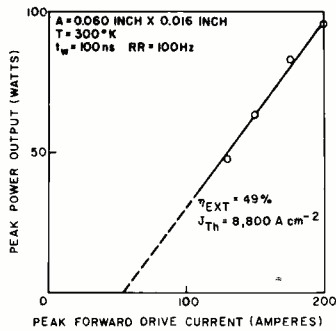


Fig. 7—High-power laser performance.

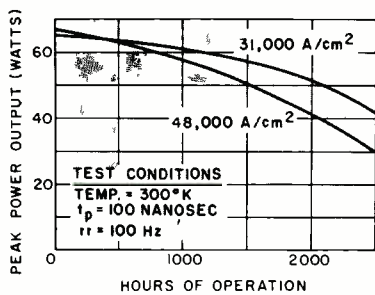


Fig. 8—Life test data for high-power laser diodes at two different current densities (laser geometry: $W = 0.056$ in.; $L = 0.018$ in.)

TESTS	MIL STD 750 REF.	CONDITIONS	SYMBOL	LIMITS MIN. MAX.	UNITS
1. RADIANT PEAK POWER		$T_c = 25^\circ\text{C}$ $P_{rr} = 100\text{ Hz}$ $t_p = 100\text{ ns}$ $I_{fm} = \text{TYPE A} = 250\text{ A}$ $\text{TYPE B} = 275\text{ A}$ $\text{TYPE C} = 300\text{ A}$	P_{pk}	60 80	WATTS
2. VISUAL AND MECHANICAL INSPECTION	2071				
3. WAVE LENGTH			λ	9000 9100	ANGSTROMS
4. BEAMSPREAD— —HALF ANGLE AT HALF POWER— POINT				15 15	DEGREES
5. OPTICAL ALIGNMENT				-10 +10	DEGREES

Fig. 9—Electrical and optical performance specifications.

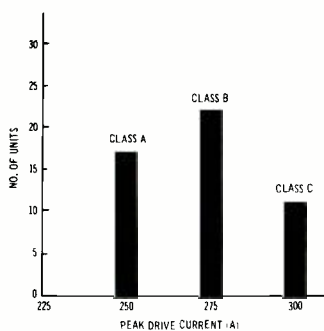


Fig. 10—Distribution of drive current for fifty 60-W lasers.

terized. The 9-mil diodes generally were fabricated from all wafers to evaluate the relative quality and uniformity of one wafer with respect to another. Single-ended laser diodes having external differential quantum efficiencies up to 50% have been obtained during these wafer evaluations.⁵ Wafers which exhibited good uniformity and yielded high quality 9-mil diodes were then used to fabricate the larger diodes.

Fig 6 shows the peak power emitted as a function of forward drive current for both a single-laser and a double-laser stack consisting of diodes having 21-mil emission lengths. Stacks were formed by soldering laser pellets one on top of another. While some variations in unit-to-unit performance were noted, device uniformity within a given wafer generally is sufficient to produce, in small stacks, the expected multiple increase in emission power. The operating conditions for these devices have been extended to nearly 3-W emission/mil of facet—primarily to demonstrate the linear dependence of emission on forward drive and the freedom of these devices from saturation or cross modes. These lasers and all others discussed in this paper are single-ended emitters because they contain a reflective optical coating on one facet of the laser cavity.

In general, devices can be produced that will maintain a peak-power-emission density 2 to 3-W/mil of emitting facet for 100 to 200-ns pulse widths for a short duration; however, the peak power must be limited to less than 1.5 watts/mil of facet, if long-term device stability is to be realized for single heterojunction lasers in their present form.

Fig. 7 contains the performance characteristic of a low-threshold 60-mil laser. In this device, the drive current was limited to 32,000 A/cm² to prevent possible catastrophic damage to the laser. The absence of cross modes encountered by Nelson⁶ in his earlier work appears to be associated with the wire sawing process used to generate the pellets. The coarse cutting grit used in this process sufficiently roughens the laser ends to suppress these modes.

Fig. 8 shows life test data obtained on two 56-mil lasers of initially com-

parable power, but driven at significantly different current densities. As expected, the laser operated at the lower current density degraded at a substantially lower rate than the other. The total degradation for this unit, after 2500 hours operation, was about 35%. These data illustrate the feasibility of stable device operation under reasonable conditions.

Pilot production and sample device tests

With the support of the Industrial Engineering Division, U.S. Army Electronics Command, Philadelphia, Pa., a small production operation for large-area high-power lasers was established. A portion of the performance specifications for these devices is shown in Fig. 9. The basic 56×18-mil lasers were divided into three groups of devices having output powers in the range of 60 to 80 watts, at 250, 275, and 300 amperes. An upper limit of 80 watts was established for these devices to assure elimination of possible catastrophic degradation and to insure an operational lifetime in excess of 1000 hours. Sample devices were subjected to mechanical and environmental assurance testing which included shock, vibration, and constant acceleration tests as well as exposure to controlled environments and thermal cycling. In the course of the production device sampling, no failures were encountered.

Fig. 10 shows the class distribution of the 50, 60-W lasers. Approximately 80% of the devices are contained in the low and moderate drive current groups with the center group containing 46% of the devices. The maximum drive current density for these devices is 47,000 A/cm². The threshold current distribution for this device lot is shown in Fig. 11. Threshold current densities ranged from 7500 to 18,000 A/cm². The typical threshold current for these devices was 12,000 A/cm².

Fig. 12 shows the peak power distribution for the same group of devices. Lasers were obtained having peak powers ranging from 60 to 71 watts at the appropriate drive current. The emission pattern for one of the devices is shown in Fig. 13. The non-uniformity in the emission pattern perpendicular to the junction indicates diffraction of the emitted beam

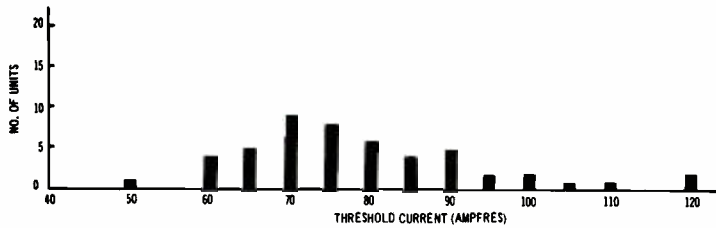


Fig. 11—Distribution of threshold current for fifty 60-W lasers.

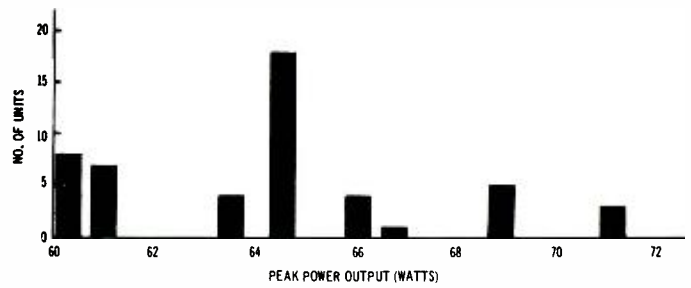


Fig. 12—Distribution of peak power output at maximum drive current for fifty 60-W lasers.

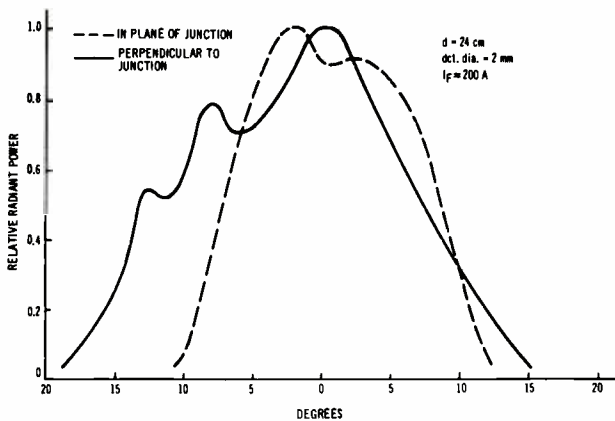


Fig. 13—Typical beam-spread characteristics of large-area diodes.

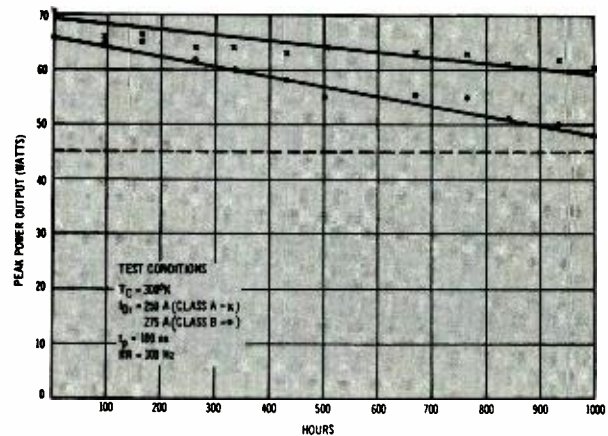


Fig. 14—Life test data on two units for 1008 hours of operation.

as a result of the 2- μ m cavity. The irregularity in the beam emitted in the plane of the junction is probably caused by a variation in emission intensity across the facet of the device. For a beam pattern of this type, approximately 90% of the total power would be collected by an f/1.0 optical system, 70% by an f/2.0 system and 50% by an f/3.0 system.

Life test results on class-A and class-B lasers are shown in Fig. 14. As before, the unit driven at the lower current density exhibits more stable performance. After 1000 hours of operation, its performance was 84% of its initial value. At the same point, the class-B unit was 74% of its initial value. The devices generated during this program met or exceeded all of the design specifications shown in Fig. 9.

Commercially available lasers

Following this successful pilot production run, RCA made two commercially available developmental high-power single heterojunction GaAs lasers: RCA Type Nos. TA7705 and the TA7787. Both devices have a typical lasing threshold current of 70 A at 23°C and are rated at a maximum peak forward drive current of 250 A.

At this drive current, the minimum peak power output is 60 W for the TA7787 and 40 W for the TA7705. These devices represent the highest peak-power single-unit GaAs lasers commercially available to date.

Summary

Single-ended GaAs single heterojunction close-confinement lasers have been fabricated emitting up to 100-W peak power at 200-A drive current. These devices exhibited a linear dependence of emitted power on forward drive current above lasing threshold and showed no effects which could be attributed to either emission saturation or cross modes.

A pilot production operation for 60- to 80-watt lasers was successfully established and the feasibility of manufacturing these devices determined. Life studies on high-power devices and the smaller laser stacks have indicated that operational lifetimes in excess of 1000 hours can be obtained on these devices within reasonable current drive and power emission limitations. The success of the pilot production run has resulted in the commercial availability of two high

power GaAs single heterojunction lasers, the TA7705 and the TA7787.

Acknowledgment

The authors thank S. Berkman who supplied all of the GaAs single crystal substrate; L. Elbaum and S. Watson for the technical assistance; and R. S. Myers who designed and fabricated the high-current pulser.

References

1. Kressel, H. and Nelson, H., "Close-confinement Gallium Arsenide p-n Junction Lasers with Reduced Optical Loss at Room Temperature" *RCA Rev.* vol. 30 (March 1969) p. 106.
2. Hayashi, I., Panish, M. B., and Foy, P. W., "A Low-threshold Room-temperature Injection Laser", *IEEE J. Quantum Electronics (correspondence)* vol. QE-5 (April 1969) p. 211.
3. Panish, M. B., Hayashi, I., and Sumski, S., "A Technique for the Preparation of Low-threshold Room-temperature GaAs Laser Diode Structures", *IEEE J. Quantum Electronics*, vol. QE-5 (April 1969) pp. 210-211.
4. Kressel, H., Nelson, H., McFarlane, S. H., Abrahams, M. S., LeFevre, P., and Buiocchi, C. J., "Effect of Substrate Imperfections on GaAs Injection Lasers Prepared by Liquid-phase Epitaxy", *J. Appl. Phys.* vol. 40, (Aug 1969) p. 3587.
5. Gill, R. B., "Room-temperature Close-confinement GaAs Laser with Overall External Quantum Efficiency of 40 Percent", *Proc. of IEEE (correspondence)* vol. 58, No. 6, (June 1970) p. 949.
6. Nelson, H., "High-Power Pulsed GaAs Laser Diodes Operating at Room Temperature", *Proc. of IEEE*, vol. 55, No. 8, (Aug 1967) pp. 1415-1419.

Laboratories RCA Ltd—a profile

R. F. Holtz, Managing Director



The Zurich Laboratories were established by RCA in 1955 to relate carefully and fully with the work of the scientific and technical communities in Europe. Its international staff has been drawn from many wide ranging backgrounds. The resulting spectrum of specific interests and disciplines and the varying philosophic views and patterns of approach to scientific problems have made for a richly diversified staff performance. Beyond this, the small size of the Zurich laboratory has preserved a working atmosphere

conductive to a high order of performance on work assignments, and relatively unstructured relationships among individuals.



Established as a wholly owned Swiss subsidiary of RCA, Laboratories RCA Ltd. in Zurich has grown considerably over the past 15 years in size and in scope of program. Late in 1970, a relocation was begun into the present new building, occupying 40,000 square feet of space. Full resumption of research and development projects was marked by an Inauguration in June, highlighted by an all day Technical Symposium.

The larger part of the Labs-Zurich program lies in the area of fundamental and applied research in the fields of solid state materials and holography, integrated carefully with related work at the Laboratories in Princeton. Independent of this research operation, the installations in Zurich include a development laboratory and a technical service laboratory with programs in the field of color television including: video signal generation and transmission, international television standards, and particularly the problems of multiple technical standards in television recording and reception.

Current programs are summarized in the following series of monographs prepared by members of the Zurich Labs Technical Staff. The monographs contain sufficient detail to give an insight into objectives, approaches, and findings—and to yield a meaningful profile of the RCA Technical center in Europe.

Editor's Note: The following articles, originally submitted as a part of this article, have been removed and will appear as Engineering and Research notes in our next issue:

"Thyristor horizontal deflection and high-voltage circuits," by G. Forster, "Electrophotography," by H. Kiess, and "Preparation of single crystals and thin films," by B. Curtis, J. Kane, H. Lehmann, H. von Philipsborn, and R. Widmer.

Engineering

R. A. Mills, Manager



The development and technical service laboratories are staffed by some 12 electronic engineers aided by a smaller group of technicians and electromechanics. Intensive team efforts are mounted to deal with the continuously changing array of system and circuitry problems arising in Europe in the field of color television. The results of this work is frequently shared with the industry through the medium of meetings and conferences sponsored by the Zurich Laboratories and held in Zurich or at other convenient locations in Europe.

SECAM color TV reception with PAL receivers



R. Peter
Licensee Technical Service
Engineering

A circuit has been devised to convert a SECAM signal in such a way that it can be demodulated by a normal unmodified PAL decoder. Thus an economical means is provided of adding SECAM reception facilities to a PAL receiver.

Principle of SECAM conversion

In the SECAM system, the two color-difference signals $R-Y$ and $B-Y$ are frequency modulated onto a subcarrier and are then transmitted sequentially (first line= $R-Y$, second line= $B-Y$). In the system shown in Fig. 1, the two difference signals are demodulated sequentially in a single frequency-discriminator and the demodulated signal is then applied to a phase modulator. This modulator remodulates the sequential SECAM color-difference signal onto a PAL subcarrier. The subcarrier, provided by the oscillator in the PAL decoder, is switched line-by-line from 0° to 90° and supplied to the phase modulator. In this modulator, the $R-Y$ signal is modulated with 0° subcarrier phase, the $B-Y$ signal with 90° subcarrier phase. The output signal of the modulator is applied to the delay-line input of the PAL decoder.

Demodulation of the converted SECAM signal in an unmodified PAL decoder

The modulated difference signals are delayed in a $64\text{-}\mu\text{s}$ delay line and are added and subtracted to the direct input signals. The delay line produces a phase shift of 180° . At the subtraction output we find

$$\begin{aligned} \text{—In the 1st line: } & (R-Y) - [- (B-Y)] = (R-Y) + (B-Y) \\ \text{—In the 2nd line: } & (B-Y) - [- (R-Y)] = (R-Y) + (B-Y) \end{aligned}$$

These signals are applied to the $B-Y$ demodulator that is a normal part of the PAL decoder. At the addition output we find

$$\begin{aligned} \text{—In the 1st line: } & (R-Y) + [- (B-Y)] = (R-Y) - (B-Y) \\ \text{—In the 2nd line: } & (B-Y) + [- (R-Y)] = - (R-Y) + (B-Y) \end{aligned}$$

These signals are applied to the $R-Y$ demodulator that is a normal part of the PAL decoder and which includes (as part of its normal PAL function) a switch that inverts the signal polarity on successive lines. Thus, the signal for the first line is demodulated directly while that for the second line is inverted and demodulated, the third line is again demodulated directly, and so on for alternate lines.

Reprint RE-17-2-21

Final manuscript received June 14, 1971.

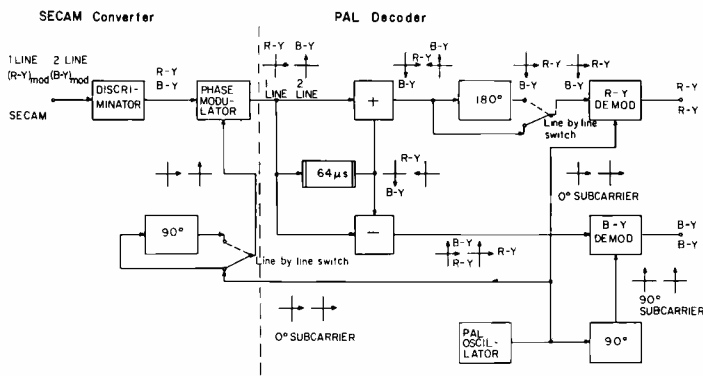


Fig. 1—SECAM-PAL Demodulation System

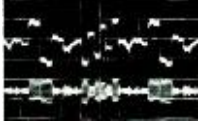


Fig. 3—Demodulated SECAM signal (after discriminator) 1 V/div (above). Remodulated signal output of SECAM-PAL converter 5V/div (below).

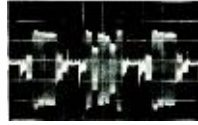


Fig. 4—Signal at the PAL delay line input 2V/div.

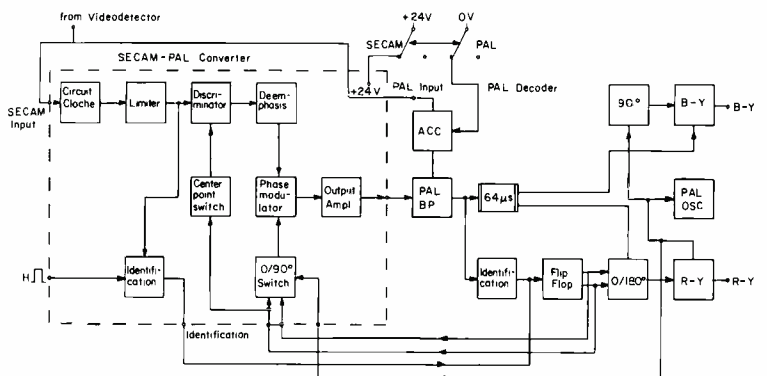


Fig. 2—SECAM-PAL Converter

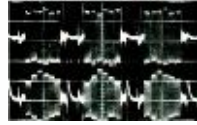


Fig. 5—Input of B-Y demodulator 2 V/div (above). Input of R-Y demodulator 2 V/div (below).

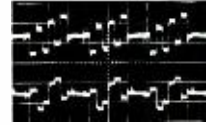


Fig. 6—B-Y output 2 V/div (above). R-Y output 2 V/div (below).

Since the $B-Y$ demodulator is insensitive to signals having $R-Y$ phase and the $R-Y$ demodulator is likewise unresponsive to signals having $B-Y$ phase, the outputs of the two demodulators contain only the desired $B-Y$ and $R-Y$ signals. This, of course, depends upon the maintenance of the correct phase relations at the phase modulator and at the two PAL demodulators. Since the modulator and the demodulators receive their subcarrier from the same oscillator (the reference oscillator that is a normal part of the PAL decoder) this condition can be met to the required accuracy ($\pm 5^\circ$ phase error) without difficulty. It may be noted that the demodulators here are used to separate the $R-Y$ and $B-Y$ signals as in a standard NTSC color receiver; however, with the great advantage that both phase modulator and phase demodulator share the same subcarrier-source (whereas for NTSC the modulator is at the transmitter and the demodulator at the receiver) so that none of the usual sources of phase error and therefore of hue error are present in the system here described.

New circuit and its connection to the PAL decoder

Fig. 2 shows the converter circuit at the left side and an ordinary PAL decoder at the right. In the SECAM circuit, a filter called the "cloche circuit" and a limiter are placed in front of the discriminator. The filter compensates for the supplementary amplitude modulation of the subcarrier that is employed in the SECAM system to improve the chroma signal-to-noise ratio (a form of pre-emphasis). The limiter serves for further noise suppression as in all FM systems. Due to the different center frequencies of the FM carriers for the two difference signals ($R-Y=4.406$ MHz; $B-Y=4.25$ MHz), the zero point of the discriminator must be shifted from line to line. This function is shown in the block diagram and in practice can be accomplished in a conventional way by means of a diode or transistor switch. At the output of this single discriminator, the demodulated difference signals, $R-Y$ and $B-Y$, are available sequentially on alternate lines. These difference signals are remodulated in the phase modulator which is DC connected to the discriminator output to maintain the correct black level. The subcarrier on which the difference signals are phase modulated is taken from the PAL decoder and, as described earlier, is switched sequentially on alternate lines to 0° or 90° phase-angle.

The rectangular line-by-line pulses for this switch are taken from the PAL flip-flop (already present in a normal PAL decoder). To get the correct switching mode ($R-Y$ should be modulated with a 0° phase subcarrier, $B-Y$ with 90° phase subcarrier), an identification system provides identification pulses which are fed to the PAL identification system. As identification, the SECAM burst is gated line-by-line and given to a frequency discriminator. The burst frequencies are 4.406 MHz for $R-Y$, 4.25 MHz for $B-Y$. The output of the discriminator delivers therefore a rec-

tangular waveform which is similar to the PAL identification signal.

The output signal of the converter is fed directly to the delay line, after the PAL bandpass circuit. This is a necessary feature since the PAL bandpass has a signal delay time which is approximately equal to the delay of the SECAM signal caused by demodulation and remodulation; consequently, bypassing the SECAM signal around the PAL bandpass circuit provides a simple way of equalizing the delay of the chroma signal for PAL and SECAM operation. Thus, at the output of the PAL decoder, the delay time of the difference signals relative to the luminance signal is substantially the same in PAL and SECAM.

The switching operation between PAL and SECAM is achieved simply by switching the supply voltage for the converter and applying zero bias voltage to the automatic gain control of the PAL decoder to interrupt this signal-path when receiving a SECAM signal

Fig. 3 shows the remodulated SECAM signal. The same signal amplified at the input of the PAL decoder delay line is shown in Fig. 4. The signals at the input of the PAL decoder demodulators are given in Fig. 5 and those at the output of the demodulators of the wanted $R-Y$ and $B-Y$ signals are given in Fig. 6.

Conclusions

Any PAL decoder can be driven by the converter and no modifications in the PAL decoder itself are necessary. Thus, an economical means is provided of adding SECAM reception facilities to a PAL receiver. The inputs of the converter for the signals of the PAL decoder are of relatively high impedances. Therefore, no readjustment of the PAL decoder is necessary

Vertical deflection system with a low voltage power supply for wide-angle color tubes



H. P. Lambrich
Licensee Technical Service
Engineering

The design of a solid-state color-TV power supply can be complicated by the requirement for a variety of different voltages for the various sections of the TV receiver. Therefore, a vertical deflection circuit capable of operating from the same low-voltage used for the low-level signal circuits offers a useful simplification. This has recently become feasible by the introduction of a low impedance toroidal yoke for wide-angle color tubes.

The L/R ratio of the toroidal yoke which is much smaller than that of saddle-types (0.6 ms) enable this yoke to be driven by

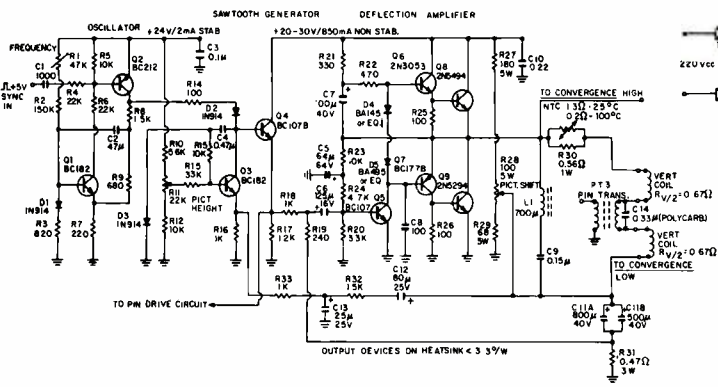


Fig. 1—AC-coupled vertical sweep circuit.

transformerless circuits with a supply voltage in the order of 20 V. The complete receiver then can be operated from two power supply sections: +270 V for horizontal sweep and video output stages and +24 V for the rest of the receiver.

In the vertical output circuits proposed, the quasi-complementary principle is favored. Tests and experience have shown that up to now npn power transistors have a superior reliability and safety against second breakdown than similar pnp devices. This especially applies to the types made by the 'hometaxial' process. However, all the circuits shown can also be realized with complementary pairs; the decision on this depends mostly on the semiconductor price situation.

AC-coupled sweep circuit

Both deflection circuits dealt with are composed of a sawtooth generator and a linear power amplifier using current feedback. To minimize drift, these amplifiers are capacitively connected to the pulse-former stages. The sawtooth generator consists of a relaxation-type oscillator, followed by a Miller run-down integrating stage and an emitter follower (Fig. 1). The oscillator, which is very stable against variations in temperature and supply voltage, periodically charges C4 via Q2 and R14, D2, and D3. This charging action takes place within 400 μ s; however, if the pulse at the collector of Q2 is to be used for vertical retrace blanking, the duration can be set to 800 μ s by increasing R3 to 2.7 kilohms. After being charged, C4 is discharged with a constant current via R16, Q3, R15, R13, R11 and R12. The magnitude of this discharging current is determined by the base current applied to Q3, which can be adjusted by R11. If perfect tracking between the vertical and horizontal picture dimensions is required, this base voltage should be derived from rectified line flyback pulses.

Emitter follower Q4 acts as a current amplifier which drives the low-impedance input of the output amplifier. In addition, its output amplitude of approximately 15 V, peak to peak, can also be used to drive other circuits, such as pincushion correction. If properly designed, it could also be used to drive the vertical convergence.

The output amplifier consists of a pre-driver stage operating in class-A and a pair of complementary drivers. The output voltage is applied to the yoke via a resistor/NTC (Negative Temperature Coefficient device) combination, the purpose of which will be explained later. The coupling capacitor and a current-sampling resistor are placed at the lower end of the yoke coils. This capacitor must be relatively large in accordance with the low coil impedance and the high peak current; however, a low voltage rating is adequate (peak working voltage 18 V). The AC voltage developed across this capacitor is parabolic and after appropriate 'shaping' this voltage is used for *S-correction* of the sawtooth drive voltage. A second feedback loop compares the voltage across R31 (which is proportional to the deflection current) against the drive voltage applied to the input of the output amplifier. This ensures that the output current accurately reproduces the input voltage waveform and provides good de-

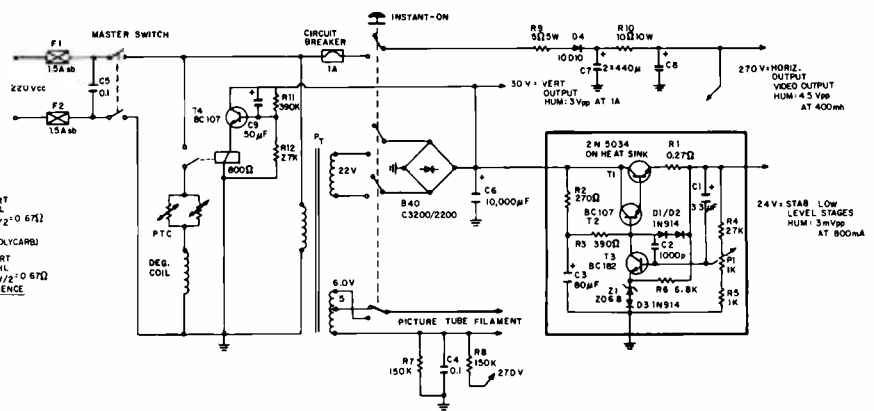


Fig. 2—Example of complete power supply for thin-neck receiver.

flection linearity that is unaffected by tolerances of the yoke parameters (L , R) or of other components in the output circuit.

A third DC feedback loop stabilizes the operating point of the amplifier via R23 and R24. The output voltage is the sum of a sawtooth waveform, a parabola (across C11), and a retrace pulse. For this composite AC waveform, the negative peak value (measured from the mean level) is smaller than the positive peak; consequently, to provide an optimized output voltage swing, the center-point voltage should be set at less than one-half the B+. The optimum value is 8 V for a B+ voltage of 24 V. The DC feedback loop also maintains the correct DC level of the amplifier when a DC current providing picture shift is fed into the cold end of the yoke coil. The potentiometer network was made unsymmetrical in accordance with the non-symmetrical DC level of the output stage. For the same reason, both the dissipation and the peak current of Q6 and Q8 is higher than that of Q7 and Q9. Consequently, devices of slightly higher rating have been chosen in these positions.

Diodes D4 and D5 eliminate residual crossover distortion by maintaining an idling current of approximately 20 mA through the output devices. This was found to be the lowest value which avoids visible velocity modulation in the center of the screen. It must be realized that the magnitude of this quiescent current changes with different diode voltages and base-emitter voltages of Q6 and Q7; therefore, it may be necessary to provide a potentiometer of about 20 ohms in series with D4 and D5 to take care of these tolerances.

To minimize power requirements, the dynamic vertical convergence was connected in parallel with the deflection yoke. As a consequence, it is necessary to stabilize the voltage applied to it against temperature changes of the yoke. An NTC resistor (which will finally be built into the yoke) shunted by a resistor R30 serves this purpose.

The pincushion-correcting signal is fed into the center tap of the yoke in order not to upset the symmetry of the correction. A series-tuned circuit, L1 and C9, provides the return path for this correction current and at the same time prevents the line frequency from entering into the vertical deflection circuit.

Top-bottom pin correction

Since the top-bottom distortion of the RCA 110° system amounts to approximately 8.5% of the total picture height, a correction current of about 0.6 A and a related voltage of about 40 V, peak-to-peak, is required. Not to increase the load upon the output stage, a separate circuit is preferably used for achieving pin correction. However, a circuit serving the double purpose of deflection and pin correction could also be employed.

Power supply circuits

The power supply of a complete receiver becomes very simple, if the horizontal sweep circuit and the video output stages can operate from a non-stabilized supply. Fig. 2 shows an example of such a supply designed in conjunction with the vertical deflection according to Fig. 1.

In this power supply, an instant-on feature is provided to make maximum use of an all-solid-state chassis. For this purpose, the filament of the picture tube is continuously connected to 5.0 V, which voltage is increased to 6.0 V after switch-on. As a consequence, the picture appears after only two seconds. A further advantage is that the life expectancy of the picture tube is increased due 1) to the reduced thermal stresses applied to the guns and 2) to the lower cathode temperature that results from operation at a filament voltage (6.0) slightly below the nominal value (6.3). Without preheating, this lower voltage would not be permitted because the warm-up period would be too long, with drift of gun characteristics extending over several minutes.

In the power supply shown in Fig. 2, a transformer core size P68 or M74 is adequate. By using a relatively large reservoir capacitor, C6, so that the amplitude of the ripple-voltage at the input to the stabilizer is kept small, the required mean DC voltage is reduced (since the minimum voltage at the negative peaks of the ripple must never fall below about 25 V). Consequently, the transformer secondary voltage can be reduced, which in turn decreases the transformer loss and in the present case the M74 core size is then sufficient.

Novel PAL identification and color killer circuit



P. Carnt
Development Engineering

J. Hemme
Licensee Technical Service
Engineering

The killer circuit in the PAL system presents a special problem that has no counterpart in the NTSC system. This arises because of the need for a binary circuit operating at half the horizontal scanning frequency which, in the PAL system, is required to restore a constant sign to the V or $R-Y$ component.

Should the mode of the $f_{H/2}$ binary be incorrect in the PAL system, an intended $R-Y$ component will be reproduced as a $-(R-Y)$ component (and vice versa). The resulting displays are unacceptable: in PAL, an intended pure red will be reproduced as green. Fleshtones, under this condition, are clearly objectionable.

In the PAL system, therefore, the killer circuit is required to operate when no burst is transmitted (exactly as in NTSC), but it should also operate when the mode of the binary is incorrect. In other words, color should be enabled only when a burst is present and also when the binary mode is correct. Naturally, PAL receivers include circuitry to ensure that the binary mode is always correct.

Referring to Fig. 1, a voltage (which can be positive or negative) is developed at point P (base of go/stop transistor Q1), when the mode of operation of the flip-flop is correct (voltage at point P negative), the flip-flop is allowed to operate normally; when the mode is incorrect, the flip-flop is stopped. Thus, the flip-flop stops and starts until the correct mode is statistically achieved.

Under either of these conditions, therefore, the Q2 collector is at -20 V. However, when the mode is correct (and only under this condition), the DC potential at P is negative (-0.7 V), Q2 conducts, and its collector is virtually at ground. Thus, the Q2 collector is at -20 V unless the mode is correct. Killing action is now simply obtained by returning the base of the chroma output transistor Q3 to Q2 collector.

Apart from the extreme simplicity of this killer circuit, it has the inherent advantage of being intimately connected with the identification-circuit command DC voltage; in fact, it uses this identical voltage source. The identification circuit shown will fail only when the signal is too small or noisy to allow the

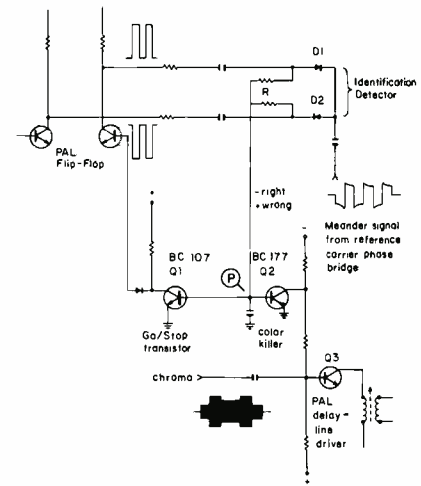


Fig. 1—PAL identification and color killer system.

subcarrier-generator automatic-phase-control loop to lock. In this event, however, the phase detector (D1, D2) output at P cannot reach a sufficiently large negative value to forward bias Q3, and the display will be color killed. Thus, the killer circuit enables color only if a correct picture can be displayed. Capacitor C of Fig. 1 at the output of the identification detector integrates the AC component of the output voltage and removes any disturbance due to noise, in weak signal conditions, from disturbing the flip-flop action.

The DC voltage at P is derived by a synchronous detection process which has, inherently, superior noise performance because the noise components are bi-directional and therefore tend to integrate out to zero, while this is not true for a simple amplitude-detection process.

Research



W. J. Merz, Director

Research efforts are carried on by a professional staff of 25 scientists: solid state physicists including experimentalists and theoreticians, chemists and crystallographers, and specialists in various areas of electronics, all supported by a corps of laboratory assistants. Carefully devised research projects seek new or refined scientific results pointing to directions meriting further applied work on ongoing development or yielding insights into hitherto not understood phenomena. In any case, most of the work of the research laboratory finds its way to scientific publications, or, in one manner or another through colloquia or symposia or other meetings, is shared with the European scientific community in university, government and other industrial laboratories.

Holography

M. T. Gale
D. L. Greenaway
J. P. Russell
T. Bart
Optics Research
Development Engineering

Initial demonstrations of holography involved the interference between two coherent beams of



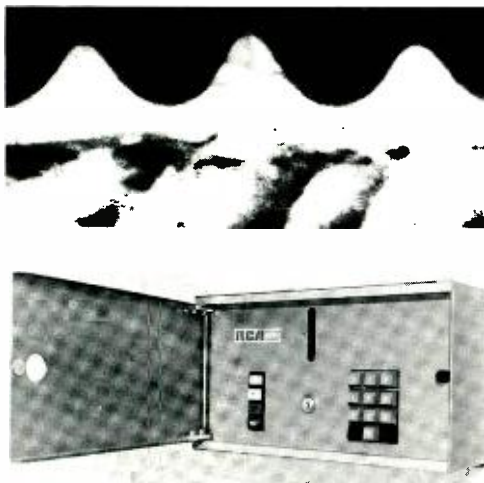


Fig. 1—Part of a diffraction grating in photoresist on a glass substrate. The picture was obtained with a scanning electron microscope at 10,000X magnification under conditions of near-grazing incidence to the grating surface. The grating period is about 1.3 microns.

Fig. 2—One of the wall-mounted door-units of the Hololock system now in use at the Zurich RCA Laboratories. The picture shows the slit for insertion of the card, the keyboard for entry of the users code, and signal lamps which indicate the sequence of operations to be performed when using the unit.

light—the so-called object beam and reference beam—and quickly revealed the amazing effect of three-dimensional imaging, which has become the most popular aspect of the field. Numerous applications have since been investigated in detail and described in the scientific literature. In the Zurich laboratory, holographic research has concentrated on new applications, such as integrated circuit manufacture, diffraction grating techniques, personal identification systems, and security systems.¹

Applications to integrated circuit manufacture

Two techniques for holographic projection printing of integrated circuit masks have received detailed attention. Both are designed to remove the currently used contact printing steps when the mask information is transferred to the final device wafer. A description of these methods has already appeared in the RCA Engineer,¹ and the reader is referred to this article for more information.

Simple diffraction grating generation

Holographically generated diffraction gratings represent a convenient way to investigate the properties of different recording media. In most of the work described above the photographic medium was photoresist. Gratings were made in the material by simply interfering two beams of coherent light on the surface of a resist-coated plate. While a normal photographic plate would have given an absorption grating which can only be used in transmission, photoresist yields a phase grating usable either in transmission or, because of the consequent surface relief, in reflection after suitable metallization. The distribution of light in the various diffraction orders from such a phase grating gives detailed information about the profile of the groove structure. One can calculate the amount of light in the various orders as a function of the grating profile and the maximum phase difference, which is proportional to the height of the surface relief. For example, a sinusoidal grating diffracts a maximum of 34% of the incident light into each of the two first orders; a square-wave grating diffracts 40%. As an example of the type of groove profile obtainable by coherent laser beam exposure of photoresist, Fig. 1 shows scanning electron micrograph of a cross-section of the developed resist surface. The inherent smoothness of the surface revealed by this picture is a good indication of the very low scatter present in this type of grating.

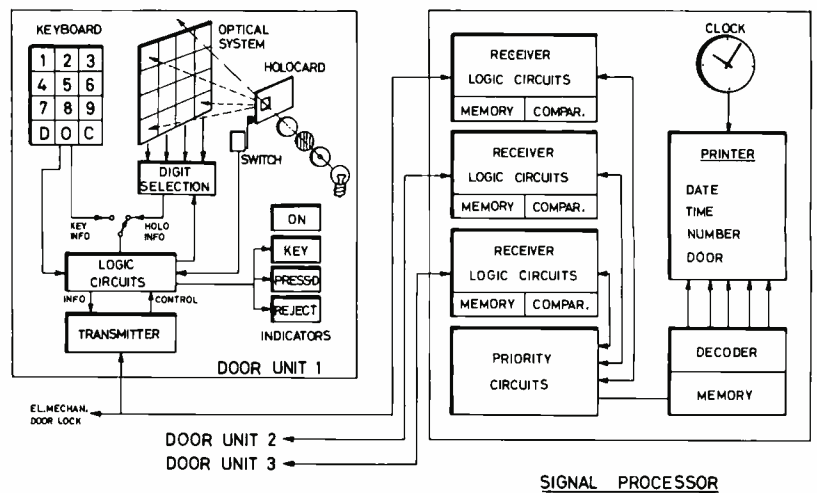


Fig. 3—Block diagram of the Hololock System.

Holocard systems

Working from the basic concept of using a small hologram as an integral part of a credit or identification card, the Zurich Laboratory has developed a secure personal identification system. The hologram contains coded digital information about the card holder. Part or all of this information is held by the card owner, but does not appear on the card in printed form. In use, the card must be inserted into a verifier and a verification code punched sequentially into a keyboard by the user. This number is compared electronically with the number coded in the hologram. This generates an "OK" or "reject" signal which can be used to trigger additional operations depending on the application of the system.

In the prototype systems, small phase holograms derived from a simple matrix of point sources are recorded in photoresist on plastic cards. Readout of the holograms in the verifier units is accomplished using a tungsten lamp and low-cost CdS photoresistors. As a demonstration, RCA Zurich Laboratories have been equipped with a "Hololock" restricted entry system. Small holograms are incorporated into the standard personnel identification cards which must be used by employees to gain entrance to the laboratories outside normal working hours. The verification operation is performed in small wall-mounted units (see Fig. 2) located near the entrances, and the doors are unlocked electrically. A central processor, remotely located, prints on paper tape the door used, the card number, the date, and the time.

In the hololock system, the information is stored holographically and, besides being difficult to forge or duplicate without highly specialized technical knowledge, it is redundant and immune to dust, scratches, mutilation, or alternation. The demand made upon the user is that he record separately (or remember) what in effect amounts to an additional telephone number, but this would appear to be a small price to pay for the high degree of security that the system can give. The system does not require lasers in the verification equipment, and the decoding operations are well suited to the use of integrated-circuit techniques. In the verifier described below, no great precision is required when the Holocard is inserted; a positional accuracy of a few millimeters is sufficient.

Hololock system

The organization of the Hololock system is shown schematically in Fig. 3. The system consists of a central signal processor which controls up to seven door units; two are currently installed. Each door unit contains a simple optical system which, upon insertion of a card, creates a pattern on the photocell array. The digital information thereby generated is processed by logic circuits within the door unit and transmitted via a two-wire line to the central processor together with the number entered manually from the keyboard. If the two num-

bers match, a signal is returned to the door unit which is used to actuate the electromagnetic door lock. As fast operation of the system is not required, a priority technique is employed to block other door units while one is being used. A flashing red light indicates this condition.

Verification in the processor is performed with conventional digital techniques. The number from the card is stored in a scratch-pad memory and the incoming number from the keyboard is compared bit by bit with the stored one. To prevent the user from leaving his card in the unit, the card must be removed before pressing the button which opens the door lock. An incorrect number entered into the keyboard results in a "reject" signal and a "clear" key is provided to allow the number to be re-entered.

The central processor also contains a clock mechanism which can be used to control the door locks so that free entry is possible during normal working hours.

Reference

I. Greenaway, D. L., "Holographic Research at at the Zurich Labs," *RCA Engineer*, Vol. 16, No. 1 (1970) p. 19.

Light scattering in solids

G. Harbeke | J. R. Sandercock
E. F. Steigmeier
Solid State Physics Research



An article on the application of laser sources for light scattering in solids was published in *RCA Engineer*, Vol. 15, No. 5 (1970) p. 82 and in the special reprint *RCA Lasers* (1970). The reader is referred to this article for a discussion of the basic mechanisms in light scattering. In the following we describe some new techniques and results.

The experimental arrangement is shown schematically in Fig. 1. A laser beam, whose polarization can be adjusted, is focused into the bulk of the sample. Light scattered at 90° is collected and analyzed for polarization and frequency. The type of spectrometer used is determined by the experiment being performed. For Brillouin scattering, the phonon frequencies ν_s are a factor of 10^4 to 10^5 smaller than the laser frequency ν_0 . Therefore, a spectrometer of high resolving power such as the Fabry-Perot interferometer is needed. The useful range of such an instrument is limited to between about 10^{-4} and 20 cm^{-1} . [The inverse centimeter, or wavenumber, is a spectroscopic unit equal to the reciprocal of the wavelength and as such is proportional to frequency and energy. One cm^{-1} is equivalent to a frequency of 30 GHz or to an energy of 0.124 meV.] In Raman scattering, on the other hand, frequency differences between a few cm^{-1} and a few thousand cm^{-1} occur. For this purpose, a double-grating spectrometer which is designed for an extremely low internal stray light level is usually employed. The output from either spectrometer is detected by a photomultiplier and recorded as a function of frequency.

Figure 2 shows a Brillouin spectrum of the ferroelectric *SbSI*. This particular example demonstrates impressively a new interferometric technique developed in this laboratory. The upper curve shows the spectrum obtained using the conventional method. The Stokes and anti-Stokes Brillouin doublet is barely separable from the very intense Rayleigh component. The Brillouin-to-Rayleigh intensity ratio is about 10^{-3} . In the lower curve, the same spectrum is presented after passing twice through the interferometer. In this case, Brillouin signals as weak as 10^{-6} of the Rayleigh peak can be measured. The peaks T_1 and T_2 , corresponding to transverse phonons, are clearly resolved. The technique has been further improved using five passes through the interferometer which permits signals with an intensity ratio of 10^{-9} to be observed. A novel electronic stabilizing system has also been constructed which maintains the

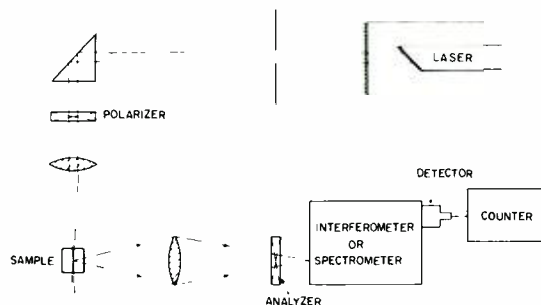


Fig. 1—Schematic representation of the experimental arrangement for the measurement of Brillouin spectra (interferometer) or of Raman spectra (spectrometer).

long-term stability of the instrument for measurement of weak signals. Such a technique is particularly useful for materials which are not transparent to the laser light. Since the light penetrates only a short distance into the crystal, measurements must be made in backscattering, unavoidably giving rise to a strong central component from the surface imperfections.

From Brillouin spectra, one can determine the velocity of sound or the elastic constants in the crystal, for various crystallographic orientations. In addition, the effect of such external parameters as temperature and pressure can be examined. From the line width, information about the sound attenuation in the GHz region can be obtained.

While there are only three branches of acoustic phonons, there can be many branches of optical phonons depending on the number of atoms per unit cell. Fig. 3 shows a section from the Raman spectrum of *SbSI* for eight different temperatures. Note that the wavelength scale is increased one hundredfold compared to that of Fig. 2. The spectra have been placed one above the other to make the dramatic change below 50 cm^{-1} clearly visible. The strong temperature dependence is related to the crystallographic phase transition and the onset of ferroelectric ordering which occurs at the Curie temperature T_c (292 K). The measurements of Fig. 3 refer to the low temperature (ferroelectric) phase. In agreement with theoretical predictions, the frequency of one optical mode goes to zero as the temperature approaches the Curie point. This so-called "soft mode" is the dynamic form of the static displacements which the atoms undergo at the transition. The strong decrease in the frequency and the correspondingly large amplitude point to an approaching lattice instability where the oscillating atoms become "frozen in" at their displaced positions. The corresponding Raman line is the strongest one in the uppermost spectrum of Fig. 3. Of particular interest is the interaction that occurs between this

Fig. 2—Back scattered Brillouin spectrum of *SbSI* at 295 K taken by single-pass (upper) and the double-pass (lower) techniques. T_1 , T_2 refer to transverse acoustic phonons; L to longitudinal. Anti-Stokes lines are to the right of the central component and Stokes lines to the left.

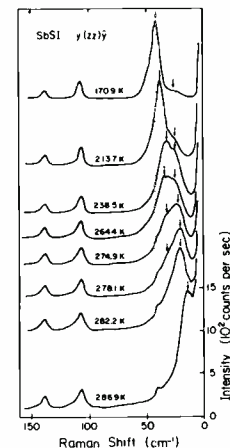
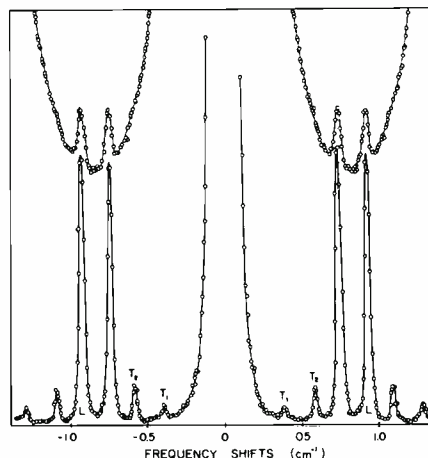


Fig. 3—Back-scattered Raman spectrum (Stokes lines) of *SbSI* at various temperatures. Arrows indicate the two optical phonons involved with phase transition at 292 K.

“soft mode” and another mode as the frequencies of the two modes approach each other.

The study of such critical phenomena in the vicinity of phase transitions is, at present, a problem of great interest in solid-state physics. Theoretically one can show, for example, that the frequency, line width, and intensity can be expressed in powers of $|T - T_c|$ with different, well-defined exponents which can be determined from experiments. A detailed analysis of the spectra of Fig. 3 shows that, in addition to the soft mode, the Rayleigh intensity exhibits critical behavior. The measurements give a well defined value for the exponent of $|T - T_c|$. The study of critical phenomena by light scattering techniques complements the results obtained by other methods, such as neutron scattering and ultrasonic absorption (see “Ultrasonic Studies of Solids”).

The above described examples are intended to illustrate the usefulness of light scattering as a tool for basic solid-state research. Among other problems currently being investigated are the interaction between lattice vibrations and the spin system in magnetic semiconductors, the lattice dynamics of phase transitions in ferroelectric materials with near-metallic electron concentrations, and light scattering in metals and antiferromagnets.

Luminescence spectroscopy in solids.



W. Czaja | L. Krausbauer
Applied Research
Optics Research

The current understanding of atomic and molecular physics has been a direct consequence of experimental results obtained in the mutually complementary fields of optical emission and absorption spectroscopy. An analogous situation exists in solid state spectroscopy, where optical absorption and reflectance spectra yield information about the electronic structure of pure crystals (energy bands), about the vibrational spectrum of the lattice (phonons), and about the effects of impurities. Surprisingly it is only in the last 10 to 15 years that emission spec-

troscopy has taken its place as an equal counterpart to the others.

For historical reasons it is usual to refer to light emission from solids as *luminescence* and to distinguish between various forms of luminescence depending on the excitation mechanism. Among these are: *photoluminescence*, excitation by light; *cathodoluminescence*, excitation by an electron beam; and *electroluminescence*, direct electrical excitation (c.f. “Visible injection electroluminescence”). However different the excitation processes may be, the resulting emission is basically the same. We will therefore limit ourselves to the discussion of photoluminescence since the phenomena observed under this excitation condition are comparatively easy to interpret and there already exists a large amount of experimental data.

A striking example of photoluminescence is the donor-acceptor pair spectrum of *GaP* shown in Fig. 1. If *GaP* is doped with equal amounts of donors and acceptors (e.g. sulfur and carbon, respectively) the dopants compensate each other, and as a result, the impurity atoms are ionized. If electron-hole pairs are created by exciting the crystal with light, the donors will capture the electrons, and the acceptors will trap the holes. These localized charge carriers have overlapping wave functions; consequently the trapped electron can recombine with a trapped hole emitting a photon. The spectrum of this emission is rich in fine structure, as is evident from Fig. 1, which can be understood as follows.

In the quiescent state of the crystal, prior to the illumination, the donors and the acceptors are charged and a Coulomb attraction exists between them. After capturing an electron and a hole respectively, the impurities are neutral and the Coulomb interaction is inhibited. The energy difference between this excited state and the quiescent state is proportional to the electrostatic interaction and, as such, is dependent on the donor-acceptor separation. In a crystal, the distances between lattice sites varies discontinuously so that the energy differences are discrete. This reflects itself in the spectrum of the emitted light as a set of sharp lines. Sometimes an additional fine structure is observed which can yield quantitative information about the charge distribution on an impurity (multipole moments).

The luminescence associated with excitonic processes provides a further example. An exciton can be visualized as an electron-hole pair which is bound together by the Coulomb interaction and which behaves very similarly to a hydrogen atom. This quasi-particle is neutral and can move freely in the crystal. It is also unstable and after a characteristic lifetime the electron and the hole recombine and emit a photon. This recombination can occur both from the ground state and from hydrogen-like excited states of the exciton. The result is a series of sharp lines in the spectra, similar to hydrogenic term sequences, which have been observed in a number of crystals, e.g. *Cu₂O* and *CdS*.

Excitons can also be bound to chemical impurities. Since the particle itself is neutral, however, it cannot be bound by electrostatic forces and more subtle forces of quantum-mechanical origin come into play. Such is the case for nitrogen atoms which substitute for phosphorous in the *GaP* lattice. Since *N* and *P* are isoelectronic, i.e. they have the same number of valence electrons, an electrically neutral impurity is formed. Excitons bound to these atoms emit a sharp line spectrum when they recombine. In addition to the single exciton it has been found that the *N* atom can bind whole excitonic complexes in *GaP*. One such complex consisting of two electrons and two holes is analogous to the H^2 molecule. We have evidence for another complex in *GaP*, consisting of two electrons and a hole, also bound to nitrogen.

From the study of these and other emission spectra, insights may be gained into the microscopic behavior of solids. The understanding of such phenomena is of more than just academic interest as they play an important role in the optimization of materials properties for light emitting devices which are currently under development.

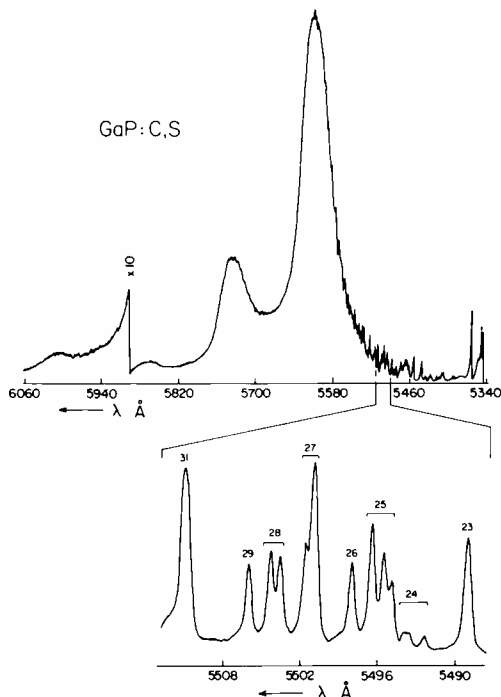


Fig. 1—Photoluminescence spectrum of *GaP* doped with C and S. The intensity scale is arbitrary. Line 31 corresponds to a donor-acceptor separation of 21.5 Å; line 23 to 18.5 Å. Concentration $\sim 10^{16} \text{cm}^{-3}$ compensation $\sim 70\%$ excitation 4880 Å temperature 2.1 K

Visible injection electroluminescence



B. Binggeli
D. P. Bortfeld | H. P. Kleinknecht
A. E. Widmer
Optics Research
Applied Research

Electroluminescence is the production of light in a solid directly from electrical energy without the necessity of heat. It comes about through the excitation of electrons from lower to higher

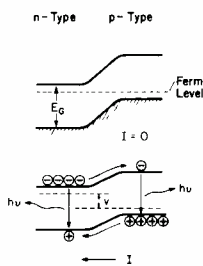
energy states or bands and the subsequent transformation of the recombination energy into photons. Such processes for the production of visible light can be observed in semiconductors of various forms. The common electroluminescent panel lights which contain a thin layer of a crystalline powder in an organic binder are one example. Although such large-area devices can be technically attractive we will limit ourselves here to single-crystalline structures as these promise higher light emission and are physically easier to understand. In particular we will consider *injection electroluminescence* which is realized best in a p-n junction.

Fig. 1 shows such a junction at zero bias (a) and at a forward bias voltage V (b). The forward bias causes current, I , composed of a flow of electrons in the conduction (upper) band from the n- to the p- region and an opposed flow of holes in the valence (lower) band. The injected carriers find themselves in regions of opposite conductivity type effectively in an excited state from which they decay through electron-hole recombination with the emission of a photon. The ideal material for such electroluminescence must fulfill three requirements:

- 1) The *bandgap* (E_g), the energy difference between the conduction and valence bands, must be greater than or equal to the photon energy (1.8 eV for red light and 2.2 eV for green).
- 2) P-n-junctions must be possible. Therefore, the material must be such that *both n- and p-type* can be formed by doping. Unfortunately many attractive luminescent materials do not fulfill this condition. These crystals react to attempts at doping with particular impurities by the creation of an equal number of lattice defects which exactly compensate the doping effect (self-compensation).
- 3) The probability of a radiative recombination between an electron and a hole must be high. This is only possible in materials which possess a particular band-structure, so-called *direct bandgap* materials. In contrast, there are many semiconductors which exhibit an "indirect" bandstructure in which any electron-hole recombination must include the simultaneous emission or absorption of a phonon which is less probable than a direct radiative transition. As a result, radiative recombination processes in such materials are less able to compete with non-radiative ones.

Table I compares a number of semiconductors with respect to the above requirements. Only *SiC* and the *III-V* alloys meet all three requirements. Experience has shown that the technology of *SiC* is very difficult. In addition the metallurgical problems associated with the *III-V* alloys are serious and have only been solved for *GaAs_{1-x}P_x*, which yields only red light. Thus, compromises must be made.

Fig. 1—Energy band diagram of a p-n junction: (a) Zero bias state; (b) Under forward bias V . In (b) the injection of holes (+) into the n-region and of electrons (-) into the p-region leads to radiative recombination (vertical arrow).



Relaxing requirement 3), *GaP* becomes an interesting material. Dropping requirement 2) instead, the *II-VI* materials (e.g. *ZnTe*) become very attractive. Finally, requirement 1) may be circumvented by using a frequency-doubling phosphor

excited by a *GaAs* electroluminescent diode, a technique which will not be further discussed here. Rather, the *GaAs_{1-x}P_x*, *GAP* and *ZnTe* cases will be examined in somewhat more detail.

GaAs_{1-x}P_x

Developmental work in this field is basically complete. Electroluminescent diodes and integrated arrays for alphanumeric displays are on the market. Quantum efficiencies (emitted photons/injected carrier) of 0.2% at $\sim 6500 \text{ \AA}$ (1.9 eV) have been achieved with a brightness of about 700 footlamberts (fL). (For comparison a tv screen has about 50 fL). The *GaAs_{1-x}P_x* material is made by gas-phase epitaxy on a *GaAs* substrate.

GaP

As this material has an indirect bandgap one must use special means to increase the probability of a radiative electron-hole recombination. This can be accomplished by the introduction of so-called isoelectronic dopants which act as traps for an electron-hole pair (an exciton). The exciton becomes localized in the neighborhood of the trap which increases the recombination probability (see *Luminescent Spectroscopy of Solids*). By using a *Zn-O* complex for the isoelectronic trap, red light is produced; nitrogen doping leads to green. In either case, care must be exercised to minimize the non-radiative decay channels, which can arise from impurities and from lattice defects. As a result, the fabrication of *GaP* layers is very critical.

The best electroluminescent results have been obtained through the liquid-phase epitaxy process in which a *GaP*-saturated gallium melt is slowly cooled so that a layer grows on a *GaP* substrate. Such epitaxial material is nearly free from mechanical defects and can be controllably doped. Red emitting diodes made by this process exhibit quantum efficiencies of up to 7%; green diodes of 0.6% efficiency have been made. In both cases, brightness values of 10,000 fL have been achieved. The Zurich Laboratory has a continuing program on the liquid-phase process itself to improve the purity, through control of the starting material, the doping, the kind of boat used; and the mechanical quality, by varying the substrate orientation and type.

Studies have also been made of diodes prepared from gas-phase epitaxial material as this process should be more controllable from a technical point of view. However, the electroluminescent results obtained by this method are distinctly inferior to those from the liquid-phase process. While the electrical characteristics of the diodes are the same, the much higher strain and dislocation density in the gas-phase material may have an adverse effect on the light emission.

ZnTe

Although *ZnTe* cannot be amphoterically doped (requirement 2), electroluminescence has been observed under metallic contacts to the material. In attempting to cultivate and extend this effect, diodes have been fabricated by alloying an *Al*-doped indium dot to the surface of the p-type *ZnTe* and slowly cooling from the alloying temperature. In the process, a thin ($\sim 1 \mu\text{m}$) high-resistivity layer is produced between the metallic contact and the bulk forming an m-i-p structure. Such diodes emit green light at 77K with a quantum efficiency of up to 2%; at room temperature, deep red emission with an efficiency of 0.1% is observed. It is believed that the i-layer becomes photo-n-type as a result of its own light emission such that, above a critical voltage, a "photo p-n junction" is formed.

By comparison of the electroluminescent spectra of the diodes with the photo- and cathodoluminescent spectra of specially doped crystals of *ZnTe*, it was possible to assign all the observed lines to certain electronic transitions associated with levels caused by these dopants.

Finally, there is another way to circumvent the second condition: through the use of heterojunction structures, i.e. junctions

between materials with differing bandgaps. The fabrication of such structures using alloying techniques as well as gas-phase epitaxy is under investigation.

Table I—Comparison of electroluminescent materials

Material	Req. 1) Eg(eV)	Req. 2) Type	Req. 3) Structure
Ge	0.67	p,n	indirect
Si	1.11	p,n	indirect
SiC	2.4-3.3	p,n	direct
InP	1.26	p,n	direct
GaAs	1.43	p,n	direct
GaP	2.24	p,n	indirect
GaAs _{1-x} P _x	x<0.51	<2.06	p,n
	x>0.51	>2.06	p,n
In _{1-x} Ga _x P	x<0.7	<2.2	p,n
	x>0.7	>2.2	p,n
Ga _{1-x} Al _x As	x<0.37	<1.92	p,n
	x>0.37	>1.92	p,n
CdTe	1.44	p,n	direct
CdSe	1.67	n	direct
ZnTe	2.25	p	direct
CdS	2.41	n	direct
ZnSe	2.7	n	direct
ZnS	3.6	n	direct

Theory of interacting phonons



R. Klein | R. K. Wehner
Solid State Physics Research

Many properties of dielectric crystals depend on the vibrations of the atoms which constitute the lattice. Well-known phenomena are the T^3 law for the specific heat at low temperature and the phenomena of thermal expansion and thermal conductivity. As long as the restoring force acting on a displaced atom is linear in the displacement, the vibrations of the lattice can be described in terms of normal modes with characteristic frequencies and amplitude vectors. Applying quantum theory to this system of independent oscillators leads to the concept of the phonon as the energy quantum of an oscillator. In this way, a kind of particle description emerges for the collective motion of the atoms in a lattice. Using this particular picture, the thermal energy of a solid can be represented by a gas of "thermal" phonons.

As long as the lattice forces remain linear in the displacement, the phonons are independent and there are no interactions between them; these are called harmonic phonons. Nonlinear (or anharmonic) forces lead to interactions between the phonons analogous to the collisions between the particles of a real gas. A study of the phenomena which can be interpreted in terms of phonon-phonon interactions improves our knowledge of the interatomic forces.

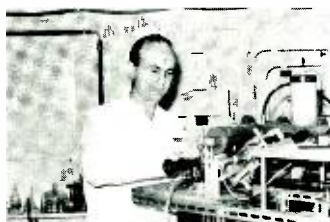
In general, there are two classes of processes in which the interactions between phonons play an important role: either only a few phonons take part in the process or the gas of thermal phonons participates as a whole. The former comprises typical quantum processes similar to those which occur in absorption or scattering experiments where the energy absorbed by the crystal is made up of only a few special phonons. These are usually high-frequency processes at low temperatures. In contrast, the latter kind of phenomena are generally low-frequency processes at temperatures which are not too low. Under these circumstances, the gas of phonons can be treated by hydrodynamical methods. For example, the "normal component" of superfluid helium at low temperature consists of phonons. If one considers a non-equilibrium situation in this hydrodynamical regime, for instance an external perturbation by a sound wave or a temperature fluctuation, there will be many collisions during one period of the perturbation. In contrast to processes of the first kind, where the

collisions can be regarded as a small perturbation, the second process is in a collision-dominated regime. When the external disturbance changes sufficiently slowly, so many collisions occur that we can define a local equilibrium and a local temperature.

Ordinary perturbation theory cannot be used in the hydrodynamic regime. Only the modern methods of many-body theory are able to give a basic description of the dynamics of the phonon gas in terms of a transport equation. In this way, the microscopic, interatomic forces are related to the macroscopic, experimentally observable effects. Work at the Zurich Laboratory extends from the derivation of such a general transport equation for interacting phonon systems to the application of the equation to the specific problems listed below:

- 1) The phonon spectrum in superfluid helium is relatively simple when compared with that of solids. The latter have at least three branches and are often anisotropic. In contrast, only phonons from an isotropic longitudinal branch can be excited below 0.6 K in liquid helium. Since the anharmonic coupling between the phonons is experimentally known, one can approximately solve the integral equation which describes the transport in the system. What results is a much better understanding of the ultrasonic attenuation than is possible on the basis of ordinary perturbation theory. In particular, by using the theory to analyze experimental results, one obtains information on rather detailed features of the phonon spectrum of superfluid helium.
- 2) In the static and homogeneous limit, the microscopic theory in the hydrodynamic regime must coincide with thermodynamics. In this connection, the question arises as to how one can describe adiabatic and isothermal processes within the microscopic theory. So far, there is no general answer, but one can hope to find some important indications as to what it might be by studying the special cases of the adiabatic and the isothermal elastic constants. That phonon transport is of vital importance in the calculation of these quantities is evident from the existence of temperature changes connected with adiabatic processes. We were able to find limiting forms of the microscopic theory which fulfill the relations among the elastic constants known from thermodynamics.
- 3) Temperature fluctuations are also fluctuations of the phonon density. Two rather interesting aspects of temperature fluctuations are under consideration. The first is the phenomenon of "second sound" in which the fluctuation propagates as a weakly damped temperature wave. As this effect has only been observed in a few solids, we are studying the conditions under which light scattering experiments can be used to detect it. The second is the "critical scattering" of light at phase transitions. In both cases the transport equation is used for a quantitative calculation of the spectrum of the scattered light.

Ultrasonic studies of solids



W. Rehwald
Solid State Physics Research

The role of ultrasonics in the testing of construction materials for cracks and in the cleaning of parts is well known. The solid-state physicist uses ultrasonics as a sensitive tool, since the elastic strain resulting from the sound wave, sinusoidally varying in space and time, influences a number of physical properties. Among these are the magnetization in a ferromagnet, the dielectric polarization in a ferroelectric, the position of the energy bands in a semiconductor or insulator, and the intensity of the thermally excited lattice vibrations (the density of thermal phonons) in any solid. The study of the final type of interactions is the main subject of our experimental investigations.

The ultrasonic frequencies used in solid-state physics are, for the most part, considerably higher than those used in parts

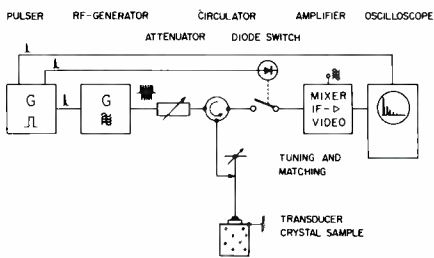


Fig. 1—Block diagram of the ultrasonic plus-echo system. The version shown covers the frequency band 200 to 2000 MHz. For higher frequencies a tuneable coaxial resonator is used to achieve a high electric field in the transducer.

testing and cleaning; they range from about 10 MHz to several GHz. We are interested primarily in the ultrasonic attenuation and also the sound velocity as a function of frequency, temperature, and crystallographic direction—and possibly as a function of such external parameters as an electric or a magnetic field. From the behavior of the sound velocity and the attenuation, conclusions may be drawn about the above-mentioned interaction mechanisms.

The pulse-echo method offers a convenient way to measure both parameters at the same time. A series of short ultrasonic pulses is generated by a piezoelectric transducer at one end of the sample which is ground and polished flat and parallel to optical precision. The sound pulse is reflected from the opposite face of the crystal, and after each round trip, it is detected by the same transducer. The resulting electrical signal is amplified, normally in a heterodyne receiver, and displayed as a video signal on an oscilloscope. Fig. 1 shows a block diagram of the pulse-echo measurement system.

The signal on the oscilloscope screen appears as a train of decaying pulses as is shown in Fig. 2. Sound velocity is obtained from the interpulse distance and attenuation from the decay rate. If the pulses are to be separated in time, the pulse length must be short compared with one round-trip transit time. Effectively, this means pulse widths of a microsecond or less. In the simplest case, the transducer consists of a properly cut quartz disc which is bonded to the sample by a viscous fluid or by a cold-welded indium layer. Every inhomogeneity in the sound path whether in the sample, in the bond, or in the transducer—can considerably distort the shape of the echo envelope. Similar effects are caused by deviations of the end faces from planarity and parallelism. The stringency of latter requirement for high frequencies can be seen from the fact that a wedge angle of several seconds of arc is sufficient to change the envelope function from an exponential to something similar to a $|\sin x/x|$ behavior.

Since such wedge effects are produced primarily in the bond, attempts have been made to grow a layer of a piezoelectric material directly on the sample surface. Under certain conditions, evaporated or sputtered films of CdS or ZnO can be put down such that all of the crystallites have their c -axes aligned parallel. Such thinfilm transducers can generate sound in the range between 300 MHz and 10 GHz with relatively good efficiency. In samples which are themselves piezoelectric, it is possible to excite the ultrasonic wave directly at the surface. Under such circumstances, the highest coherently-detected sound frequencies (>100 GHz) have been obtained.

As a consequence of the anharmonicity of the lattice forces, the sound wave in the crystal is coupled to the thermally excited lattice vibrators (phonons). [In radio, this nonlinear phenomenon is known as mixing.] For the description of the resulting sound attenuation, two limiting cases can be distinguished. Up to moderately high frequencies at room temperature, the period of the sound wave is long compared with the mean time between two phonon-phonon interactions. Roughly speaking, the sound wave modulates the density of the phonons which, in seeking to re-establish thermal equilibrium, draw power from the sound wave. In this region, the sound attenua-

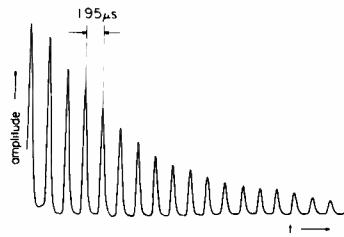


Fig. 2—Oscilloscope of a pulse-echo measurement in a $SrTiO_3$ single crystal (7.7mm long; Frequency 120 MHz; Pulse width $\sim 0.5\mu s$). The exponential envelope corresponds to an absorption of 1.1 dB/cm.

tion increases quadratically with the frequency but is not as strongly temperature dependent.

In the limit of low temperatures and high frequencies, the time between phonon-phonon interactions becomes long with respect to a period, and we can describe the effect of the sound wave as collision processes between a quantum of ultrasound and a thermal phonon. Here the temperature dependence is strong, like T^n where $4 \leq n \leq 9$ depending on sophisticated details, but the frequency dependence is small. Further details are discussed under "Theory of Interacting Phonons".

Since sound velocities are 10^5 times less than the velocity of light, acoustic delay lines are technically interesting. In the transducer, the electrical signal is converted to sound and later reconstructed after passing, for a time, through the crystal. Delays between 1 and 4 $\mu s/cm$ of path length can be obtained. Materials for this application must have low attenuation in the GHz regime. From experience, we know that these are to be found among crystals which are composed of light elements and which have a complicated structure. An example is the spinel $MgAl_2O_4$ which can be obtained both naturally and synthetically. In single crystals of spinel at room temperatures we find an attenuation for longitudinal waves of 2 to 5 db/cm at 4.5 GHz. The comparable value for crystalline quartz lies between 50 and 70 dB/cm.

Scientifically, it is interesting to investigate deviations from the usual temperature dependence of the attenuation as occur, for example, in the vicinity of a structural phase transition. Such transitions are usually accompanied by anomalies in the phonon spectrum (e.g., "soft modes") which show themselves by changes in the sound attenuation and velocity in the various crystal directions. Fig. 3 shows the behavior of these two quantities in the neighborhood of a structural transition in $SrTiO_3$. Such an effect is known as critical scattering, a phenomenon which can also be seen by optical means. Thus, ultrasonic investigations complement light scattering studies.

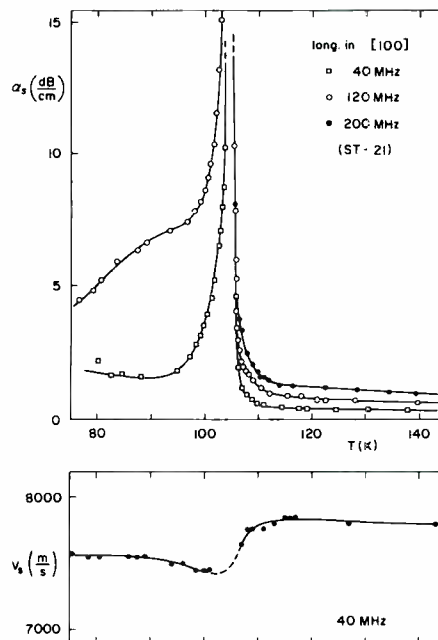


Fig. 3—Temperature dependence of the sound absorption α_s and the sound velocity v_s of longitudinal waves in $SrTiO_3$ near the phase transition at 104°K. The crystal is cubic above this temperature and weakly tetragonal below. The absorption peak indicates critical fluctuations in the order parameter.

Piezoceramic device applications

P. Nelson

Piezoelectric ceramics are materials whose characteristics make them, in many cases, excellent mechanical-to-electrical transducers. Two possible areas of application of these ceramics—piezoelectric sensing devices (geophones) and safety and arming devices—will be discussed in this paper. An engineering model of a piezoelectric geophone was designed, built, and tested. It proved to have a very high signal-to-noise ratio and extremely high sensitivity. It also had the capability of offering frequency information on a complex waveform, thus inherently providing the first stage of frequency analysis. Feasibility studies were conducted on the use of piezoelectric ceramics as active portions of a safety-and-arming device for certain types of shells and rockets. It would have the advantages of being all electronic and triple-safe.

Perry L. Nelson

Design and Development Engineering
Advanced Technology Laboratories
Van Nuys, California

received the BS in physics and mathematics from St. Olaf College, Minnesota, and did graduate work in physics at Montana State University. While at RCA, Mr. Nelson has been actively engaged in IR&D work specializing in research and first-stage design of new projects. He has been engaged in programs such as a near-surface burst capacitive fuze for bombs, an optical fuze employing GaAs laser diodes, and optical portions of a signaling system for submarines. Following this, Mr. Nelson studied possible uses of piezoelectric ceramics in the ordnance area. He developed and tested a unique piezoceramic sensor and has done work on a solid state piezoelectric transformer and a piezoelectric S&A device. In 1970, he became active in the area of voice-response techniques. This project includes a holographic storage and he has specifically been responsible for the holographic facility and research leading to a random access non-moveable store of audio and video information.



PIEZOELECTRICITY or pressure electricity is not a new phenomenon. However, only in the last few years have piezoelectric ceramics been refined to a point where they have become very useful transducer materials.

Certain crystals and compositions are *piezoelectric* if their physical dimensions change when they are subjected to an electrical stress and if they generate an electrical charge when subjected to a mechanical stress. If the electrodes are not short circuited, a voltage associated with this charge appears. The applied stresses and the resulting responses are functionally related by the piezoelectric properties of the ceramics, their geometries, and the direction of the applied electrical or mechanical stresses.

The most common ceramics possessing piezoelectric properties are compositions of lead zirconate-lead titanate. These compositions do not exhibit the piezoelectric properties in their original state but do exhibit them after polarization in a directional high-voltage field. This induces a polarization direction within the material, and voltage-output to stress-input ratios are related to this direction.

Applications

Possible applications of piezoceramics as transducer devices are many and varied. Studies were conducted on three of these applications: sensing de-

vices with direct application as geophones; an all-electric safety and arming device for missiles; and a solid-state high voltage transformer. The work being done on the transformer is not completed and will not be discussed here.

Sensing devices

Sensing devices, probably the most common of which is the geophone, are in use in many disciplines. Their primary purpose is to detect the presence of any disturbing functions above the normal background noise. A highly desirable secondary function of a sensor is to offer information as to the cause of the disturbing function; the information provided is analyzed by associated logic. Because of the many applications where sensors are needed to detect but not to be seen, size and weight are critical requirements.

Characteristics

With these two functions as goals, and with size as a limitation, a study was conducted to determine if piezoelectric ceramics could serve as sensing devices.

The ceramics used would be in the form of benders (rectangular beams). If one end of these benders is clamped to a base, an impulse motion of the base will cause each bender to resonate at a frequency determined by its dimensions and material. If several of these benders are combined in one unit and each bender tuned to a separate frequency, the resulting sensor unit will respond to many driving functions.

The response curve of most existing geophones forsakes high gain to achieve a broad bandpass. The output must then be amplified and analyzed for information (predominately time and phase relationships). By making use of the inherently high Q of a mechanically tuned piezoceramic beam and combining several of these tuned elements, the total response curve becomes nearly level. This scheme results in broad bandpass but it also makes use of resonant amplification which is considerably above existing geophone output levels. Thus, amplification requirements are reduced to a nominal level, and at the same time such problems as RF noise are almost eliminated. Information analysis at

Reprint RE-17-2-7

Final manuscript received January 26, 1971.

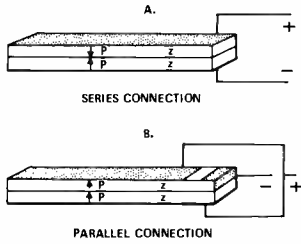


Fig. 1—Commercially available piezoelectric bender elements.

this point becomes much more complete than an ordinary geophone in that relative amplitudes of various frequencies are offered as a result of the narrow bandpass filtering provided by the tuned elements.

Piezoelectric benders

The commercially available piezoelectric bender elements are of the general construction shown in Fig. 1. Two identical pieces of ceramic, Z , are bonded together by epoxy about a center metal vane. Depending upon the type of connection desired, the polarizations of the ceramics are oriented relative to each other and silvered contacts deposited on the outer faces. Comparison of the output voltages of the two types of connections, when subjected to the same amount of stress force as shown in Fig. 2, gives the relationship that the voltage output for the series-connected bender is twice that of the parallel-connected bender and the capacitance of the parallel is twice that of the series.

Geometrically, benders can be obtained in sizes up to 2 inches long and in a range of 10 to 30×10^{-3} inches thick and 30 to 60×10^{-3} inches wide.

Cantilever beam equations

Preliminary investigation of a system started with the approximation that the ceramic benders can be described by the equations for cantilever beams clamped at one end (see Fig. 3).

The deflection, δ , of a beam clamped in this manner and acted upon by a force F is

$$\delta = FL/3EI \quad (1)$$

where F is force; L is length; I is moment of inertia $= bh^3/12$; E is Young's modulus; b is width; and h is height.

The maximum shear force S that a given beam can withstand is determined by

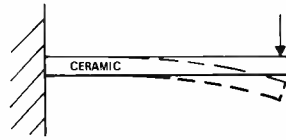


Fig. 2—Ceramic bender subjected to a stress force.

$$S_{\max} = FL/Z \quad (2)$$

where $Z = bh^2/6$

Thus, the maximum force to bend a given beam to breakage is given by

$$F = (S_{\max})bh^2/6L \quad (3)$$

The piezoelectric ceramic by itself is very brittle. The construction of a total bender with the center vane and two silvered faces, however, adds considerable strength. The vendor specifications on a beam $1 \times 0.06 \times 0.02$ inches put the shear force at approximately 15,000 lbf/in².

The resonant frequency f of a beam in this mode of operation is

$$f = (K/M)^{1/2}/2\pi \quad (4)$$

where K is the modulus of elasticity and M is mass.

This, to a very good approximation, is

$$f \approx (10/\delta)^{1/2} \quad (5)$$

Single-beam parameters

The first geophone model was designed and constructed around benders which were available in-house. These were parallel-connected ceramics from Gulton Industries, with dimensions of $0.6 \times 0.06 \times 0.019$ inches. Maximum shear for these units was rated at 9,000 lbf/in² with shear of ceramic by itself at 3,000 lbf/in².

Breakage force and deflection

From Eq. 3, the maximum force this beam will take to reach shear is

$$F_{\max} = S_{\max}bh^2/6L \\ = \frac{(3 \times 10^3 \text{ lb/in}^2)(6 \times 10^{-2} \text{ in})(2 \times 10^{-2} \text{ in})^2}{6(6 \times 10^{-1} \text{ in})} \\ = 0.02 \text{ lb} = 9 \text{ gms.}$$

Thus, total σ to breakage will be the distance caused by a 9-gram force; but because of the composite construction, this σ won't be reached before

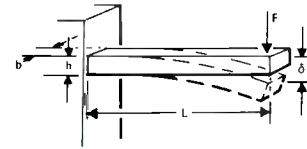


Fig. 3—Ceramic bender may be described as a cantilever beam clamped at one end.

the force becomes 27 grams. From Eq. 1, the static deflection δ of the beam will be

$$\delta = 4FL^3/Ebh^3$$

where

$$F = (9\text{gm})(9.80 \times 10^2 \text{cm/sec}^2) = 0.0882\text{N}; \\ L = 0.6 \text{ in } (1.524 \text{ cm}); E = 4.85 \times 10^9 \\ \text{n/cm}^2; b = 0.06 \text{ in } (0.1524 \text{ cm}); \text{ and } \\ h = 0.02 \text{ in } (0.0508 \text{ cm}). \\ \delta = \frac{(4)(8.8 \times 10^{-2})(1.52)^3}{(4.85 \times 10^9)(1.52 \times 10^{-1})(5.08 \times 10^{-2})^3} \\ = 0.15 \text{ cm} = 6 \times 10^{-3} \text{ inches}$$

Later experiments proved that these figures were very conservative, with the total deflection to reach breakage being 3 to 4 times this distance.

Resonance frequency

Using 6×10^{-3} inches as breakage distance and allowing 2 mils of this as usable distance (the other 4 mils being safety margin), the resonant frequency associated with the beam becomes $f \approx (10/\delta)^{1/2} = [(10/2) \times 10^{-3}]^{1/2} = 71 \text{ Hz.}$

Since $\delta \propto F$ and breakage deflection of 6 mils is caused by 27 grams, a force of 9 grams at one end of the beam should give the desired deflection of 2 mils.

Loading mass

To approach this mass with materials that could be obtained and tooled meant either brass or lead. The dimensions of a brass block weighing 9 grams are large: 0.500 inches in diameter \times 0.34 inches high. There obviously had to be some change in dimensions.

Arbitrarily setting the maximum dimensions of the mass as 0.25×0.25 inches with reasonable height and cutting the total volume to $1/4$ of its original, a mass was made. It was designed in a cylinder form 0.250 inches in diameter, 0.285 inches high, and weighing 2.57 grams. This in itself obviously raised the resonant fre-

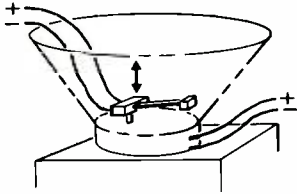


Fig. 4—Single ceramic beam mounted on the vibration table.

quency, but, by extending the center of mass, the theoretical resonance was approximately 108 Hz.

Geometrical dimensions and expected test values

Final dimensions and theoretical expected values on the first test model to be built were as follows:

- Ceramic bender— $L=0.625$ inches; $h=0.020$ inches; $b=0.060$ inches; Mass (brass)—area= 0.250×0.250 inches; ht= 0.324 inches; vol= 0.021 in³; wt.= 2.57 gms.
- Static deflection— 0.85 mil
- Resonant frequency— 108 Hz
- Breakage force— 24.5 gms
- Breakage deflection— 6.5 mil

Electrical leads

The most prominent methods for attaching leads to the ceramic are conductive epoxying, welding or soldering, and pressure contacts. Conductive

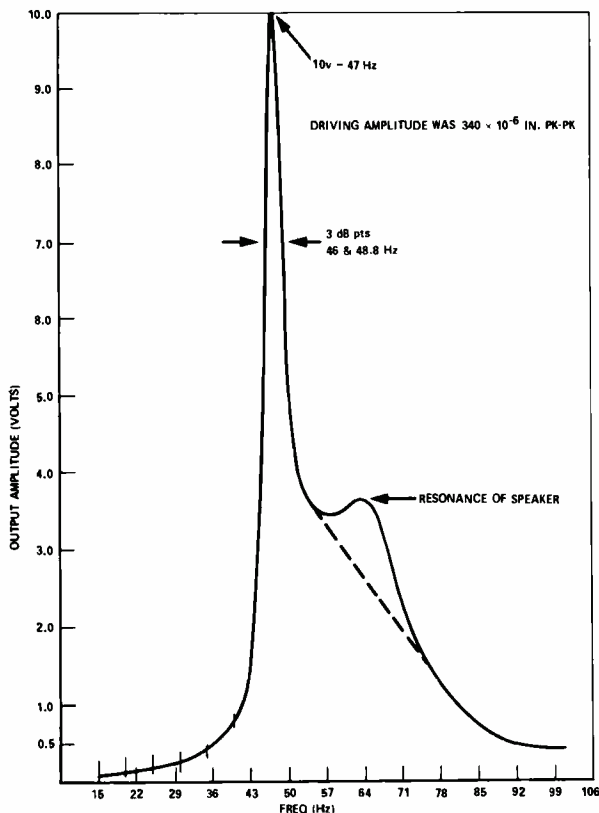


Fig. 5—Frequency response of a single tuned ceramic beam.

epoxy was attempted first but proved to be a slow, cumbersome process resulting in a bulky, weak contact point. Soldering was left for later study because of the temperatures involved. The present unit has pressure contacts.

Test equipment

Original tests run on a commercial vibration table were inconclusive and incomplete because the table lacked a low frequency, low amplitude drive. An excellent vibration table was improvised using an 8-inch speaker. The speaker was calibrated by plotting deflection versus drive current. The calibrated vibration table was capable of duplicating movements as low as 100×10^{-6} in. (pp) at 10 Hz.

With the single ceramic beam mounted on the vibration table as shown in Fig. 4, tests were run to find the resonant points, output signal, and Q of the sensor (output is shown in Fig. 5). Restrictions were imposed on total movement to assure that the unit would not break. These restrictions were dropped as soon as first tests showed that the ceramic was quite capable of withstanding drive amplitudes of under $500 \mu\text{in}$.

First tests were as expected, with high voltage output and narrow band resonance. The fact that the actual resonance frequency did not match the theoretical value is believed to be due to the varying material constants of the ceramic.

Tone burst

One of the more important results from the lab tests was the response time of the beam to bursts of its resonant frequency. It was quite easy to obtain outputs of up to 50% full resonance operation after an excitation burst of only 1 to 2 cycles.

System parameters

The next step was to expand to a system consisting of several tuned ceramic beams, thus covering a frequency range. Optimization between frequency range and physical size now drew first priority. Proper choice of dimensions and physical constants should have provided resonant beams covering a wide range of frequencies. We were interested here in a sensor responsive to frequencies predominant

in earth vibrations caused by men and vehicles. This set the frequency range at 10 to 100 Hz and the physical dimensions of the sensor had to be fitted to this range.

Dimensions

The deflection needed by any cantilever beam to be resonant at 10 Hz is, from Eq. 5:

$$\delta = 10/f^2 = 10/100 = 0.100 \text{ in.} \quad (6)$$

Setting an arbitrary limit on the mass at 5 gms, Eq. 1 is reduced to one variable.

$$\text{Solving } \delta = 4FL^3/Ebh^3 \text{ for Length, } L = (Ebh^3/4F)^{1/3}:$$

$$\delta = 1.0 \times 10^{-1} \text{ in} = 2.54 \times 10^{-1} \text{ cm}; E = 5 \times 10^6 \text{ N/cm}^2; b = 6.3 \times 10^{-2} \text{ in} = 1.5 \times 10^{-1} \text{ cm}; h = 2.1 \times 10^{-2} \text{ in} = 5.33 \times 10^{-2} \text{ cm}; F = (5 \times 10^{-3} \text{ kg}) (9.8 \text{ M/sec}^2) = \text{N}.$$

Therefore,

$$L = \left(\frac{(2.54 \times 10^{-1}) (5 \times 10^6) (1.5 \times 10^{-1}) (5.33 \times 10^{-2})^3}{4 (5 \times 10^{-3}) (9.8)} \right)^{1/3}$$

$$L = 5.2 \text{ cm} = 2.04 \text{ in.}$$

This length of ceramic posed a problem because the maximum length that could be prepared with a high yield was 2.0 inches.

To bypass the problem of exceptionally long piezoceramics, an alternate path of incorporating a short ceramic bender into a metal beam was studied. At first glance, it appeared that by lowering the length of the ceramic the high output voltage would be reduced. The non-resonant relationship of voltage output V to length is

$$V = (3FL/2bh) g_{31} \quad (7)$$

where g_{31} = piezoelectric constant of the material.

Thus, voltage is directly proportional to the length. However, since piezoceramics act electrically as capacitors, voltage output is inversely proportional to the capacitance. The relationship of capacitance to length is $C = K_{\text{const}} Lb/h$. Voltage output is thus inversely proportional to length. Because of this and Eq. 7, voltage depends only on the piezoceramic parameters.

Several quick tests proved this to be true. We could now achieve the high voltage output with easily available short piezoceramics. To approach the 2-inch length required for 10 Hz reso-

nance meant incorporating the ceramic as a part of a larger metal beam.

Beam construction

For ease in mathematically describing the action of the bi-material beam, the beam constant Ebh^3 was matched to that of the metal. This also assured that the tensile stress at the base would be no greater than if the entire beam were ceramic. The extension beam, using spring steel, was 0.15×0.062 inches in cross section and 1.75 inches long, leaving a ceramic length of 0.250 inches.

The combination beam worked very well and provided the same output and bandpass as expected.

Shock mounting

The next development step was to provide shock mounting of the ceramic. This was done in two steps: 1) using a round wire as the extension beam, thus giving Y-axis protection; and 2) using a coil spring as the extension beam, providing both Y- and Z-axis shock mounting.

Spring extension

In designing a spring for the beam, it was important that 1) the lateral spring constant, K_x , matched that of the ceramic; and 2) the longitudinal spring constant, K_y , was soft enough to provide protection.

The constants of a coil spring are described by two equations:

$$K_y = Gd^4 / 8D^3n \quad (8)$$

$$K_x = 10^6 d^4 / nD(K_1 L^2 + K_2 D^2) \quad (9)$$

where G is the modulus of elasticity; d is the diameter of wire; D is the diameter of coil; n is the number of turns; and, for materials with Y/G ratios of from 2.0 to 2.5, $K_1 = 0.204$ and $K_2 = 0.265$.

The springs in the present model were of phosphor-bronze with $d = 0.035$ inch; $n = 8$; $D = 0.165$ inch; and $L = 1.80$ inches.



Fig. 6—A shock-mounted ceramic beam; the ceramic is epoxied into the end of the spring. This set the constant K_x at 0.05 gm/mil, which was the K_x of the ceramic, and the constant K_y at 2 gm/mil. To combine the spring and the ceramic into one beam, the ceramic was epoxied into the end of the spring as shown in Fig. 6.

Frequency range and tuning masses

By making several of these beams identical, the only variable left in tuning the resonance frequency was the loading mass at the free end. The variables were already set so that the lowest frequency (10 Hz) needed a 5-gm weight. From Eq 1, $\delta = 4FL^2 / Ebh^2$, and from Eq 5, $f \approx (10/\delta)^{1/2}$ $f \propto 1/F^{1/2}$. By using varying weights on one beam, a test was run to determine frequency response and crossover points. Because of the high gain and narrow bandpass, a crossover point of -24 dB between neighboring resonances seemed quite reasonable. As expected, the bandwidth increased considerably as resonant frequency increased. Results and proper tuning frequencies are shown in Fig. 7. There is some question as to the redundancy of information provided by spacing the ceramics at crossover points of -24 dB. This is probably the minimum spacing that is needed, but a sensor unit may be able to provide the same information with fewer elements. To keep the volume at a reasonable level, twelve ceramics were used in building the first model.

System assembly

After the active portion of the sensor was completed, a shell was designed to provide stops for maximum movement of the free end of the beam and provide a solid base for the ceramics.

A top plate, as shown in Fig. 8, was designed to provide stops for the X-Y movement.

The radii of the holes allowed for normal sway space of the mass loaded beams but provided stops before the shear point of the ceramic was reached. The base plate was designed with a simple printed circuit board as an integral part, providing leads for

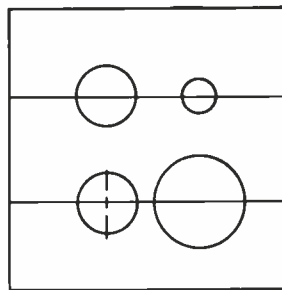


Fig. 8—Top plate, providing stops for the X-Y movement.

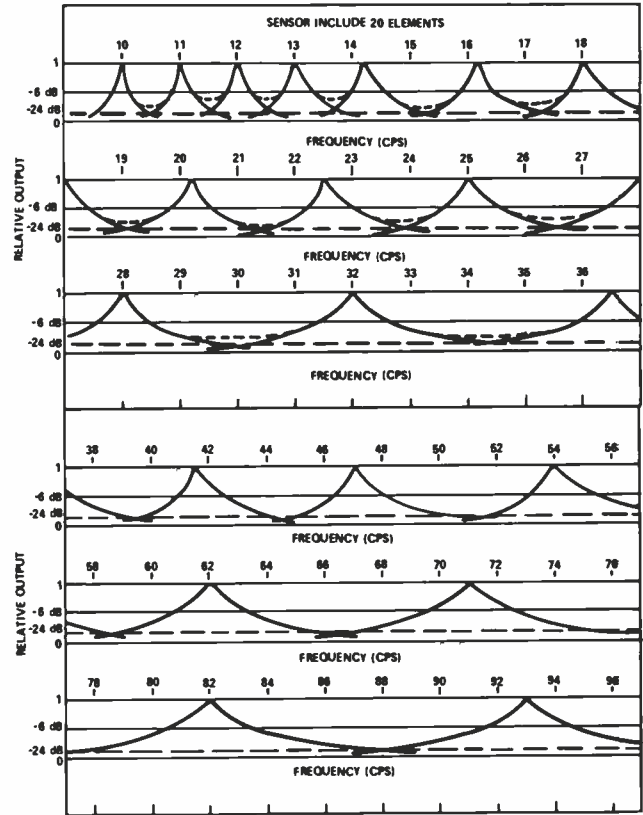


Fig. 7—Frequency response of sensor covering 10 to 100 Hz.

output. This is shown as part of the total assembly in Fig. 9.

Testing

It remained now to test the completed assembly. First step was to check single-beam resonance points. These varied slightly from planned values because of variations in construction of the laboratory model. After pinpointing resonance frequencies, outputs at low amplitude drives were studied and total system response to sweep frequencies and rates was noted. Response of any single beam to tone bursts of its resonant frequency for 50% full resonance output was from 1 to 2 cycles.

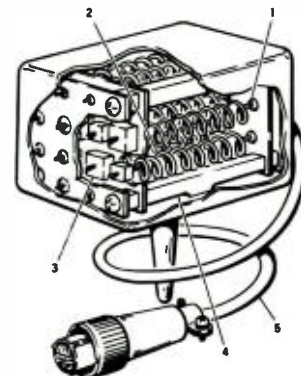


Fig. 9—Sensor array: 1) piezoelectric bender element; 2) coil spring; 3) mass; 4) shock-mounting structure; 5) electrical leads.

Response to complex signals

The final test of the model as a practical sensor rested on its ability to respond to actual complex waveforms. Laboratory simulation of this was carried out by driving the vibration table with the output of a tape recording, made in Asia, of walking men and moving trucks. There was some problem in simulating the recording level so that the vibration table could duplicate the actual field vibrations.

The first test was to determine the relative signal-to-noise ratio regardless of absolute recording levels. By driving the vibration table with a recording of quiet background, an output of from 0.2V to 0.3V on each sensor beam was recorded. Leaving the amplitude level set, the drive tape was turned to a section of 13 Thais walking. Signal outputs covered a wide range of amplitudes. Mean amplitudes ranged from 0.75V at 12 Hz to 5 to 6V mean at 24 Hz with peaks ranging from 2 to 8V.

Switching the tape to a section of moving trucks, output amplitudes were again studied. Amplitudes now ranged from 0.75V mean at 12 Hz to a new predominant frequency of 29 to 31 Hz where output was 5 to 6V pp. Output at 24 Hz was now at a 2 to 3V pp level.

Quick comparison of the frequency outputs for the two tests—13 Thais walking and moving trucks—showed three important results: 1) the sensor can respond to complex waveforms; 2) the output of any single channel

is 40 to 90 dB above the unamplified composite output of an ordinary geophone; and 3) the sensor is able to detect and show the frequency information contained in a complex waveform.

Conclusion

The results of the limited testing prove quite readily that piezoelectric ceramics as active parts of sensing devices can provide detection and information far superior to present geophones. The sensitivity of the present model ranges from 26 mV/ μ in at 12 Hz to 78 mV/ μ in at 65 Hz. This can be compared to a sensitivity of present geophones of approximately 1 mV/ μ in. The frequency information provided directly from the sensor can be incorporated with time and phase relationships of the composite signal, giving a very complete signature of the disturbance causing source. The size of the present model is 2 x 2 x 2 1/4 inch. This size is presently being studied and plans are being prepared for a 1 x 1 x 1 inch model. The present size is not out of question and the new one-inch cube model will compare excellently with the size of present geophones.

Safety-and-arming device

A safety-and-arming device has a two-fold function. One is providing a complete break in the detonation train for the entire time up until launch and for a prescribed "safe" time after launch of the shell or missile of which it is a part. The other function, happening at this point of safe separation,

is to fully align the detonation train, making the shell live and responsive to the fuzing assembly.

Any safety-and-arming device must provide a very high degree of reliability; thus it must be able to detect at least two and sometimes three environmental factors (such as initial acceleration, velocity, altitude, time of flight, etc.) before arming. Most of the present safety-and-arming devices are mechanical and an attempt was made here to show that an electrical safety-and-arming device could be made using the output of a piezoelectric ceramic sensor. A flow diagram is shown in Fig. 10; the sequence of events is shown in Fig. 11.

Environmental forces

The idea was to detect and monitor, through the voltage output of piezoelectric ceramics, three distinctly different but related environments acting upon the system. These environments were acceleration, length of acceleration, and velocity. The safety mode would not be switched to the arm mode until certain conditions of all three environments were satisfied.

Sensors

The sensors were loaded piezoelectric ceramics, either in the form of benders or round discs.

Functions of sensors

One set of ceramics was loaded so that any change in acceleration caused a force to act upon them. The force of interest, in this case, was the setback

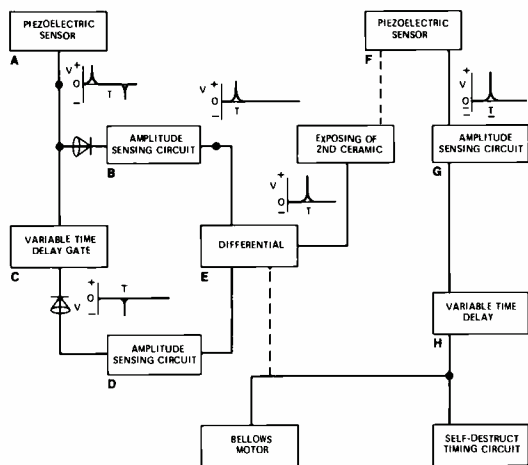


Fig. 10—Piezoelectric safety-and-arming device. A. Sensor gives voltage pulse proportional to acceleration. B. Safety 1 opens gate if acceleration pulse greater than preset level. C. Safety 2 sets gate which will not open for set time interval. D. Safety 3 senses amplitude and decides if motor has burned at full amount for entire time. E. Fires only when both pulses arrive; output exposes 2nd ceramic to air flow and activates associated circuitry. F. Velocity sensor senses air pressure. G. Safety 4 decides if velocity is at least at minimum value. H. Sets safe separation distance by length of time delay.

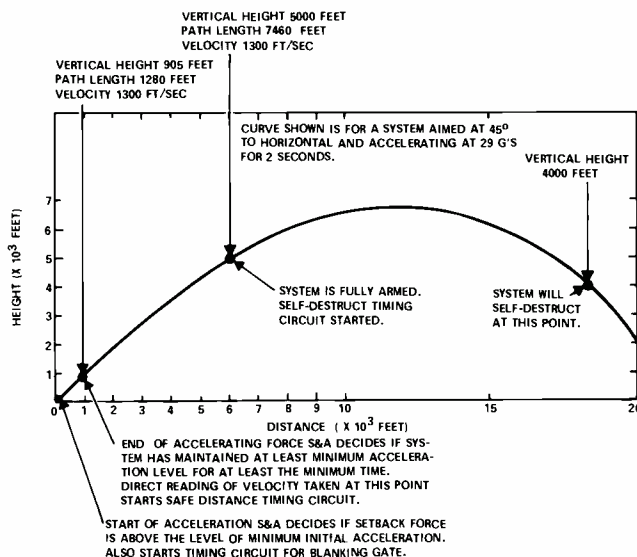


Fig. 11—Sequence of events—piezoelectric safety and arming device.

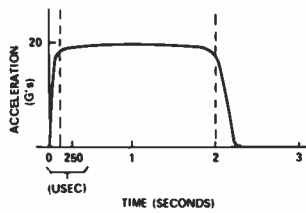


Fig. 12—Acceleration vs. time for a typical rocket.

force due to the initial acceleration and the sudden deceleration at the termination of the constant acceleration period. (A typical acceleration curve is shown in Fig. 12.) At this point, by monitoring the instantaneous air pressure on another ceramic, a direct reading of velocity was taken.

Systems

The output of the piezoelectric sensors should be capable of triggering and sustaining all of the decision circuitry needed for an all-electric system. It could be modified, however, so that the ceramics only provide the signals, and another source provides power for the circuitry.

During the initial acceleration change, a setback force exerted on the piezoceramics causes the ceramic to deform and generate a voltage pulse. During the period of constant acceleration, there is no change in force upon the ceramics—thus, no energy generated. At the end of this period of constant acceleration, a brief restoring force acts upon the ceramics as the driving force stops. This force causes a voltage pulse from the ceramics which is proportional to the thrust of the engines at this point. If the engine holds at full power over the entire length of the burning period, this pulse would be of opposite polarity and approximately the same amplitude as the initial pulse.

The first half of the signal operating the device is now generated, consisting of a positive pulse proportional to initial acceleration, a non-signal time proportional to the burn time of the accelerating force, and a negative pulse proportional to the deceleration at the end of the burn (Fig. 13).

The initial positive pulse performs two functions. It feeds an amplitude-sensing device at the same time that it initiates a variable-time-delay circuit. The level-sensing circuit verifies that the initial pulse is proportional to an

acceleration (which is at least the minimum level called for in the system). The variable-time-delay circuit generates a gate which does not open following this initial pulse until after a certain time duration. This duration is long enough to block out the possibility of passing a false signal caused by a fall. This is highly reliable because the times involved between the positive and negative pulses of a signal caused by a fall are in microseconds; and the times of burn of powered rockets, for instance, are several times that long.

Assuming that the acceleration pulse is above the minimum level of the sensing circuit, it then opens one side of a differential circuit. This same pulse, after initiating the time delay gate, is blocked from going any further.

Assuming now that the accelerating impulse lasts for the specified time of the system, the negative pulse (proportional to the end thrust of the motor) is generated at a time slightly following the opening of the time-delay circuit. This pulse is now blocked from entering the level-sensing circuit of the positive pulse but is permitted to pass through the time-delay gate to another level-sensing circuit. The level set here determines if the magnitude or energy of this pulse is compatible with the previously determined amplitude of the acceleration pulse. If the negative pulse is able to pass this test, the system has safely reached the minimum values of acceleration magnitude and length.

At this point, a direct reading of the velocity is taken. There are several methods of doing this, but one method (using another ceramic) is to use the signal from the previous two conditions to quickly uncover a ceramic in the surface of the missile. This ceramic experiences a force, due to air pressure, which changes from ambient to the pressure of the velocity attained. The voltage pulse from this sensor is sent through yet another level-sensing circuit to determine if the actual velocity, related to the acceleration and burn time of the engine, is at least equal to a minimum level. If this test is passed, a time-delay circuit is initiated to determine safe separation distance.

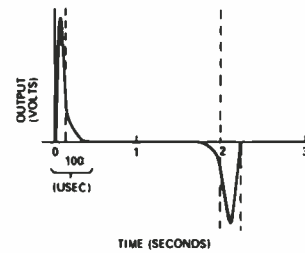


Fig. 13—Output of piezoceramic vs. acceleration.

Alignment of detonation train

At the end of this time delay, a charge is activated, causing a bellows motor to align the detonation train.

Safety

All accidental falls cause one of two types of signal. These signals occur only on impact with some object, since a fall would be under the acceleration of 1 g which is a constant force and at no time generates a signal. Depending upon orientation upon impact, the signal is either a positive pulse only or a positive pulse followed very closely (microseconds) by a negative pulse. In the first case, where there is no negative acceleration pulse, the differential does not see the required energy and reverts to a full-safe position. In the second case, assuming the acceleration is enough to pass through the level-sensing circuit, the gate which was triggered by this pulse is closed for at least a few milliseconds so that the quick negative pulse caused by the rebound appears much too soon to pass through. There is no apparent way that an accidental fall could cause a false signal to appear and open the velocity sensing ceramic. If this happens, however, there is no velocity at this point and the signal to the bellows motor is never generated.

Conclusion

There is much work to be done on the circuitry concerned with the safety-and-arming concept but the use of piezoelectric ceramics as sensors appears to warrant further design and testing. The circuitry could be set up so that individual parameters would be dialed in to set the length of the time-delay gates. Redundance of the system could easily provide the reliability desired. Cost of a system such as this seems quite comparable with existing mechanical safety-and-arming devices.

Speech bandwidth compression by analytic rooting

E. J. Sass | G. E. Mackiw

The analytic rooter system described in this paper accepts speech signals with a bandwidth from 238 to 2856 Hz, compresses this bandwidth by a factor of two to 119 to 1428 Hz for transmission, and reconstitutes the signal at the receiver to its original form. The device was submitted to a Diagnostic Rhyme Test (DRT), which measures the intelligibility of the signal. A score of 91.2 was achieved; for the bandwidth being considered, a DRT score of 96.1 would be perfect. This is the first known unit of such simplicity and potentially small size that has achieved a DRT score this high. With medium-scale integration, the analytic rooter will fit beneath the base of a telephone handset.



Earl J. Sass, Ldr.

Communications Equipment Engineering
Government Communications Systems
Communications Systems Division
Camden, N.J.

received the BSEE in 1945 from the University of Nebraska; and the MSEE in 1954 from the University of Pennsylvania. He joined RCA after receiving his undergraduate degree and worked on RF and IF coils and transformers and the first RCA printed-circuit television tuner. He was then assigned responsibility for product design of picture and sound IF amplifiers for RCA's first commercial color television receivers. Next, he supervised half of the electrical design of commercial color television receivers and remote control receivers. To further broaden his background, he transferred to RCA's Government Communications Systems Division where he was responsible for the design 1) of the ground receiving equipment for the DYNA-SOAR Project and 2) a part of the GRC and 744 project. Later he was responsible for the design and development of the AN/TRC-97 exciter, receiver, and shelter. At present, he is Group Leader in charge of the development and design of military frequency division multiplex terminal equipment and is responsible for the AN/UCC-5(V) FDM equipment. He was in charge of the completion of the Analog Voice Compression Study program which included the development of the Analytic Rooter. He holds three U.S. patents and is the co-author of four published articles. He is a Senior Member of the IEEE, is a registered Professional Engineer in the State of New Jersey, is a member of the Armed Forces Communications and Electronics Association, and is a member of Sigma Tau and Pi Mu Epsilon.

George E. Mackiw

Communications Equipment Engineering
Government Communications Systems
Communications Systems Division
Camden, N.J.

received the BSEE in 1959 and the MSEE in 1962 from Drexel Institute of Technology. In 1959 he joined Philco Corporation Communications Group where he participated in design of the Courier communication satellite and AN/TRC-56 radio-multiplex equipments. In 1963 he joined RCA Communications System Division. There he participated in AN/TRC-97 program as a design project engineer responsible for diversity combiner, threshold extender demodulator, baseband and orderwire circuits. In 1966, he conducted two IR&D programs to develop and evaluate techniques for a 300-channel baseband combiner and for a 300-channel phase-locked demodulator (threshold extender). In 1967, he became part of TACSATCOM design team where he was responsible for beacon receiver subsystem, parametric amplifier, and overall system integration and evaluation. During 1969-1970, he performed Analog Voice Compression study in which an analytic rooter system was constructed and evaluated. Currently he is assigned to IR&D program in the telecommunication field. He has post graduate work beyond his Masters Degree, is the author/co-author of four TR's, and is a member of Eta Kappa Nu.

Reprint RE-17-2-10

Final manuscript received January 26, 1971

A FUNDAMENTAL PROBLEM in telecommunications is making the most efficient use of the transmission media available. The increasing demand for more voice communications channels, both analog and digital, has given added importance to the investigation and development of a special bandwidth compression system that is simple, small, economical, and provides acceptable intelligibility and quality. These criteria exclude such complex analog bandwidth compression techniques as are applied in channel vocoders, format vocoders, autocorrelation vocoders, etc., where bandwidth compressions on the order of 10:1 are typically provided. Rather, the candidate list includes only those techniques primarily intended to provide a lower order of bandwidth compression, such as:

VOBANC¹
CODIMEX,² etc.³
Harmonic compressor⁴
Phase vocoder⁵
Analytic rooter⁶

Broadly speaking, all of the listed techniques split the speech band into a number of contiguous sub-bands at the transmitter and operate on each sub-band, by various means, to effect division of its output frequency by a factor of 2 (or more). Likewise, at the receiver, all of the techniques effect a frequency multiplication of 2 (or more) in each sub-band, and thereafter combine the sub-band outputs to obtain reconstituted speech. Preliminary study of these candidates indicated that:

The VOBANC inherently distorted speech to an unacceptable degree.

The CODIMEX, etc., techniques were closely related to the analytic rooter technique described in this paper, but were judged to be less-advanced as well as less-available (foreign source).

The harmonic compressor inherently distorted unvoiced speech an undesirable amount, and required an excessive number of narrow-band subchannels (50 or so) which would probably be too expensive.

The phase vocoder yielded fairly good speech quality but required an excessive number of narrowband subchannels (30 or so) plus other circuit complications which would be too expensive.

The analytic rooter promised to yield good speech quality and was judged to be the best analog processing technique to consider.

Thus, the Analytic Rooter was selected as a most promising bandwidth compression technique, and was developed, built, and tested for the R&D Division of the Defense Communications Agency. A Diagnostic Rhyme Test (DRT) intelligibility score of 91.2% was achieved. This compares favorably with a normal telephone circuit, which achieves a DRT score of 94-95%.

An Analytic Rooter employing medium scale integration (MSI) could be packaged to fit under the base of a conventional telephone handset. The size would be approximately 9-in. long by 5½-in. wide by 1-in. high (volume less than 50 cubic inches).

Analytic rooter theory

If $S(t)$ is a real, bandlimited signal, the corresponding analytic signal is defined as $S(t) + jS'(t)$, where $S'(t)$ is the Hilbert transform of $S(t)$. It can be shown that, for signals with a spectral width due primarily to large-index frequency modulation, the "square rooted" signal, defined as

$$S_{\frac{1}{2}}(t) = \text{Re}[S(t) + jS'(t)]^{\frac{1}{2}} \quad (1)$$

has approximately one-half the bandwidth of $S(t)$.

A signal having approximately this spectral property is speech filtered to remove all but one formant. [A *Formant* is "one of the regions of concentration of energy, prominent on a sound spectrogram, which collectively constitute the frequency spectrum of a speech sound." For example, if speech is filtered by a bandpass filter passing frequencies from about 238 to 714 Hz, the output of that filter will nominally contain the first formant,

$F1$, of the speech. If by additional filtering, the Hilbert transform of $F1$ is next obtained and appropriately added in quadrature to $F1$, the analytic signal of $F1$ results. If the real part of the square root of this analytic signal is then obtained via appropriate circuitry, a new signal (containing only frequencies from about 119 to 357 Hz and thus having only about half the bandwidth of $F1$) is obtained.

Not only the first formant $F1$, but also the second, third, and fourth speech formants can be so processed. Thus,

2:1 bandwidth compression of speech can be introduced via this analytic-signal rooting technique.

Even higher compression factors are possible by using higher roots of the analytic signal, but in the interest of utilizing the technique to a degree consistent with maximum result per unit complexity, present considerations have been constrained to 2:1 bandwidth compression.

At the receiver, the original signal $S(t)$ must be recovered from the half-band version, $S_{\frac{1}{2}}(t)$, with acceptable

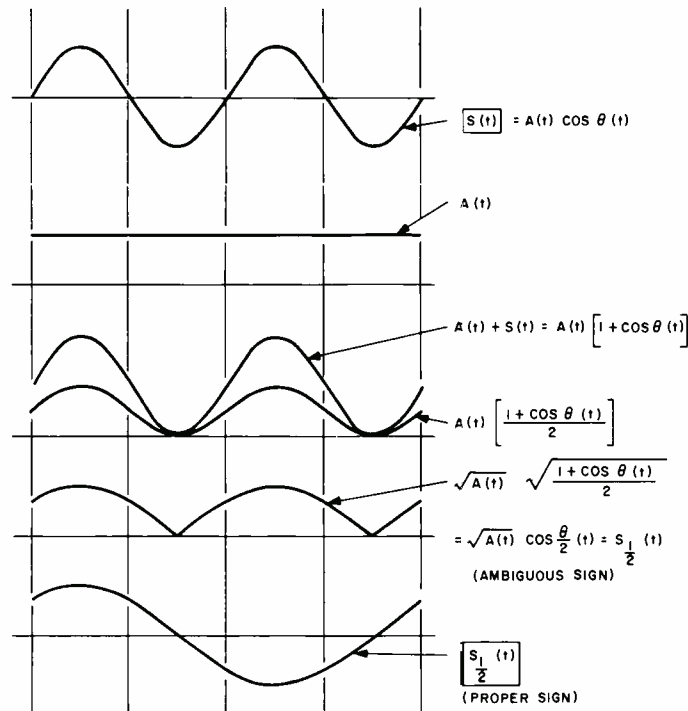


Fig. 1—Sinewave signals in analytic rooter transmit section.

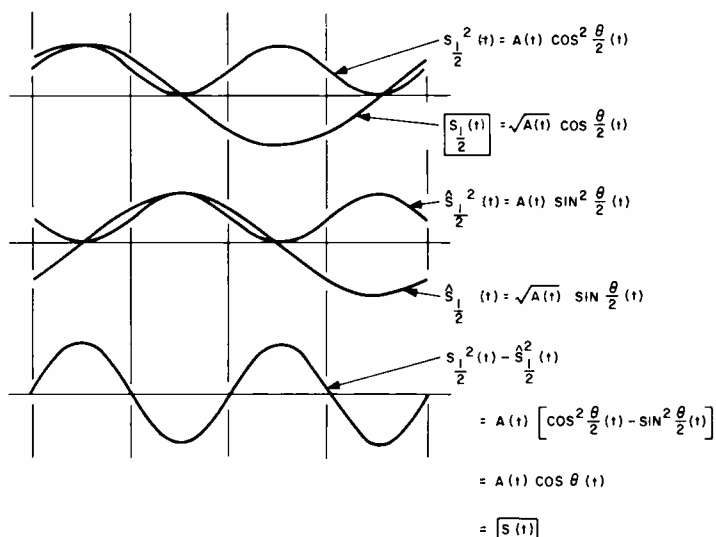


Fig. 2—Sinewave signals in analytic rooter receive section.

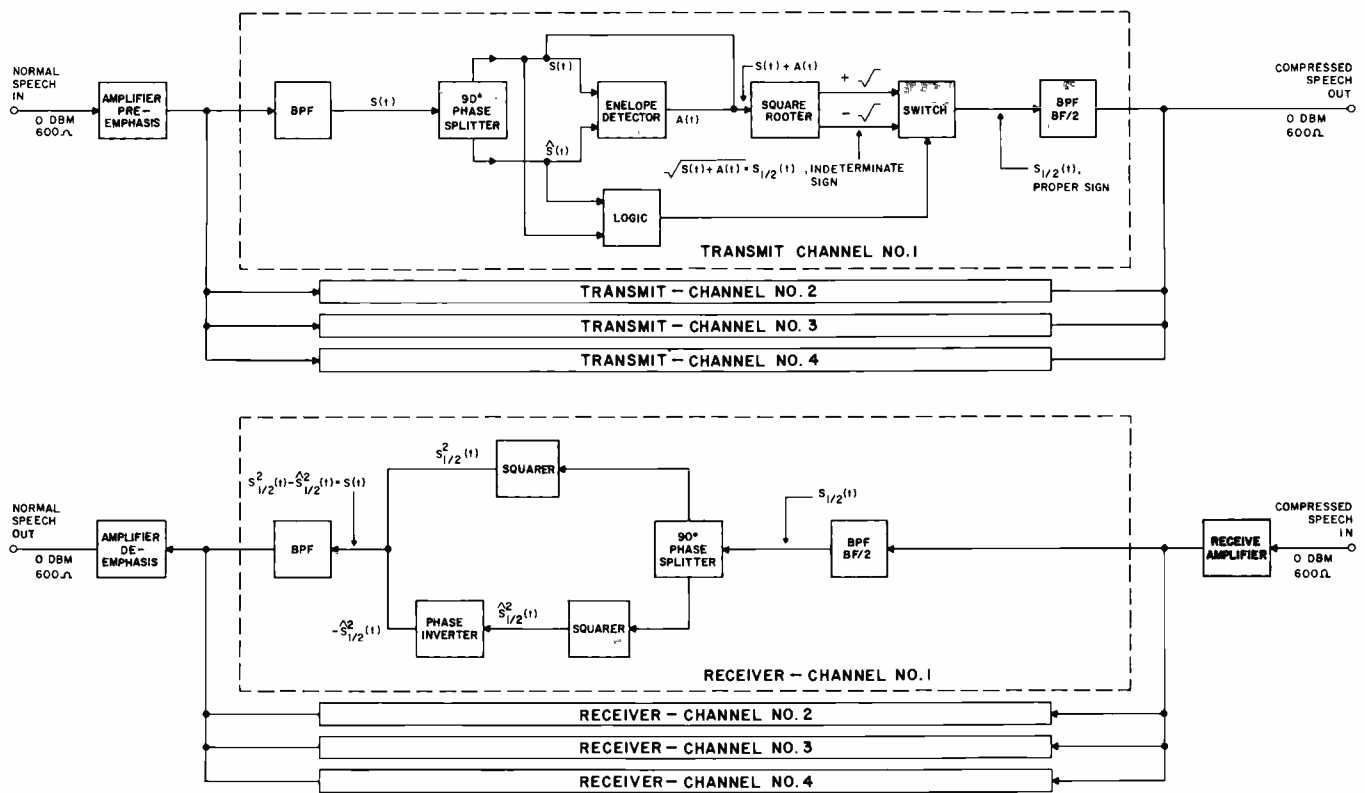


Fig. 3—Block diagram of the analytic router.

fidelity. It can be shown that this may be accomplished by squaring the analytic signal corresponding to $S_{1/2}(t)$ whence:

$$S(t) = \text{Re} [S_{1/2}(t) + jS'_{1/2}(t)]^2. \quad (2)$$

Implementation of the bandwidth compression and expansion functions of Eqs. 1 and 2 may be accomplished as described below. If $S(t)$ is expressed in terms of its "envelope," $A(t)$, and its phase, $\phi(t)$,

$$S(t) = A(t) \cos [\phi(t)], \quad (3)$$

then it can be shown that

$$S'(t) = A(t) \sin [\phi(t)] \quad (4)$$

$$A(t) = [S^2(t) + S'^2(t)]^{1/2}, \quad (5)$$

and

$$S_{1/2}(t) = (1/2)^{1/2} [A(t) + S(t)]^{1/2}. \quad (6)$$

Unfortunately, the sign of the square root in Eq. 6 is indeterminate. However, the proper sign can be recovered by changing the sign of the square root in Eq. 6 every time the phase, $\phi(t)$, of the original signal, $S(t)$, goes through an integral multiple of 2π . According to Eqs. 3 and 4, this occurs when $S'(t) = 0$, while $S(t) < 0$. Application of this logic to Eq. 6, therefore, provides a practical solution to implementing Eq. 1 at the transmitter.

It can also be shown that Eq. 2 may be rewritten in the form

$$S(t) = S_{1/2}^2(t) - S'_{1/2}^2(t). \quad (7)$$

The latter provides a practical solution to implementing Eq. 2 at the receiver. Pictorial representations of sinewave signals as they progress through the system are presented in Figs. 1 and 2.

Configuration

A block diagram of the analytic router is shown in Fig. 3. The speech spectrum is first divided into four contiguous passbands, each nominally containing no more than one formant. After division, each of the four spectral segments is independently processed in circuitry consisting of a 90° phase splitter, envelope detector, square rooter, analog switch, and logic. The processed signals are then passed through the corresponding half-bandwidth filters that prevent inter-channel coupling. These filtered signals are then summed and form the composite compressed transmitter output.

In the receiver, the composite compressed signal is divided into four formant channels by half-bandwidth filters. Each channel is processed in

the phase splitter, squarer, and inverter circuits to return the signal to its original form. The four signals are then filtered and summed to provide the composite reconstituted output.

Common equipment for the four channels consists of transmit input amplifier with preemphasis, receive input amplifier, and a receive output amplifier with de-emphasis. The transmit amplifier pre-emphasis circuit, located at the transmitter input, provides interface with a 600-ohm 0-dBm input line, provides pre-emphasis for the high frequency spectrum of speech, and provides the input signal to the four roter channels.

The receive input amplifier, located at the receiver input, provides gain and interface between the 600-ohm 0-dBm half-bandwidth transmission line and the receiver circuits.

The receive amplifier de-emphasis circuit, located at the receiver output, provides de-emphasis and 600-ohm 0-dBm interface to the output line.

Bandpass filters

Four bandpass filters are used in each channel. All filters are active and of identical structure. Two filters in each channel (transmit input and receive

output) have full channel bandwidth; the other two (transmit output and receive input) have bandwidths exactly one-half of the full channel. The first filter (transmit input) defines the channel bandwidth and separates the corresponding spectral segment $S(t)$ from the input speech signal. The second filter (transmit output) serves to restrict any out-of-compressed-band spectral component, generated in the transmitter circuits, from adjacent-channel coupling in compressed signal multiplexing. The third filter (receive input) separates the corresponding spectral segment $S_{\frac{1}{2}}(t)$ from the compressed input speech signal. Finally, the fourth filter (receive output) prevents any out-of-band signal, generated in the receiver circuits, from distorting the reconstituted output signal. The specified filter characteristics are summarized in Table I.

Table I—Analytic roter filter characteristics

Channel	Filter frequency range (Hz)	
	BW	BW/2
1	238 to 714	119 to 357
2	714 to 1428	357 to 714
3	1428 to 2142	714 to 1071
4	2142 to 2856	1071 to 1428

Phase splitter

The Hilbert transforms $S'(t)$ and $S'_{\frac{1}{2}}(t)$ are formed in the transmitter and receiver, respectively, by the same 90° phase-splitter networks. These networks are of the so-called Weaver^{8,9} type, synthesized with active all-pass stages. The phase-splitter networks were designed for 90° phase shift, bandwidth of one decade, and accuracy of ± 0.5 degree.

Envelope detector

As described above, in the analytic roter theory section, detection of the envelope signal $A(t)$ is required. The envelope detector must be very linear over a wide dynamic range and should produce no significant delay.

Theoretically, ideal envelope detection of a signal $X(t)$ may be obtained by taking a square root of the sum of the squares of a signal and its Hilbert transform $A(t) = [X(t)^2 + X'(t)^2]^{\frac{1}{2}}$. Such an envelope detector was initially constructed, but it proved to be too sensitive to offset. Another type of envelope detector was finally used: a "quadrature" envelope detector. The "quadrature" detector consists of two active full-wave detectors followed by a summing circuit. A signal and its

Hilbert transform (quadrature signal) are applied to the two detector inputs. The resulting operation is basically that of a two-phase full-wave detector. A small ripple at four times the signal frequency is then filtered out without introducing a significant envelope delay. This detector is very stable and performs very well in the system.

Square roter

In this circuit, a signal envelope $A(t)$ and a signal $S(t)$ are summed and the square root of the sum taken. Two outputs, $+[A(t)+S(t)]^{\frac{1}{2}}$ and $-[A(t)+S(t)]^{\frac{1}{2}}$ are provided so that the sign ambiguity of $S_{\frac{1}{2}}(t)$, indicated by Eq. 6, may be resolved by the use of selective switching. The final square-roter circuit used two operational amplifiers to provide forward gain and phase inversion, and a multiplier circuit in the feedback loop to shape the transfer characteristics. This non-linear feedback forms the square-rooting forward response.

Switch/logic

Selection of the sign of $S_{\frac{1}{2}}(t)$ is accomplished by the switch/logic module, the algebraic sign of $S_{\frac{1}{2}}(t)$ being changed whenever $S'(t)$ goes through zero while $S(t) < 0$. This is accomplished by determining the $S'(t)$ zero crossing in a sense amplifier, combining this condition in AND gate with the negative polarity of $S(t)$. The output

of the AND gate commutates a flip flop which drives a field-effect-transistor switch. The other inputs to the switch are the two outputs of the $[A(t)+S(t)]^{\frac{1}{2}}$ square-roter module. Based on the logic just described, the ambiguity of sign of the square-rooted signal, $[A(t)+S(t)]^{\frac{1}{2}} = S_{\frac{1}{2}}(t)$, is resolved, giving the correct sign for $S_{\frac{1}{2}}(t)$.

Squarer

In this module, both the compressed signal, $S_{\frac{1}{2}}(t)$, and its Hilbert transform $S'_{\frac{1}{2}}(t)$ are squared, and a difference of these squared signals taken, to provide the reconstituted signal, $S(t)$. The function of this module is mathematically described by Eq. 7. The module consists of two four-quadrant multipliers connected for squaring and an operational amplifier stage where the difference between the squared signals is taken.

Dynamic range

The dynamic range of the complete analytic-roter system is linear over a range exceeding 50 dB for each channel frequency, with the resulting data shown in Fig. 4. Subjective tests with speech signals prove that a useful signal can be received when the average speech level is varied over a range of 30 dB. Because of this satisfactory dynamic range obtained with the analytic roter alone, use of compandor circuitry is not required.

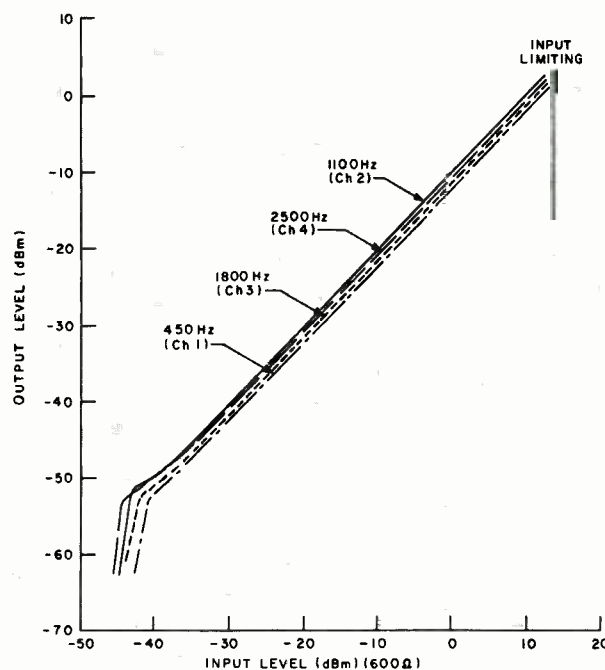


Fig. 4—Dynamic range of analytic roter.

The absolute signal levels shown in Fig. 4 refer to the input signal measured at the common transmitter filter point (output of the amplifier pre-emphasis circuit), and the output signal measured at the summed receiver point (input to the amplifier de-emphasis).

Intermodulation distortion

The spectrum produced by rooting a complex signal has components which fall outside the allocated compressed bandwidth. As a result, some energy is rejected in the half-bandwidth filters and consequently upon signal reconstitution some distortion occurs. This is confirmed by tests which were performed with the half-bandwidth filters bypassed; the DRT score improved from 91.2 to 93.6%.

If a signal which falls within any of the formant channels is of a pure FM form, a perfect compression in bandwidth results. Since, however, a speech formant does not have a pure FM structure but contains AM components also, a perfect compression is not realized. To determine the mechanism by which intermodulation between the non-FM spectral components within a formant channel occurs, mathematical analysis of transmission of a two-tone signal through the analytic roter system was performed. The analysis shows that the transmitted spectrum is not compressed but in fact becomes wider, and non-symmetrical, as shown in Fig. 5. The relative positions of the input and output spectral components in respect to the input and output (half-bandwidth) filters is shown in Fig. 6. When the output spectrum is passed through the output filter, the spectral components become modified both in phase and in amplitude.

The calculated and measured distortion as a function of normalized frequency is shown in Fig. 7. The distortion is a function of frequency separation between the signals, their position with respect to the filter pass-band, and of their relative levels. The close agreement between the calculated and measured distortion indicates that the system performance is inherently limited by the filters.

To determine whether phase equalization of the filters could improve the performance, analysis was performed where the filter was followed by an

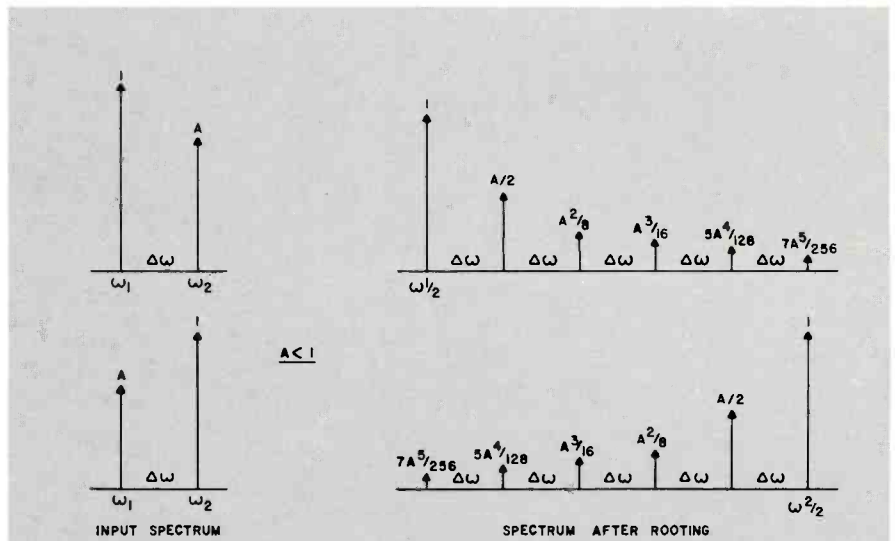


Fig. 5—Spectra produced by the analytic roter transmitter from a two-tone input.

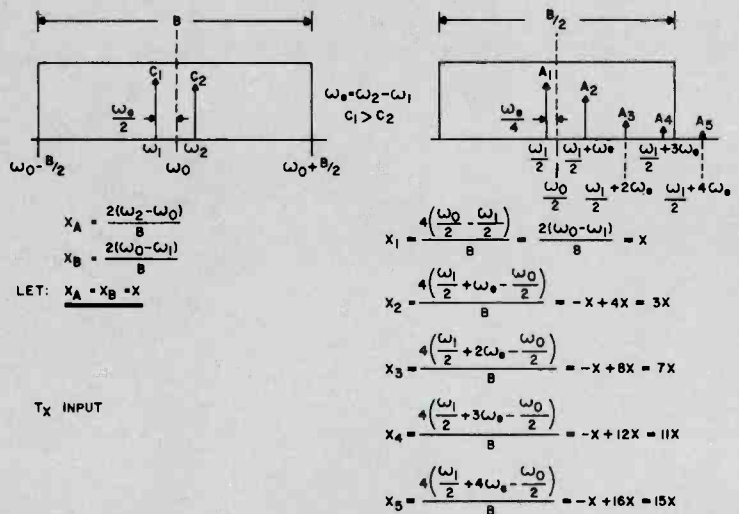


Fig. 6—Spectral components normalized with respect to bandwidth.

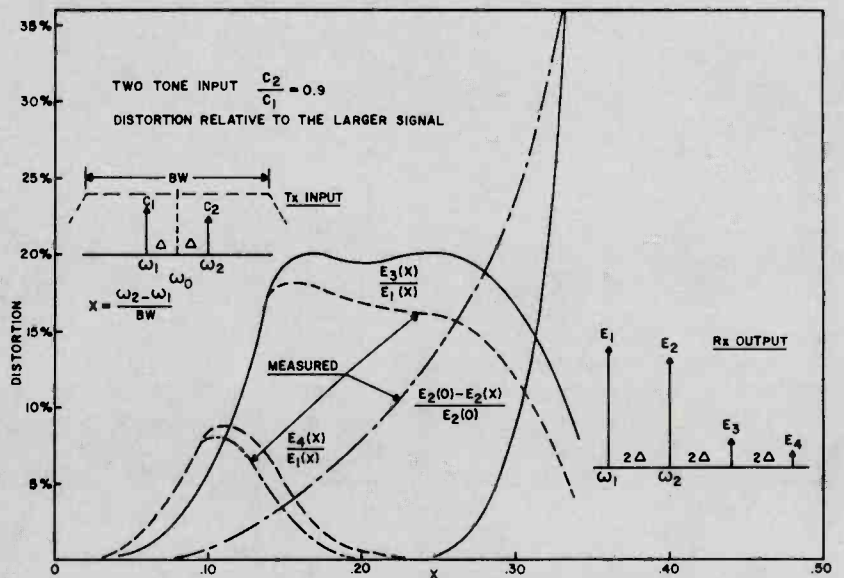


Fig. 7—Measured and computed distortion due to $BW/2$ filter in analytic roter system.

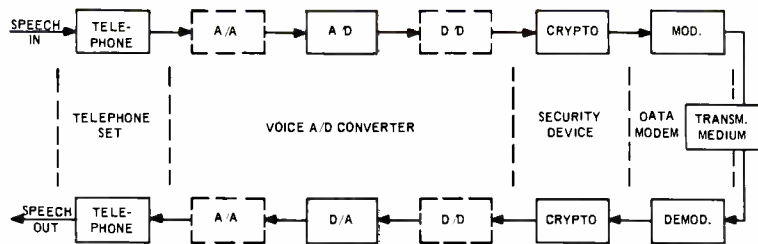


Fig. 8—Secure-voice-terminal functions, block diagram.

ideal phase equalizer. The resulting distortion, although slightly different in shape, indicated only minor improvement over a real system where no equalization was used.

Intelligibility

Since the analytic-roter bandwidth compression system is intended for speech signal transmission, the most significant characteristics are those associated with speech intelligibility. Therefore, various DRT intelligibility tests were performed. The DRT test is a two-choice test of consonant discriminability which yields a gross measure of speech intelligibility and additional scores relating to specific aspects of the performance of the speaker, listener, or system under test. It utilizes a corpus of 192 words (96 rhyming pairs selected such that the initial consonants of each pair differ in terms of a single phonemic attribute). The results of these intelligibility tests are presented in Table II. The DRT result for the analytic roter (tape number 1) is only approximately 5% less than obtained with the analytic roter bypassed (tape number 3), for the speech input bandwidth for which it was designed (238 to 2856 Hz). The DRT result for the complete analytic roter system (tape number 1)—despite the compressed transmission band (119 to 1428 Hz)—is approximately 15% better than the result over a near-perfect filter (tape number 4) of the same band (119 to 1428 Hz). If the analytic roter were designed to accept a somewhat broader band of speech (3500 Hz), the DRT score might approach a value of 95%.

Table II—Results of DRT tests.

Tape No.	Experimental condition	Total DRT score (%)	Standard error
1	Complete analytic roter	91.2	0.84
2	Analytic roter without BW/2 filters	93.6	0.82
3	Bandpass filter 238 to 2856Hz	96.1	0.61
4	Bandpass filter 119 to 1428Hz	76.1	1.01

Quality

Speech quality through the analytic roter is a good for male voices but only fair for female voices. The quality is constant for 25 dB of dynamic range and useable for 30 db of range. There is no noticeable distortion when the half-bandwidth filters are removed.

Tests with the speech signal exhibiting varying degrees of signal/noise have not been conducted.

Potential applications

Acceptable-quality digitized speech has been achieved at bit rates of 9.6 kb/s or less with vocoders of several types but these are characteristically bulky, heavy, complex, and costly. Direct absolute digitization, such as PCM, which yields good quality at high bit rates, produces unacceptable speech performance at 9.6 kb/s. Certain direct delta techniques and adaptive delta techniques have shown a good compromise between speech quality and equipment size, weight, and cost at 19.2 kb/s. However, at the present state-of-the-art, no direct A/D or D/A converter (signified by the solid-line A/D and D/A blocks in Fig. 8) is capable of yielding acceptable speech performance at the 9.6 kb/s rate.

It is, therefore, presently necessary to introduce other appropriate processing functions (dashed-line blocks in Fig. 11) before and/or after, respectively, the basic A/D and D/A conversion functions, if a 9.6 kb/s bit rate capability is to be realized. Although such hybrid converters exist (for example, voice-excited vocoders) they are undesirably complex and costly. With a view to correcting this deficiency, the analytic roter could provide an analog-to-analog conversion unit (block A/A in Fig. 11) that would be relatively inexpensive, small, and light weight.

Police departments want to increase information handling capacity of their assigned channels; e.g., by adding tele-

type, the patrol cars could have a hard copy of the received commands. Police also desire communications privacy to prevent monitoring by unauthorized personnel. Through the use of analytic rooting, the voice-information bandwidth would be reduced by a factor of two, leaving the remaining portion of the band for transmission of other information. Since the transmitted bandwidth is halved, the signal is unintelligible; thus privacy is preserved.

By using two analytic routers and two dual-channel frequency division multiplexers, two voice channels can be operated full duplex over one S-1 telephone line; thus halving the cost of the leased line.

Through the use of analytic rooting and modified frequency division multiplex equipment, the voice channel capacity of any system can be doubled.

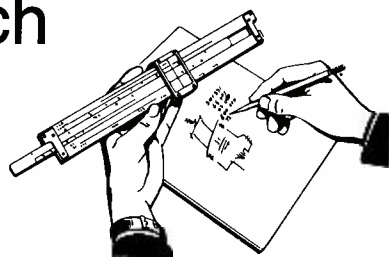
Acknowledgment

The authors wish to give special credit to Harold M. Straube and his group at the then Defense Advanced Communication Laboratory, West Windsor, N.J., who obtained the contract from the Defense Communication Agency, Washington, D.C. and who did the initial systems and development work.

References

- Bogert, B. P., "The VOBANC—A Two-to-One Speech Bandwidth Reduction System", *JASA*, Vol. 28, No. 3 (May 1956).
- Marcou, P. and Daguét, J., "New Methods of Speech Transmission", *Proc. 3rd Symp. on Information Theory*, London (1955). Also Daguét, J., "CODIMEX' Speech Compression System", *Proc. Stockholm Speech Comm. Seminar*, R.I.T., Stockholm, Sweden (Sep 1962).
- Seki, H., "A New Method of Speech Transmission by Frequency Division and Multiplication", *J. Acoust. Soc. Japan*, Vol. 14 (1958) pp. 138-142.
- Schroeder, M. R., Logan, B. F., and Prestigiacomo, A. J., "New Methods for Speech Analysis—Synthesis and Bandwidth Compression", *Proc. Stockholm Speech Comm. Seminar*, R.I.T., Stockholm, Sweden (Sep 1962).
- Flanagan, J. L. and Golden, R. M., "Phase Vocoder", *BSTJ*, (Nov 1966) pp. 1493-1509.
- Schroeder, M. R., Flanagan, J. L., and Lundry, E. A., "Bandwidth Compression of Speech by Analytic-Signal Rooting", *Proc. IEEE*, Vol. 55, No. 3, (March 1967) pp. 396-401.
- The Random House Dictionary of the English Language* (Random House, Inc., New York; 1967).
- Weaver, D. K., "Design of RC Wideband 90-degree Phase-Difference Network", *Proc. IRE*, Vol. 32 (April 1954) pp. 671-676.
- Bedrosian, S. D., "Normalized Design of 90-degree Phase Difference Networks", *IRE Transactions on Circuit Theory* (June 1960) pp. 128-136.

Engineering and Research Notes



Brief Technical Papers
of Current Interest

Phase-change heat-transfer techniques

B. Shelpuk
Advanced Technology Laboratories
Camden, New Jersey



Temperature control of the Lunar Communication Relay Unit (LCRU) used in the final Apollo missions is accomplished through the use of phase-change heat transfer.

The LCRU operates for 6 hours at a relatively high dissipation rate and then remains inoperative for 14 hours. Because of this cyclic operation, all of the dissipated energy does not have to be rejected as it is generated but can be stored in the thermal mass of the equipment. As long as the heat rejection means of the system is adequate to reject the stored heat during the inoperative period, no cumulative effects occur and the system can be cycled indefinitely.

The thermal storage capacity of the LCRU equipment, which weighs 50 pounds, is 330 Btu or 98 watt hours when the equipment is heated from 90°F to 120°F. By adding 5.75 pounds of phase-change material, the thermal capacity can be raised to over 945 Btu, almost a three-fold increase. Thus, the rate of temperature rise can be cut to 1/3 of its former value.

The key elements to using phase-change material are the selection of appropriate material and application of the packaging techniques required for its effective use. In the LCRU, a temperature limitation of 120°F dictated the temperature at which heat had to be absorbed. Two types of materials which undergo transitions at approximately 120°F are presented in Tables I and II. The first group, listed in Table I, undergoes hydration at this temperature. This process is accompanied by a large heat absorption or rejection, depending on the process. It suffers from difficulty in promoting reversibility and from the corrosive nature of the chemicals required. While this type of material has excellent properties for a phase change heat sink, it requires a modest amount of additional development to assure its successful use. The second group of materials, listed in Table II, undergo a fusion process which is reversible. In addition, the materials in this group are virtually inert and offer a wide latitude in packaging. These materials are hydrocarbons and have heats of fusion of approximately 100 Btu/pound. Other hydrocarbons in this family have similar heat absorbing characteristics with the melting point temperature increasing with the number of carbon atoms. A key factor in achieving the maximum values of heat absorption involves the purity of the material used. As much as 40% of the capacity of the material can be lost by using commercial grades of the material. Highly refined docosane ($C_{22}H_{46}$) or a synthesized version of the same material has been used to achieve performance consistent with the data in the tables. The

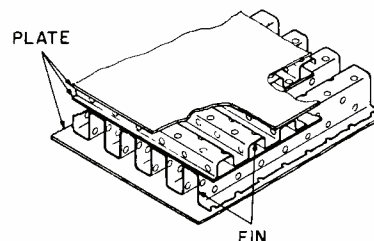


Fig. 1—Brazed aluminum plate fin container structure, sectional view.

final material selected was a mixture of 90% docosane and 10% eicosane.

The second factor bearing on performance is the packaging container. Since the material has low thermal conductivity, large temperature gradients can develop as the hydrocarbon melts. Several techniques to increase conductivity were explored before the brazed aluminum plate fin structure was selected. One technique was the use of metal powder mixed with the hydrocarbon. Another was the use of a honeycomb structure. The brazed-aluminum plate fin structure, shown in Fig 1, provides a high-strength lightweight container for the hydrocarbon material and provides effective thermal paths to all parts of the material.

Table I—Hydrated materials.

Material	Hydration Temperature (°F)	Heat of Hydration (Btu/lb)	Specific Gravity	Remarks
Dibasic Sodium Phosphate ($Na_2HPO_4 \cdot 12H_2O$)	97	120	1.52	Forms protective film against corrosion
Sodium Sulfate ($Na_2SO_4 \cdot 10H_2O$)	88	92	1.464	Used as thermal storage in solar heating
Lithium Bromide ($LiBr \cdot 7H_2O$)	112	78.5	3.46	Used in absorption A/C equipment
Potassium Fluoride ($KF \cdot 2H_2O$)	105	120	2.45	Corrosive and toxic

Extensive testing of a system that uses docosane in a plate fin container has shown that the full thermal capacity of such a system can be realized with a maximum temperature gradient of less than 7°F from the electronic chassis to melting thermal material. Flexibility in geometry and melting temperature make application of this technique to other problems a straightforward matter.

Table II—Fusion materials.

Material	Melting Point (°F)	Heat of Fusion (Btu/lb)	Specific Gravity	Remarks
n-Docosane ($C_{22}H_{46}$)	112	107	0.794	Includes heat of transition at 109°F
n-Octadecane ($C_{18}H_{38}$)	82.4	105	0.782	
n-Nonadecane ($C_{19}H_{40}$)	89.8	80.6	0.785	
n-Eicosane ($C_{20}H_{42}$)	98	106	0.789	

Reprint RE-17-2-22 | Final manuscript received February 2, 1971.

Drilling chip collection

Marvin Novick
Astro-Electronics Division
Princeton, New Jersey



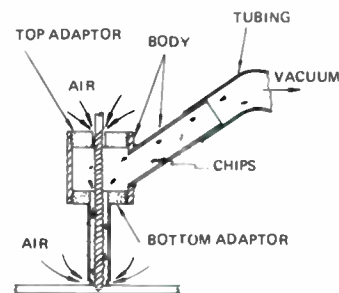
Often in manufacturing, it is necessary to drill during assembly or in a Clean Room environment. Both instances pose the problem of confining the chips.

To resolve this problem, the Astro-Electronics Division has designed a chip collector that allows for drilling, at various stages of assembly and in Clean Room environments, without fear of particle contamination. Fig. 1 illustrates a typical way in which the tool is used.



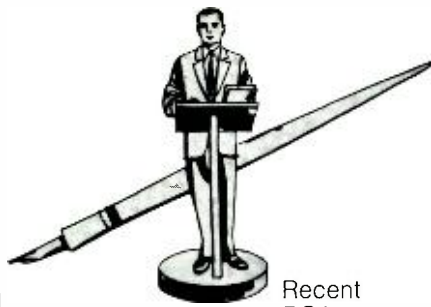
A close-up exploded view of the chip collector, shown in Fig. 2, clearly indicates the simple three-part construction of the tool, which consists of a brass body, a top adaptor, and a bottom adaptor. The adaptors may be fabricated from Delrin, Nylon, Teflon, or other low-friction, abrasive-resistant materials.

Functionally speaking, the chip collector simply confines the drill chips within a given space that is constantly being purged. The velocity of the air used for purging is dependent on the clearance at the top adaptor, the size of the slots at the tip of the bottom adaptor, and the amount of vacuum applied. A cross sectional view (Fig. 3) of the chip collector illustrates the relationship between the air flow and the chips generated during a drilling operation.



In general, there are two usable sources of vacuum for this type operation. One makes use of a central vacuum system, assuming there is sufficient negative pressure available at the inlet; the other employs the use of a transducer to convert shop compressed air to a vacuum. In most cases, the choice of which source to use is a matter of availability and convenience.

Reprint RE-17-2-22 | Final manuscript received April 20, 1971.



Pen and Podium

Recent RCA technical papers and presentations

Both published papers and verbal presentations are indexed. To obtain a published paper, borrow the journal in which it appears from your library, or write or call the author for a reprint. For information on unpublished verbal presentations, write or call the author. (The author's RCA Division appears parenthetically after his name in the subject-index entry.) For additional assistance in locating RCA technical literature, contact: RCA Staff Technical Publications, Bldg. 2-8, RCA, Camden, N.J. (Ext. PC-4018).

This index is prepared from listings provided bimonthly by RCA Division Technical Publications Administrators and Editorial Representatives—who should be contacted concerning errors or omissions (see inside back cover).

Subject index categories are based upon standard announcement categories utilized by Technical Information Systems, Corporate Engineering Services, Bldg 2-8, Camden, N.J.

Subject Index

Titles of papers are permuted where necessary to bring significant keyword(s) to the left for easier scanning. Authors' division appears parenthetically after his name.

SERIES 100 BASIC THEORY & METHODOLOGY

110 Earth & Space Sciences

... geology, geodesy, meteorology, atmospheric physics, astronomy, outer space environment, etc.

VENUS Atmospheric Turbulence on: Venera 4,5,6, and Mariner 5 Estimates—D. A. de Wolf (Labs, Pr) *J. of Geophysical Research*, Vol. 76, No. 13; 5/1/71

125 Physics

... electromagnetic field theory, quantum mechanics, basic particles, plasmas, solid-state, optics, thermodynamics, solid mechanics, fluid mechanics, motion, acoustics, etc.

see also: 110 EARTH & SPACE SCIENCES

205 MATERIALS (ELECTRONIC)

ACOUSTIC PHONON SPECTROMETER, A New—C. H. Anderson, E. S. Sabisky (Labs, Pr) *J. of Acoustical Society of America, Memorial Issue*, Vol. 49, No. 3, Part 3; 3/71

ELECTRON TRAJECTORIES in Television Camera Tubes, Computer Calculation of—O. H. Schade, Sr., (EC, Harsn) *RCA Review*; 3/71

LOW-FIELD ACOUSTOELECTRIC INTERACTION and Thermal Brillouin Scattering—R. W. Smith (Labs, Pr) *J. of Acoustical Society of America, Memorial Issue*, Vol. 49, No. 3; Part 3; 3/71

130 Mathematics

... basic & applied mathematical methods

see also: 140 CIRCUIT & NETWORK THEORY
370 COMPUTER PROGRAMS (SCIENTIFIC)

NON-LINEAR DIFFERENTIAL GAMES, Computational Algorithms for Optimal Solution of—W. Gaskell (M&SR, Mrstn) Ph.D. Thesis, University of Penn; 5/71

140 Circuit & Network Theory

... methods for circuit synthesis & analysis; network topology; matrix analysis applied to circuits; equivalent circuit methods; etc.

(for specific circuit applications, see the appropriate 200-series category)

CONTINUOUS NONLINEAR SYSTEMS with Discrete Nonlinear Observations—G. Sparks (M&SR, Mrstn) 14th Midwest Symp. on Circuit Theory, Denver, Colorado; 5/6-7/71

MULTI-DIMENSIONAL ANALOG DEMODULATION—A. E. Smith (M&SR, Mrstn) Thesis. Univ. of Penn; 4/16/70

160 Laboratory Techniques & Equipment

... experimental methods & equipment, lab facilities, testing, data measurement, spectroscopy, electron microscopy, dosimeters, etc.

ATOMIC ABSORPTION SPECTROPHOTOMETRY, Determination of Dopants (In, Ag, and Cu) in Single Crystal CdCr₂S₄ and CdCr₂Se₄, by—K. Ametani, F. Okamoto, T. Oka (Labs, Pr) 33rd Annual Conf. of the Japanese Society for Analytical Chemistry; 6/5-6/71

ELLIPSOMETRY and Its Use in the Measurement and Control of Dielectric Films, A Review of—A. N. Saxena (Labs, Pr) Electrochemical Soc. Mtg., Washington, D.C.; 5/9-14/71

MASS SPECTROSCOPY to the Analysis of Solids: A Review, Application of—R. E. Honig (Labs, Pr) Proc. of the Int'l Conf. on Mass Spectroscopy, Kyoto, Japan, Univ. of Tokyo Press, 1970

MODULATED WAVELENGTH OPTICAL MONITORING of Thin Film Deposition—H. O. Hook (Labs, Pr) AVS Symp., David Sarnoff Research Center, Princeton, N.J.; 5/20/71

SCANNING ELECTRON MICROSCOPY Techniques—E. R. Levin (Labs, Pr) 4th Annual Failure Analysis Seminar, Univ. of Penn, Philadelphia, Pa.; 5/20/71

X-RAY SPECTROMETRIC ANALYSIS, Principles and Practice of—E. P. Bertin (Labs, Pr) Seminar on X-Ray Spectrometry, Stevens Institute of Technology, Hoboken, N.J.; 6/1/71

170 Manufacturing & Fabrication

... production techniques for materials, devices, & equipment
see also: 175 RELIABILITY, QUALITY, CONTROL, & STANDARDIZATION

MICROELECTRONICS PROCESSING, ADVANCED, Diffusion Technology for—W. Grieg, K. Cunniff, H. M. Hyman, S. Muller (SSD, Som) Proc. of the Symp. on Silicon Device Processing; 6/70

175 Reliability, Quality Control, & Standardization

... value analysis, reliability analysis, standards for design & production, etc.
see also: 170 MANUFACTURING & FABRICATION
325 CHECKOUT, MAINTENANCE, & USER SUPPORT

INTEGRATED CIRCUIT DEVICE RELIABILITY, The Achievement of—G. F. Granger (SSD, Som) 4th Annual Failure Analysis Seminar & Proc., 5/20/71

LONG-DURATION MISSION RELIABILITY, The Multiprocessing Computer—Answer to—M. L. Johnson (ASD, Burl) ASQC All Day Conf. and Technical Exhibit on Quality Control and Reliability, Seattle, Washington; 6/29/71

QUALITY Gap—Communications—S. Price (M&SR, Mrstn) ASQC Meeting; Pennsauken, N.J.; 5/13/71

RELIABILITY Data Base—R. Killion (M&SR, Mrstn) ASQC Reliability Seminar—Leeds & Northrup Tech. Center, North Wales, Pa.; 5/26/71

SESSION MODERATOR and Technical Program Chairman—W. J. Gray (ASD, Burl) Boston Spring IEEE Reliability Conf.; Lynnfield, Mass.; 4/29/71

VECP GROWTH, A Program for—S. Robinson (M&SR, Mrstn) Nat'l Conf., Society of Amer. Value Engrs. Miami, Fla.; 5/24-26/71

180 Management & Business Operations

... organization, scheduling, marketing, etc.

CONFIGURATION MANAGEMENT for the American Institute of Industrial Engineers, Workshop Seminar on Industry—J. E. Finnegan (M&SR, Mrstn); 4/20/71

PROGRAM MANAGEMENT Check List—R. D. Black (M&SR, Mrstn) Vol. 1—Management Check Lists; 4/71; Spartan Books

SYSTEMS ANALYSIS & the Computer for Business Planning & Management Problem Solving, Using Modern—M. Buckley (M&SR, Mrstn) South Jersey AIEE Group; Silver Lake Inn; 4/20/71

UNFAIR COMPETITION—Trade Secrets—Enforcement of Licensing Agreements—I. Krittman (Labs, Pr) *Seton Hall Law Review*, Vol. 2, No. 2; Spring 1971

SERIES 200 MATERIALS, DEVICES, & COMPONENTS

205 Materials (Electronic)

... preparation & properties of conductors, semiconductors, superconductors, magnetics, electro-optics, etc.

see also: 125 PHYSICS
160 LABORATORY TECHNIQUES & EQUIPMENT
170 MANUFACTURING & FABRICATION

Ca in the (Cs)Na₂K₂Sb (S-20 Multialkali Photocathode, The Role of—W. H. McCarroll, R. J. Paff, A. H. Sommer (EC, PR) *J. of Applied Physics* 2/71

CARBON MONOFILAMENT as Substrate for CVD Filaments—R. M. Mehalso, R. J. Diefendorf (Labs, Pr) 10th Biennial Int'l Conf. on Carbon, Bethlehem, Pa.; 6/27-7/20/71

CERAMIC MATERIALS as Substrates for Epitaxial Semiconductor Devices, The Use of—C. C. Wang (Labs, Pr) Electrochemical Society Mtg., Washington, D.C.; 5/9-14/71

CuCr₂V₂S₄ SPINELS, NMR of—S. B. Berger, T. J. Burch, J. I. Budnick, L. Darcy (Labs, Pr) *J. of Applied Physics*, Vol. 42, No. 4; 3/15/71

ELECTROLESS PLATING BATHS and the Mechanism of Electroless Nickel Plating, A New Technique for Investigating the Electrochemical Behavior of—N. Feldstein, T. C. Lancsek (Labs, Pr) Institute of Metal Finishing, Brighton, England; 5/25/71

F CENTER, Stress Parameters of the—R. C. Alig (Labs, Pr) *Crystal Lattice Defects*, Vol. 2; 1971

FERRITES, Relation Between Fundamentals and Properties of—I. Gordon (Labs, Pr) Midwest Electronics Materials Symp., Notre Dame Univ., South Bend, Indiana; 6/4/71

FILM PROPERTIES by RF Sputtering Techniques, Control of—J. L. Vossen (Labs, Pr) American Vacuum Society Symp. on New Developments in Film and Device Fabrication, Yorktown Heights, New York; 5/18/71

FLAME FUSION, FLUX, AND CZOCHRALSKI SPINEL, A Comparison of the Hole Mobility and Early Growth of Epitaxial Silicon on—G. W. Cullen, C. C. Wang (Labs, Pr) *J. of the Electrochemical Soc.* Vol. 118, No. 4; 4/71

GaAs-Al_xGa_{1-x}As OPTOELECTRONIC COLD-CATHODE STRUCTURES, Efficient Electron Emission from—H. Schade, H. Nelson (Labs, Pr) *Applied Physics Letters*, Vol. 18, No. 10; 5/15/71

GaN, Electroluminescence in—J. I. Pankove, E. A. Miller, D. Richman, J. E. Berkeyheiser (Labs, Pr) Device Research Conf., Univ. of Michigan; 6/28-7/1/71

GaP, On the Czochralski Growth of—E. A. Miller, L. R. Weisberg, W. K. Liebmann (Labs, Pr) *J. of the Electrochemical Society*, Vol. 118, No. 5; 1971

GRANULAR FILMS, Superconducting and Semiconducting Phases of—B. Ables, J. J. Hanak (Labs, Pr) *Physics Letters*, Vol. 34A, No. 3; 2/22/71

GROUP IV and III-V SEMICONDUCTORS, On the Ground State Energy of Free Excitons in—W. Czaja (Labs, Pr) *Physik der kondensierten Materie*, Vol. 12, 1971

LIQUID CRYSTALS, Electro-Optic Properties of—J. A. Castellano (Labs, Pr) 21st Electronic Components Conf., Washington, D.C.; 5/10-12/71

LIQUID CRYSTALS V. Nematic Materials Derived from p-Alkylcarbonato-p' Alkoxyphenyl Benzoates—J. A. Castellano, M. T. McCaffrey, J. E. Goldmacher (Labs, Pr) Molecular Crystals and Liquid Crystals, Vol. 12; 1971

LIQUID HELIUM, Acoustic Interference in Thin Films of—E. S. Sabisky (Labs, Pr) Physics Colloquium, Polytechnic Institute of Brooklyn; 5/6/71

LIQUID HELIUM, Phonon Interference in Thin Films of—C. H. Anderson (Labs, Pr) Colloquia, Harvard University, Cambridge, Mass.; 5/5/71

LIQUID HELIUM, Phonon Interference in Thin Films of—C. H. Anderson (Labs, Pr) Colloquia, Rutgers University, New Brunswick, N.J.; 5/11/71

M-NITROANILINE, Anomalous High Nonlinear Optical Effects in—P. D. Southgate, D. S. Hall (Labs, Pr) *Applied Physics Letters*, Vol. 18, No. 10; 5/15/71

MAGNETOSTRICTIVE FILMS, Dispersion Effects in—H. Kurlansik, L. Onyskevych (Labs, Pr) *J. of Applied Physics*, Vol. 42, No. 4; 3/15/71

MnF₂, Excited State Exchange in—S. Freeman (Labs, Pr) *J. of Applied Physics*, Vol. 42, No. 4; 3/15/71

NEMATIC LIQUID CRYSTALS, Light Scattering from Electric-Field Driven—L. Goodman (Labs, Pr) Society for Information Display Symp., Phila., Pa.; 5/4-6/71

NEMATIC LIQUID CRYSTALS, A Simplified Electrophydrodynamic Treatment of Threshold Effects in—G. H. Heilmeyer (Labs, Pr) Proc. of the IEEE, Vol. 59, No. 3; 3/71

NEW RED-EMITTING INFRARED-EXCITED PHOSPHORS, Y₂O₃:Yb, Er, and Gd₂O₃:Yb, Er—I. Ladany, P. N. Yocom, J. P. Wittke (Labs, Pr) Electrochemical Society Meeting, Washington, D.C.; 5/9-14/71

P-N JUNCTION ELECTROLUMINESCENCE, Zone-Leveled In_{0.5}Ga_{0.5}P for—L. Kudman, C. J. Nuese (Labs, Pr) Electrochemical Society Meeting, Washington, D.C.; 5/9-14/71

PHOTOCONDUCTANCE IN CdCr₂Se₄, Spectral Dependence of the—A. Amith, S. B. Berger (Labs, Pr) *J. of Applied Physics*, Vol. 42, No. 4; 3/15/71

PHOTORESIST ADHESION—The Characterization of Photoresists by Determination of the Critical Surface Tension for Spreading—E. B. Davidson (Labs, Pr) Electrochemical Society Mtg., Washington, D.C.; 5/9-14/71

PLASMA-GROWN Al₂O₃ FILMS ON SILICON Using X-Ray Diffraction, Stress Analysis of—F. B. Michelletti, S. H. McFarlane (Labs, Pr) Electrochemical Society Mtg., Washington, D.C.; 5/9-14/71

PLASMA-GROWN Al₂O₃ FILMS, Properties of—P. E. Norris (Labs, Pr) Electrochemical Society Meeting, Washington, D.C.; 5/9-14/71

PULSED LIQUID CRYSTAL CELLS, On the Transient Scattering of Light by—L. S. Cosentino (Labs, Pr) Soc. for Information Display Symp. Philadelphia, Pa.; 5/4-6/71

SEMICONDUCTING MONOTRIDES of Sc, Y, and the Rare Earth Elements, Vapor Deposition of—J. P. Dismukes, W. M. Yim, J. J. Tietjen (Labs, Pr) *J. of Crystal Growth*, Vol. 9; 1971

SEMICONDUCTOR SURFACE CONTAMINATION III Radiochemical Study of Deposition of Trace Impurities on Germanium and Gallium Arsenide—W. Kern (Labs, Pr) *RCA Review*, Vol. 32, No. 1; 3/71

SILICON with Chlorine, Gas-Phase Etching of—J. P. Dismukes, R. Ulmer (Labs, Pr) *J. of the Electrochemical Society*, Vol. 118, No. 4; 4/71

STOICHIOMETRIC MAGNESIUM ALUMINATE SPINEL SINGLE CRYSTALS, Dielectric and Optical Properties of—C. C. Wang, P. J. Zanzucchi (Labs, Pr) *J. of the Electrochemical Society*, Vol. 118, No. 4; 4/71

TUNGSTEN FILMS for Microelectronic Devices, Electrochemical Delineation of—W. Kern, J. M. Shaw (Labs, Pr) Electrochemical Society Meeting, Washington, D.C.; 5/9-14/71

VAPOR DEPOSITED AIs, Properties of—A. G. Sigai (Labs, Pr) Electrochemical Society Mtg., Washington, D.C.; 5/9-14/71

Y₂O₃ by Tb, Intensification of Sm³⁺, Yb³⁺, and Eu³⁺ Emission in—P. N. Yocom, R. E. Shrader, M. R. Royce (Labs, Pr) Electrochemical Society Mtg., Washington, D.C.; 9/9-14/71

210 Circuit Devices & Microcircuits

... electron tubes & solid-state devices (active & passive); integrated, array, & hybrid microcircuits; molecular circuits; resistors & capacitors; modular & printed circuits; circuit interconnection; waveguides & transmission lines; etc.

see also: 205 MATERIALS (ELECTRONIC) 215 CIRCUIT & NETWORK DESIGNS 140 CIRCUIT & NETWORK THEORY

Ag-O-Cs (S-1) PHOTOCATHODE, The Relationship Between Photoelectric and Secondary Electron Emission, with Special Reference to the—A. H. Sommer (EC, Pr) *J. of Applied Physics*; 2/71

AVALANCHE DIODES, Anti-Parallel Pair of High-Efficiency—H. Kawamoto, S. G. Liu (Labs, Pr) *Proc. of the IEEE*, Vol. 59, No. 3; 3/71

CHARGE-COUPLED DEVICES with Strong Drift-Aiding Fringing Fields, Free Charge Transfer in—J. E. Carnes, W. F. Kosonocky, E. G. Ramberg (Labs, Pr) 1971 Device Research Conf., Univ. of Michigan, Ann Arbor, Michigan; 6/28-7/1/71

COLOR PICTURE TUBES 110° and Deflecting Yoke, Development and Performance of the RCA 19V and 18V—W. D. Masterton, R. L. Barbin (EC, Lanc) *Electronics Magazine*; 4/71

DIELECTRIC FILMS in Monolithic Integrated Circuit Technology—K. H. Zaininger (Labs, Pr) Electrochemical Soc. Mtg., Washington, D.C.; 5/9-14/71

FERRITE-DIODE LIMITER, A Hundred-Kilowatt X-Band—W. W. Siekanowica, R. W. Paglione, R. Steinhoff (EC, Pr) Int'l Symp. on Microwave Theory & Techniques; 5/71

GALLIUM ARSENIDE FIELD-EFFECT PHOTOTRANSISTOR, A New Type of—G. A. Swartz, A. Gonzalez, A. Dreeben (Labs, Pr) *RCA Review*, Vol. 32, No. 1; 3/71

HELICAL DISLOCATIONS in Semiconductors, The Formation and Elimination of—M. S. Abrahams, J. Blanc, C. J. Buicocchi (Labs, Pr) *Philosophical Magazine*, Vol. 23, No. 183, 4/71

HIGH POWER RF TRANSISTORS, Recent Development in—H. C. Lee (SSD, Som) Petroleum Industry Electrical Association & Petroleum Electrical Supply Association Conf., 4/20/71

HYPER-ABRUPT TUNING DIODES, Design Considerations of—P. J. Kannan, S. Ponczak, J. Olmstead (SSD, Som) IEEE Electron Devices; 2/71

KINESCOPE, Molecular Gas Flow in—J. C. Turnbull (EC, Lanc) Int'l Symp. on Residual Gases in Electron Tubes, Italy; 4/14/71

MOS COMPLEMENTAIRE, Les Circuits Integres De Technologie—R. Griffin (SSD, Sunbury) Destines A L'Industrie Horlogere, French & German Industry Conf., Grenoble; 6/11-13/71

MOS IC's in Linear Circuit Application—S. Reich (SSD, Som) EEE Paris Seminar 3/30-4/2/71; EEE Seminar Integrated Circuits; 3/22-25/71

PHOTOCONDUCTIVE DETECTOR for 10.6 μm, A Packaged System of a, Solid-State Microwave-Biased—C. Sun, T. E. Walsh (EC, Pr) *Proc. of the IEEE*; 10/70

RECTIFIER, Transcatal (Silicon Power)—R. M. McKechnie, S. W. Kessler (EC, Lanc) 2nd IEEE Power Conditioning Specialists Conf., 4/19-20/71

RETURN BEAM VIDICON with Electrical Input, The High Resolution—M. J. Cantella (ASD, Burl) Chapter 18: Vol. II: *Photoelectronic Imaging Devices*; Plenum Publishing Corp, New York; 4/71

SILICON-ON-SAPPHIRE: The Optimum Technology for MOS Digital Circuits—E. J. Boleky (Labs, Pr) IEEE High Speed Circuits Workshop, Denver, Colorado, 5/20-21/71

THERMAL SWITCHING in an Avalanche Diode, Stroboscopic Investigation of—R. A. Sunshine, M. A. Lampert (Labs, Pr) *Applied Physics Letters*, Vol. 18, No. 10; 5/15/71

TRANSFERRED ELECTRON DEVICES, Wideband Microwave Amplification Using—B. S. Perlman (EC, Pr) IEEE Conv.; 3/22-25/71

TRANSFERRED-ELECTRON DEVICES in Prototype Filter Equalization Networks, Microwave Amplification Using—B. S. Perlman (EC, Pr) *RCA Review*; 3/71

TRANSFERRED ELECTRON OSCILLATORS, Microwave Circuits for High Effi-

ciency Operation of—J. T. Reynolds, B. E. Berson, R. E. Enstrom (EC, Pr) *IEEE Trans. on Microwave Theory and Techniques*; 1/71

215 Circuit & Network Designs ... analog & digital functions in electronic equipment; amplifiers, filters, modulators, modems, a-d converters, encoders, oscillators, switches, etc.; logic & switching networks; masers & microwave circuits; timing & control functions: fluidic circuits

see also: 210 CIRCUIT DEVICES & MICROCIRCUITS 225 ANTENNAS & PROPAGATION 140 CIRCUIT & NETWORK THEORY

ACOUSTIC SURFACE WAVE FREQUENCY GENERATORS & Matched Filters with Adjustable Taps—D. Gandolfo (EASD, Calif) IEEE/SMIT Microwave Symp., Washington, D.C.; 5/17-19/71; Symp. Proc.

BIPOLAR MEMORIES, High Speed—R. A. Bishop (SSD, Sunbury) Man Made Memory Conf., London; 3/22/71

COS/MOS MEMORIES—R. A. Bishop (SSD, Sunbury) Man Made Memory Conf., London; 3/22/71

COS/MOS RANDOM ACCESS MEMORIES—H. S. Miller (SSD, Som) Man-made Memories Conf., England; 3/30/71

COS/MOS TECHNOLOGY, Advantages of Logic Implementation Using—R. Griffin (SSD, Sunbury) Int'l Electronic Components Exhibition, Paris; 3/31-4/6/71

CW POWER MODULE for Phased Arrays, S-Band—E. Belohoubek (EC, Pr) *Micro-wave Journal*; 2/71

EPITAXIAL GaAs TRAVELING-WAVE AMPLIFIER: Properties and Modulation Capabilities—R. H. Dean (Labs, Pr) 1971 Device Research Conf., University of Michigan, Ann Arbor, Michigan; 6/28-7/1/71

HIGH-SPEED COUNTER, An Efficient—A. T. Turecki (CS, Fla) *Computer Design*; 8/71

HYBRID POWER SERIES REGULATOR, Design Considerations for a—R. M. Engler, W. R. Peterson (SSD, Som) Electronic Components Conf., 5/10-12/71

IF SUBSYSTEM for Color and B&W TV Receivers, A Completely Integrated—S. Reich, R. T. Peterson (SSD, Som) IEEE Conf. and Record; 3/22-25/71

IMPACT DIODE OSCILLATORS, A Simple and Direct Accounting for the Noise in—H. Johnson, B. B. Robinson (Labs, Pr) 1971 Device Research Conf., Univ. of Michigan, Ann Arbor, Michigan; 6/28-7/1/71

MICROSTRIP AMPLIFIERS Can be Simple to Design—G. D. O'Clock (EASD, Calif) *Electronic Design*; 7/8/71; Vol. 19, No. 14

MICROWAVE AMPLIFIER Using Anti-Parallel Avalanche-Diode Pair, High-Power—H. Kawamoto (Labs, Pr) IEEE G-MTT Int'l Microwave Symp., Washington, D.C.; 5/17-20/71

MICROWAVE INTEGRATED CIRCUITS—H. Sobol (Labs, Pr) 1971 European Microwave Conf., Royal Institute of Technology, Stockholm, Sweden; 8/23-28/71; 1971 National Electronics Conf. Chicago, Ill.; 10/18-20/71

POWER SUPPLY PROTECTION Techniques—F. C. Easter (EASD, Calif) 14th Midwest Symp. on Circuit Theory, Univ. of Denver; 5/6-7/71; Symp. Proc.

SEMICONDUCTOR MEMORIES, High Speed and Low Power—A. Bishop (SSD, Sunbury) Munich Int'l Seminar on Memories; 6/7/71

TRANSCONDUCTANCE AMPLIFIERS—L. Avery (SSD, Sunbury) Paris Components Show; 3-4/71

VIDEO AMPLIFIER, Hybrid Microelectric—L. J. Thorpe (CSD, Camden) Montreux Int'l Symp., Montreux, Switzerland; 5/21

225 Antennas & Propagation

... antenna design & performance; feeds & couplers; phased arrays; radomes & antenna structures; electromagnetic wave propagation; scatter; effects of noise & interference

see also: 320 RADAR, SONAR, & TRACKING SYSTEMS

WIDEBAND SCATTERING ANALYSIS, A New Method—S. Sherman, C. Campopiano (M&SR, Mrstn) URSI Spring Meeting, Washington, D.C.; 4/8-10/71

240 Lasers & Related Electro-optical Components

... design & characteristics of lasers; components used with lasers in electro-optical systems (excludes: masers)

see also: 205 MATERIALS (ELECTRONIC) 210 CIRCUIT DEVICES & MICROCIRCUITS 215 CIRCUIT & NETWORK DESIGNS 245 DISPLAYS

ARGON LASER AMPLIFIERS and Oscillators, A Comparative Analytical Study of the Performance of—I. Gorog (Labs, Pr) *RCA Review*, Vol. 32, No. 1; 3/71

FIELD-EMITTER ARRAY, Analysis and Optimization of a—J. D. Levine (Labs, Pr) *RCA Review*, Vol. 32, No. 1; 3/71

He-Cd LASERS Using Re-Circulation Geometry—K. Hernqvist (Labs, Pr) 1971 IEEE/OEA Conference on Laser Engineering and Applications, Washington, D.C.; 6/2-4/71

GaAs INJECTION LASER ARRAYS, High Average Power—P. Nyul, A. Limm (SSD, Som) Electro-Optical Int'l Conf., England; 3/23-25/71

GaAs LASER and Non-Coherent (Re-Emitting) Diodes, Technology and Design of—R. Glicksman (SSD, Som) *Solid State Technology*; 9-10/71

GaAs TRANSFERRED-ELECTRON DEVICES, CW Microwave Amplification from Circuit-Stabilized Epitaxial—B. S. Perlman (EC, Pr) *Solid-State Circuits*; 12/70

HIGH-POWER DIODE Fabricated by Novel Techniques, Small Area—K. P. Weller, C. P. Wen (Labs, Pr) 1971 Device Research Conf., Univ. of Michigan, Ann Arbor, Michigan; 6/28-7/1/71

HOLOGRAPHIC STORAGE APPLICATIONS, Improved Electro-Optic Materials for—J. J. Amodei, W. Phillips, D. L. Staebler (Labs, Pr) 1971 IEEE/OEA Conf. on Laser Engineering and Applications, Washington, D.C.; 6/2-4/71

IR COVERT ILLUMINATORS, Effectiveness of—F. J. Gardiner (ASD, Burl) Electro-Optical Systems Design Conf. and Exhibition for Western America; Anaheim, Calif.; 5/18-20/71

IR EMITTING LASING AND NON-LASING DIODES, Characteristics and Applications of—R. Glicksman (SSD, Som) Cleveland Electronics Conf. (CECON '71); 4/13-15/71

ISOELECTRONIC TRAP NITROGEN IN GaP, A New Quasiparticle Bound to the—W. Czaja, K. Krausbauer, B. J. Curtis (Labs, Pr) *Solid State Communications*, Vol. 8, No. 14; 1971

LIGHT VALVE DEVICES, System Techniques for Overcoming Material Limitations in—G. W. Taylor (Labs, Pr) Society for Information Display Symp., Philadelphia, Pa.; 5/4-6/71

LIQUID CRYSTAL MATRIX Displays—J. van Raalte (Labs, Pr) Panel Discussion on Matrix Displays, SID, Philadelphia, Pa.; 5/4-6/71

SATURABLE EMISSION: The Cause of Broad Beams in Injection Lasers—H. S. Sommers, Jr., D. O. North (Labs, Pr) 1971 Device Research Conf., Univ. of Michigan, Ann Arbor, Michigan; 6/28-7/1/71

245 Displays

... equipment for the display of graphic, alphanumeric, & other data in communications, computer, military, & other systems; CRT devices, solid state displays, holographic displays, etc. (excludes: television)

see also: 205 MATERIALS (ELECTRONIC) 345 TELEVISION & BROADCAST SYSTEMS

GRAPHIC INFORMATION DISTRIBUTION SYSTEM TERMINAL, An Experimental Low Cost—I. Gorog, P. M. Heyman, H. K. Kim, M. D. Lippman (Labs, Pr) Soc. for Information Display Symp., Philadelphia, Pa.; 5/4-6/71

IMAGERY Simulation of ERTS [Earth Resources Technology Satellite] RBV [Return Beam Vidicon]—B. P. Miller, J. M. Barletta, O. Weinstein (AED, Pr) Remote Sensing Mtg., Proc.; Univ. of Michigan; 5/19/71

250 Recording Components & Equipment

... tape, disk, drum, film, holographic, & other assemblies for audio, image, & data systems; magnetic tape, tape heads, pickup devices, etc.

see also: 360 COMPUTER EQUIPMENT 345 TELEVISION & BROADCAST SYSTEMS

BISMUTH TITANATE FE-PC Optical Storage Medium—Further Developments—S. A. Keneman, G. W. Taylor, A. Miller (Labs, Pr) IEEE Symp. on the Applications of Ferroelectrics, IBM, Yorktown Heights, N.Y.; 6/7-8/71

ELECTRO-OPTIC CRYSTALS, Holographic Fixing in—D. L. Staebler, J. J. Amodei (Labs, Pr) IEEE Symp. on Applications of Ferroelectrics, IBM, Yorktown Heights, N.Y.; 6/7-8/71

ELECTRONIC IMAGE STORAGE Utilizing a Silicon Dioxide Target—R. S. Silver, E. Luedicke (Labs, Pr) IEEE Trans. on Electron Devices, Vol. ED-18, No. 4; 4/71

ELECTRONIC MUSIC SYNTHESIS for Recordings—H. F. Olson (Labs, Pr) IEEE Spectrum, Vol. 8, No. 3; 4/71

MOTION PICTURE LOOPING SYSTEMS, Computer Techniques as Applied to—D. R. Brewer (CSD, Camden) SMPTE, Los Angeles, Calif.; J. of the SMPTE: 6/71

X-RAY IMAGES, Contrast Characteristics of—I. P. Csorba (EC, Lanc) RCA Review; 3/71

280 Thermal Components & Equipment

... heating & cooling components & equipment; thermal measurement devices; heat sinks & thermal protection designs; etc.

FUSIBLE PHASE-CHANGE TEMPERATURE CONTROL for Modern Packaging Design—B. Watson (M&SR, Mrstn) IEEE Conf. Hilton Hotel, Washington, D.C.; 5/8-10/71

SERIES 300 SYSTEMS, EQUIPMENT & APPLICATIONS

305 Aircraft & Ground Support ... airborne instruments, flight control systems, air traffic control, etc.

OBSTACLE WARNING SYSTEMS for Helicopters, Miniature—H. C. Eckhardt (ASD, Burl) J. of the American Helicopter Soc.; Vol. 16, No. 2; 4/71; pages 10-16

WEATHER RADAR for General Aviation, A New—G. C. Jung (EASD, Calif) Microwave Symp., Washington, D.C.; 5/17/71; Digest of Symp. Papers

315 Military Weapons & Logistics

... missiles, command & control, etc.

see also: 325 CHECKOUT, MAINTENANCE, & USER SUPPORT 320 RADAR, SONAR, & TRACKING SYSTEMS

SYSTEMS FUNCTION, Advanced Planning for the—F. P. Congdon (ASD, Burl) J. of Systems Management; 8/70

320 Radar, Sonar, & Tracking Systems

... microwave, optical, acoustic, & other techniques for detection, acquisition, tracking, & position location

see also: 305 AIRCRAFT & GROUND SUPPORT 225 ANTENNAS & PROPAGATION

E-O COUNTERMEASURES, Intercept Receiver Requirements for—H. Wetzstein (ASD, Burl) Electro-Optical Systems Design Conf. and Exhibition for Western America; Anaheim, Calif.; 5/18-20/71

325 Checkout, Maintenance, & User Support

... automatic test equipment, maintenance & repair methods, installation & user support, etc.

see also: 175 RELIABILITY, QUALITY CONTROL, & STANDARDIZATION

AUTOMATIC TEST SYSTEMS—Dedicated or Integrated—A. M. Greenspan (ASD, Burl) Electrical Engineering Measurements and Test Instrumentation Conf., Ottawa, Ontario; 7/1-3/71

TEST-DATA ACQUISITION AND PROCESSING SYSTEM, RUDI—A Computer-Controlled—R. Herrmann, B. Mangolds (AED, Pr) IEEE 1971 Electrical & Electronic Measurement & Test Instrument Conf.; Ottawa, Ont.; 6/1-3/71

345 Television & Broadcast Systems

... television & radio broadcasting, receivers, transmitters, & systems; television cameras, recorders, & other studio equipment; closed circuit, spacecraft, & special-purpose television

see also: 210 CIRCUIT DEVICES & MICROCIRCUITS 250 RECORDING COMPONENTS & EQUIPMENT

TELEVISION EQUIPMENT, Development of—E. G. Ramberg (Labs, Pr) Encyclopedia Americana, pp. 445-449; 1971

360 Computer Equipment

... processors, memories, & peripherals

see also: 370 COMPUTER PROGRAMS (SCIENTIFIC) 250 RECORDING COMPONENTS & EQUIPMENT

HIGH SPEED COMPUTER APPLICATIONS, A Case History—Combining Wire Wrap and Stripline Multilayer Board for—S. Patrakis, J. Furnstahl (ASD, Burl) Electronic Components Conf. Washington, D.C.; 5/10-12/71

OPTICAL MEMORIES, Ferroelectric Light Valve Arrays for—G. W. Taylor, W. F. Kosonocky (Labs, Pr) IEEE Symp. on the Applications of Ferroelectrics, IBM, Yorktown Heights, N.Y.; 6/7-8/71

SYSTEMS DESIGN Considerations—L. C. Kaye (ASD, Burl) 1971 Computer Designs Conf., Anaheim, Calif.; 1/19-21/71; 1971 Computer Designers Conf. Proc.; pages 444-450

370 Computer Programs (Scientific)

... specific programs & techniques for scientific use; computation, simulation, computer aided design, etc.; (entries in this category generally consist of program documentation, listings, use instructions, decks, or tapes)

see also: 370 COMPUTER PROGRAMS (SCIENTIFIC) 360 COMPUTER EQUIPMENT

FORTRAN TRANSLATOR, A Decision Table for—B. J. Gulledge (CS, Fla) ACM Southeastern Regional Conf., Mobile, Alabama; 6/18/71

REAL-TIME DATA PROCESSING Software for Instrumentation Radars—E. Crenshaw, W. T. Vollmer, S. Steele (M&SR, Mrstn) I.S.A. Aerospace Instrum. Symp.; 5/10-12/71

STORAGE UTILIZATION in a Memory Hierarchy when Storage Assignment is Performed by a Hasing Algorithm—J. G. Williams (Labs, Pr) Communications of the ACM, Vol. 14, No. 3; 3/71

380 Graphic Arts & Documentation

... printing, photography, & typesetting; writing, editing, & publishing; information storage, retrieval, & library science; reprography & microstorage

COST-COMPETITIVE AUTOMATION, The Search by One Publication for—D. B. Dobson (ASD, Burl) J. of Technical Writing and Communication; Vol. 1 (2) 4/71; Pages 155-160

Author Index

Subject listed opposite each author's name indicates where complete citation to his paper may be found in the subject index. An author may have more than one paper for each subject category.

Astro-Electronics Division

Barletta, J. M. 245
Herrmann, R. 325
Mangolds, B. 325
Miller, B. P. 245
Weinstein, O. 245

Aerospace Systems Division

Cantella, M. J. 210
Congdon, F. P. 315
Dobson, D. B. 380
Eckhardt, H. C. 305
Furnstahl, J. 360
Gardner, F. J. 240
Gray, W. J. 175
Greenspan, A. M. 325
Johnson, M. L. 175
Kaye, L. C. 360
Patrikis, S. 360
Wetzstein, H. 320

Computer Systems

Gulledge, B. J. 365
Turecki, A. T. 215

Communications Systems Division

Brewer, D. R. 250
Thorpe, L. J. 215

Electromagnetic and Aviation Systems Division

Easter, F. C. 215
Gandolfo, D. 215
Jung, G. C. 305
O'Clock, G. D. 215

Electronic Components

Barbin, R. L. 210
Belohoubek, E. 215
Berson, B. E. 210
Csorba, I. P. 250
Enstrom, R. E. 210
Kessler, S. W. 210
Masterton, W. D. 210
McCarroll, W. H. 205
McKechnie, R. M. 210
Paff, R. J. 205
Paglione, R. W. 210
Perlman, B. S. 210
Perlman, B. S. 240
Reynolds, J. T. 210
Schade, Sr., O. H. 125
Siekanowica, W. W., 210
Sommer, A. H. 205
Sommer, A. H. 210
Steinhoff, R. 210
Sun, C. 210
Turnbull, J. C. 210
Walsh, T. E. 210

RCA Laboratories

Ables, B. 205
Abrahams, M. S. 210
Allig, R. C. 205
Ametani, K. 160
Amith, A. 205
Amodei, J. J. 240
Amodei, J. J. 250
Anderson, C. H. 125
Anderson, C. H. 205
Berger, S. B. 205
Berkeyheiser, J. E. 205
Bertin, E. P. 160
Blanc, J. 210
Boleky, E. J. 210
Budnick, J. I. 205
Buiochi, C. J. 210
Burch, T. J. 205
Carnes, J. E. 210
Castellano, J. A. 205
Cosentino, L. S. 205
Cullen, G. W. 205
Curtis, B. J. 240
Czaja, W. 205
Czaja, W. 240
Darcy, L. 205
Davidson, E. B. 205
Dean, R. H. 215
de Wolf, D. A. 110
Diefendorf, R. J. 205
Dismukes, J. P. 205
Dreeben, A. 210
Feldstein, N. 205
Freeman, S. 205
Goldmacher, J. E. 205
Gonzalez, A. 210
Goodman, L. 205

Gordon, I. 205
Gorog, I. 240
Gorog, I. 245
Hall, D. S. 205
Hanak, J. J. 205
Heilmeyer, G. H. 205
Hernqvist, K. 240
Heyman, P. M. 245
Honig, R. E. 160
Hook, H. O. 160
Johnson, H. 215
Kawamoto, H. 210
Kawamoto, H. 215
Keneman, S. A. 250
Kern, W. 205
Kim, H. K. 245
Kosonocky, W. F. 210
Kosonocky, W. F. 360
Krausbauer, L. 240
Krittman, I. 180
Kudman, I. 205
Kurfanski, H. 205
Ladany, I. 205
Lampert, M. A. 210
Lancsek, T. C. 205
Levin, E. R. 160
Levine, J. D. 240
Liebermann, W. K. 205
Lippman, M. D. 245
Liu, S. G. 210
Luedicke, E. 250
McCaffrey, M. T. 205
McFarlane, S. H. 205
Mehalso, R. M. 205
Micheletti, F. B. 205
Miller, A. 250
Miller, E. A. 205
Neilson, H. 205

Norris, P. E. 205
 North, D. O. 240
 Nuese, C. J. 205
 Oka, T. 160
 Okamoto, F. 160
 Olson, H. F. 250
 Onyshkevych, L. 205
 Pankove, J. I. 205
 Phillips, W. 240
 Ramberg, E. G. 210
 Ramberg, E. G. 345
 Richman, D. 205
 Robinson, B. B. 215
 Royce, M. R. 205
 Sabisky, E. S. 125
 Sabisky, E. S. 205
 Saxena, A. N. 160
 Schade, H. 205
 Shaw, J. M. 205
 Shrader, R. E. 205
 Sigai, A. G. 205

Silver, R. S. 250
 Smith, R. W. 125
 Sobol, H. 215
 Sommers, H. S. 240
 Southgate, P. D. 205
 Staebler, D. L. 240
 Staebler, D. L. 250
 Sunshine, R. A. 210
 Swartz, G. A. 210
 Taylor, G. W. 240
 Taylor, G. W. 250
 Taylor, G. W. 360
 Tietjen, J. J. 205
 Ulmer, R. 205
 van Raalte, J. 240
 Vossen, J. L. 205
 Wang, C. C. 205
 Weisberg, L. R. 205
 Weller, K. P. 240
 Wen, C. P. 240
 Williams, J. G. 365
 Witke, J. P. 205

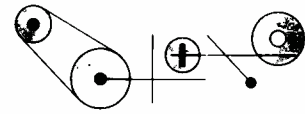
Yocom, P. N. 205
 Zaininger, K. H. 210
 Zanzucchi, P. J. 205

Solid State Division

Avery, L. 215
 Bishop, A. 215
 Cunniff, K. 170
 Engler, R. M. 215
 Glicksman, R. 240
 Granger, G. F. 175
 Greig, W. 170
 Griffin, R. 210
 Griffin, R. 215
 Hyman, H. M. 170
 Kannam, P. J. 210
 Lee, H. C. 210
 Limm, A. 240
 Miller, H. S. 215
 Muller, S. 170
 Nyul, P. 240
 Olmstead, J. 210
 Peterson, W. R. 215
 Ponczak, S. 210
 Reich, S. 210
 Reich, S. 215

Patents Granted

to RCA Engineers



As reported by RCA Domestic Patents, Princeton

Graphic Systems

Constant Sized Halftone Dot Image Generator—R. J. Klensch (GS, Dayton) U.S. Pat. 3,580,995; May 25, 1971

Electronic Components

Display Device for Providing Graticules of Various Configurations—W. J. Dodds (EC, Harsn) U.S. Pat. 3,581,002; May 25, 1971

Method for Metallizing Phosphor Screens—T. A. Saulnier (EC, Lanc) U.S. Pat. 3,582,389; June 1, 1971

Method of Metallizing Phosphor Screens Using an Aqueous Emulsion Containing Hydrogen Peroxide—T. A. Saulnier (EC, Lanc) U.S. Pat. 3,582,390; June 1, 1971

Method of Coating Wide-Angle Cathode Ray Picture Tube Envelopes—R. E. Salveter, Jr. (EC, Marion) U.S. Pat. 3,582,394; June 1, 1971

High Voltage Integrated Circuit Including an Inversion Channel—G. F. Granger H. Khajezadeh (EC, Som) U.S. Pat. 3,582,727; June 1, 1971

Low Reluctance Resonant Structure in Waveguide for Isolating D.C. Magnetic Fields—W. W. Siekanowicz, T. E. Walsh, D. J. Blattner (EC, Clark) U.S. Pat. 3,582,831; June 1, 1971

Shadow-Mask Cathode Ray Tube Including a Masking Member Comprising a Skirt Having Indentations and Projections Overlapping and Attached to a Frame—K. A. Long (EC, Lanc) U.S. Pat. 3,585,431; June 15, 1971

Miniature Ceramic Capacitor and Method of Manufacture—B. Schwartz, W. H. Liederbach (EC, Som) U.S. Pat. 3,585,460; June 15, 1971

Microwave Power Transistor with a Base Region Having Low-and-High-Conductivity Portions—W. P. Imhauser (EC, Som) U.S. Pat. 3,585,465; June 15, 1971

Semiconductor Hybrid Power Module Package—W. L. Oates (EC, Som) U.S. Pat. 3,586,917; June 22, 1971

Method of Assembly of Electron Tubes—D. V. Henry (EC, Harsn) U.S. Pat. 3,587,148; June 28, 1971

Rectangular Shadow Mask Type Color Picture Tube with Barrel Shaped Mask Frame—F. M. Sohn (EC, Lanc) U.S. Pat. 3,588,568; June 28, 1971

High Voltage Electron Discharge Tube—C. M. Morris (EC, Som) U.S. Pat. 3,588,575; June 28, 1971

Integrated Circuit—A. H. Medwin (EC, Som) U.S. Pat. 3,588,635; June 28, 1971

Control Circuits—M. S. Fischer (EC, Som) U.S. Pat. 3,590,275; June 29, 1971

High Voltage Electron Discharge Tube Having Anode Target—J. L. Deckert (EC, Woodbridge) U.S. Pat. 3,590,308; June 29, 1971

Complementary Field-Effect Transistor Buffer Circuit—J. A. Dean, R. C. Heuner (EC, Som) U.S. Pat. 3,591,855; July 6, 1971

Photographic Printing of Cathode-Ray Tube Screen Structure—H. R. Frey (EC, Lanc) U.S. Pat. 3,592,112; July 13, 1971
Display Device Including Resilient Mounting Means—N. L. Lindburg (EC, Som) U.S. Pat. 3,594,602; July 20, 1971

Circuit and Method for Measuring the Amplification Factor of an In-Circuit or Out-of-Circuit Transistor—S. L. Knanishu (EC, Harsn) U.S. Pat. 3,594,640; July 20, 1971

Missile and Surface Radar Division

Automatic Impedance Matching Circuits for variable Frequency Source—W. I. Smith (M&SR, Mrstn) U.S. Pat. 3,581,244; May 25, 1971

Video Logarithmic Amplifier—H. F. Inacker, M. C. Johnson (M&SR, Mrstn) U.S. Pat. 3,571,618; March 23, 1971

High Speed Double Rank Shift Register—E. L. Henderson (M&SR, Mrstn) U.S. Pat. 3,585,113; June 15, 1971

Corporate-Network Printed Antenna System—O. M. Woodward (M&SR, Mrstn) U.S. Pat. 3,587,110; June 22, 1971

Consumer Electronics

Keyed Burst Separator—J. N. Pratt (CE, Ind) U.S. Pat. RE 27134; June 1, 1971

Electromagnetic Deflection Yoke Having Bypassed Winding Turns—R. L. Barbin (CE, Ind) U.S. Pat. 3,588,566; June 28, 1971

RCA Laboratories

Projection of Color-Coded B and W Transparencies—P. J. Donald (Labs, Pr) U.S. Pat. 3,582,202; June 1, 1971

Magnetostrictive Element—L. S. Onyshkevych (Labs, Pr) U.S. Pat. 3,582,408; June 1, 1971

Light Aperture Matrix—G. W. Taylor, P. Goldstein (Labs, Pr) U.S. Pat. 3,582,907; June 1, 1971

Crosstalk Reduction in Film Player—R. E. Flory, W. J. Hannan (Labs, Pr) U.S. Pat. 3,584,147; June 8, 1971

Continuous Motion Apparatus for TV Scanning—R. E. Flory (Labs, Pr) U.S. Pat. 3,584,148; June 8, 1971

Registration Apparatus for Television Film Projection System—R. E. Flory (Labs, Pr) U.S. Pat. 3,584,149; June 8, 1971

Process for Fabricating Replicating Masters—C. H. Morris, Jr. (Labs, Pr) U.S. Pat. 3,585,113; June 15, 1971

Coding Arrangements for Multiplexed Messages—R. F. Sanford (Labs, Pr) U.S. Pat. 3,585,290; June 15, 1971

Missile and Surface Radar Division

Black, R. D. 180
 Buckley, M. 180
 Campopiano, C. 225
 Crenshaw, E. 370
 Finnegan, J. E. 180
 Gaskell, W. 130
 Killion, R. 175
 Price, S. 175
 Robinson, S. 175
 Sherman, S. 225
 Smith, A. E. 140
 Sparks, G. 140
 Steele, S. 370
 Vollmer, W. T. 370
 Watson, B. 280

Video Amplifier—P. E. Haferl (Labs, Switzerland) U.S. Pat. 3,585,295; June 15, 1971

Structural Corner—E. P. Cecelski (Labs, Pr) U.S. Pat. 3,586,359; June 22, 1971

Field-Excited Semiconductor Laser Which Uses a Uniformly Doped Single Crystal—P. D. Southgate (Labs, Pr) U.S. Pat. 3,586,999; June 22, 1971

Adjustable Bandwidth Optical Filter—D. H. Pritchard (Labs, Pr) U.S. Pat. 3,588,224; June 28, 1971

High Resolution Laser Engraving Apparatus—M. E. Heller, H. J. Gerritsen (Labs, Pr) U.S. Pat. 3,588,439; June 28, 1971

UHF or L Band Non-Free-Running Avalanche Diode Power Amplifying Frequency Synchronized Oscillator—H. J. Prager, K. K. N. Chang, S. Weisbrod (Labs, Pr) U.S. Pat. 3,588,735; June 28, 1971

Method and Apparatus for Manufacturing Magnetic Recording Tape—D. F. Martin (Labs, Pr) U.S. Pat. 3,588,771; June 28, 1971

Projection of Color-Coded B and W Transparencies—P. J. Donald (Labs, Pr) U.S. Pat. 3,591,274; July 6, 1971

Photochromic Display Device—Z. J. Kiss (Labs, Pr) U.S. Pat. 3,592,528; July 13, 1971

Image Device Having 100 Angstrom Bandwidth Phosphor Emissive in Blue Region—S. Larach (Labs, Pr) U.S. Pat. 3,593,054; July 13, 1971

High Power Avalanche Diode Microwave Oscillators Having Output Frequency Above Diode Transit Time Frequency—S. Liu, J. J. Risko, K. K. N. Chang (Labs, Pr) U.S. Pat. 3,593,193; July 13, 1971

RCA Service Company

Test Signal Generator for Producing Test Patterns for a Television Receiver—S. Wlasuk (ServCo, Cherry Hill) U.S. Pat. 3,582,544; June 1, 1971

Test Signal Generator—S. Wlasuk (ServCo, Cherry Hill) U.S. Pat. 3,586,755; June 22, 1971

Communications Systems Division

Automatic Black Level Video Signal Clipping and Clamping System—L. J. Thorpe (CSD, Camden) U.S. Pat. 3,582,545; June 1, 1971

Signal Transmission in Recorder Systems with Impedance Transformation—J. T. Heizer (CSD, Camden) U.S. Pat. 3,585,312; June 15, 1971

Digital Signalling System—M. Rosenblatt (CSD, Camden) U.S. Pat. 3,585,596; June 15, 1971

Video Tape Reproducer System Having Automatic Standard Selection—J. C. Kmiec, A. C. Luther, Jr. (CSD, Camden) U.S. Pat. 3,586,769; June 22, 1971

Servo System—M. Horrii, K. Sadashige (GCS, Camden) U.S. Pat. 3,586,946; June 22, 1971

Digital Companding Loop for Monobit Encoder/Decoder—E. King (CSD, Camden) U.S. Pat. 3,587,087; June 22, 1971

Electro-Optic Devices for Portraying Closed Images—L. J. Nicastro (CSD,

Camden) U.S. Pat. 3,588,225; June 28, 1971

Gamma Correction and Shading Modulation Circuitry for a Television Camera—R. A. Dischert, L. J. Thorpe (CSD, Camden) U.S. Pat. 3,588,338; June 28, 1971

Television Blanking and Synchronizing Signal Generator—L. J. Baun (CSD, Camden) U.S. Pat. 3,588,351; June 28, 1971

Speech Synthesizer Utilizing Timewise Truncation of Adjacent Phonemes to Provide Smooth Formant Transition—T. B. Martin (CSD, Camden) U.S. Pat. 3,588,353; June 28, 1971

Word Recognition System for Voice Controller—M. B. Herscher, T. B. Martin (CSD, Camden) U.S. Pat. 3,588,363; June 28, 1971

Electronic Check Cashing System—T. G. Paterson (CSD, Camden) U.S. Pat. 3,588,449; June 28, 1971

Feature Abstractor—G. J. Dusheck, Jr., T. P. Kelley, and P. B. Scott (GCS, Camden) U.S. Pat. 3,588,075; March 2, 1971
Gyromagnetic Notch Filter—A. Boornard (GCS, Camden) U.S. Pat. 3,594,665; July 20, 1971

Transmission Including Toothed Belt and Partially Toothed Pulley—R. M. Kongelka (CSD, Meadowlands) U.S. Pat. 3,583,250; June 8, 1971

Reed Armature Valves for Controlling Fluid Flow—D. G. Macaulay (CSD, Plymouth) U.S. Pat. 3,584,650; June 15, 1971

Optical Flaw Detector—D. A. Wisner (CSD, Plymouth) U.S. Pat. 3,584,963; June 15, 1971

Apparatus for Comparing Two Dimensions—D. A. Wisner (CSD, Plymouth) U.S. Pat. 3,593,133; July 13, 1971

Systems Development Division

Trigger Pulse Circuits—K. H. Hoffman (SDD, Palm Beach) U.S. Pat. 3,584,240; June 8, 1971

Astro-Electronics Division

Self Righting Vessel—V. P. Head (AED, Pr) U.S. Pat. 3,585,952; June 22, 1971

Control System for Spinning Bodies—H. Perkel, W. H. Comerford (AED, Pr) U.S. Pat. 3,591,108; July 6, 1971

Radio Facsimile Postal System—D. S. Bond (AED, Pr) U.S. Pat. 3,594,495; July 20, 1971

Electromagnetic and Aviation Systems Division

Clamp Assembly—A. A. Smalzarz (EASD, Van Nuys) U.S. Pat. 3,586,356; June 22, 1971

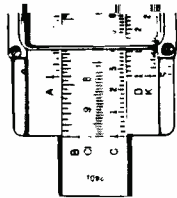
Agitation Switch—J. R. Hall, P. B. Korda (EASD, Van Nuys) U.S. Pat. 3,594,520; July 20, 1971

Aerospace Systems Division

Flash Lamp—B. R. Clay, T. A. Haddad (ASD, Burl) U.S. Pat. 3,560,787; February 2, 1971

RCA Limited

Differential Phase Distortion Compensator for Color Television Equipment—P. Labarre (Ltd, Mont) U.S. Pat. 3,593,041; July 13, 1971



Fellowship Honors Dr. Engstrom

Dr. Malcolm Moos, President of the University of Minnesota, and H. W. Levenenz, Staff Vice President and Chairman of the RCA Educational Aid Committee, have jointly announced an RCA Fellowship in Science and Engineering honoring Dr. Elmer W. Engstrom, former President of RCA.

Dr. Engstrom graduated from the University of Minnesota in 1923 and currently is a Trustee of the University of Minnesota Foundation. He served as President and then Chief Executive Officer of RCA before retiring as an employee in 1969 after more than 45 years of service. He continued on the Board of Directors and as Chairman of the Executive Committee until he chose earlier this year not to stand for re-election to the Board.

Candidates for the Engstrom Fellowship should be full time pre-doctoral graduate students in electronics, electrical engineering, computer/information science or engineering, physics or mathematics. Selection of the Fellow and administration of the Fellowship will be handled by the University. RCA will sponsor the Fellowship, including payment of full tuition, a stipend to the Fellow, and a grant to the department in which the Fellow is majoring. The Fellowship is expected to start with the coming 1971-72 academic year and to continue for 10 years.

D. F. Schmit, former RCA Engineering Vice President

Dominic F. Schmit, former RCA research and engineering management executive, died July 16 at the age of 68.

Mr. Schmit graduated in 1923 from the University of Wisconsin with a BSEE degree. He worked as an engineer at General Electric Company and E. T. Cunningham Co. of New York before joining RCA in 1930.

During his 37 years at RCA Mr. Schmit held a succession of increasingly important engineering and management positions. Early in his career, he was responsible for supervision of engineering and development of metal electronic vacuum tubes, miniature tubes, and kinescopes for television. In 1938 he became Manager of Research and Engineering, RCA Radiotron Division, Harrison, N.J.

In 1940, he was named Manager of the New Products Division, Camden, N. J. and four years later was appointed Assistant Chief Engineer of the RCA Victor Division; he was closely associated with the development of RCA's first pre-war commercial television receivers. During World War II, Mr. Schmit coordinated engineering on the airborne "Block" Tele-

Gilbertson named to post at Electromagnetic & Aviation Systems Division

Appointment of **Donald K. Gilbertson** as Manager, Advanced Systems, has been announced by **Frederick H. Krantz**, Division Vice President and General Manager of RCA Electromagnetic and Aviation Systems Division, Van Nuys, Calif.

Mr. Gilbertson is responsible for directing the Division's systems engineering and new technology for application to advanced programs and new business opportunities. Prior to being named to the new post he had been Manager, Electronic Warfare Systems, for the Aerospace Systems Division at Burlington, Mass. for the past several years.

Rabinowitz named Manager, Systems Engineering at Missile and Surface Radar Division

Appointment of Dr. **Samuel J. Rabinowitz** as Manager, Systems Engineering, was announced by **Dudley M. Cottler**, Chief Engineer of RCA's Missile and Surface Radar Division, Moorestown, N. J. In the new post, Dr. Rabinowitz will be responsible for directing the division in fulfilling customers' systems requirements and developing new program concepts to meet the advanced technological demands of the future.

Staff Announcements

Anthony L. Conrad, President and Chief Operating Officer has announced his organization as follows: **L. Edwin Donegan, Jr.**, Vice President and General Manager, Computer Systems; **John B. Farese**, Executive Vice President, Electronic Components; **Edgar H. Griffiths**, Executive Vice President, Services; **Howard R. Hawkins**, President, RCA Global Communications, Inc.; **William C. Hittinger**, Vice President and General Manager, Solid State Division; **Irving K. Kessler**, Executive Vice President, Government and Commercial Systems; **Barton Kreuzer**, Executive Vice President, Consumer Electronics; **Anthony L. Conrad**, Acting Vice President, Subsidiary Operations.

Electromagnetic & Aviation Systems Division

Frederick H. Krantz, Division Vice President and General Manager of RCA Electromagnetic and Aviation Systems Division, Van Nuys, Calif., has appointed **Donald K. Gilbertson**, Manager, Advanced Systems.

RCA Taiwan Limited

J. W. Good, President, RCA Taiwan Limited, has announced the organization as follows: **S. R. Cha**, Chief, Security; **S. Y. Chen**, Manager, Plant Engineering; **S. C. Chow**, Controller; **R. A. Donnelly**, Manager, Solid State Division; **J. J. McDowell**, Manager, Consumer Electronics Division; **E. G. Shagen**, Manager,



vision System, and other military electronics equipments and tubes. After the war, he became active in shifting engineering activities back to entertainment and commercial products such as black-and-white television receivers, electron tubes and broadcasting equipment. He

was promoted to Director of Engineering in March, 1945, and was elected Vice President, RCA Victor Division Engineering Dept. in March, 1946.

High on the list of his post-war projects were the RCA Victor "45" Record Player and Records. Mr. Schmit was deeply involved in the early development, field testing, and FCC hearings which led to the approval and establishment of the color television system in use today—a project involving numerous interrelated electronic products.

In 1954, D. F. Schmit was promoted to the position of Vice President, Product Engineering, reporting to the Executive Vice President, Research and Engineering. In this capacity, he was responsible for coordinating and administering product engineering programs and procedures on a company-wide basis. This included specialized guidance on product engineering matters, corporate engineering support of line management, and provision for a corporate-wide standardization program.

Mr. Schmit who had joined IRE as an Associate Member in 1925 received an IRE Fellow Award in 1951. He was a registered professional engineer in New Jersey.

Industrial Relations; **H. L. Wang**, Manager, Import/Export; **R. H. Yen**, Manager, Memory Products Division.

Government & Commercial Systems

Dr. Harry J. Woll, Division Vice President, Government Engineering has appointed **Robert Trachtenberg**, Manager, Technical Planning, for RCA Government and Commercial Systems.

Solid State Division

William C. Hittinger, Vice President and General Manager has appointed **Julius S. Lemper**, Marketing Manager, Linear Integrated Circuits Products, for the Solid State Division.

Electronic Components

Joseph H. Colgrove, Division Vice President and General Manager, Entertainment Tube Division, RCA Electronic Components has appointed **Gordon W. Farmer**, Manager, Receiving Tube Operations.

Advanced Technology

Eugene D. Savoye, Manager, Advanced Technology, has announced the organization as follows: **Thomas W. Edwards**, Engineering Leader, Product Development (Structures Technology); **Charles P. Hadley**, Engineering Leader, Product Development (Photoconductor Technology); **Frederick R. Hughes**, Engineering Leader, Product Development (Emission Technology); **Paul W. Kaseman**, Engineering Leader, Product Development (Camera Tube Technology); **James L. King**, Manager, Development Shop; **Brown F. Williams**, Manager, Electro-Optics Devices Laboratory (Princeton).

Awards

Communications Systems Division

Robert T. Fedorka has received an Individual Technical Excellence Award for his outstanding work on the Radar Data Link Decoder/Converter used in the AN/TPQ-27 Radar Course Directing Central.

Roy H. Brader of Communications Equipment Engineering Advanced Development has received the August Technical Excellence Award for his outstanding work in developing an electronically tuned, high dynamic range front end for the receiver portion of the Ultra Reliable Radio System.

Aerospace Systems Division

Donald J. Morand has been cited as Engineer of the Month for April for his synthesis and subsequent analysis of a complex Thermal Analytical Model (TAM) for the Laser Altimeter Program.

Ray Boyle of Technical Staff, Data Systems Development, was chosen as May Engineer of the Month for his work on the disc routines for the Walt Disney World AM&CS.

The team of **Glenn Anderson**, **George Dodson**, **John Harrison**, **Steven Schlosser**, and **Eldon Sutphin** received the April Technical Excellence Award for out-

Degrees Granted

W. N. Abrams, Labs, Pr A.A. in Applied Science, Mercer County Community Col.
E. M. Botnick, Labs, Pr B.A. in Chemistry, Rutgers Univ.
C. J. Buiocchi, Labs Pr B.A. in Chemistry, Rutgers Univ.
B. DeMarinis, AED, Pr M.S.E.E., Brooklyn Polytechnic Inst.
S. D. Dierk, Labs, Pr M.S. in Information Science, Drexel Univ.
L. J. French, Labs, Pr Ph.D. in E.E., Columbia Univ.
J. J. Gibson, Labs, Pr Teknologie Licentiat, Inst. of Tech., Chalmers, Sweden
G. E. Gottlieb, Labs, Pr Ph.D. in Ceramics, Rutgers Univ.
D. I. Harris, Labs, Pr M.S.E.E. Polytechnic Inst. of Brooklyn
F. Hornbuckle, AED, Pr M.S.E.E., Rutgers Univ.
C. K. Hu, Labs, Pr Ph.D. in Chemistry, Rutgers Univ.
K. Johnson, AED, Pr M.S. in Engineering Management, Newark Col. of Eng.
D. L. Matthies, Labs, Pr M.S.E.E., Princeton Univ.
T. J. McKnight, AED, Pr M.S. in Engineering Management, Drexel Univ.
J. J. O'Neill, Jr., Labs, Pr B.S. in Mktg., Rutgers Univ.
W. Rauch, AED, Pr B.S.E.E., Monmouth Col.
H. Solomon, AED, Pr B.S. in Electronic Physics, LaSalle Col.
H. C. Wasserman, Labs, Pr Ph.D. in Linguistics, Univ. of Penn.

standing creativity and inventiveness in the improvements of the LCSS switching matrix and measurements functions associated with the Test Adapter and Waveform Converter assemblies.

The team of **Dominick Aievoli**, **Dick Cahoon**, **George Cahoon**, **George Chambers**, **Anthony Helies**, **David Johnson**, **Noel Lanham**, **Joe Newell**, and **Gene Veilleux** was selected for the May Technical Excellence Team Award for the successful completion of the design, development, fabrication, test, and sell-off of the first prototype Data Acquisition Assembly (DAA), a portion of the AEGIS—Operational Readiness Test System (ORTS).

Astro-Electronics Division

The following groups have been selected as winners of the 1971 I-R 100 New Product Competition Award:

A. Holmes-Siedle and **W. Poch** for the "Mosimeter" radiation dose measuring device.

G. Barna, **L. Freedman**, **B. P. Miller**, and **S. Ravner** for the return beam vidicon camera and Laser Beam Image Reproducer (LBIR).

W. Haneman, **R. Hoedemaker**, **G. Martch**, **F. Scearce** and **A. Schnapf** for the ITOS-1 satellite.

Licensed Professional Engineers

When you receive a professional license, send your name, PE number (and state in which registered,) RCA division, location, and telephone number to: **RCA Engineer**, Bldg. 2-8, RCA, Camden, N.J. As new inputs are received they will be published.

Astro Electronics Division

A. W. D'Amanda, AED, Princeton, N.J., PE-19326, N.J.

Aerospace Systems Division

E. D. Veilleux, ASD, Burlington, Mass., PE-19197; Mass.

Communications Systems Division

A. J. Risko, CSD, Meadow Lands, Pa., PE-7334-E; Pa.

C. J. Springer, CSD, Meadow Lands, Pa., PE-61992-E; Pa.

Computer Systems Division

J. Chisholm, CS Palm Beach Garden, Fla., PE-11404; Mass.

D. J. Enxing, CS Marlboro, Mass., PE-24534; Mass.

G. V. Jacoby, CS Marlboro, Mass., PE-001950E, Pa.

J. M. Stevens, CS Palm Beach Gardens, Fla., PE-13814; Fla.

Electromagnetic and Aviation Systems Division

R. A. Holt, EASD, Van Nuys, Calif., PE-EE-6940; Calif.

Electronic Components

P. Zell, EC, Woodbridge, N.J., PE-13494; N.J.

J. E. Kelley, EC, Harrison, N.J., PE-009538; Pa.

RCA Laboratories

L. K. Jurskis, RCA Labs, Princeton, N.J., PE-012317E; Pa., PE-15429; N.J.

RCA Purchasing Company, NV

E. Montoya, Resident Engineering, Tokyo, Japan, PE-06584; Ind.

Solid State Division

L. C. Linesch, Mountaintop, Pa., PE-E-03026; Ohio.

Service Company

A. J. Schmidt, SvCo., Cherry Hill, N.J., PE-011152E; Pa.

Missile and Surface Radar Division

R. S. Milne, M&SR, Moorestown, N.J., PE-10347E; Pa.

C. T. Olson, M&SR, Moorestown, N.J., PE-13757; N.J.

A. L. Tennenbaum, M&SR, Moorestown, N.J., PE-7233; Md.

W. C. Powell, M&SR, Moorestown, N.J., PE-26824; Ohio; PE-7950; Wash.

Patents and Licensing

M. De Camillis, P&L, Princeton, N.J., PE-12131; Mich.

RCA Global Communications, Inc.

V. Lim, GlobCom, Phillippines, PE-474; Phillippines

Government and Commercial Systems

L. P. Dague, ATL, Camden, N.J., PE-5392; N.J.

M. E. Siegal, GPSD, Camden, N.J., PE-24174; Mass.

Promotions

Solid State Division

U. Roundtree from Engr., Product Develop. to Engr. Ldr., Product Develop. (J. A. Amick, Somerville)

W. F. Allen, Jr., from Engr., Product Develop. to Engr. Ldr., Product Develop. (R. A. Santilli, Somerville)

S. Middings from Engr., Product Develop. to Engr. Ldr., Product Develop. (R. A. Santilli, Somerville)

Communications Systems Division

I. Joffe from Ldr., Design & Develop. Engrs. to Mgr., Comm. Eng. Tactical Engr. (D. T. Gross, Camden)

Astro Electronics Division

J. E. Croft from Ind. Engr. to Mgr., Ind. Svcs. (M. Sasso, Hightstown)

A. S. Baran from Engr. to Mgr., Adv. Develop. (M. Sasso, Hightstown)

J. H. Feingold from Ind. Engr. to Mgr., Ind. Engr. (M. Sasso, Hightstown)

T. C. McNelis from Mfg. Engr. to Mgr., Process Engr. (M. Sasso, Hightstown)

Electronic Components

J. H. Bamford from Engr. Mfg. Engrg. to Mgr. Tube Prod. Engrg. (J. J. Florek, Harrison)

G. D. Cartwright from Engr., Mfg. to Engr. Ldr., Mfg. (J. A. Zollman, Lancaster)

J. C. Decker from Mgr., Miniature & Special Purpose Tube Prod. Engrg. to Mgr., Prod. Engrg. (R. Nearhoff, Woodbridge)

Electronic Components

T. M. DeMuro from Res. Engr, Tube Mfg. Engrg. to Mgr., Tube & Parts Prep., Prod. Engrg. (J. J. Florke, Harrison)

T. W. Edwards, Engr., Prod. Develop. to Engr. Ldr., Prod. Develop. (E. D. Savoye, Lancaster)

J. J. Florek from Mgr., Tube and Parts Prep., Prod. Engrg. to Mgr., Tube Mfg. (C. W. Hear, Harrison)

C. W. Hear from Mgr. Tube Mfg. to Mgr. Rec. Tube Prod. (G. W. Farmer, Harrison)

F. R. Hughes from Engr., Prod. Develop. to Engr. Ldr., Prod. Develop. (E. D. Savoye, Lancaster)

P. W. Kaseman, Prod. Develop. to Engr. Ldr., Prod. Develop. (E. D. Savoye, Lancaster)

J. G. Kindbom from Supt., Electro-Optics Prod. Mfg. to Mgr., Mfg. & Prod. Engr. (H. W. Sawyer, Lancaster)

Errata

On page 17 of Vol. 16, No. 6 of the RCA Engineer co-authors Jose Raij and James H. Leppold are erroneously listed as being assigned to Systems Development Division. Actually, both men are assigned to Systems Manufacturing.

Gunther Retires After 40 Years with RCA

Clarence A. Gunther, Division Vice President, Technical Programs for RCA's Government and Commercial Systems, has retired after more than 40 years' service with the company.

Mr. Gunther joined RCA in 1930 as a development and design engineer. Since that time he moved into a number of increasingly important engineering posts in the company, gaining his position at the Moorestown-based operation in 1962. Prior to that he served as Chief Engineer for six years and Assistant Chief Engineer for nine years.

Mr. Gunther earned his BSEE from Princeton University in 1926 and joined the General Electric Company upon graduation. He is an active member in a number of industrial, technical and military societies and is a Fellow in the Institute of Electrical and Electronic Engineers. He has received citations from both the U.S. Army and Navy for his contributions in the field of electronics for military use.

Professional Activities

Electromagnetic & Aviation Systems Division

Robert M. Illson, Administrator, Program Product Assurance, has been named Chairman of the Los Angeles Section of the American Society for Quality Control. The National Group has approximately 25,000 members; the Los Angeles Section, the second largest, has almost 700 members.

D. W. Koch, Manager, Customer and Product Support, has been elected Chairman of the San Fernando Chapter of the Society of Logistics Engineers. SOLE has over 2000 members nationally, with approximately 120 in the San Fernando Chapter.

Melvin M. Miller, ASD-Burlington, was moderator at a recent meeting at MIT on the subject of "Engineering Education . . . the Challenge of the 70's and 80's." Principal speakers included: Dr. Eino Johnson, Director, Higher Education, HEW, Region 1; Dr. John Leech, Assistant Dean of Engineering, Boston University; Dr. Harold Raemer, Chairman, EE Dept., Northeastern University; and Dr. Paul Grey, Chancellor of MIT and former Dean of Engineering. Mr. Miller is chairman of the IEEE Education Group in Boston.

James Hillier, Executive Vice President in charge of Research and Engineering, has been elected to the Council of the National Academy of Engineering.

Electronic Components

W. E. Harbaugh participated as one of six lecturers at the University of Tennessee Space Institute, Tullahoma, Tennessee on April 24 and 25, 1971. Mr. Harbaugh gave a short course on heat pipe technology as his part in the lecture series.

A ten session color television course for factory and quality rating lab technicians and supervision was promoted by S. L. Babcock, Woodbridge Resident Engineer, and taught by J. P. Wolff of Application Engineering at the Woodbridge plant location during April, May, and June 1971. The course was designed to upgrade the ability to maintain color television sets used in receiving tube testing.

Kocher on ENGINEER Staff

Christopher P. Kocher has been appointed Administrator, RCA Technical Publications, and Assistant Editor, RCA ENGINEER; he reports to W. O. Hadlock, Manager, Technical Publications, Corporate Engineering Services.

Mr. Kocher will maintain close contact with the TPA's and the RCA ENGINEER Editorial Representatives, and the authors of RCA technical papers.

Mr. Kocher received the BA in Chemistry from the University of Pennsylvania in 1971; he earned scholastic honors at Deerfield Academy and at Lafayette College prior to his study at U. of P. Mr. Kocher's major academic interests were in math, science, and technical journalism. He served as Managing Editor, and Editor-in-Chief of the *Pennsylvania Triangle* in which he published ten technical or semi-technical articles; he also conducted interviews, and published editorials, and a nationally awarded series of essays. His industrial experience includes work at the Borden Chemical Company research laboratory as Senior Laboratory Technician. At Borden, Mr. Kocher designed and carried out tests of the physical properties of polymers intended for adhesive use; in this work, he programmed and used a time-sharing computer.



Editorial Representatives

The Editorial Representative in your group is the one you should contact in scheduling technical papers and announcements of your professional activities.

Government and Commercial Systems

Aerospace Systems Division

Electromagnetic and Aviation Systems Division

Astro-Electronics Division

Missile & Surface Radar Division

Government Engineering

Government Plans and Systems Development

Communications Systems Division

Commercial Systems

Industrial and Automation Systems

Government Communications Systems

Computer Systems

Systems Development Division

Data Processing Division

Magnetic Products Division

Memory Products Division

Research and Engineering

Laboratories

Electronic Components

Entertainment Tube Division

Industrial Tube Division

Solid State Division

Consumer Electronics

Services

RCA Service Company

RCA Global Communications, Inc.

National Broadcasting Company, Inc.

RCA Records

RCA International Division

RCA Ltd.

Patents and Licensing

Engineering, Burlington, Mass.

Engineering, Van Nuys, Calif.
Engineering, Van Nuys, Calif.

Engineering, Princeton, N.J.
Advanced Development and Research, Princeton, N.J.

Engineering, Moorestown, N.J.

Advanced Technology Laboratories, Camden, N.J.
Defense Microelectronics, Somerville, N.J.
Advanced Technology Laboratories, Camden, N.J.
Central Engineering, Camden, N.J.

Engineering Information and Communications, Camden, N.J.

Chairman, Editorial Board, Camden, N.J.
Mobile Communications Engineering, Meadow Lands, Pa.
Professional Electronic Systems, Burbank, Calif.
Studio, Recording, & Scientific Equip. Engineering, Camden, N.J.
Broadcast Transmitter & Antenna Eng., Gibbsboro, N.J.

Engineering, Plymouth, Mich.

Engineering, Camden, N.J.

Palm Beach Product Laboratory, Palm Beach Gardens, Fla.
Marlboro Product Laboratory, Marlboro, Mass.
Systems Programming Product Laboratory, Riverton, N.J.

Service Dept., Cherry Hill, N.J.

Development, Indianapolis, Ind.

Engineering, Needham, Mass.

Graphic Systems, Dayton, N.J.

Research, Princeton, N.J.

Chairman, Editorial Board, Harrison, N.J.

Receiving Tube Operations, Woodbridge, N.J.
Receiving Tube Operations, Cincinnati, Ohio
Television Picture Tube Operations, Marion, Ind.
Television Picture Tube Operations, Lancaster, Pa.

Industrial Tube Operations, Lancaster, Pa.
Microwave Tube Operations, Harrison, N.J.

Solid State Power Device Engrg., Somerville, N.J.
Semiconductor and Conversion Tube Operations, Mountaintop, Pa.
Semiconductor Operations, Findlay, Ohio
Solid State Signal Device Engrg., Somerville, N.J.

Chairman, Editorial Board, Indianapolis, Ind.
Engineering, Indianapolis, Ind.
Radio Engineering, Indianapolis, Ind.
Advanced Development, Indianapolis, Ind.
Black and White TV Engineering, Indianapolis, Ind.
Ceramic Circuits Engineering, Rockville, Ind.
Color TV Engineering, Indianapolis, Ind.
Engineering, RCA Taiwan Ltd., Taipei, Taiwan

Consumer Products Service Dept., Cherry Hill, N.J.
Consumer Products Administration, Cherry Hill, N.J.
Tech. Products, Adm. & Tech. Support, Cherry Hill, N.J.
Missile Test Project, Cape Kennedy, Fla.

RCA Global Communications, Inc., New York, N.Y.
RCA Alaska Communications, Inc., Anchorage, Alaska

Staff Eng., New York, N.Y.
Record Eng., Indianapolis, Ind.

New York, N.Y.

Research & Eng., Montreal, Canada

Staff Services, Princeton, N.J.

* Technical Publication Administrators listed above are responsible for review and approval of papers and presentations.

RCA Engineer

A TECHNICAL JOURNAL PUBLISHED BY CORPORATE ENGINEERING SERVICES
"BY AND FOR THE RCA ENGINEER"